STUDIES OF RUMINANT DIGESTION, ECOLOGY, AND EVOLUTION

A Thesis

presented to

the Faculty of the Graduate School

at the University of Missouri-Columbia

In Partial Fulfillment

of the Requirements for the Degree

Master of Science

---

by

TIMOTHY HACKMANN

Dr. James Spain, Thesis Supervisor

DECEMBER 2008

The undersigned, appointed by the dean of the Graduate School, have examined the thesis entitled

STUDIES OF RUMINANT DIGESTION,
ECOLOGY AND EVOLUTION

presented by Timothy Hackmann,

a candidate for the degree of Master of Science,

and hereby certify that, in their opinion, it is worthy of acceptance.

Professor James Spain

Professor Monty Kerley

Professor Joshua Millspaugh

ACKNOWLEDGEMENTS

The author is indebted to

- Dr. James Spain, Julie Sampson, and Benjamin Nielson, for varied support and insight that turned the impossible into the possible
- Lucas Warnke, Chad McNeal, Eric Meyer, Zach Brockman, Reagan Bluel, Ruthie Dietrich, Marin Summers, Asa Spain, and Denise Frietag, for additional assistance in the lab and the field
- Dr. Joshua Millspaugh, for his ecological perspective and reaffirming the value of mathematical modeling
- Dr. Monty Kerley, for additional review and teaching me the importance of originality
- Drs. William Lamberson and John Fresen, for introducing me to much of the statistical analysis used herein
- Drs. James Williams, Ronald Belyea, and Deke Alkire, for additional critical review
- Matthew Brooks, Illana Barasch, and Nicole Barkley, for academic and non-academic conversations alike
- My parents, other family, and friends, for listening to me during the joys and frustrations of research
- Kate Kocyba, for being special
- Father God for orchestrating it all.

This thesis belongs to them as much as it does to me.

TABLE OF CONTENTS

LIST OF FIGURES

LIST OF TABLES

STUDIES OF RUMINANT DIGESTION,

ECOLOGY, AND EVOLUTION

Timothy Hackmann

Dr. James Spain, Thesis Supervisor

ABSTRACT

This thesis examines ruminant digestion, ecology, and evolution, particularly where they can improve livestock production systems. We performed an experiment that estimated ruminal in situ degradation parameter values of grass and legume forages. In one analysis, we showed the relative feed value system did not explain variation in these parameter estimates, underscoring a biological limitation of this system. In a subsequent analysis, we found that ruminal digestibility estimated from mean parameter estimates had large 95% confidence limits (81% of digestibility means), suggesting digestibility values so estimated have little meaning.

We performed another experiment that monitored concentrations of labeled forage particles within the reticulorumen. We inferred that once a particle escapes from the dorsal sac for the final time, it must escape from ventral regions soon after entry.

We also developed a mechanistic model of ruminant gastrointestinal tract function (based on chemical reactor theory) that predicted feed intake of wild and domestic ruminants precisely (generally $R^2 > 0.9$, root mean square prediction error < 1.4 kg·d^{-1}). We then used this mechanistic model, along with allometric equations and the fossil record, to demonstrate the pattern of large BW within the Ruminantia is a response to nutritional resource limitations.

Our final study recapitulates key points in the ecology and evolution of wild ruminants, then discusses how these points and others presented in the thesis offer insight to improving livestock production systems.

CHAPTER 1

LITERATURE REVIEW

INTRODUCTION

Owing to ruminants' ability to digest fiber, ruminant livestock production systems convert low-quality fibrous and other feedstuffs into highly-nutritious meat and milk. In total, these systems produce nearly 30 and 100% of the world's supply of these meat and milk products (FAO, 2008a). Because these systems play a keystone role in the world's food supply, it is crucial to understand the ruminant animal underlying their operation. This review examines the evolution, ecology, and domestication of the ruminant to give a comprehensive overview of this animal.

ECOLOGY AND EVOLUTIONARY HISTORY OF WILD RUMINANTS

For the purpose of this review, a ruminant includes any artiodactyl (member of the mammalian order Artiodactyla) possessing a rumen, reticulum, omasum or isthmus homologous to the omasum, and abomasum. Ruminants also possess certain skeletal features—such as loss of upper incisors, presence of incisiform lower canines, and fusion of cubiod and navicular bones in the tarsus—that are useful in fossil identification (e.g., Gentry, 2000) but not of primary consideration here.

Ruminant Families

The six extant (i.e., non-extinct) ruminant families include the Tragulidae, Moschidae, Bovidae, Giraffidae, Antilocapridae, and Cervidae. Table 1.1 provides a

description of these families, including the number of species and genera (from Nowak [1999]).

The Tragulidae (chevrotains) (4 sp.) are small, reclusive, forest-dwelling, deer-like ruminants (Figure 1.1). They are the most primitive of all living families and have changed little morphologically over evolutionary history—this has led them to being called "living fossils" (Janis, 1984). Their primitiveness is demonstrated by (1) their very simple social behavior, (2) retention of a gallbladder and appendix (Janis, 1984), (3) lack of a true omasum (Langer, 1988), and (4) possession of many skeletal characters (e.g., short, unfused metapodials) considered ancestral (Webb and Taylor, 1980). While still considered ruminants, the Tragulidae are not included in the same infraorder (Pecora) as other ruminant families (Moschidae, Bovidae, Giraffidae, Antilocapridae, Cervidae) because of these ancestral features.

The Moschidae (musk deer) (5 sp.) are small tropical Asiatic deer whose males possess a musk gland anterior to the genitals. Like tragulids, the moschids are hornless (other families possess horns or antlers) and the males have large upper canines instead (Figure 1.2). The remaining families, the Bovidae (e.g., cattle, sheep, goats, antelope; 140 sp.), Giraffidae (giraffe and okapi), Cervidae (true deer; e.g., white-tailed deer, caribou, moose; 41 sp.), and Antilocapridae (pronghorn), include species familiar to most readers. Standard mammalogy textbooks (e.g., Feldhamer et al., 2007) and encyclopedias (e.g., Nowak, 1999) provide additional information for all these families.

There are 5 additional extinct families that are generally recognized (Carroll, 1988), the Hypertragulidae, Leptomerycidae, Gelocidae, Palaeomerycidae, and Dromomerycidae. The Hypertragulidae and Leptomerycidae were small, hornless

ruminants that were non-Pecorans (and thus primitive) but still possess the defining skeletal characteristics of present-day ruminants (Webb and Taylor, 1980; Webb, 1998b). Figure 1.3 shows a restoration of a leptomerycid (*Archaeomeryx optatus*) that is broadly representative of these early ruminants. Their appearance and behavior is probably best approximated by the Tragulidae and Moschidae (Webb, 1998b). The Gelocidae is another hornless ruminant family but more advanced—it is considered a true Pecoran (Webb and Taylor, 1980)—and with no close living relatives. Roughly, it members might most closely resemble the Moschidae or the African water chevrotain (family Tragulidae) (Webb, 1998b). Despite living in different locales, Palaeomerycidae (of Eurasia) and Dromomerycidae (of North America) appear very similar; they are medium-to-large-sized with giraffe-like horns but deer-like limb proportions (Janis and Scott, 1987). A restoration of a dromomerycid (*Dromomeryx borealis*) in Figure 1.4 shows the intermixing of these deer and giraffe-like features. Their ecological niche probably resembled that of a subtropical deer (Janis and Manning, 1998b), though they are not closely related to deer or any other living ruminants.

Phylogeny and Evolution

The phylogeny of these families is not well-resolved, but one possible scenario (a simplified and updated version presented by Gentry [2000]) is shown in Figure 1.5. The Hypertragulidae are the most primitive and thus probably the first to appear (Webb and Taylor, 1980), around 50 million years ago (**Ma**; early Eocene) in SE Asia (Fernández and Vrba, 2005; Métais and Vislobokov, 2007). The Tragulidae and Leptomerycidae (or close ancestors thereof) arose shortly thereafter, again in Asia (Colbert, 1941; Métais et al., 2001), but quickly dispersed to North America (Webb, 1998b). During this time,

tropical, closed-canopy forests were widespread (Janis, 1993) and temperatures were very warm (near their highest point in the last 65 million years; Zachos et al., 2001). The Gelocidae appeared at approximately 40 million years ago (middle Eocene), when the climate had already cooled (about 5°C relative to 50 Ma; Zachos et al., 2001) and temperate woodlands appeared (Janis, 1993).

When these first ruminant groups emerged, they were rabbit-sized (<5 kg; Métais and Vislobokov, 2007), but as demonstrated in the North American fossil record, their size progressively increased over time (Figure 1.6). Their skull and dental morphology (low-crowned teeth, small incisors, long and narrow skulls) was optimal for consuming fruits, shoots, and insects (Webb, 1998b). This evidence in addition to the observed habitat and diet of living tragulid and moschid species (which are taken as rough analogues for these first groups) suggests the first ruminants were small, reclusive, forest-dwelling omnivores (Webb, 1998b). Foregut fermentation and rumination was not extensive when these first ruminants emerged but developed by approximately 40 Ma, as indicated by dental morphology (Janis, 1976) and molecular techniques (Jermann et al., 1995).

The remaining families evolved about 18 to 23 Ma (early Miocene) during a second radiation (Janis, 1982) in Eurasia (Antilocapridae, Cervidae, Moschidae, Dromomerycidae, Bovidae, Palaeomerycidae) and Africa (Giraffidae) (Gentry, 2000). Many of these families (Moschidae, Dromomerycidae, Antilocapridae) dispersed to North America shortly after their emergence (Janis and Manning, 1998a,b; Webb, 1998b). By this time, the climate was drier (Janis, 1993) and cooled substantially (first Antarctic ice sheets formed; Zachos et al., 2001) and open, temperate woodlands were the

dominant flora (Janis, 1982, 1993). Dental wear patterns and craniodental morphology suggests these groups ate primarily leaves (Janis, 1982; Solounias and Meolleken, 1992) or grass and leaves (Solounias et al., 2000; Semprebon et al., 2004; Semprebon and Rivals, 2007; DeMiguel et al., 2008). Body mass of these groups was larger (20-40 kg; Janis, 1982) and increased over time, continuing the prior trend (Figure 1.6).

By about 5 to 11 Ma (Late Miocene), grasslands expanded (Jacobs et al., 1999), and some species began including more grass in their diets, again suggested by dental wear patterns and craniodental morphology (Semprebon et al., 2004; Semprebon and Rivals, 2007). At the end of this period (5 Ma), bovids and cervids migrated to North America (Webb, 1998a, 2000). Later (2 Ma; Latest Pliocene) deer would migrate to SA (Webb, 2000).

Distribution, Abundance, BW, and Dietary Preferences of Living Ruminants

Today there exist nearly 200 ruminant wild species (Nowak, 1999), most of which are Bovidae and Cervidae (Table 1.1). A conservative estimate places the world population of wild ruminants at 75.3 million, with 0.28 million tragulids, 0.28 million moschids, 44.6 million cervids, 29.1 million bovids, 0.15 million giraffids, and 0.88 million antilocaprids (Table 1.2). The majority of wild ruminants, in terms of species and population numbers, are thus bovids and cervids.

Following their distribution in the fossil record, living ruminants are natively found on all continents except Antarctica and Australia, though most species are found in Africa and Eurasia (Table 1.3, constructed from data in van Wieren [1996]). The Bovidae and Cervidae both enjoy an almost world-wide distribution, while the range of the

remaining families is much more restricted (Table 1.3). Only the Cervidae are found in South America (Table 1.3).

Ruminants not only have a wide geographic distribution but are also found across many climates and habitats. Though the classification system of habitats and climates used in this review (adopted from van Wieren [1996]) is admittedly crude, it still gives a general sense of this distribution. As a whole, ruminant species are evenly spread across open, ecotone, and forested habitats, but they prefer warm to other types of climates (Table 1.3). The distribution of the Bovidae and Cervidae is generally representative of this overall pattern, whereas other families individually inhabit a more restricted range of habitats and climates (Table 1.3).

As reported in Table 1.4 (data from van Wieren [1996]), median BW of modern ruminants is 45 kg, near that expected from the historical trend (Figure 1.6). Body mass ranges greatly, from approximately 2 kg (Salt's dik to dik [*Madoqua saltiana*], royal antelope [*Neotragus pygmaeus*], lesser Malay mouse deer [*Tragulus javanicus*]) to 800 kg (American bison [*Bison bison*], wisent [*Bison bonasus*], gaur [*Bos gaurus*], Asian water buffalo [*Bubalus bubalis*], kouprey [*Bos* sauveli]; van Wieren, 1996). Though not shown in Table 1.4, some individuals from the largest species achieve BW ≥1,000 kg, with maximum size of male reticulated giraffe (*Giraffa camelopardalis*) reaching 1,400 kg (Clauss et al., 2003). By family, the Giraffidae are the largest; Antilocapridae, Bovidae, Cervidae intermediate; and Moschidae and Tragulidae smallest (Table 1.4). The Bovidae and Cervidae have species at or near these BW extremes, while the other families display a much more restricted range in BW (Table 1.4).

Ruminant species display innate dietary preferences, and these differ greatly across species. A concise way of classifying these preferences is with the feeding class system (first proposed by Hoffman and Stewart [1972]), which categorizes species as either (1) browsers, which innately prefer browse like fruits, shoots, and leaves (typically from shrubs, forbs, and trees), (2) grazers, which innately prefer grasses and other roughage, or (3) intermediate feeders, which switch between browse and grass, usually depending on their seasonal availability. For most of their evolutionary history, ruminant species were predominately or exclusively browsers. Today, a plurality of ruminant species is still classified as browsers (Table 1.5), and only about a quarter are grazers. The Bovidae and Cervidae have species represented in all three feeding classes; the other families are exclusively browsers.

DOMESTICATION OF RUMINANT SPECIES

Details of Domestication

The following details of domestication are from Clutton-Brock (1999) (except where noted) and summarized in Table 1.6. The first livestock species to be domesticated (ruminant or non-ruminant) was the goat at approximately 10 000 B.C. in the Fertile Crescent of the Near East (Zeder and Hesse, 2000). The goat was initially domesticated to supply meat to burgeoning, congested human populations whose hunting had depleted large prey populations in the wild (Clutton-Brock, 1999; Diamond, 2002). Most of the other 8 domesticated ruminant species (sheep, European and Zebu cattle, water buffalo, mithan, reindeer, yak, Bali cattle) were brought under human control by 2500 B.C. in either the Near East or southern Asia. Some of these species were initially

domesticated for meat, like the goat, but reasons for domestication varied greatly, including for milk, draft, transportation, sacrifice, and barter.

Molecular approaches (Bruford et al., 2003) have determined each domestic species is probably derived from several wild species; at least 12 species can claim ancestry to the 9 domesticated species. Of the multitude of available wild species, these twelve were chosen for domestication because they were gregarious, submissive to human captors, unexcitable, and easy to breed (Clutton-Brock, 1999; Diamond, 2002).

Characteristics of Domestic Species

Except where noted, points in the discussion below are summarized in Table 1.7. The total population size of domestic species is 3.57 billion, nearly 50-fold larger than that of wild ruminants. As might be anticipated, cattle, sheep, and goats comprise most (about 95%) of the domestic ruminant population. All but reindeer belong to the family Bovidae.

Most species are grazers, with goats and reindeer the notable exceptions. Sheep were classified by Hoffman (1989) as grazers, though others (e.g., Pfister and Malechek, 1986) argue that they are instead intermediate feeders.

Though BW varies greatly by sex and across breeds, the rough averages in Figure 1.7 demonstrates that BW of domestic ruminants is large in comparison to many wild ruminants. The smallest species (sheep, goat) are near the median BW of wild ruminants (45 kg) and many species (cattle, mithan, Bali cattle) approach the maximum observed in the wild (800 kg; Table 1.4).

SUMMARY AND EXPERIMENTAL OBJECTIVES

The first ruminants evolved approximately 50 million years ago and were small (<5 kg) forest-dwelling omnivores. Today there are almost 200 living ruminant species in 6 families. Wild ruminants number about 75 million, range from about 2 to more than 800 kg, and generally prefer at least some browse in their diet. Eight species have been domesticated within the last 12,000 years, currently numbering 3.6 billion. In contrast to wild ruminants, domestic species naturally prefer at least some grass in their diets, are of large BW (roughly from 35 to 800 kg), and, excepting reindeer, belong to one family (Bovidae).

The goal of the following work is to enhance our understanding of ruminant digestive function, ecology, and evolution, particularly where they intersect with and thus can improve livestock production systems. A myriad of approaches are used herein. Chapters 2 and 3 both discuss an experiment that measured the ruminal in situ degradation of a large number of grass and legume forages. Chapter 2 uses the degradation data collected in this experiment to identify (1) the mathematical model that optimally fits these data and should be used estimate values of degradation parameters (e.g., rate and extent of digestion) from them, (2) the relationship between the degradation parameter values so estimated and relative feed value system (RFV), in order identify biological reasons for RFV's poor performance. Many feed evaluation systems use mean degradation parameter values to estimate in vivo ruminal digestibility, and Chapter 3 shows how variability around these mean values can lead to gross imprecision in this estimation.

Chapter 4 summarizes an experiment that monitored concentrations of labeled forage across sites in the bovine reticulorumen to infer general patterns of digesta particle flow therein. Chapter 5 presents a holistic mechanistic model of the ruminant gastrointestinal tract function. This chapter emphasizes the model as a practical tool to predict intake, though it has other uses (as Chapters 6 and 7 will show).

The focus of Chapters 6 and 7 is ruminant ecology and evolution. Chapter 6 attempts to demonstrate the pattern of large BW in ruminants (whose median BW is 500-fold greater than mammals as a whole) is evolutionary strategy adopted by ruminants to overcome nutritional resource limitations. The mechanistic model of Chapter 5, allometric equations of digestive parameters, and the ruminant fossil record are used as supporting evidence for the chapter's arguments. Chapter 7 briefly recapitulates the summary of ruminant ecology and evolution first presented in the literature review. It then attempts to show how points from Chapter 6, among others in ruminant ecology and evolutionary research, can offer insight into livestock research and production.

APPENDIX

Global population estimates of wild ruminants were compiled from several sources (Whitehead, 1971; Ohtaishi and Gao, 1990; East, 1999; Nowak, 1999; Wiener, 2003; Ulvevadet and Klokov, 2004; IUCN, 2008), many of which are compilations themselves. We excluded from our estimates domesticated, feral, captive, and non-natively introduced populations or species. We also excluded species for which estimates were judged very fragmentary (included only a few isolated or subspecies populations) and were unlikely to approach anything of a global estimate.

In all, we obtained estimates for 150 species (78% of total). This includes 1 species from Antilocapridae (100% of family total), 116 from Bovidae (83% of total), 26 from Cervidae (63% of total), 2 from Giraffidae (100% of total), 4 from Moschidae (80% of total), and 1 from Tragulidae (25% of total). Poor or non-existent census data accounts for missing species. Also note that estimates for many Asian species include numbers only in China, again due to poor census data.

The population sizes reported here are clear underestimates. In total they are still more comprehensive and up-to-date than the last apparent global census (McDowell, 1977), which estimated population numbers for only 11 species (excluding feral and currently unrecognized species) in two families (Bovidae, Cervidae), for a total of 27 million ruminants overall.

Table 1.1. Description of extant ruminant families, including number of genera and species and example species.[1]

family	Number of genera	Number of species	Example species
Antilocapridae	1	1	Pronghorn
Bovidae	49	140	Cattle, sheep, goats, antelope
Cervidae	17	41	White-tailed deer, caribou, moose
Giraffidae	2	2	Giraffe, okapi
Moschidae	1	5	Muskdeer
Tragulidae	3	4	Chevrotains
total	73	193	

[1]Data from Nowak (1999)

Table 1.2. Estimated global population sizes of wild ruminant species.

family	species name: common	species name: scientific	population	source
Antilo-capridae	Pronghorn	*Antilocapra americana*	875,000	Nowak (1999)
		total for Antilocapridae	875,000	
Bovidae	blue duiker	*Cephalophus monticola*	7,000,000	East (1999)
	Maxwell's duiker	*Cephalophus maxwelli*	2,137,000	East (1999)
	Impala	*Aepyceros melampus*	1,990,000	East (1999)
	Grey duiker	*Sylvicapra grimmia*	1,660,000	East (1999)
	Bushbuck	*Tragelaphus scriptus*	1,340,000	East (1999)
	Common wildebeest	*Connochaetes taurinus*	1,200,000	East (1999)
	Kirk's dik-dik	*Madoqua kirki*	971,000	East (1999)
	Oribi	*Ourebia ourebi*	750,000	East (1999)
	Bay duiker	*Cephalophus dorsalis*	725,000	East (1999)
	African buffalo	*Syncerus caffer*	687,000	East (1999)
	Steenbok	*Raphiceros campestris*	663,000	East (1999)
	Thomson's gazelle	*Gazella thomsoni*	650,000	East (1999)
	Peter's duiker	*Cephalophus callipygus*	570,000	East (1999)
	Gunther's dik-dik	*Madoqua guentheri*	511,000	East (1999)
	Salt's dik-dik	*Madoquo saltiana*	485,600	East (1999)
	Alpine chamois	*Rupicapra rupicapra*	400,000	Nowak (1999)
	Sable antelope	*Hippotragus niger*	373,000	East (1999)
	Suni	*Neotragus moschatus*	365,000	East (1999)
	Greater kudu	*Tragelaphus strepsiceros*	352,000	East (1999)
	Black-fronted duiker	*Cephalophus nigrifons*	300,000	East (1999)
	Mongolian gazelle	*Procapra gutturosa*	300,000	Nowak (1999)
	Topi	*Damaliscus lunatus*	300,000	East (1999)
	Kob	*Kobus kob*	295,000	East (1999)
	White-bellied duiker	*Cephalophus leucogaster*	287,000	East (1999)
	Common hartebeest	*Alcelaphus buselaphus*	280,000	East (1999)
	Bontebok	*Damaliscus dorcas*	237,500	East (1999)
	Pygmy antelope	*Neotragus batesi*	219,000	East (1999)
	Lechwe	*Kobus lechwe*	212,000	East (1999)

Bison	*Bison bison*	202,500	Nowak (1999)
Waterbuck	*Kobus ellipsiprymnus*	200,000	East (1999)
Red-flanked duiker	*Cephalophus rufilatus*	170,000	East (1999)
Sitatunga	*Tragelaphus spekei*	170,000	East (1999)
Yellow-backed duiker	*Cephalophus sylvicultor*	160,000	East (1999)
Grant's gazelle	*Gazella granti*	140,000	East (1999)
Comon eland	*Tragelaphus oryx*	136,000	East (1999)
puku	*Kobus vardoni*	130,000	East (1999)
Muskox	*Ovibos moschatus*	122,600	Nowak (1999)
Lesser kudu	*Tragelaphus imberbis*	118,000	East (1999)
Dall sheep	*Ovis dalli*	112,000	Nowak (1999)
Bohor reedbuck	*Redunca fulvorufula*	101,000	East (1999)
Black duiker	*Cephalophus adersi*	100,000	East (1999)
Goitred gazelle	*Gazella subgutturosa*	100,000	Nowak (1999)
Serow	*Capricornis crispis*	100,000	Nowak (1999)
Tibetan antelope	*Pantholops hodgsoni*	100,000	Nowak (1999)
Gerenuk	*Litocranius walleri*	95,000	East (1999)
Sharpe's grysbok	*Raphiceros sharpei*	95,000	East (1999)
Argali	*Ovis ammon*	80,000	Nowak (1999)
Roan antelope	*Hippotragus equinus*	76,000	East (1999)
Mountain goat	*Oreamnos americanus*	75,000	Nowak (1999)
Southern reedbuck	*Redunca arundinum*	73,000	East (1999)
Oryx	*Oryx beisa*	67,000	East (1999)
Royal antelope	*Neotragus pygmaeus*	62,000	East (1999)
Bighorn sheep	*Ovis canadensis*	58,000	Nowak (1999)
Iberian wild goat	*Capra pyrenaica*	50,000	IUCN (2008)
Saiga	*Saiga tatarica*	50,000	IUCN (2008)
Speke's gazelle	*Gazella spekei*	50,000	East (1999)
Klipspringer	*Oreotragus oreotragus*	42,000	East (1999)
Red forest duiker	*Cephalophus natalensis*	42,000	East (1999)
Urial	*Ovis vignei*	40,000	Nowak (1999)
Dorcas gazelle	*Gazella dorcas*	37,500	East (1999)
Mountain reedbuck	*Redunca redunca*	36,350	East (1999)
Blackbuck	*Antilope cervicapra*	36,000	Nowak (1999)
Lichtenstein's hartebeest	*Alcelaphus lichtensteini*	36,000	East (1999)
Nile lechwe	*Kobus megaceros*	36,000	East (1999)
Ogilby's duiker	*Cephalophus ogilbyi*	35,000	East (1999)

Nyala	*Tragelaphus angasi*	32,000	East (1999)
Ibex	*Capra ibex*	31,670	IUCN (2008)
Cape grysbok	*Raphiceros melanotis*	30,500	East (1999)
Piacentinis's dik-dik	*Madoquo piacentinii*	30,000	East (1999)
Bongo	*Tragelaphus eurycerus*	28,000	East (1999)
Zebra duiker	*Cephalophus zebra*	28,000	East (1999)
Blue sheep	*Pseuodois nayaur*	25,000	Nowak (1999)
East Caucasian tur	*Capra caucasica*	25,000	Nowak (1999)
Red-fronted gazelle	*Gazella rufifrons*	25,000	East (1999)
Springbok	*Antidorcas marsupialis*	24,000	East (1999)
Harvey's red duiker	*Cephalophus*	20,000	East (1999)
Black wildebeest	*Connochaetes gnou*	18,000	East (1999)
gray rhebuck	*Pelea capreolus*	18,000	East (1999)
Grey rhebok	*Pelea capreolus*	18,000	East (1999)
Giant Eland	*Tragelaphus derbianus*	17,650	East (1999)
Pyrenean chamois	*Rupicapra pyrenaica*	15,000	IUCN (2008)
Yak	*Bos grunniens*	15,000	Wiener et al. (2003)
Soemmering's gazelle	*Gazella Soemmerring*	14,000	East (1999)
Mountain gazelle	*Gazella gazella*	12,000	Nowak (1999)
Indian gazelle	*Gazella bennetti*	10,000	Nowak (1999)
Nilgai	*Boselaphus tragocamelus*	10,000	Nowak (1999)
Tibetan gazelle	*Procapra picticaudata*	10,000	Nowak (1999)
West Caucasian tur	*Capra caucasica*	10,000	Nowak (1999)
Mouflon	*Ovis aries*	7,500	IUCN (2008)
Beira	*Dorcatragus megalotis*	7,000	East (1999)
Four-horned antelope	*Tetracerus quadricornis*	5,500	Nowak (1999)
Markhor	*Capra falconeri*	5,200	Nowak (1999)
Jentink's duiker	*Cephalophus jentinki*	3,500	East (1999)
Water buffalo	*Bubalus bubalis*	3,500	Nowak (1999)
Abbott's duiker	*Cephalophus spadix*	2,500	East (1999)
Dama gazelle	*Gazella dama*	2,500	East (1999)
Dibatag	*Ammodorcas clarkei*	2,500	East (1999)
Mountain nyala	*Tragelaphus buxtoni*	2,500	East (1999)
European wild goat	*Capra hircus*	2,335	IUCN (2008)
Nilgiri tahr	*Hemitragus hylocrius*	2,200	Nowak (1999)

	Nilgiri tahr	*Hemitragus jayakari*	2,000	Nowak (1999)
	Wisent	*Bison bonasus*	1,800	IUCN (2008)
	Zanzibar duiker	*Cephalophus adersi*	1,400	East (1999)
	Banteng	*Bos javanicus*	1,000	Nowak (1999)
	Gaur	*Bos gaurus*	1,000	Nowak (1999)
	hirola	*Betragus hunteri*	1,000	East (1999)
	Slender-horned gazelle	*Gazella leptoceros*	1,000	East (1999)
	Cuvier's gazelle	*Gazella cuvieri*	560	Nowak (1999)
	Arabian oryx	*leucoryx*	500	Nowak (1999)
	Walia ibex	*Walia ibex*	400	Nowak (1999)
	Addax	*Addax nasomaculatus*	350	East (1999)
	Saola	*Pseudoryx nghetinhensis*	350	Nowak (1999)
	Tamaraw	*Anoa mindorensis*	350	Nowak (1999)
	Przewalskii's gazelle	*Procapra przewalskii*	200	Nowak (1999)
	Scimitar-horned oryx	*Oryx dammah*	200	Nowak (1999)
		total for Bovidae	29,119,715	
Cervidae	Roe deer	*Capreolus capreolus*	15,000,000	IUCN (2008)
	White-tailed deer	*Odocoileus virginianus*	14,000,000	Nowak (1999)
	Mule deer	*Odocoileus hemionus*	5,500,000	Nowak (1999)
	Caribou	*Rangifer tarandus*	4,421,500	Ulvevadet and Klokov (2004)
	Moose	*Alces alces*	1,500,000	IUCN (2008)
	Elk/red deer	*Cervus elaphus*	1,000,000	Nowak (1999)
	Siberian roe deer	*Capreolus pygargus*	1,000,000	Nowak (1999)
	Wapiti	*Cervus canadensis*	782,500	Nowak (1999)
	Reeves muntjac	*Muntiacus reevesi*	650,000	Nowak (1999)
	Tufted deer	*Elaphodus cephalophus*	500,000	Nowak (1999)
	red muntjac	*Muntiacus muntjac*	145,000	Nowak (1999)
	White-lipped deer	*Cervus albirostris*	75,000	Nowak (1999)
	Black muntjac	*Muntiacus crinifrons*	10,000	Nowak (1999)
	Javan rusa	*Cervus timorensis*	10,000	Whitehead (1971)
	Water deer	*Hydropotes inermis*	10,000	Nowak (1999)
	Marsh deer	*Blastoceros dichotomus*	7,000	Nowak (1999)
	Sika deer	*Cervus nippon*	5,935	Ohtaisha and Gao (1990)
	Barasingha	*Cervus duvaucelii*	3,565	Nowak (1999)

	Eld's deer	*Cervus eldi*	2,619	Nowak (1999)
	Pampas deer	*Ozotoceros bezoarticus*	1,500	Nowak (1999)
	Chilean huemel	*Hippocamelus bisulcus*	1,300	Nowak (1999)
	Peruvian huemal	*Hippocamelus antisensis*	1,300	Nowak (1999)
	Calamian deer	*Axis calamianensis*	550	Nowak (1999)
	Bawean deer	*Axis kuhli*	300	Nowak (1999)
	Fallow deer	*Dama dama*	140	Nowak (1999)
	Père David's deer	*Elaphurus davidianus*	100	Ohtaisha and Gao (1990)
		total for Cervidae	44,628,309	
Giraffi-dae	Giraffe	*Giraffa camelopardalis*	141,000	East (1999)
	Okapi	*Okapia johnstoni*	10,000	East (1999)
		total for Giraffidae	151,000	
Moschi-dae	Alpine muskdeer	*Moschus sifanicus*	150,000	Zhou et al. (2004)
	Black muskdeer	*Moschus fuscus*	100,000	Zhou et al. (2004)
	Himalayan musk deer	*Moschus leucogaster*	20,000	Zhou et al. (2004)
	Siberian muskdeer	*Moschus moschiferus*	10,000	Zhou et al. (2004)
		total for Moschidae	280,000	
Traguli-dae	Water chevrotain	*Hyemoschus aquaticus*	278,000	East (1999)
		total for Tragulidae	278,000	
		grand total for wild ruminants	75,332,024	

Table 1.3. Native distribution of species (% of total within family) across continents and habitat and climate types[1]

	Continent[2,3]				Habitat			Climate		
family	EA	AF	NA	SA	forest	ecotone	open	warm	temperate	cold
	----------% of total within family----------									
Antilo-capridae	0	0	100	0	0	0	100	0	100	0
Bovidae	28.4	67.6	4.9	0	25.4	32.4	42.2	74.5	16.7	8.8
Cervidae	63.3	0[4]	13.3	30.0	50.0	30.0	20.0	46.7	46.7	6.7
Giraffidae	0	100	0	0	50.0	50.0	0	100	0	0
Moschidae	100	0	0	0	0	100	0	0	0	100
Tragulidae	75.0	25.0	0	0	100	0	0	100	0	0
total	37.6	51.1	7.1	6.4	32.6	31.9	35.5	68.8	22.0	9.2

[1]Data from van Wieren (1996)

[2]EA = Eurasia, AF = Africa, NA = North America, SA = South America

[3]Percentages for continent may not sum to 100 within family because some species may be located on multiple continents.

[4]Does not include species which have a limited range in Africa.

Table 1.4. Body mass of wild ruminant species by family[1]

	Body mass (kg)		
Family	Median	Min	Max
Antilocapridae	40	40	40
Bovidae	52.5	2	800
Cervidae	47.5	6	550
Giraffidae	475	250	700
Moschidae	11.5	11	12
Tragulidae	2	2	8
total	45	2	800

[1]Data from van Wieren (1996)

Table 1.5. Dietary preferences of species (% of total within family), according to their assignment as browser (BR), intermediate feeder (IM), or grazer (GR)[1]

	Feeding class		
Family	BR	IM	GR
	----------% of total species within family----------		
Antilocapridae	100	0	0
Bovidae	35.3	26.5	39.2
Cervidae	46.7	36.7	16.7
Giraffidae	100	0	0
Moschidae	100	0	0
Tragulidae	100	0	0
total	41.1	31.9	27.0

[1]Data from van Wieren (1996)

Table 1.6. Domesticated ruminant species and details of their domestication[1]

		Details of domestication		
Species	Wild ancestors	date	region	initial reason
Goat (*Capra hircus*)	Benzoar goat (*C. aegagrus*), markhor (*C. falconeri*)	10,000 B.C.	Near East	meat
Sheep (*Ovis aries)*	Mouflon (*O. musimon*), Marco Polo sheep (*O. ammon*), Urial (*O. vignei*)	7,000-8,000 B.C.	Near East	meat
European cattle (*Bos taurus*)	European auroch (*B. primigenius primigenius*)	>6,200 B.C.	Near East	sacrifice, barter
Zebu cattle (*Bos indicus*)	Indian auroch (*B. p. namadicus*)	>2,500 B.C.	SW Asia, India	sacrifice, barter
Water buffalo (*Bubalus bubalis*)	Wild water buffalo subspecies (*B. b. bubalis*, *B. b. carabanesis*)	>2,500 BC	S China, Indo-China	draft, milk
Mithan (*Bos frontalis*)	Gaur (*B. gaurus*)	2,500 BC	India, SE Asia	sacrifice, barter
Reindeer (*Rangifer tarandus*)	Caribou (*R. tarandus*)	<1st millennium A.D.	N Europe, Asia	meat, draft, transportation, milk
Yak (*Bos mutus*)	Wild yak (*B. grunniens*)	unknown	The Himalayas and nearby ranges	pack, meat, milk
Bali cattle (*Bos javanicus*)	Banteng (*B. javanicus*)	unknown	Borneo and islands of SE Asia	draft, meat

[1]Data from Clutton-Brock (1999), except domestication date for goat (from Zeder and Hesse [2000]) and wild ancestors of goat, sheep, European cattle, Zebu cattle, and water buffalo (from Bruford et al. [2002]).

Table 1.7. Characteristics of domestic species, including population size, BW, and feeding class

Species	Population size[1]	BW[2]	Feeding class[3,4]
	millions		
Goat (*Capra hircus*)	850	35	IM
Sheep (*Ovis aries)*	1,113	50	IM/GR
European and zebu cattle (*Bos taurus, Bos indicus*)[5]	1,390	600	GR
Water buffalo (*Bubalus bubalis*)	202	400	GR
Mithan (*Bos frontalis*)	NA	800	GR
Reindeer (*Rangifer tarandus*)	2	140	IM
Yak (*Bos mutus*)	14	700	GR
Bali cattle (*Bos javanicus*)	4	700	GR
total	3,574		

[1]Data for goat, sheep, cattle, and water buffalo from FAO (2008a); for reindeer from Ulvevadet and Klokov (2004); for yak from Wiener et al. (2003) and for Bali cattle from FAO (2008b)

[2]Data for sheep, cattle, and goats are from typical literature studies (those summarized in Tables 5 and 6 of Clauss et al., [2005]); for water buffalo from Popenoe (1981); for yak from Wiener et al. (2003); and for all other species from van Wieren (1996), taking BW of wild ancestors.

[3]IM = intermediate feeder, GR = grazer

[4]Data for goat, cattle, and water buffalo from Hoffman (1989); for sheep from Hoffman (1989) and Pfister and Malechek (1986); and for all other species from van Wieren (1996), taking feeding class of wild ancestors.

[5]Figures for European and Zebu cattle are presented together because separate data are generally not available for these species.

Figure 1.1. A greater Malay chevrotain (*Tragulus napu*), a member of the family Tragulidae and one of the most primitive ruminants. Note small size (approximately 3 kg), short limbs, and absence of horns, all of which are characteristic of early ruminants. Enlarged upper canines are absent because this specimen is a female. Photo courtesy of Dr. Ellen S. Dierenfeld.

Image removed for electronic publication because copyright permission could not be obtained. Reader is referred to Figure 3 of source (Colbert, 1941) for original image.

Figure 1.2. A member of the family Moschidae, probably Alpine musk deer (*Moschus chrysogaster*). Note large upper canines and absence of horns. Reproduced from Wemmer (1998).

Image removed for electronic publication because copyright permission could not be obtained. Reader is referred to Figure 3 of source (Colbert, 1941) for original image.

Figure 1.3. Restoration of *Archaeomeryx optatus*, one of the earliest ruminants. *Archaeomeryx* belonged to the Hypertragulidae, but aspects of its appearance (small size, short front legs, absence of horns) are representative of other early ruminant families (Tragulidae, Leptomerycidae). Reproduced from Colbert (1941).

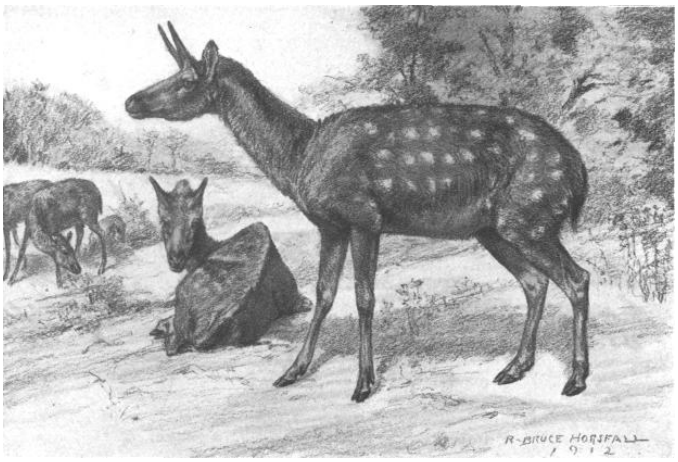

Figure 1.4. Restoration of *Dromomeryx borealis* (from Scott 1913). *Dromomeryx* belonged to the Dromomerycidae, but its size and giraffe-like horns are also characteristic of Palaeomerycidae. Reproduced from Scott (1913).

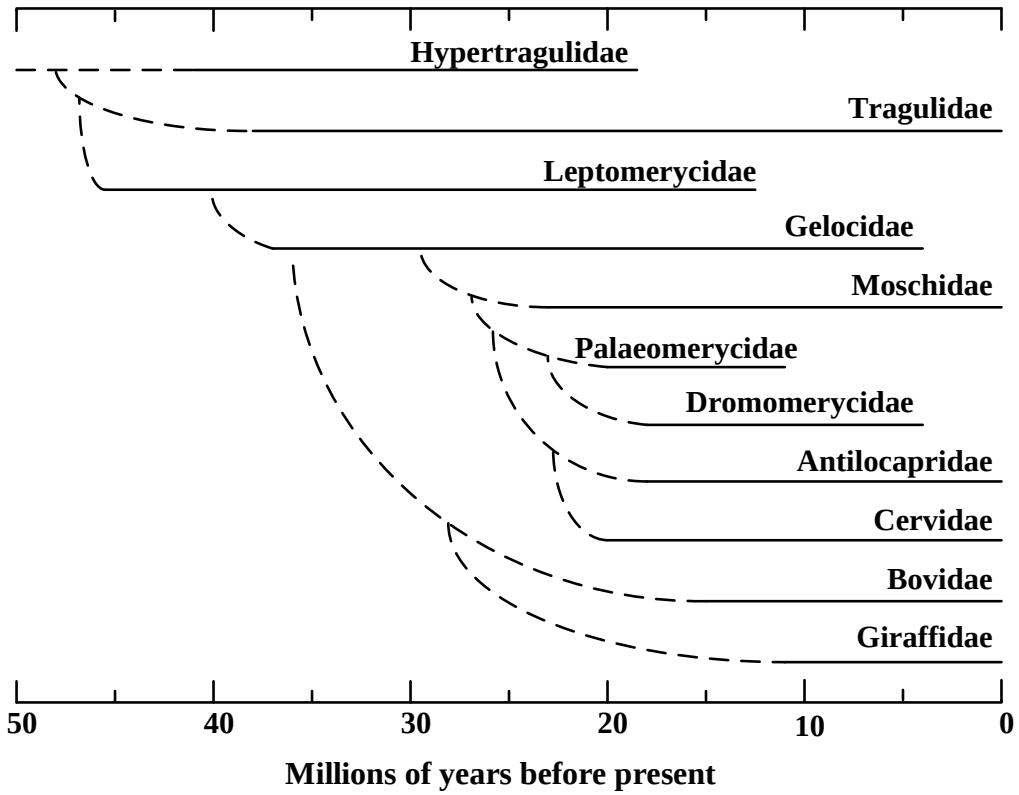

Figure 1.5. A phylogeny of ruminant families. Families included are the Hypertragulidae, Tragulidae, Leptomerycidae, Gelocidae, Moschidae, Dromomerycidae, Palaeomerycidae, Antilocapridae, Giraffidae, Cervidae, and Bovidae—i.e., those recognized by Carroll (1988). Solid lines indicate age ranges documented in the fossil record (adapted from Métais et al. [2001] for Tragulidae; Webb [1998] and Gentry [2000] for Gelocidae; and Gentry [2000] for all other families, assuming *Archaeomeryx* belongs to Leptomerycidae [Webb and Taylor 1980]); stippled lines indicate inferred age ranges and family relationships (adapted from Gentry [2000]).

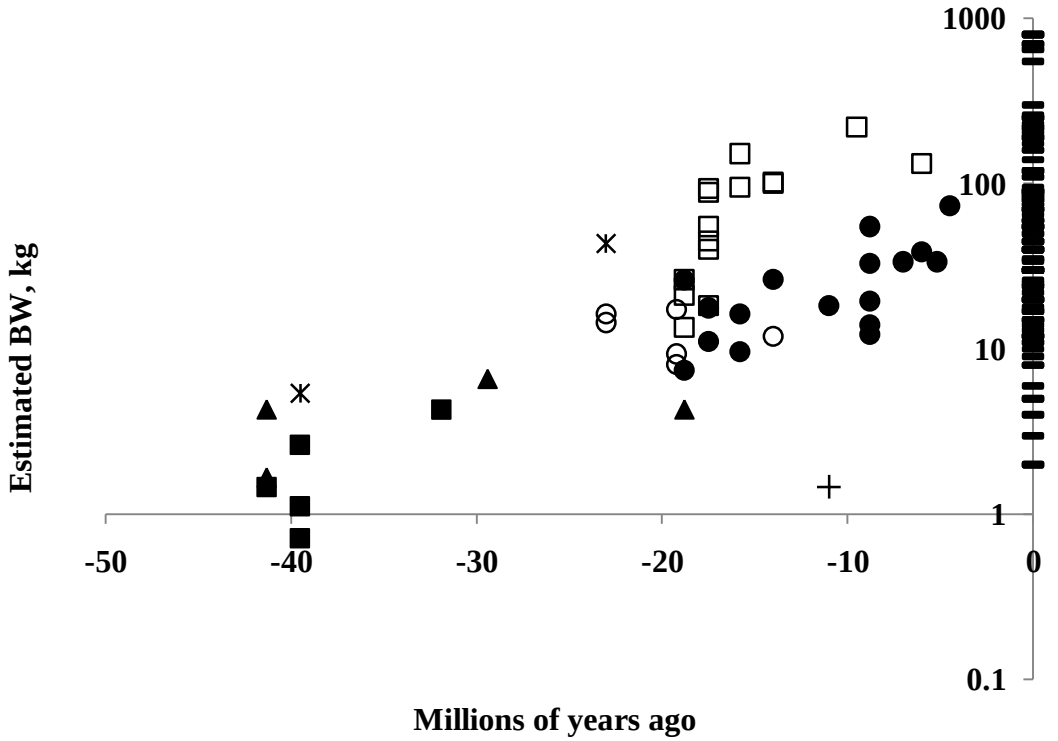

Figure 1.6. Increase in BW of ruminants over evolutionary time (millions of years), as shown in fossil record of the North American Tertiary (2 to 65 million years ago). Each point represents the appearance date of a single genus within the Hypertragulidae (■), Leptomerycidae (▲), Antilocapridae (●), Dromomerycidae (□), Moschidae (○), Gelocidae (+), or an indeterminate hornless ruminant family (*). Masses were estimated from lengths of fossilized molars. For comparison, BW of all extant ruminant species (-) are included. Note plot is semi-logarithmic for BW. Chapter 6 describes the methodology used in constructing this figure in more detail.

CHAPTER 2

COMPARING RFV TO DEGRADATION PARAMETERS OF GRASS AND LEGUME FORAGES

ABSTRACT

Relative feed value (RFV) was evaluated relative to in situ degradation parameters of grass and legume forages. Early-cut alfalfa (n = 20), late-cut alfalfa (n = 26), cool season grass (n = 11), warm season grass (n = 4), and grass/legume (n = 20) samples were collected from duplicate hay bales submitted to the 2002 and 2003 MO State Fair Hay Contests. Sub-samples were incubated in the rumen of 2 lactating Holstein cows for 0, 6 or 8, 12, 24, and 48 h to determine in situ degradation of DM, ADF, NDF, CP, and hemicellulose over time. Degradation data were fit to a variety of candidate models to estimate degradation parameters. Correlation coefficients were determined between degradation parameter estimates (sorted according to forage [early-cut alfalfa, late-cut alfalfa, grass/legume, grass]) and RFV. For further comparison, correlations between NDF degradation parameter estimates and digestible DMI were determined with data from a previous study. Degradation data were best fit to a single, gamma 2-distributed pool model without a lag phase. Relative feed value was significantly correlated ($P <$ 0.05) to potentially digestible DM and CP for early-cut alfalfa, potentially digestible DM for late-cut alfalfa, and potentially digestible DM, NDF, and hemicellulose for grass/legume. The percentage of significant correlations (10.7%) across the entire dataset

was low and no correlations were significant for grass. Relative feed value did not account for variation in degradation parameters, especially for grasses. A further correlation analysis, which compared digestible DMI with degradation parameter estimates reported by another dataset, revealed that digestible DMI and degradation parameter estimates were related for grass but not alfalfa forages. These results suggest that RFV is limited by its failure to include degradation parameters.

INTRODUCTION

Numerous systems have been developed to predict quality of forages fed to ruminants (Moore, 1994). Relative feed value (**RFV**; Rohweder et al., 1978) is the most widely employed. Relative feed value grades forages according to their predicted digestible DMI (**DDMI**), the product of DMI and percentage digestible DM (**DDM**). Predicted DDMI is divided by a base DDMI to establish an index with a typical full bloom legume hay scoring 100. To parameterize the RFV system, the National Forage Testing Association selected equations that relate forage NDF and ADF to DMI and DDM, with a base DDMI of 1.29% (Linn and Martin, 1989).

Despite the extensive use of the RFV system parameterized according to the National Forage Testing Association recommendations, RFV has been criticized. In their summary, Moore and Undersander (2002) demonstrated NDF and ADF are inconsistent and poor predictors of DDMI. Sanson and Kercher (1996) found that RFV prediction equations accounted for less than 1% of total variation in DDMI for 20 alfalfa hays fed to lambs.

Whereas RFV's poor performance has been identified statistically, further work needs to ascertain the underlying biological reasons for this performance. One area that deserves attention is degradation characteristics. Degradation characteristics, such as degradation rate and extent, are linked to DMI and DDM (Mertens, 1973), the two factors on which RFV is based. Many studies have measured degradation characteristics but only for a limited number of forages or chemical fractions. Furthermore, degradation characteristics have rarely been collected to evaluate RFV; only Canbolat et al. (2006) has done so, finding variable correlations between in vitro gas production characteristics and RFV for 1 alfalfa sample collected over 3 maturities.

To further evaluate RFV, this study was designed to determine degradation characteristics of legume and grass hays that are representative of those graded by the RFV system.

MATERIALS AND METHODS

Hay Types and Sampling Procedures

Hay samples were obtained from entries submitted to the Missouri State Fair Hay Contest in 2002 and 2003. The entries came from across the state of Missouri and included early-cut alfalfa (**ECA**), late-cut alfalfa (**LCA**), cool season grass (**CSG**), warm season grass (**WSG**), and grass/legume (**GL**) samples. A detailed description of the forages, including number of samples collected by year of harvest, class, variety, and cutting within year is reported in Table 2.1.

Each entry was submitted as duplicate hay bales. Each bale was cored with a hay probe (Penn State Forage Sampler; Nasco, Ft. Atkinson, CO), and the core samples of

duplicate bales were combined to give a representative sample of each entry. Samples were ground in a Wiley mill (Arthur H. Thomas Company, Philadelphia, PA) to pass through a 2-mm screen. Ground samples were placed in sealed plastic bags and stored at room temperature for further analysis.

In Situ and Chemical Analysis

In situ degradation characteristics were determined for all samples. The samples were analyzed over 3 different 2-d time periods, two 2-d periods for 2002 samples and one 2-d period for 2003 samples (as discussed below). Air-dry dacron bags (10 x 20 cm; 50 ± 15μm pore size; ANKOM Technology, Macedon, NY) were filled with 5 ± 0.1 g of air-dry sample for 2002 hay samples and 4 ± 0.1 g of sample for 2003 hay samples; sample mass to surface area ratio was approximately 12.5 $mg \cdot cm^{-2}$ and 10 $mg \cdot cm^{-2}$ for 2002 and 2003 samples, respectively, which are within those suggested by Nocek (1988). Duplicate bags were prepared for insertion into 2 cows, giving a total of 4 bags per sample at each incubation time. Bags were heat sealed (AIE-200; American International Electric, Wittier, CA), secured to plastic cable ties, and tied in bundles to nylon retrieval cords according to their incubation time.

Two ruminally cannulated, multiparous Holstein cows housed in free-stall facilities at the University of Missouri-Columbia Foremost Dairy Center were selected for in situ procedures. All procedures involving the animals were approved by the Animal Care and Use Committee, University of Missouri-Columbia. Each animal was provided ad libitum access to a standard lactation diet. The diet was a corn silage, alfalfa hay, alfalfa haylage-based diet (240 g corn silage, 123 g alfalfa hay, 150 g alfalfa

haylage, 467 g concentrate and 190 g CP, 240 g ADF and 410 g NDF·kg DM^{-1}) fed as a total mixed ration. Bags were inserted into the ventral rumen of the cows in reverse order. Incubation times chosen were 0, 8, 12, 24, and 48 h for 2002 hay samples (for original run; see below) and 0, 6, 12, 24, and 48h for 2003 hay samples. All samples within year (2002 or 2003) were to be incubated during a single 2-d period, giving two 2-d periods total. However, one of the cows used to incubate the 2002 samples stopped ruminating during the 2-d period sampling period, and the samples from this cow for that period were discarded. New subsamples of the 2002 hay samples were incubated in this cow for an additional 2-d period, with incubation times of 0, 6, 12, 24, and 48 h. Samples from 2003 were incubated during a single 2-d period as originally planned, giving a total of three 2-d periods during which the forages were incubated. A standard forage was not used to correct for differences between runs because all samples within a cow·period were incubated in one run, and any systematic differences between cow·periods could be detected by comparing degradation parameter values across cow·periods with an ANOVA (see below). During all runs, 0h bags were exposed to rumen fluid briefly (approximately 5 min) to allow hydration. All bags were removed simultaneously, as suggested by Nocek (1988).

After removal from the rumen, the bags were doused with cold (approximately 15°C) water to halt fermentation and were rinsed until the wash water ran relatively clear. Bags were then washed in a domestic washing machine until the wash water ran completely clear, as suggested by Cherney et al. (1990b). Samples were airdried in a 55°C convection oven to a constant mass and then were completely dried in a 105°C

oven. Bags were then air-equilibrated and weighed to determine their residue mass. Residues were then removed, composited by duplicates within cow, and stored at <0°C for further analysis.

Bag residue and original forage samples were ground with a Wiley mill to pass through a 1-mm screen. All material was subsequently analyzed for DM by drying at 105°C for 24 h; NDF and ADF using an ANKOM^{200} Fiber Analyzer (ANKOM Technology); and total N by combustion analysis (LECO FP-428; LECO Corporation, St. Joseph, MI). Hemicellulose (**HEM**) was calculated by difference between NDF and ADF. No assay to determine microbial contamination was made; previous work where bags were washed in a similar manner reported negligible microbial contamination of residues (Coblentz et al., 1997).

Calculations and Statistical Analysis

All degradation data were expressed as fractional disappearance ($g \cdot g^{-1}$). Using a variant of an equation from Weisbjerg et al. (1990; as cited by Stensig et al., 1994), NDF, HEM, and ADF degradation data at each incubation time were corrected for insoluble material washed from the bag. Because NDF, ADF, and HEM are insoluble entities, it was assumed that the truly soluble fraction, *W*, was 0, and so the equation of Weisbjerg et al., (1990) was simplified and applied as follows:

$$K(t_i) = M(t_i) - P(1 - \frac{M(t_i) - P}{1 - P})$$

where $K(t_i)$ = corrected degradation at time t_i ($g \cdot g^{-1}$), $M(t_i)$ = measured (uncorrected) degradation at time t_i ($g \cdot g^{-1}$), and P = insoluble fraction washed from 0h bag (total fraction washed from 0h bag; $g \cdot g^{-1}$).

A method was developed to eliminate aberrant bag observations, which might be caused by undetected bag rupture or other errors. Whereas such observations can be identified and eliminated using conventional statistical methods (e.g., studentized residuals and Cook's distance [Kaps and Lamberson, 2004]), such methods require the data to be fit to a pre-determined model. However, because several models were under consideration, conventional methods could not be applied, and an alternative method for removing outliers was formulated. Bag observations that satisfied any one of the following conditions were considered for removal, as described below:

(1) Those whose disappearance values were 20% greater than the mean disappearance value of the next incubation time of the same cow;

(2) Those whose disappearance values were 20% less than the mean disappearance value of the prior incubation time of the same cow;

(3) Those which created >15% replicate error relative to duplicate bag at the same incubation time and cow.

Condition 1 is based on the premise that degradation increases monotonically; those that fulfill condition 1 violate that premise. For illustration, Figure 2.1A shows a 6 h bag observation from a 2002 GL sample that fulfilled condition 1 and was removed. If a bag observation had an aberrantly low disappearance value, it could cause the bag at the next incubation time to fulfill condition 1, even if the bag at the next incubation time was not aberrant. For this reason, condition 2 was enacted to identify such bags with aberrantly low disappearance values and prevent non-aberrant bags from being removed. Figure 2.1B shows a 12 h bag observation from a 2002 CSG sample that fulfilled condition 2

and was removed. Condition 3 was designed to remove bag observations that failed to fulfill conditions 1 and 2 yet were still grossly aberrant; most duplicate bag pairs repeated well (median replicate error was 2.4% after removing bags that fulfilled conditions 1 and 2), and a large replicate error (>15%) indicated that 1 of 2 bags in a duplicate pair was aberrant. If condition 3 was fulfilled by a duplicate bag pair, the aberrant bag of the pair was identified visually as an outlier from the degradation curve and removed. Though a subjective selection, the offending bag of the duplicate pair was usually identified easily; Figure 2.1C illustrates an example where a bag from a poorly replicated (16.55% replicate error) 48 h bag pair (2002 LCA sample) was identified as aberrant because its disappearance (0.990 $g \cdot g^{-1}$) was abnormally high, both absolutely and relative to the asymptotic disappearance value suggested by observations prior to 48 h.

However, for some 0 h bags, the aberrant bag could not be identified because disappearance values of both bags were reasonable based on the behavior of the degradation curve >6 h; Figure 2.2 gives an example of a 0 h bag pair from which an aberrant bag could not be identified for removal despite poor repeatability (30.56% replicate error) of disappearance values within the pair. In this case, no correction could be made, and both bag observations were retained.

Models based on the gamma distribution (Pond et al., 1988; Ellis et al., 1994; Ellis et al., 2005) were considered for describing the in situ degradation data. Due to the limited number of incubation times, only single pool models reported in Table 2.2 could be considered. The G1 and G1L models are equivalent to the commonly used first-order kinetics models of Ørskov and McDonald (1979) and McDonald (1981), respectively,

and were considered with less frequently used age-dependent G2, G2L, G3, and G3L models.

The PROC NLIN procedure of SAS (SAS Institute, Inc., Cary, NC) was used to estimate parameters in the models for DM, NDF, ADF, HEM, and CP degradation data. Parameters estimated include the age-dependent degradation rate, λ_d (h^{-1}); fraction degraded at $t = 0$, a ($g \cdot g^{-1}$); potential extent of degradation, $(a + b)$ ($g \cdot g^{-1}$); fraction not degraded at $t = 0$ that is potentially degradable, b ($g \cdot g^{-1}$); and discrete lag time before onset of degradation, τ (h).

Note that most degradation rates reported in the literature are age-independent rates—that is, refer to specific degradation rates (g substrate degraded · g total substrate^{-1} · h^{-1}) that remain constant over time. The specific degradation rate associated with λ_d (an age-dependent rate) increases asymptotically to λ_d (Pond et al., 1988; Ellis et al., 1994). For this reason, comparison between age-independent rates reported by most literature and the age-dependent rate λ_d is not commensurate and leads to the finding that age-dependent rates are greater than age-independent ones. To allow more commensurate comparison, the mean degradation rate of λ_d , k, was calculated as $0.59635 \cdot \lambda_d$ (Pond et al., 1988). This mean rate is the specific degradation rate associated with λ_d averaged over time. It is effectively an age-independent equivalent of an age-dependent rate and can be compared to age-independent rates commonly reported in the literature.

Because NDF, ADF, and HEM degradation data had been corrected to make disappearance 0 at $t = 0$, the value of a was constrained to 0 for fitting procedures for

these fractions. For all fractions, the value of ($a + b$) was bounded between 0 and 1 $g \cdot g^{-1}$, the theoretical limits of degradation.

Using the criteria for eliminating aberrant bag observations, nearly all NDF, ADF, and HEM bag observations had to be eliminated for one 2003 ECA sample. So few bag observations were left after this elimination that NDF, ADF, and HEM degradation data could not be fit to a model for this forage sample.

At first, degradation data of each cow were kept separate for the fitting procedure. However, after a preliminary ANOVA indicated that degradation parameter values did not consistently differ across cow·periods, cow·period data were pooled by year of forage (2002 or 2003), entailing that data of 2 cows (n = 2, 2002 and n = 2, 2003) were used to construct each degradation curve. The results of model fit using this pooled data set were employed in all subsequent statistical analysis.

Models were evaluated using residual sums of squares ($\mathbf{SS_{RES}}$), residual mean square ($\mathbf{MS_{RES}}$), and Akaike information criterion (**AIC**) values for DM, CP, and NDF degradation data. The model with the lowest numerical value for each test was considered best (Kaps and Lamberson, 2004).

Relative feed value and forage degradation parameter estimates (λ_d, k, a, b, and $[a + b]$) were sorted according to forage class (ECA, LCA, grass, or GL). The PROC CORR procedure of SAS was used to determine correlation coefficients between RFV and degradation parameter estimates. Correlations with $P < 0.05$ were considered significant.

Comparison with Data of Mertens (1973)

For comparison, correlations between RFV, NDF degradation parameters, and DDMI reported by Mertens (1973) were determined. Data for 15 grass (11 CSG and 4 WSG) and 15 alfalfa forages were selected to create a dataset with similar forage varieties and chemical composition (mean and SD) as the forage populations examined in this study. Cutting of alfalfa was not reported by Mertens (1973), and thus alfalfa samples were pooled under a common alfalfa class. A GL class was not examined because only 4 GL samples were appropriate for correlation analysis; the other 8 GL samples in Mertens (1973) included birdsfoot trefoil, which was not examined in this study. Digestible DM intake was reported for sheep or cattle or both; if DDMI was reported for both animals, then average DDMI was calculated and used.

Mertens (1973) fit degradation data to a model similar to the G1L model (Table 2.2), which includes degradation parameters k_d and τ but not λ_d. The parameter λ_d was estimated from mean lifetime (Ellis et al., 2005), which is related to k_d , τ ,and n as follows:

$$mean\ lifetime = n/(\lambda_d / 100) = 1/(k_d / 100) + \tau$$

and hence

$$\lambda_d = n \cdot k_d /(1 + k_d /100 \cdot \tau)$$

where n = order of the gamma distribution associated with λ_d.

Relative feed value, DDMI, and forage degradation parameter estimates, (λ_d, k_d, a, b, $[a + b]$, and τ), were sorted according to forage class (alfalfa or grass). The PROC

CORR procedure of SAS was used to determine correlation coefficients between RFV and degradation parameters. Correlations with $P < 0.05$ were considered significant.

RESULTS AND DISCUSSION

Chemical Composition

The chemical composition and RFV of the forages is reported in Table 2.3. The mean and SD of the chemical composition data were generally similar to those summarized by the Dairy NRC (2001), indicating a representative range of forages were included in this study. However, WSG generally had lower NDF, ADF, and HEM as well as greater CP than bermudagrass reported in the NRC (2001). Warm season grasses in this study were generally of better quality than those summarized by the NRC. This difference is related to contestants of MO State Fair Hay Contest submitting only higher quality WSG.

Model Selection

Table 2.4 illustrates values of SS_{RES}, MS_{RES}, and AIC values obtained when fitting G1, G1L, G2, G2L, G3, and G3L models to DM, CP, and NDF degradation data of all forages. These values were used as criteria for model fit, with lower values for a given model indicating better fit (Kaps and Lamberson, 2004). On this basis, models (G1, G1L, G2, G2L, G3, and G3L) were assigned a rank of model fit (1 to 6, where 1 indicates best fit and 6 the worst) relative to other models within each chemical fraction (DM, CP, and NDF). Table 2.5 reports the mean and range of these rankings across fractions (DM, CP, and NDF).

Across chemical fractions, values of SS_{RES} are lowest for the G1L model, and values of SS_{RES} were lower for lagged (G1L, GL2, GL3) models than their non-lagged counterparts (G1, G2, G3; Table 2.4). As such, the G1L model was ranked best and lagged models ranked better than non-lagged according to the SS_{RES} criterion (Table 2.5). However, the use of SS_{RES} as a model selection criterion is not commensurate in this case because SS_{RES} decreases with increasing parameters, and the lagged models contain 1 more parameter than the non-lagged models.

As the ratio of SS_{RES} to error degrees of freedom, MS_{RES} accounts for the number of parameters in the model and is a more appropriate selection criterion than SS_{RES} where the number of parameters varies across models, as is in the case in the present study. However, MS_{RES} still tends to decrease with increasing number of parameters (Kaps and Lamberson, 2004), and thus one risks bias towards selection of larger models when employing MS_{RES} as a selection criterion. The expression for AIC ($n \log [SS_{RES} / n] + 2p$, where n = number of observations and p = number of parameters) penalizes for excessive parameters in a given model to avoid such biased selection, and, for this reason, AIC is the most preferable model selection criterion in this study.

Values of both MS_{RES} and AIC were lowest for the G2 models and, with the exception of the MS_{RES} for the G1 model, were lower for non-lagged (G1, G2, G3) models than their lagged counterparts (G1L, G2L, G3L; Table 2.4). Consequently, the G2 model was ranked best and non-lagged models ranked better than their lagged counterparts. These results indicate the G2 model is optimal. They also suggest that the

decrease in total error (SS_{RES}) by the inclusion of a lag term is not justified by the addition of a model parameter in so doing.

The above discussion refers to mean SS_{RES}, MS_{RES}, and AIC values and rankings. Values of SS_{RES}, MS_{RES}, and AIC values differed by chemical fraction and so did the rankings in some cases (Tables 4 and 5). Still, the rankings based on AIC, the most preferred criterion, showed unequivocally that the G2 model was best, as it was ranked 1 across all chemical fractions.

Difference in performance among models may be understood by considering model shapes. Figure 2.3 shows the fit of G2 vs. G1 (A), G1L (B), and G3 (C) models to DM disappearance data of a 2003 LCA sample (where the 2 observations at each incubation time represent mean values from each of the 2 cows) to illustrate these shapes. The G2 and other age-dependent models represent degradation as following a sigmoidal curve, with an increasingly more protracted sigmoidal shape as the order increases from G2 to G*N* (where *N* represents the order of the model; see Figure 2.3C; Pond et al., 1988; and Ellis et al., 1994). The G1 model, by contrast, represents degradation as an abrupt first-order decay process lacking the smooth sigmoidal shape of the age-dependent models (Figure 2.3A). A lag phase is often added to the G1 model, yielding the G1L model (Figure 2.3B), because degradation does not begin instantaneously but rather shows a phase of slow degradation at early time points followed by more rapid degradation later (see Figure 2.3 of Van Milgen et al., 1991); this lag phase may also be added to the age-dependent models, as done in this study for comparative purposes, as discussed below.

In this study, the sigmoidal shape of the G2 model appears to accommodate the transition between these slow and fast degradation phases better than a G1 model, as indicated by better fit to degradation data between 6 to 12 h (Figure 2.3A) and the lower error (SS_{RES}) for the G2 model relative to the G1 model. A similar analysis suggests that the G3 model (and higher order models) appears to possess too protracted of a sigmoidal shape to properly model degradation data (Figure 2.3C).

Though the addition of a lag phase in the G1L model decreased total error (SS_{RES}) relative to the G1 model, it did not improve fit to match the parsimony of the G2 model, as indicated by lower values of MS_{RES} and AIC for the G2 model. Figure 2.3B shows a typical example where error of the G1L model fit ($SS_{RES} = 8.29 \cdot 10^{-2}$) is indeed lower than that of the G2 model ($SS_{RES} = 8.36 \cdot 10^{-2}$) but is so marginal the increased complexity of the G1L model (where model complexity is measured in terms of number of parameters) is not justified. The addition of a lag term in the G2L and G3L models did not appreciably lower total error relative to non-lagged counterparts and caused MS_{RES} and AIC values to rise; the sigmoidal shape of the age-dependent curves already represented the transition between slow and fast degradation phases, and thus the addition of a lag phase was redundant and reduced parsimony. Often, as in the case of the LCA sample shown in Figure 2.3, the estimated value of the lag phase for G2L and G3L models was 0 h, yielding a model shape identical those of the G2 and G3 models and demonstrating that the lag term was an superfluous addition.

The conclusion that a two-compartmental model such as the G2 model performs better than the G1L agrees with Van Milgen et al. (1991). This report along with Ellis et

al. (2005) suggest that multi-compartmental age-dependent models often perform better than the oft-used G1 and G1L models and should be considered in future in situ and in vitro degradation experiments.

Influence of Incubation Times on Model Selection and Parameter Estimates

To maximize the number of forages that could be analyzed, the number of degradation observations was limited to only five (0, 6 or 8, 12, 24, and 48h), with relatively few observations at early and late time points. Some may suggest including more early degradation observations would have led to better performance of lagged vs. non-lagged models, particularly when considering the first non-0h observation (6 or 8h) falls beyond most values of lag phase (typical values ranging from 1 to 6 h; Mertens, 1973; von Keyserlink et al., 1996). If there indeed exists a discrete lag phase before onset of degradation, as represented by the lagged models, the omission of early degradation observations would have artificially improved fit of non-lagged models. However, if degradation follows a more sigmoidal response as represented by the G2 and G3 models, fit of lagged models would have been artificially improved. Thus, the limited number of observations at early incubation times makes the selection of the G2 more uncertain but does not inherently support that the G1L or other lagged model is more appropriate. For the present purposes, the statistical procedures identify the G2 model as the best for use with this dataset, and thus all degradation parameter estimates presented hereon pertain to the G2 model.

Conversely, the terminal observation is less than the time required to approach asymptotic degradation (approximately 24 to 60h for high and 48 to 72h for poor-quality

forages; Ørskov et al., 1980). Asymptotic degradation was probably not approached by the 48h terminal observation for some samples, particularly for the poorer-quality WSG. At first consideration, the use of a 48h terminal observation may seem to greatly underestimate ($a + b$), the estimate of asymptotic degradation, but note that ($a + b$) was not measured as the value of the 48h terminal observation but was rather estimated during the model fitting procedure. Using nonlinear regression to estimate ($a + b$), in comparison to employing a log-linear transformation, decreases the sensitivity of ($a + b$) to the value of the terminal observation and appears to report more realistic values of ($a + b$) when terminal observations of 48h or less are used (Van Milgen et al., 1991).

The G1 and G1L models estimated the value of ($a + b$) as 1 $g \cdot g^{-1}$, the upper bound set during fitting procedures for 16 and 4 of the 402 total degradation curves, respectively; these represent a small number of instances where ($a + b$) was clearly overestimated, despite the use of non-linear regression. These cases of overestimation may be due more to poor model fit than the relatively early terminal incubation time per se; as Figure 2.3A shows, the G1 model (and G1L model to a lesser extent) was often forced to overestimate degradation values of later incubation times in order to better fit the sigmoidal shape of the degradation profile at early time points, which led to overestimation of ($a + b$) in some cases. The G2 and other higher-order models did not appear to display this overestimating property (c.f., Figures 3A,B,C) and did not reach the 1 $g \cdot g^{-1}$ bound of ($a + b$) in any case. Because the G2 model was ultimately adopted to estimate all degradation parameters, because non-linear regression has been shown to deliver more realistic estimates of ($a + b$; Van Milgen et al., 1991), and because values of

(a + b) are similar to those in published reports (Mertens, 1973; Brown and Pitman, 1991; von Keyserlingk et al., 1996), one may infer overall that *(a + b)* was underestimated minimally if at all by using a 48 h terminal incubation.

Degradation Parameter Estimate Means

Table 2.6 reports means of degradation parameter estimates λ_d, *k*, *a*, *b*, and *(a + b)* using the G2 model. These means, with the exception of $\lambda_{d,}$ (see below), are similar to those presented by other reports (Smith et al., 1971; Mertens, 1973; von Keyserlingk, 1996), indicating they are suitable for the subsequent correlation analysis comparing degradation parameter estimates with RFV. As discussed in Materials and Methods, values of λ_d generated in this study are numerically greater than degradation rate values reported by other investigators because λ_d is a rate-dependent degradation rate whereas most degradation rates reported in the literature are age-independent rates. For commensurate comparison between degradation rates in this and prior studies, the mean degradation rate *k* should be used for reference (Materials and Methods).

Correlation between RFV and Degradation Parameter Values

Results of the correlation analysis between degradation parameter estimates and RFV scores are listed in Table 2.7. Six of the 56, or 10.7%, of tested correlations were significant. This percentage only slightly exceeds that which is expected by random chance (5%) due to incidence of type I error with $\alpha = 0.05$. Furthermore, no correlations were significant for grasses. Correlations were thus poor overall. Statistically, this is likely because the relationship between NDF degradation characteristics and NDF concentration is fair to poor: with 275 legume and CSG forages, Mertens (1973) found

the correlation coefficient between NDF and NDF degradation rate, extent, and lag to be 0.59, -0.28, and 0.22, respectively. Because RFV is essentially a reexpression of NDF (Weiss, 2002), only fair to poor correlations would be expected between RFV and degradation characteristics. Biological reasons for this poor relationship are discussed in the Shortcomings of the Conceptual Structure of RFV section below.

Despite the general lack of correlations, a few patterns were observed in the correlation analysis. The parameter $DM_{(a+b)}$, the potential extent of degradation of DM ($g \cdot g^{-1}$), was consistently significant with RFV scores of ECA, LCA, and GL. The value of the correlation coefficient, *r*, for these correlations and all significant correlations was always positive. Though it is not apparent why $DM_{(a+b)}$ alone was consistently significant with RFV, the positive values of *r* for this and other correlations indicate that RFV accounts for the correct, positive relationship between degradation parameter values and RFV scores.

Whereas a few patterns were observed in the correlation analysis, it must be emphasized that degradation parameter values were poorly correlated to RFV overall. Given that degradation parameters are often linked to DMI and DDM (Mertens, 1973), the factors on which RFV is based, it may be concluded tentatively that RFV is inadequate because of weak correlations between it and degradation parameters.

Assumption in Correlation Analysis

This tentative conclusion rests on an assumption that degradation characteristics are related to DDMI. Because RFV is an index of DDMI, the most direct evaluation of RFV would involve a comparison between DDMI and RFV. Still, if degradation

characteristics are related to DDMI, as assumed, RFV can be compared to degradation characteristics as if it is being directly compared to DDMI. The assumption is supported by the observation that DMI, DDM, and degradation parameters are related (Mertens, 1973). Still, it has not been tested directly because it has not been shown whether a simple linear relationship exists between DDMI and degradation values for an extensive forage dataset.

Comparison with Data of Mertens (1973)

To test this assumption directly, the data of Mertens (1973) were used to determine the correlation between NDF degradation parameters and in vivo DDMI, which were reported for a wide range and number of grass and alfalfa forages. Table 2.8 reports correlations found between DDMI and NDF degradation parameter values reported by Mertens (1973). Correlations between DDMI and NDF degradation parameters were consistently significant for grass; correlations involving k_d, λ_d, and τ were all significant ($P < 0.001$, $P < 0.001$, and $P = 0.048$, respectively), and the correlation involving b showed a statistical trend ($P = 0.065$; data not shown). Curiously, NDF_b alone was significantly correlated with DDMI for alfalfa. These findings support that DDMI is linearly related to degradation parameters of grass but not alfalfa, and thus our assumption that degradation characteristics are related to DDMI was not supported for alfalfa.

Because degradation parameter values were not strongly correlated with DDMI for alfalfa, one might infer that correlations measured in this study cannot be used to demonstrate RFV is inadequate for alfalfa. However, there are several limitations in the

analysis with the data of Mertens (1973) that should caution the drawing of this inference. First, cutting time of alfalfa could not be considered because it was not reported by Mertens (1973). Because alfalfa degradation parameter values differ by cutting time (Hackmann, T.J., Sampson, J.D., and Spain, J.N., unpublished data), the relationships between degradation parameter values, DDMI, and RFV may differ by cutting time, as well. Hence, examining these relationships as they pertain to a general alfalfa class only, as done in the analysis involving the dataset of Mertens (1973), ignores potential differences between ECA and LCA that may significantly impact the correlation results. For example, degradation parameter values and DDMI were poorly correlated for the alfalfa class from Mertens (1973), but it is possible that stronger correlations exist for ECA and LCA when each cutting is considered separately, and these stronger correlations were simply masked in the analysis of Mertens (1973) by pooling cutting times. The analysis is also limited because degradation parameters of non-NDF chemical fractions could not be considered, as the necessary data were lacking in Mertens (1973). As such, the conclusions drawn from the analysis involving Merten's data do not necessarily apply to specific cuttings times of alfalfa or to non-NDF degradation parameter values.

Shortcomings of the Conceptual Structure of RFV

Noting the limitations in the analysis involving the dataset of Mertens (1973), and considering other studies that find RFV inadequate (Sanson and Kercher, 1996; Moore and Undersander, 2002; Weiss, 2002), the findings of this study suggest RFV may be limited by its poor relationship with degradation parameter values. Because degradation

parameters are related to DMI and DDM (Mertens, 1973), the lack of relationship between RFV and degradation parameters potentially limits the accuracy of RFV equations.

The lack of a relationship between degradation parameters and RFV indicates a pivotal, but not isolated, shortcoming in the conceptual structure of RFV. Relative feed value is a simple empirical prediction system which fundamentally relies on linear equations to predict DMI from NDF and DDM from ADF. It does not explicitly include terms for degradation parameters or any other factors.

In representing DMI and DDM as functions of NDF and ADF alone, RFV does not explicitly consider plant-related factors that impact DMI and DDM. A multitude of non-mutually exclusive plant-related factors affect DMI and DDM, including forage species, growth conditions (soil type, fertilization, climate), maturity, cutting date, morphology (proportion of leaf and stem), physical properties (density, resistance to breakdown), disease, and processing method (chopping, pelleting; Van Soest et al., 1978; Minson, 1990; Van Soest, 1994). At least in some cases, these factors may change DMI and DDM independently of NDF and ADF concentrations, contrary to the conceptual structure of RFV. For example, Cherney et al. (1990a) found that intake and DDM of twelve grass hays by sheep changed with plant morphology—intake increased with increasing proportion of leaf blade, and intake and DDM decreased with increasing proportion of stem—despite similar concentrations of NDF (658 ± 7 g·kg DM^{-1}; mean ± SEM) and ADF (289 ± 8 g·kg DM^{-1}) across the hays.

Note that most plant-related factors not accounted by RFV affect degradation characteristics (forage species, growth conditions, maturity, cutting date, morphology; review by Mertens, 1993). We suggest that variation in degradation characteristics may capture some variation in plant-related factors that affect DMI and DDM, such that incorporation of degradation characteristics in a forage quality prediction system may improve prediction accuracy of specific forage classes and cuttings. Incorporating degradation parameters into a forage quality prediction system is unlikely to account for all factors influencing forage quality, such as animal-related factors that interact with forage quality (Minson, 1990), but it is a suitable first step in improving forage quality prediction systems.

Whether such a forage quality system should employ an empirical approach (such as RFV) or a more mechanistic approach (*sensu* Baldwin, 1995) is subject to results of future study. If incorporating degradation characteristics into a forage quality prediction system shows further promise, it must be determined how degradation characteristics should be estimated or measured, for conventional in situ/in vitro procedures are too laborious for routine analysis.

Table 2.1. Description of hays used for in situ analysis

Year	Class[1]	n	Variety
2002	ECA	15	alfalfa 2nd cutting
	LCA	16	alfalfa 3rd cutting
	CSG	4	brome 1st cutting
			orchard 1st cutting (n=1)
			timothy 1st cutting (n=1)
			canary grass 2nd cutting (n=1)
	WSG	1	unspecified 1st cutting
	GL	16	alfalfa/orchardgrass 2nd cutting (n=4)
			alfalfa/canary grass 2nd cutting (n=2)
			alfalfa/orchardgrass 3rd cutting (n=2)
			alfalfa/timothy 2nd cutting (n=1)
			alfalfa/bromegrass 2nd cutting (n=1)
			alfalfa/unspecified grass 1st cutting (n=1)
			alfalfa/unspecified grass 2nd cutting (n=1)
			alfalfa/unspecified grass 3rd cutting (n=1)
			red clover/fescue 2nd cutting (n=1)
			red clover/timothy 1st cutting (n=1)
			unspecified grass/legume 2nd cutting (n=1)
2003	ECA	5	alfalfa 2nd cutting
	LCA	10	alfalfa 3rd cutting
	CSG	7	orchardgrass 2nd cutting (n=2)
			brome/orchardgrass 1st cutting (n=1)
			orchardgrass 1st cutting (n=1)
			orchardgrass hay 2nd cutting (n=1)
			reed canary grass 2nd cutting (n=1)
			rye grass hay 3rd cutting (n=1)
	WSG	3	bermudagrass hay 2nd cutting (n=2)
			bermudagrass hay 3rd cutting (n=1)
	GL	4	alfalfa/orchardgrass hay 3rd cutting (n=2)
			alfalfa/timothy hay 1st cutting (n=1)
			unspecified grass/legume 2nd cutting (n=1)

[1]ECA = early cutting alfalfa, LCA = late cutting alfalfa, CSG = cool season grass, WSG = warm season grass, GL = grass/legume mix

Table 2.2. Degradation models considered for describing in situ data

Model	Description	Equation[1]
G1	single, gamma 1-distributed pool model without lag phase	$Y(t) = a + b \cdot (1-e^{-kd \cdot t})$
G1L	single, gamma 1-distributed pool model with lag phase	$Y(t) = a + b \cdot [1-e^{-kd \cdot (t-\tau)}]$
G2	single, gamma 2-distributed pool model without lag phase	$Y(t) = a + b \cdot [1-e^{-\lambda d \cdot t} \cdot (1+\lambda_d \cdot t)]$
G2L	single, gamma 2-distributed pool model with lag phase	$Y(t) = a + b \cdot [1-e^{-\lambda d \cdot (t-\tau)} \cdot (1+\lambda_d \cdot [t-\tau])]$
G3	single, gamma 3-distributed pool model without lag phase	$Y(t) = a + b \cdot [1-e^{-\lambda d \cdot t} \cdot (1+\lambda_d \cdot t+[\lambda_d \cdot t]^2/2)]$
G3L	single, gamma 3-distributed pool model with lag phase	$Y(t) = a + b \cdot [1-e^{-\lambda d \cdot (t-\tau)} \cdot (1+\lambda_d \cdot [t-\tau]+[\lambda_d \cdot (t-\tau)]^2/2)]$

[1] $Y(t)$ = disappearance ($g \cdot g^{-1}$), t = time (h), τ = discrete lag time before onset of degradation (h), k_d, λ_d = degradation rate (h^{-1}), a = fraction degraded at $t = 0$ ($g \cdot g^{-1}$), $(a + b)$ = potential extent of degradation ($g \cdot g^{-1}$), b = fraction not degraded at $t = 0$ that is potentially degradable ($g \cdot g^{-1}$)

Table 2.3. Chemical composition and RFV[1] of forages

	n	Mean	Minimum	Maximum	SD
		----------g·kg DM^{-1}----------			
ECA					
DM	20	870	842	896	14
NDF	20	431	329	502	45
ADF	20	304	218	369	45
HEM[3]	20	127	95	184	28
CP	20	208	150	293	38
RFV	20	143	119	203	23
LCA					
DM	26	859	825	880	15
NDF	26	384	268	463	51
ADF	26	265	195	354	43
HEM[3]	26	119	66	185	37
CP	26	222	194	260	20
RFV	26	169	125	254	30
CSG					
DM	11	876	867	892	7
NDF	11	658	452	772	81
ADF	11	338	299	380	28
HEM[3]	11	320	123	392	73
CP	11	123	60	174	33
WSG					
DM	4	867	845	886	17
NDF	4	623	395	732	155
ADF	4	266	233	343	52
HEM[3]	4	357	155	484	154
CP	4	180	104	233	54
RFV	11	90	71.5	130	15
GL					
DM	20	868	819	890	18
NDF	20	453	355	613	52
ADF	20	304	241	384	36
HEM[3]	20	149	101	272	41
CP	20	204	124	308	40
RFV	20	136	95	184	20

[1]RFV = relative feed value
[2]ECA = early cutting alfalfa, LCA = late cutting alfalfa, CSG = cool season grass, WSG = warm season grass, GL = grass/legume mix
[3]HEM = hemicellulose

Table 2.4. Values of model selection criteria (SS_{RES}, MS_{RES}, and AIC) obtained when fitting DM, CP, and NDF degradation data to models

	Model[1,2]					
Item[3]	G1	G1L	G2	G2L	G3	G3L
SS_{RES}[4,5]						
DM	1.80	1.61	1.57	1.43	1.67	1.32
CP	4.41	3.50	3.96	3.82	4.15	3.69
NDF	7.31	6.20	6.79	6.22	6.95	6.93
mean	4.41	3.77	4.11	3.82	4.26	3.98
MS_{RES}[4,6]						
DM	2.58	2.69	2.25	2.38	2.38	2.19
CP	5.88	5.83	5.66	6.36	5.93	6.15
NDF	9.13	8.86	8.49	8.89	8.69	9.91
mean	5.87	5.79	5.46	5.88	5.67	6.08
AIC[4]						
DM	-8.21	-6.99	-8.54	-6.97	-8.46	-7.06
CP	-6.40	-4.90	-6.57	-4.74	-6.51	-4.79
NDF	-7.28	-5.74	-7.50	-5.78	-7.44	-5.45
mean	-7.30	-5.88	-7.54	-5.83	-7.47	-5.77

[1]G1= single, gamma 1-distributed pool model without lag phase, G1L= single, gamma 1-distributed pool model with lag phase, G2 = single, gamma 2-distributed pool model without lag phase, G2L = single, gamma 2-distributed pool model with lag phase, G3 = single, gamma 3-distributed pool model without lag phase, G3L = single, gamma 3-distributed pool model with lag phase

[2]See Table 2.2 for model equations.

[3]SS_{RES}= residual sums of squares, MS_{RES}=residual mean square, AIC = Akaike information criterion

[4]Values of SS_{RES}, MS_{RES}, and AIC by chemical fractions (DM, CP, and NDF), and the mean value across chemical fractions

[5]Values listed are actual values$\cdot 10^2$

[6]Values listed are actual values$\cdot 10^3$

Table 2.5. Relative ranking (1-6) of degradation models according to average values of model selection criteria (SS_{RES}, MS_{RES}, and AIC)[1]

	Model[2]					
Item[3,4]	G1	G1L	G2	G2L	G3	G3L
SS_{RES} rank						
mean	5.67	2.00	3.33	2.33	5.33	2.33
range	5-6	1-4	3-4	2-3	5-6	1-4
MS_{RES} rank						
mean	4.33	3.67	1.33	4.67	3.00	4.00
range	3-5	2-6	1-2	4-6	2-4	1-6
AIC rank						
mean	3.67	4.33	1.00	5.33	2.00	4.67
range	3-5	3-5	1	4-6	2	4-6

[1]See Table 2.2 for model equations.
[2]G1 = single, gamma 1-distributed pool model without lag phase, G1L = single, gamma 1-distributed pool model with lag phase, G2 = single, gamma 2-distributed pool model without lag phase, G2L = single, gamma 2-distributed pool model with lag phase, G3=single, gamma 3-distributed pool model without lag phase, G3L = single, gamma 3-distributed pool model with lag phase
[3]SS_{RES} = residual sums of squares, MS_{RES} = residual mean square, AIC = Akaike information criterion
[4]Mean and range ranks refer to rankings across fractions (DM, CP, and NDF).

Table 2.6. Degradation parameter estimates of forages by forage class and chemical fraction

	Chemical fraction[1]									
	DM		NDF		ADF		HEM[1]		CP	
Item[2,3,4]	mean	SEM	mean	SEM	mean	SEM	mean	SEM	mean	SEM
ECA (n=20)[5]										
λ_d, h^{-1}	0·198	0·008	0·155	0·012	0·147	0·014	0·208	0·019	0·231	0·010
k, h^{-1}	0·118	0·005	0·093	0·007	0·088	0·008	0·124	0·011	0·138	0·006
a, $g \cdot g^{-1}$	0·341	0·023	-----	-----	-----	-----	-----	-----	0·412	0·030
b, $g \cdot g^{-1}$	0·419	0·021	0·554	0·019	0·535	0·018	0·626	0·026	0·483	0·027
$(a+b)$, $g \cdot g^{-1}$	0·760	0·011	0·554	0·019	0·535	0·018	0·626	0·026	0·894	0·009
LCA (n=26)										
λ_d, h^{-1}	0·229	0·008	0·173	0·009	0·154	0·010	0·234	0·017	0·263	0·008
k, h^{-1}	0·136	0·005	0·103	0·005	0·092	0·006	0·140	0·010	0·157	0·005
a, $g \cdot g^{-1}$	0·387	0·022	-----	-----	-----	-----	-----	-----	0·442	0·025
b, $g \cdot g^{-1}$	0·407	0·018	0·537	0·016	0·514	0·015	0·584	0·025	0·481	0·022
$(a+b)$, $g \cdot g^{-1}$	0·794	0·008	0·537	0·016	0·514	0·015	0·584	0·025	0·924	0·005
CSG (n=11)										
λ_d, h^{-1}	0·109	0·007	0·098	0·005	0·098	0·006	0·104	0·011	0·130	0·010
k, h^{-1}	0·065	0·004	0·058	0·003	0·058	0·004	0·062	0·007	0·078	0·006
a, $g \cdot g^{-1}$	0·246	0·018	-----	-----	-----	-----	-----	-----	0·341	0·037
b, $g \cdot g^{-1}$	0·451	0·020	0·583	0·026	0·589	0·032	0·576	0·035	0·507	0·032
$(a+b)$, $g \cdot g^{-1}$	0·697	0·018	0·583	0·026	0·589	0·032	0·576	0·035	0·848	0·035
WSG (n=4)										
λ_d, h^{-1}	0·093	0·022	0·071	0·003	0·058	0·006	0·071	0·019	0·091	0·009
k, h^{-1}	0·056	0·013	0·043	0·002	0·035	0·004	0·042	0·011	0·054	0·005
a, $g \cdot g^{-1}$	0·250	0·016	-----	-----	-----	-----	-----	-----	0·359	0·068
b, $g \cdot g^{-1}$	0·421	0·018	0·567	0·017	0·535	0·029	0·515	0·039	0·424	0·055
$(a+b)$, $g \cdot g^{-1}$	0·670	0·008	0·567	0·017	0·535	0·029	0·515	0·039	0·783	0·016

GL (n=20)										
λ_d, h^{-1}	0·181	0·012	0·102	0·008	0·131	0·010	0·081	0·027	0·226	0·012
k, h^{-1}	0·108	0·007	0·061	0·005	0·078	0·006	0·048	0·016	0·135	0·007
a, $g \cdot g^{-1}$	0·311	0·020	-----	-----	-----	-----	-----	-----	0·394	0·025
b, $g \cdot g^{-1}$	0·452	0·021	0·420	0·017	0·564	0·021	0·435	0·019	0·493	0·025
$(a+b)$, $g \cdot g^{-1}$	0·763	0·008	0·420	0·017	0·564	0·021	0·435	0·019	0·887	0·008

[1]HEM = hemicellulose

[2]ECA = early cutting alfalfa, LCA = late cutting alfalfa, CSG = cool season grass, WSG = warm season grass, GL = grass/legume mix

[3]k, λ_d = degradation rate, a = fraction degraded at $t = 0$, $(a + b)$ = potential extent of degradation, b = fraction not degraded at $t = 0$ that is potentially degradable

[4]$k = 0.59635 \cdot \lambda_d$

[5]Value of n for DM and CP. Value of n for NDF, ADF, and HEM is 19 because NDF, ADF, and HEM degradation data of 1 sample could not be fit to a degradation model (see Materials and Methods).

Table 2.7. Significant correlations between degradation parameter estimates of forages and RFV

Item[1,2]	*r*	*P*
ECA		
$DM_{(a + b)}$	0.82	< 0.001
$CP_{(a + b)}$	0.56	< 0.01
LCA		
$DM_{(a + b)}$	0.69	< 0.001
GL		
$DM_{(a + b)}$	0.74	<0.001
NDF_b	0.52	0.02
HEM_b	0.56	0.01

[1]ECA = early cutting alfalfa, LCA = late cutting alfalfa, CSG = cool season grass, WSG = warm season grass, GL = grass/legume mixture

[2]$DM_{(a + b)}$ = potential extent of degradation of DM ($g \cdot g^{-1}$), NDF_b = NDF not degraded at $t = 0$ that is potentially degradable ($g \cdot g^{-1}$), HEM_b = hemicellulose not degraded at $t = 0$ that is potentially degradable ($g \cdot g^{-1}$)

Table 2.8. Significant correlations between NDF degradation parameters and DDMI for a subsample of alfalfa (n = 15) and grass (n = 15) forages in data of Mertens (1973)

Item[1]	*r*	*P*
Alfalfa		
b	0.83	<0.001
Grass		
k_d	0.87	< 0.001
λ_d	0.92	<0.001
τ	-0.52	0.048

[1]*b* = NDF not degraded at *t* = 0 that is potentially degradable (g/g); k_d, λ_d = degradation rate (h^{-1}); τ = discrete lag time before onset of degradation (h)

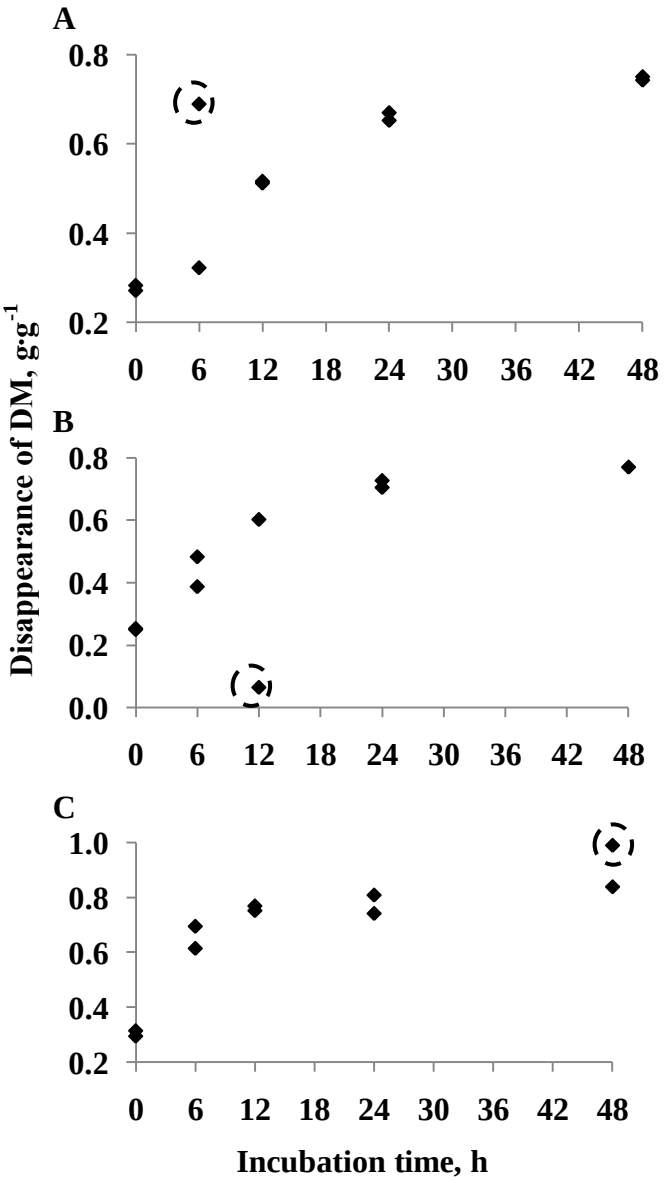

Figure 2.1. Examples of bag observations that were identified as aberrant and removed because they fulfilled one of the three conditions for bag removal described in Materials and Methods. Each of the 2 points at each incubation time represents one bag observation. (A) A 6 h bag observation (circled) from a 2002 GL sample removed because it fulfilled condition 1; its disappearance value was 34.1% greater than the mean disappearance of the 12 h bag observations (B) A 12 h observation (circled) from a 2002 CSG removed because it fulfilled condition 2; its disappearance value was 85.1% lower than the mean disappearance of the 6 h bag observations. (C) A 48 h observation (circled) from a 2002 LCA bag pair that fulfilled condition 3; the replicate error was 16.6%. The circled observation was judged to be the aberrant one of the pair because its disappearance was abnormally high (0.990 $g \cdot g^{-1}$), both absolutely and relative to the asymptotic disappearance value suggested by observations prior to 48 h.

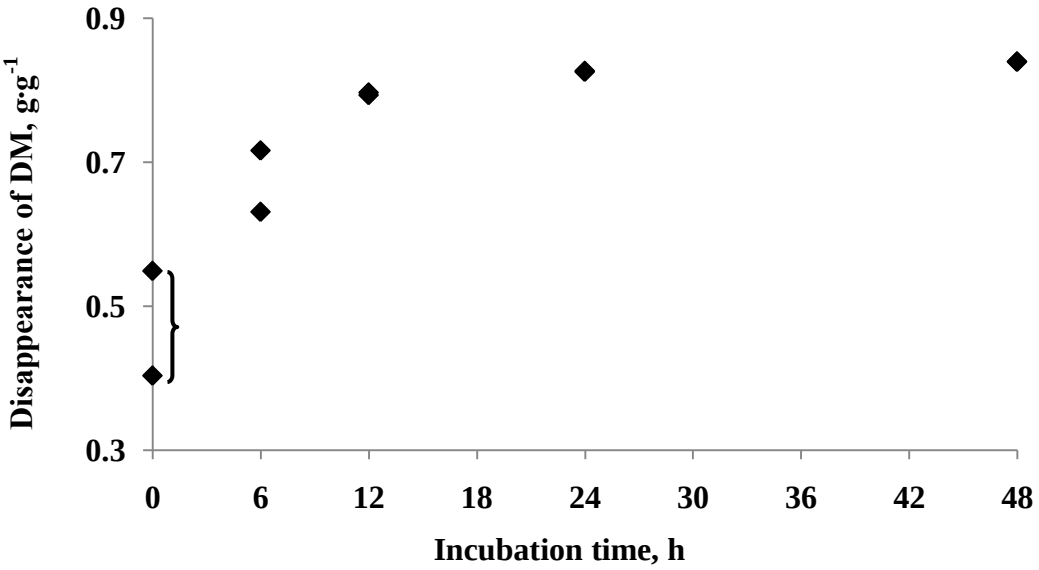

Figure 2.2. An example of a 0 h bag pair that fulfilled condition 3 of the criteria for bag removal (see Materials and Methods) but from which the aberrant bag of the pair could not be identified for removal. The 0 h observations (bracketed for emphasis) had poor repeatability (30.56% replicate error), but disappearance values of both observations were reasonable according to behavior of the curve after 6 h, and thus neither bag could be identified as aberrant and removed.

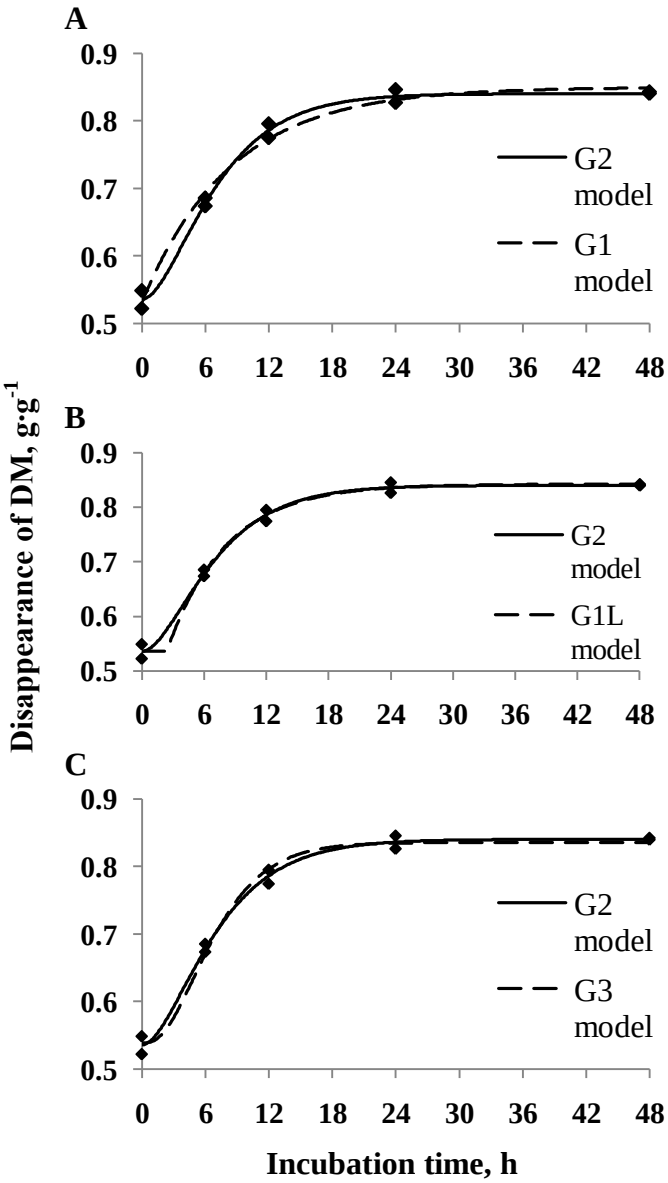

Figure 2.3. Fit of (A) single, gamma 2-distributed pool model without lag phase (G2) vs. single, gamma 3-distributed pool model without lag phase (G3), (B) G2 vs. single, gamma 1-distributed pool model without lag phase (G1), and (C) G2 vs. single, gamma 1-distributed pool model with lag phase (G1L) to observed DM disappearance data ($g \cdot g^{-1}$; ♦) of one 2003 late-cut alfalfa (LCA) sample. The 2 observations at each incubation time represent mean values from each of the 2 cows. See Table 2.2 for model equations.

CHAPTER 3

VARIABILITY IN RUMINAL DEGRADATION PARAMETERS CAUSES IMPRECISION IN ESTIMATED RUMINAL DIGESTIBILITY

ABSTRACT

Ruminal digestibility of dietary ingredients is frequently estimated with degradation parameters. Mean degradation parameters (e.g., those in a feed library) are often used, but limited data suggests considerable variation around these means, potentially leading to imprecise digestibility estimates. This experiment quantified degradation parameter variation for forage hays and determined this variation's impact on precision of ruminal digestibility estimates. Degradation data were those previously published by our lab and included degradation rate, λ_d (h^{-1}), fraction instantly degraded, a ($g \cdot g^{-1}$), degradation extent, $(a + b)$ ($g \cdot g^{-1}$), and fraction not instantly degraded that is degradable, b ($g \cdot g^{-1}$) of alfalfa, grass, grass-legume hays. Ruminal digestibilities of chemical fractions (DM, NDF, ADF, hemicellulose, CP) were estimated using these data. Ninety-five percent confidence limits of digestibility were determined using propagation of uncertainty with measured SD of degradation parameters. Values of CV for degradation parameters were large; averaged across chemical fractions, they were 24.8, 28.6, 20.7, and 12.6% for λ_d, a, b, and $(a + b)$. Ninety-five percent confidence limits of digestibility were large (80.5% of digestibility means) and often overlapped each other, even where digestibility means greatly differed numerically. Consequently, digestibility values computed with mean degradation parameters may have little biological and practical significance. When

uncertainty in all parameters but λ_d was set to zero (λ_d alone had uncertainty), 95% confidence limits still encompassed 54.5% of digestibility means. Thus, uncertainty in λ_d alone causes considerable imprecision in estimated digestibility. These results caution using mean degradation parameters to estimate digestibility.

INTRODUCTION

Grass and legume forages are key components of ruminant diets. Quality of these forages and of other components of ruminant diets is largely influenced by their digestibility (Minson, 1990), making a measure of digestibility useful in diet formulation. Because measurement of digestibility in vivo is laborious and requires large amounts of forage, digestibility is frequently estimated. Many current feed evaluation systems (e.g., Cornell Net Carbohydrate and Protein System [Sniffen et al., 1992]; Molly [Baldwin, 1995]; Beef NRC (2000); Dairy NRC [2001]) use ruminal degradation parameters (such as rate and extent of digestion) to estimate ruminal digestibility, which in turn is used with estimated post-ruminal digestion to calculate total tract digestibility. These feeding systems use simple averages of degradation parameters, such as those compiled in a feed library, to estimate ruminal digestibility. However, a limited number of sources suggest considerable variability exists for these mean values for forages and other feeds (von Keyserlingk et al., 1996; NRC, 2001; Hvelplund and Weisbjerg, 2000). This variability raises questions about the precision of using simple averages to calculate digestibility. More work needs to determine the actual variability in degradation parameters of forages and to ascertain whether use of average values is valid.

The objectives of this study were to (1) determine the variability in ruminal degradation parameters within and across hay forages, and (2) assess the impact of this variability on the precision of digestibility calculations.

MATERIALS AND METHODS

Hay Types and Sampling Procedures

Hay samples were obtained from entries submitted to the Missouri State Fair Hay Contest in 2002 and 2003. The entries came from across the state of Missouri and included early-cut alfalfa (ECA; n = 20), late-cut alfalfa (**LCA**; n = 26), cool season grass (**CSG**; n = 11), warm season grass (**WSG**; n = 4), and grass-legume (**GL**; n = 20) samples. A detailed description of the species composition of the forages has been reported in Chapter 2. Samples were collected from hay bales using a hay probe (Penn State Forage Sampler; Nasco, Ft. Atkinson, CO), ground through a 2 mm screen with a Wiley mill (Arthur H. Thomas Company, Philadelphia, PA), and stored in sealed plastic bags at room temperature for further analysis.

In Situ and Chemical Analysis

In situ degradation characteristics were determined for all samples. Dacron bags (10 x 20 cm; 50 ± 15μm pore size; ANKOM Technology, Macedon, NY) were filled with 5 ± 0·1 g (2003 samples) or 4 ± 0.1 g (2002 samples) of sample. Duplicate bags were prepared for insertion into two cows, giving a total of four bags per sample at each incubation time.

Two ruminally cannulated, multiparous Holstein cows housed in free-stall facilities at the University of Missouri-Columbia Foremost Dairy Center were selected for in situ procedures. All procedures involving the animals were approved by the

Animal Care and Use Committee, University of Missouri-Columbia. Each animal was provided ad libitum access to a lactation diet (240 g corn silage, 123 g alfalfa hay, 150 g alfalfa haylage, 467 g concentrate and190 g CP, 240 g ADF and 410 g NDF/kg DM) formulated to meet their requirements (NRC, 2001). Bags containing 2003 hay samples were inserted into 2 cows for 0, 6, 12, 24, and 48 h during one 2-d period. Bags containing 2002 hay samples were inserted into 2 cows for 0, 8, 12, 24, and 48 h during another 2-d period. However, one of the cows used to incubate 2002 samples stopped ruminating during the sampling period, and the samples from this cow for that period were discarded. New subsamples of the 2002 hay samples were incubated in this cow for an additional 2-d period, with incubation times of 0, 6, 12, 24, and 48 h. Zero hour bags were exposed to rumen fluid briefly (approximately 5 min) to allow hydration. All bags were removed simultaneously, as suggested by Nocek (1988).

After removal from the rumen, bags were doused with cold water (approximately 15°C) to halt fermentation and were rinsed until wash water ran relatively clear. Bags were stored at <0°C to await further processing. Once removed from storage, bags were thawed to room temperature and washed in a domestic washing machine until the wash water ran completely clear, as suggested by Cherney et al. (1990b). Samples were air-dried in a 55°C convection oven to a constant mass, then air-equilibrated and weighed to determine residue mass. Residues were then removed and composited by duplicates within cow. Bag residue and original forage samples were ground to pass through a 1-mm screen and subsequently analyzed for DM, NDF, ADF, HEM, and CP as described in Chapter 2.

Calculations and Statistical Analysis of In Situ Data

All degradation data were expressed as fractional disappearance. Using an equation from Weisbjerg et al. (1990) (cited by Stensig et al. [1994]), NDF, HEM, and ADF degradation data at each incubation time were corrected for insoluble material washed out of the bag. Since NDF, ADF, and HEM are insoluble entities, it was assumed that the truly soluble fraction was zero when applying the equation.

Aberrant bag observations were identified and eliminated using a method reported in Chapter 2. Using the criteria for eliminating aberrant bag observations, nearly all NDF, ADF, and HEM bag observations had to be eliminated for one 2003 ECA sample. So few bag observations were left after this elimination that NDF, ADF, and HEM degradation data could not be fit to a model for this forage sample.

In situ data were described using a single, gamma 2-distributed pool model without lag phase (G2) model from Pond et al. (1988) and Ellis et al. (1994) as follows:

$$Y(t) = a + b \cdot [1 - \exp(-\lambda_d \cdot t) \cdot (1 + \lambda_d \cdot t)]$$

where $Y(t)$ is fractional disappearance ($g \cdot g^{-1}$), λ_d is degradation rate (h^{-1}), a is fraction degraded at $t = 0$ ($g \cdot g^{-1}$), $(a + b)$ is potential extent of degradation ($g \cdot g^{-1}$), b is fraction not degraded at $t = 0$ that is potentially degradable ($g \cdot g^{-1}$), and t is time (h). The age-dependent, G2 model was chosen over oft-used age-independent models (Ørskov and McDonald, 1979) because the G2 model yielded lower values of Akaike information criterion relative to age-independent models, indicating the G2 model provided fit superior to that of first-order kinetic models for this dataset (see Chapter 2).

The PROC NLIN procedure of SAS (SAS Institute, Inc., Cary, NC) was used to estimate parameters in the models for DM, NDF, ADF, HEM, and CP degradation data.

Because NDF, ADF, and HEM degradation data had been corrected to make disappearance zero at $t = 0$, the value of a was constrained to zero for fitting procedures for these fractions.

Most degradation rates reported in the literature are age-independent whereas λ_d is an age-dependent rate (Pond et al., 1988; Ellis et al., 1994). Comparison between an age-independent rate, k_d (h^{-1}), and the age-dependent rate λ_d is not commensurate; an age-independent rate is less than an age-dependent one when describing the same degradation data. To allow more commensurate comparison, the mean degradation rate of λ_d , k, was calculated as $0.5964 \cdot \lambda_d$ (Pond et al., 1988). This mean rate is effectively an age-independent equivalent of an age-dependent rate and can be compared to age-independent rates commonly reported in the literature.

At first, degradation data of each cow were kept separate for the fitting procedure. However, after a preliminary ANOVA indicated that degradation parameter values did not consistently differ across cow·periods, cow·period data were pooled by year of forage (2002 or 2003), entailing that data of 2 cows (n = 2, 2002 and n = 2, 2003) were used to construct each degradation curve.

Values of SD and CV of degradation parameter estimates were calculated for each chemical fraction within forage class. Because values of SD and CV were similar across forage classes, values were averaged across forage classes before they were tabulated. These tabulated values should not be mistaken as SD and CV of data pooled by forage class; data were separated by forage class when values of SD and CV were calculated, and only thereafter were values of SD and CV averaged.

Statistical Analysis with Other Previously Published Degradation Data

The data of Mertens (1973), von Keyserlingk et al. (1996), NRC (2001), and Hvelplund and Weisbjerg (2000) were used to calculate CV of degradation parameter estimates for comparison with our own results. Values of CV for *(a + b)* and k_d in Mertens (1973) were calculated by compiling data in the appendix, which listed estimates of *(a + b)* and k_d individually for each experimental forage. When not reported in the original publication, values of CV for *a*, *b*, and k_d in von Keyserlingk et al. (1996) were calculated directly using reported mean and SD pooled by forage class.

Because Hvelplund and Weisbjerg (2000) reported SD by forage species and not forage class, SD for forage class was calculated by pooling variances of degradation parameter estimates across forage species within a class. Similarly, because the NRC (2001) reported SD by forage maturity and not forage class, SD for forage class was calculated by pooling variances of degradation parameter estimates across forage maturities within a class. Once values of SD were calculated in this way, values of CV were then computed as with the data of von Keyserlingk et al. (1996).

Calculation of Ruminal Digestibility and 95% Confidence Limits

Predicted ruminal digestibilities of DM, ADF, HEM, and CP by forage class were calculated using the equation

$$digestibility_{i,j} = a_{i,j} + b_{i,j} \frac{\lambda_{d|i,j}^{\ 2}}{(\lambda_{d|i,j} + k_p)^2} \qquad [1]$$

where $digestibility_{i,j}$ ($g \cdot g^{-1}$) is the ruminal digestibility of chemical fraction *i* (DM, ADF, HEM, CP) and forage class *j* (ECA, LCA, CSG, WSG, GL); $a_{i,j}$ is *a* for chemical fraction *i* and forage class *j*; $b_{i,j}$ is *b* for chemical fraction *i* and forage class *j*; $\lambda_{d|i,j}$ is λ_d for

chemical fraction *i* and forage class *j*; and k_p is the fractional rate of passage from the rumen (h^{-1}), set to a constant value of 0·06 h^{-1}. This equation is conceptually analogous to the oft-used equation

$$digestibility = a + b\frac{k_d}{k_d + k_p} \qquad [2]$$

developed by Ørskov and McDonald (1979). Eq. 1 and 2 are derived using the same biological principles and compute the same entity, though their precise mathematical forms differ because of the use of the age-dependent rate λ_d in Eq. 1 in place of the independent-rate k_d in Eq. 2. (See Appendix for the derivation of Eq. 1)

Upper and lower 95% confidence limits (CL) of calculated digestibility were determined using the law of propagation of uncertainty (e.g., Taylor, 1997; Heuvelink, 1998). Frequently used in the physical and quantitative sciences, the law of propagation of uncertainty is employed to compute the amount of uncertainty (analogous to SD) expected in a calculated quantity (e.g., digestibility) originating from uncertainty in one or more measured quantities (e.g., *a*, *b*, λ_d) used in the calculations. In general, using a first-order Taylor approximation, uncertainty in a dependent variable *y* that is a function of independent variables $x_1, x_2, \ldots, x_n$ is the following:

$$\Delta y = [\sum_{k=1}^{n}\sum_{l=1}^{n}(\frac{\partial y}{\partial x_k}\frac{\partial y}{\partial x_l}\Delta x_k \Delta x_l \rho_{x_k, x_l})]^2 \qquad [3]$$

where $\frac{\partial y}{\partial x_k}$ and $\frac{\partial y}{\partial x_l}$ are the partial derivatives of *y* in respect to x_k and x_l, respectively; Δx_k and Δx_l are the uncertainties of x_k and x_l, respectively; and ρ_{x_k, x_l} is the correlation coefficient between variables x_k and x_l. When $k = l$, the term $\Delta x_k \Delta x_l \rho_{x_k, x_l} = \Delta x_k^{\,2}$ and

when $k \neq l$, $\Delta x_k \Delta x_l \rho_{xk,xl} = \sigma_{xk,xl}$, the covariance between x_k and x_l; from these relations and from Eq. 1 and 3, the corresponding uncertainty in digestibility is expressed as

$$\begin{aligned}\Delta digestibility_{i,j} = [&(\frac{\partial digestibility_{i,j}}{\partial a_{i,j}}\Delta a_{i,j})^2 + (\frac{\partial digestibility_{i,j}}{\partial b_{i,j}}\Delta b_{i,j})^2 + \\ &(\frac{\partial digestibility_{i,j}}{\partial a_{i,j}}\Delta \lambda_{d|i,j})^2 + 2\frac{\partial digestibility_{i,j}}{\partial a_{i,j}}\frac{\partial digestibility_{i,j}}{\partial b_{i,j}}\sigma_{a_{i,j},b_{i,j}} + \\ &2\frac{\partial digestibility_{i,j}}{\partial a_{i,j}}\frac{\partial digestibility_{i,j}}{\partial \lambda_{d|i,j}}\sigma_{ai,j,\lambda_{d|i,j}} + \\ &2\frac{\partial digestibility_{i,j}}{\partial b_{i,j}}\frac{\partial digestibility_{i,j}}{\partial \lambda_{d|i,j}}\sigma_{bi,k,\lambda_{d|i,j}}]^2\end{aligned} \quad [4]$$

where $\Delta digestibility_{i,j}$ is uncertainty in $digestibility_{i,j}$; $\Delta a_{i,j}$ is uncertainty in $a_{i,j}$; $\Delta b_{i,j}$ is uncertainty in $b_{i,j}$; $\Delta \lambda_{d|i,j}$ is uncertainty in $\lambda_{d|i,j}$; $\sigma_{ai,j,bi,j}$ is covariance between $a_{i,j}$ and $b_{i,j}$; $\sigma_{ai,j,\lambda d|i,j}$ is covariance between $a_{i,j}$ and $\lambda_{d|i,j}$; $\sigma_{bi,j,\lambda d|i,j}$ is covariance between $b_{i,j}$ and $\lambda_{d|i,j}$; $\frac{\partial digestibility_{i,j}}{\partial a_{i,j}}$ is the partial derivative of $digestibility_{i,j}$ with respect to $a_{i,j}$, equal to 1; $\frac{\partial digestibility_{i,j}}{\partial b_{i,j}}$ is the partial derivative of $digestibility_{i,j}$ with respect to $b_{i,k}$, equal to $\frac{\lambda_{d|i,j}^{\ 2}}{(\lambda_{d|i,j}+k_p)^2}$; and $\frac{\partial digestibility_{i,j}}{\partial \lambda_{d|i,j}}$ is the partial derivative of $digestibility_{i,j}$ with respect to $\lambda_{d|i,j}$, equal to $2b[\frac{\lambda_{d|i,j}}{(\lambda_{d|i,j}+k_p)^2} - \frac{\lambda_{d|i,j}^{\ 2}}{(\lambda_{d|i,j}+k_p)^3}]$. As mentioned below, the value of Δk_p was set to 0; for simplicity, Eq. 4 has already been rendered with $\Delta k_p = 0$.

Examination of Eq. 3 and 4 reveals the key result that increasing uncertainty in a measured quantity (e.g., degradation parameters) increases uncertainty in a calculated quantity (e.g., digestibility). This point is illustrated by Figure 3.1, which shows how

uncertainty in *b* translates into uncertainty in digestibility. The solid black line represents values of *digestibility* (computed with Eq. 1) when *b* varies from 0 to 1 (and with *a* and λ_d set to 0 and 0·075, values similar to those for NDF of WSG). The value of Δb is 0·08 and centered around *b* = 0·60 (values similar to those for NDF of WSG); covariances and all other uncertainties are set to 0. As shown in Figure 3.1, a vertical line extending from the lower bound of Δb on the *x*-axis intersects with a horizontal line extending from the lower bound of $\Delta digestibility$ on the *y*-axis, where the point of intersection is a point on the graph of *digestibility*. A similar relationship is observed between the upper bounds of Δb and $\Delta digestibility$ (Figure 3.1). As such, when Δb is increased, $\Delta digestibility$ increases in kind. Note that the exact relationship between *b* and *digestibility* shown in Figure 3.1 exists only when covariances and all other uncertainties are equal to 0, but the general principle illustrated ($\Delta digestibility$ increases with Δb) holds true under all conditions.

Further examination of Eq. 3 and 4 also reveals that increasing the partial derivative of the measured quantity relative to the calculated quantity (i.e., $\frac{\partial y}{\partial x_k}$) increases uncertainty, as does increasing the covariances between the measured quantities (i.e., σ_{x_k, x_k}).

At first, $\Delta a_{i,j}$ and $\Delta b_{i,j}$ were set to the standard deviations of $a_{i,j}$ and $b_{i,j}$ measured in the study, and so too were covariances set to their measured values, in order to determine the composite effect of $\Delta a_{i,j}$, $\Delta b_{i,j}$, and $\Delta \lambda_{d|i,j}$ on $\Delta digestibility_{i,j}$. Next, $\Delta a_{i,j}$ and $\Delta b_{i,j}$ were set to zero in order to study the effect of $\Delta \lambda_{d|i,j}$ on $\Delta digestibility_{i,j}$ in isolation. In all analyses, the values of $\Delta \lambda_{d|i,j}$ and Δk_p were set to the SD of $\lambda_{d|i,j}$ and 0, respectively.

For calculating the composite effect of $\Delta a_{i,j}$, $\Delta b_{i,j}$, and $\Delta\lambda_{d|i,j}$ on $\Delta digestibility_{i,j}$, methods other than law of propagation of uncertainty may be employed; one alternative is to determine digestibility of each sample using Eq. 1 and then compute the SD of these digestibility values to yield $\Delta digestibility_{i,j}$ when $\Delta a_{i,j}$, $\Delta b_{i,j}$, and $\Delta\lambda_{d|i,j}$ are equal to their SD. However, only the law of propagation of uncertainty can be used for the more complex analysis in which the effect of $\Delta\lambda_{d|i,j}$ on $\Delta digestibility_{i,j}$ is studied in isolation. For this reason, the law of propagation of uncertainty was used for all analyses.

Upper and lower 95% CL were computed as the quantity

$$digestibility_{i,j} \pm \Delta digestibility_{i,j} \cdot t_{0{\cdot}025,n-1}$$

where $t_{0{\cdot}025,n-1}$ = critical value of the right tail of the *t* distribution with $\alpha / 2 = 0{\cdot}025$ and with $n - 1$ degrees of freedom (n = number of $digestibility_{i,j}$ observations).

RESULTS

The chemical composition of the forages is presented in Table 2.3. Numerically, both alfalfa classes (ECA, LCA) had higher mean concentrations of CP and lower concentrations of fiber (NDF, ADF, HEM) than for grass classes (CSG, WSG). Within alfalfa, LCA had a numerically higher mean CP concentration and lower fiber concentrations than for ECA. Within grasses, CSG had numerically higher mean CP concentration and lower fiber concentrations than for WSG.

Table 2.6 reports means of degradation parameter estimates λ_d, k, a, b, and $(a + b)$. Mean values of $(a + b)$ of DM and CP were numerically higher for alfalfa (ECA, LCA) than for grass samples (CSG, WSG). Values of $(a + b)$ of fiber (NDF, ADF, HEM) were similar across classes. Mean values of λ_d and k were numerically higher for alfalfa (ECA, LCA) than for grasses (CSG, WSG). Within alfalfa, λ_d and k were higher

for LCA than for ECA, and within grasses, these parameters were higher for CSG than for WSG. Differences in λ_d and k were consistently preserved across chemical fractions (DM, NDF, ADF, HEM, CP).

Table 3.1 reports their SD and CV of degradation parameter estimates (λ_d, k, a, b, and $[a + b]$). Values in Table 3.1 were averaged across forage classes for brevity because SD and CV did not vary appreciably across classes. Values of SD are large relative to the mean, illustrated by large values of CV. Values of CV range from 17.3 to 36.2% for λ_d and k, 24.8 to 32.4% for a, 18.0 to 23.4% for b, and 5.5 to 16.4% for $(a + b)$. Values of CV for $(a + b)$ were systematically smaller than for any other parameter, while values of CV for other parameters (λ_d, k, a, and b) were similar in magnitude. Similarly, values of CV for HEM were consistently larger than for any other chemical fraction, and while CV for CP were systematically smaller.

Table 3.2 shows digestibility means and their associated upper and lower 95% CL when $\Delta\lambda_d$, Δa, and Δb were set to the SD values of λ_d, a, and b measured in the study. The mean digestibilities of CP range from 0.513 to 0.761 $g \cdot g^{-1}$ for CP. Numerically, these are generally higher than those of DM digestibility, with values of 0.406 to 0.642 $g \cdot g^{-1}$. These values are in turn numerically higher than those of NDF, ADF, and HEM, which are themselves similar, with digestibilities ranging from 0.193 to 0.288 $g \cdot g^{-1}$ for NDF, 0.192 to 0.270 for ADF, and 0.217 to 0.396 $g \cdot g^{-1}$ for HEM.

Within ECA, 95% CL of DM and CP are distinct from NDF and ADF, and all other 95% CL overlap each other. Within LCA, 95% CL of CP digestibility are distinct from those of HEM, ADF, and NDF digestibility; 95% CL of DM digestibility are distinct from those of NDF and ADF digestibility; and all other 95% CL overlap each

other. Within CSG, the 95% CL of CP are distinct from all other chemical fractions (DM, NDF, ADF, HEM), and all other 95% CL overlap each other. Within WSG, the 95% CL of DM are distinct from all other chemical fractions (NDF, ADF, HEM, CP), and all other 95% CL overlap each other. Within GL, 95% CL of DM and CP digestibility are distinct from those of NDF and ADF, and all other 95% CL overlap each other.

When compared within the same chemical fraction, mean digestibilities for WSG and CSG are systematically lower than for other forage classes, which are themselves similar to each other (Table 3.2). As shown in Table 3.2, 95% CL of DM, NDF, ADF, HEM, and CP digestibility overlap each other across forage classes, with only one exception (95% CL of DM digestibility of WSG were distinct those of LCA).

Table 3.3 shows digestibility means and their associated upper and lower 95% CL when $\Delta\lambda_d$ was set to the SD of λ_d measured in this study (and Δa and Δb were set to zero). Mean digestibilities are the same as those reported in Table 3.2. Within ECA, LCA, and CSG, 95% CL of CP and DM digestibility are distinct from each other and of all other chemical fractions; and 95% CL of NDF, ADF, and HEM digestibility overlap each other. A similar pattern is found for WSG, except 95% CL of HEM is not distinct from that of DM. Within GL, 95% CL of CP digestibility are distinct from those of NDF, ADF, and HEM digestibility; 95% CL of DM digestibility are distinct from those of NDF and ADF digestibility; and all other 95% CL overlap each other.

Compared across forages, 95% CL of DM digestibility for CSG and WSG are distinct from those for ECA, LCA, and GL. Additionally, 95% CL of CP digestibility for WSG are distinct from those for ECA, LCA, and GL, and 95% CL for CP digestibility

for CSG are distinct from those for LCA. All other 95% CL of forage classes overlap each other.

DISCUSSION

Chemical Composition and Degradation Parameter Means

The mean and SD of the chemical composition data in Table 2.3 were generally similar to those summarized by the Dairy NRC (2001), though our samples of WSG had lower NDF, ADF, and HEM and higher CP than reported by the NRC (2001). These results suggest a representative range of forages was included in this study. With the exception of $\lambda_{d,}$ (see below), degradation parameter means in Table 2.6 are similar to those presented by other reports (Smith et al., 1972; Mertens, 1973; von Keyserlingk et al., 1996), indicating they are suitable for the digestibility analyses below. Values of λ_d generated in this study are numerically greater than degradation rate values reported by other investigators because λ_d is a age-dependent degradation rate whereas most degradation rates reported in the literature are age-independent rates. For commensurate comparison between degradation rates in this and prior studies, the mean degradation rate *k* should be used for reference (Materials and Methods).

Variation in Degradation Parameter Estimates

For comparison with values in Table 3.1, we summarize CV values for degradation parameters estimates from prior studies. In the data of von Keyserlingk et al. (1996) values of CV for *a*, *b*, and k_d of CP were 11.4, 20.1, and 35.1% for alfalfa hay and 26.3, 24.1, and 34.9% for grass hay. For DM, values of CV for *a*, *b*, and k_d were 7.9, 7.4, and 36.7% for alfalfa hay and 16.3, 25.6, and 36.8% for grass hay. Similarly, in the data of Hvelplund and Weisbjerg (2000), values of CV of *a*, *b*, and k_d were 11.1, 16.0, and

27.2% for alfalfa CP. In the same dataset, values of CV of *a*, *b*, and k_d were 21.8, 17.6, and 24.7% for CSG CP. In the data of NRC (2001), values of CV of *a*, *b*, (*a* + *b*) and k_d were 34.8, 32.2, 11.2, 46.5% for alfalfa CP. In the same dataset, values of CV of *a*, *b*, (*a* + *b*) and k_d were 22.7, 20.4, 4.8, and 35.5% for CSG CP. In Mertens (1973), values of CV of *(a + b)* and k_d for NDF were 18.1 and 21.5% for alfalfa; 14.8 and 19.6% for GL;10.9 and 29.3 for CSG; and 12.8 and 25.5% for WSG.

In sum, literature values of CV for *a* range from 7.9 to 34.8%; those for *b* range from 7.4 to 32.2%; those for (*a* + *b*) range from 4.8 to 18.1; and those for k_d range from 19.6 to 36.5%, with no clearly detectable differences across forage classes (alfalfa, GL, CSG, WSG) or chemical fractions (DM, CP, NDF). Coefficient of variation values for DM, CP, and NDF in our own dataset (Table 3.1) generally fall within these ranges. The large amount of variability we found in degradation parameters values is thus reasonable. Note that in prior reports, CV for degradation rate were larger than CV of other parameters, unlike in this experiment.

In general, the reason for variation in degradation parameter estimates is due to a combination of (1) variation truly attributable to chemical fraction and forage class and (2) procedural variation. For in situ studies (such as the current), common sources of procedural variation arise from factors such as bag characteristics (material, size, pore size, sample size:surface area), sample preparation (grind size), incubation procedure (presence or absence of pre-incubation, reticuloruminal region in which bags are incubated, incubation times, order of bag removal and insertion), replications (number of animal, day, and bag replications), rinsing technique (hand vs. mechanical rinsing), and animal-related parameters (species, diet, temporal and individual variation in

reticulorumen environment) (Nocek, 1988; Vanzant et al., 1998). Most of these factors (bag characteristics, sample preparation, incubation technique, rinsing technique, animal species, diet) were controlled in this study by adopting a standardized procedure. Other sources of variation, such as variation among animals, days, and replicate bags (Mehrez and Ørskov, 1977; Vanzant et al., 1998) were reduced by use of multiple animals (2 per forage) and bags (2 per animal).

Though extensive effort was made to minimize procedural error relative to variation attributable to chemical fraction and forage class, procedural error may have still been appreciable. In this context, it is difficult to explain systematic differences in CV across degradation parameters and chemical fractions, for these differences are confounded by the two sources of variation defined above. For example, the consistently smaller CV for *(a + b)* compared to other degradation parameters could be caused by lower measurement error due to some feature of the procedure, or lower true variation in this parameter across chemical fractions and forages, or both. Whatever its source, variation in degradation parameters was substaintial and comparable to studies using a wide range of in situ and in vitro methodology.

Calculated Digestibilities and Their 95% CL

Many feed analysis systems (e.g., Cornell Net Carbohydrate and Protein System [Sniffen et al., 1992]; Molly [Baldwin, 1995]; Beef NRC [2000]; Dairy NRC [2001]) use degradation parameter estimate means to calculate ruminal digestibility or TDN. Because of the considerable variability in degradation rate and other degradation parameter estimates, as discussed above, the precision in using simple means may be questioned. To determine variability in ruminal digestibility calculated using mean

values, 95% CL of digestibility was computed using the law of propagation of uncertainty.

Values in Table 3.2 (where λ_d, a, and b equal their SD) represent the case in which digestibility is calculated from estimated a, b, and λ_d means, such as those from a feed library. There existed large numerical differences in digestibilities across chemical fractions, with CP digestibility higher than DM digestibility, which is in turn higher than NDF, ADF, and HEM digestibilities (which are themselves similar). There existed large numerical differences across forage classes, also, with digestibilities of ECA, LCA, and GL systematically higher than those of CSG and WSG (which are themselves similar). However, these appreciable numerical differences are often not preserved when comparing 95% CL (Table 3.2). As suggested by their frequent overlapping, 95% CL span a wide range of values, equal to 80.5% of their associated digestibility means on average. These findings, together with those discussed above, suggest digestibility values calculated using mean values of a, b, and λ_d may have limited practical and biological meaning.

Note that k_p and chemical composition of the forages was assumed to have no uncertainty–i.e., there is assumed to be no error in their estimation. Because there is considerable variability in k_p and published equations predict k_p with low precision (the best equation for predicting k_p of forages in Seo et al. [2006] had a root mean square prediction error of 0·011 h^{-1} with R^2 = 0·39), 95% CL would be much greater in more practical cases–in which k_p was not known and thus had to be estimated–than in Table 3.2 where it is assumed to be known with certainty. In all likelihood, the 95% CL reported in

Table 3.2 are greatly underestimated. This further cautions the use of mean values of *a*, *b*, and λ_d to calculate digestibility.

Analysis Where* a *and* b *are Known with Certainty

Values of *a* and *b* may often be measured or estimated readily using solubility and chemical assays, such as buffer-soluble N (Krishnamoorthy et al., 1983), which is used to estimate *a* for CP, and lignin, used to predict *b* for NDF (Smith et al., 1972; Mertens, 1973; Traxler et al., 1998). To mimic cases in which *a* and *b* are measured, 95% CL were re-calculated assuming that *a* and *b* were known with certainty, and λ_d alone had uncertainty (Table 3.3).

The 95% CL in Table 3.3 overlap each less frequently than in Table 3.2, compared both within and across forage classes. However, considerable variation in calculated digestibility is still present when *a* and *b* are known with certainty. On average, 95% CL encompass values 54.4% of their associated digestibility means. This percentage is less than that when *a* and *b* are uncertain (80.5%), but it is still large enough to limit the practical and biological meaning of the calculated digestibilities.

As discussed above, k_p of the forages were assumed to have no uncertainty, and thus the 95% CL listed in Table 3.3 are likely to be smaller than realized when k_p must be estimated. Note also that it is unrealistic to assume values of *a* and *b* with absolute certainty, as done in calculating 95% CL reported Table 3.3. At the very least, analytical error in measuring *a* and *b* contributes uncertainty to the values of these parameter. Further, *a* and *b* may not be measured directly but estimated from another chemical or physical measurement; for example, *b* of NDF is often estimated from lignin content of the NDF (Smith et al., 1972; Mertens, 1973; Traxler et al., 1998); errors in this estimation

add uncertainty. Overall, due to these sources of uncertainty that were not accounted in the calculations in this report, the widths of the 95% CL in Table 3.3 are likely underestimated.

Here and throughout, one may attribute the large 95% CL we found to some suspected peculiarity in our in situ procedure, kinetic model (Eq. 1), uncertainty analysis (Eq. 4), or some other aspect of our methodology. We reemphasize that the amount of variability in degradation parameter values we found is comparable to that of in vitro and other in situ studies using a wide range of methodology. Though we fully carried out uncertainty analysis with our parameter values alone, we would expect similarly large 95% CL using values from other reports because of this comparable variability (c.f., Figure 3.1 and Materials and Methods). While largely foreign to animal and nutritional sciences, the uncertainty analysis we used is itself well-accepted in the physical sciences. The large 95% CL we found are thus not artifacts of the conditions of our study.

These results caution the use of mean degradation parameter values in estimating digestibility. As a corollary, caution should be exercised when using digestibility values garnered from feed analysis systems that rely on approaches to calculate digestibility similar to those used in this report. Because uncertainty in λ_d contributes appreciable uncertainty in calculated digestibility, techniques to efficiently measure or effectively estimate λ_d should continue to be developed. One promising approach is that of Van Soest et al. (2000), who developed multiple regression equations that accurately predict the degradation rate of forage NDF from chemical composition and in vitro digestibility. The dataset from this study could be used to further validate the equations of Van Soest et al. (2000) and formulate similar equations for non-NDF chemical fractions.

APPENDIX

Digestibility is the sum of $a_{i,j}$ and $b_{i,j}$ that is digested in the rumen:

$$digestibility_{i,j} = a_{i,j}' + b_{i,j}$$

where $a_{i,j}'$ and $b_{i,j}'$ are $a_{i,j}$ and $b_{i,j}$ that is digestible ($g \cdot g^{-1}$). The terms $a_{i,j}'$ and $b_{i,j}'$ are explicitly defined as

$$a_{i,j}' = p_{a_{i,j}} \cdot a_{i,j}$$

and

$$b_{i,j}' = p_{b_{i,j}} \cdot b_{i,j}$$

where $p_{ai,j}$ and $p_{bi,j}$ are the fractions ($g \cdot g^{-1}$ $a_{i,j}$ or $b_{i,j}$) of $a_{i,j}$ and $b_{i,j}$ that is digestible. It is assumed that the $a_{i,j}$ fraction is completely digestible—i.e. $p_{ai,j} = 1$—following its definition that it is instantly degraded. For the G2 model used in this report, $p_{bi,j}$ is equal to

$$p_{b_{i,j}} = \frac{\lambda_{d|i,j}^{\ 2}}{(\lambda_{d|i,j} + k_p)^2}.$$

This follows from the definition of fractional digestibility as the amount of material (in this case, $b_{i,j}$) that disappears by digestion divided by its total disappearance; mathematically, this is equivalent to the integral (over the interval $t = 0$ to infinity) of $r_{i,j}(t)$, the rate function for digestion of $b_{i,j}$ (h^{-1}), multiplied by $B_{i,j}(t)$, the amount of $b_{i,j}$ remaining over time ($g \cdot g^{-1}$ $b_{i,j}$):

$$p_{b_{i,j}} = \int_{t=o}^{\infty} [r_{i,j}(t) \cdot B_{i,j}(t)]dt = \frac{\lambda_{d|i,j}^{\ 2}}{(\lambda_{d|i,j} + k_p)^2}$$

(For a G2 model, $r_{i,j}(t)$ is (Pond et al., 1988; Ellis et al., 1994)

$$r_{i,j}(t) = \frac{\lambda_{d|i,j}{}^2 \cdot t}{1 + \lambda_{d|i,j} \cdot t},$$

and the term $B_{i,j}(t)$

$$B_{i,j}(t) = (1 + \lambda_{d|i,j} \cdot t)\exp[-t \cdot (\lambda_{d|i,j} + k_p)]$$

is the solution to the differential equation that describes the change of $B_{i,j}(t)$ over time by due digestion and passage:

$$\frac{dB_{i,j}(t)}{dt} = -[r_{i,j}(t) + k_p]B_{i,j}(t).)$$

Making the appropriate substitutions, the final digestibility equation (Eq. 1 in the text) is then

$$digestibility_{i,j} = a_{i,j} + b_{i,j}\frac{\lambda_{d|i,j}{}^2}{(\lambda_{d|i,j} + k_p)^2}.$$

Table 3.1. Standard deviation and CV of degradation parameter estimates, averaged by chemical fraction[1,2]

		Degradation parameter				
		λ_d	k	a	b	$(a + b)$
DM						
	SD	0.031	0.019	0.079	0.077	0.041
	CV, %	17.3	17.3	24.8	18.0	5.5
NDF						
	SD	0.032	0.019	-----	-----	0.073
	CV, %	21.7	21.7	-----	-----	12.9
ADF						
	SD	0.038	0.023	-----	-----	0.088
	CV, %	29.1	29.1	-----	-----	15.7
HEM						
	SD	0.069	0.041	-----	-----	0.097
	CV, %	36.2	36.2	-----	-----	16.4
CP						
	SD	0.037	0.022	0.127	0.111	0.065
	CV, %	19.7	19.7	32.4	23.4	10.1

[1] k_d , λ_d, degradation rate (h^{-1}); a, fraction degraded at $t = 0$ ($g \cdot g^{-1}$); $(a + b)$, potential extent of degradation ($g \cdot g^{-1}$); b, fraction not degraded at $t = 0$ that is potentially degradable ($g \cdot g^{-1}$); HEM, hemicellulose.
[2] Values of SD and CV are averaged across forage class. Units for SD are h^{-1} for λ_d and k and $g \cdot g^{-1}$ for a, b, and $(a + b)$.

Table 3.2. Calculated digestibility of chemical fractions by forage class and upper and lower 95% confidence limits (CL), using uncertainty values of λ_d, *a*, and *b* equal to their SD[1,2]

	Forage class				
	ECA	LCA	CSG	WSG	GL
	----------g·g^{-1}----------				
DM					
Digestibility[3]	0.588[a]	0.642[ab]	0.436[ab]	0.406[a]	0.570[a]
Lower 95% CL	0.456	0.508	0.301	0.324	0.434
Upper 95% CL	0.720	0.777	0.571	0.487	0.707
NDF					
Digestibility[3]	0.288[b]	0.296[c]	0.225[b]	0.193[b]	0.296[b]
Lower 95% CL	0.157	0.177	0.113	0.123	0.192
Upper 95% CL	0.420	0.415	0.337	0.264	0.401
ADF					
Digestibility[3]	0.270[b]	0.266[c]	0.226[b]	0.192[b]	0.266[b]
Lower 95% CL	0.123	0.167	0.114	0.120	0.158
Upper 95% CL	0.417	0.366	0.338	0.263	0.374
HEM					
Digestibility[3]	0.377[ab]	0.370[bc]	0.231[ab]	0.217[ab]	0.396[ab]
Lower 95% CL	0.174	0.134	0.107	0.045	0.170
Upper 95% CL	0.581	0.606	0.355	0.389	0.623
CP					
Digestibility[3]	0.716[a]	0.761[a]	0.597[a]	0.513[ab]	0.702[a]
Lower 95% CL	0.544	0.640	0.348	0.240	0.573
Upper 95% CL	0.877	0.882	0.847	0.787	0.831

[a,b,c]Means with different superscripts within column have non-overlapping 95% CL

[1]λ_d, degradation rate (h^{-1}); *a*, fraction degraded at $t = 0$ (g·g^{-1}); *b*, fraction not degraded at $t = 0$ that is potentially degradable (g·g^{-1}); *(a + b)*, potential extent of degradation; ECA, early-cut alfalfa; LCA, late-cut alfalfa; CSG, cool season grass; WSG, warm season grass; GL, grass-legume mixture; HEM, hemicellulose.

[2]Values calculated using Eq. 1 and 4 in text and passage rate of 0·06 h^{-1}.

[3]All means within rows have overlapping 95% CL; corresponding superscript symbols omitted for brevity.

Table 3.3. Calculated digestibility of chemical fractions by forage class and upper and lower 95% confidence limits (CL), using uncertainty values of λ_d equal to its SD[1,2]

	Forage class				
	ECA	LCA	CSG	WSG	GL
	----------g·g^{-1}----------				
DM					
Digestibility	0.588^{b,x}	0.642^{b,x}	0.436^{b,y}	0.406^{b,y}	0.570^{ab,x}
Lower 95% CL	0.539	0.602	0.391	0.387	0.497
Upper 95% CL	0.636	0.683	0.481	0.424	0.644
NDF					
Digestibility	0.288^{c}	0.296^{c}	0.225^{c}	0.193^{c}	0.296^{c}
Lower 95% CL	0.173	0.212	0.175	0.146	0.209
Upper 95% CL	0.404	0.381	0.275	0.241	0.383
ADF					
Digestibility	0.270^{c}	0.266^{c}	0.226^{c}	0.192^{c}	0.266^{c}
Lower 95% CL	0.136	0.169	0.143	0.104	0.145
Upper 95% CL	0.404	0.364	0.309	0.280	0.387
HEM					
Digestibility	0.377^{c}	0.370^{c}	0.231^{c}	0.217^{bc}	0.396^{bc}
Lower 95% CL	0.239	0.258	0.172	0.011	0.227
Upper 95% CL	0.516	0.483	0.290	0.423	0.566
CP					
Digestibility	0.716^{a,xy}	0.761^{a,x}	0.597^{a,yz}	0.513^{a,z}	0.702^{a,xy}
Lower 95% CL	0.664	0.722	0.530	0.436	0.640
Upper 95% CL	0.767	0.801	0.665	0.590	0.763

^{a,b,c}Means with different superscripts within column have non-overlapping 95% CL

^{x,y,z}Means with different superscripts within row have non-overlapping 95% CL

$^{1}\lambda_d$, degradation rate (h^{-1}); ECA, early-cut alfalfa; LCA, late-cut alfalfa; CSG, cool season grass; WSG, warm season grass; GL, grass-legume mixture; HEM, hemicellulose.

^{2}Values calculated using Eq. 1 and 4 in text and passage rate of 0·06 h^{-1}.

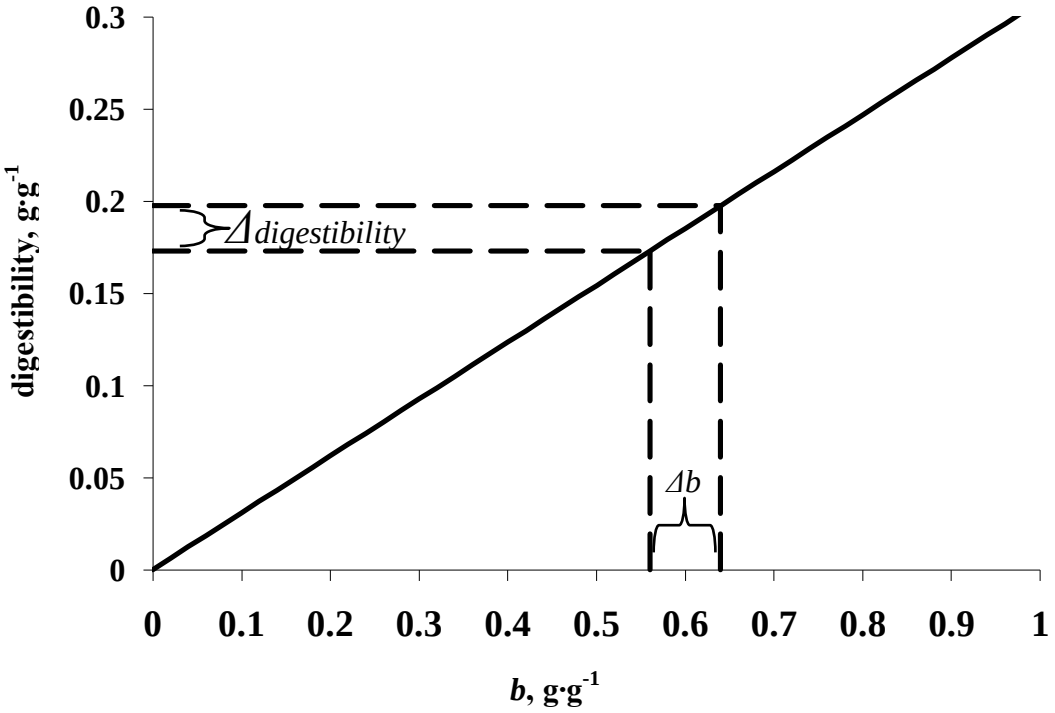

Figure 3.1. Graphical illustration of how increasing uncertainty in a measured quantity (e.g., degradation parameters) increases uncertainty in a calculated quantity (e.g., digestibility) according to the law of propagation of uncertainty. Digestibility (solid black line) is computed using Eq. 1 in the text with b (fraction not degraded at $t = 0$ that is potentially degradable [$g \cdot g^{-1}$]) varying from 0 to 1 and a (fraction degraded at $t = 0$ [$g \cdot g^{-1}$]) and λ_d (degradation rate [h^{-1}]) held constant at 0 and 0·075. The value of Δb (uncertainty in b) is 0·08 and is centered around $b = 0{\cdot}60$, with covariances and all other uncertainties set to zero. Dashed lines mark the upper and lower bounds of Δb and $\Delta digestibility$ (uncertainty in digestibility). The point of intersection between horizontal and vertical lines extending from the lower bounds of Δb and $\Delta digestibility$ is a point on the graph of digestibility; a similar relationship exists between the upper bounds of the two variables. Increasing Δb hence increases $\Delta digestibility$.

CHAPTER 4

USING YTTERBIUM-LABELED FORAGE TO INVESTIGATE PARTICLE FLOW KINETICS ACROSS SITES IN THE BOVINE RETICULORUMEN

ABSTRACT

To better understand particle flow kinetics across the reticulorumen (RR), we monitored concentrations of Yb-marked forage across several RR sites over time. We fed three forages (bromegrass, high-quality alfalfa, low-quality alfalfa) ad libitum to lactating Holstein dairy cows in an incomplete 3x3 Latin square design. After dosing Yb-marked forage in the mid-dorsal sac (DS), we determined Yb concentrations of particulate samples taken from several sites (DS, ventral sac [VS], ventral blind sac [VBS], reticulum [RT]) from 0 to 72 h. For each site we constructed marker concentration profiles and applied non-parametric (local quadratic) and parametric (two-compartmental, G2→G1→O) regression models to these profiles. We determined mean residence time (MRT) and peak marker concentration using the original profile observations and regressions. Across forage diets, intake of DM differed ($P = 0.022$) but that of other chemical fractions did not ($P = 0.125$). The local regression fit the data well visually, and MRT calculated using this model and original observations closely agreed. This suggests the local regression successfully smoothed the original observations, which had considerable stochastic variation, without changing the underlying shapes they implied. Similar considerations showed the G2→G1→O model fit the data poorly. Visually, marker profiles shapes varied greatly, but we found few differences attributable

to diet and site. Mean residence and peak marker concentration times, which reflect marker profile shape, did not strongly differ by diet (P = 0.434, 0.0824) or site (P = 0.113, 0.0824), though they did by cow (P = 0.036, 0.004). These results further show differences in profile shapes—and the particle flow kinetics they reflect—are explained poorly by diet and site but somewhat explained by unidentified animal factors. Based on studies that demonstrate particles flows through RR in the partial order DS→VBS↔VS→RT, we expected MRT values to follow the order $MRT_{DS} < MRT_{VS} \approx MRT_{VBS} < MRT_{RT}$ (where MRT_i is MRT of the i^{th} site). Our finding that MRT values were similar across sites suggests that once a particle escapes from the DS for the final time, it must escape from ventral regions (VS, VBS, RT) soon after entry. Our attempt to model these particle flow kinetics more quantitatively failed. Still, the experiment suggests that feed products designed to initially enter the ventral rumen and resist regurgitation should pass quickly from the RR.

INTRODUCTION

The kinetics of digesta flow and passage in the reticulorumen (**RR**) affect many digestive parameters, namely nutrient digestibility and voluntary feed intake. Digestibility is nutrient absorption rate divided by total disappearance rate (absorption and passage), and thus it depends on the precise kinetic pattern of digesta passage (Waldo, 1972; Allen and Mertens 1988). When steady-state conditions apply, rate of feed intake is equal to disappearance rate and thus partly a function of particle flow kinetics (Allen and Mertens, 1988).

Pulse-dosing feed particles mordanted with an external marker, then monitoring marker concentration over time to construct a marker profile, permits particle flow

kinetics to be described in detail (Ellis et al., 1979). Such methods have been repeatedly used to describe flow kinetics across the entire RR or at sites distal to it (duodenum, ileum, rectum). However, few studies have examined marker profile kinetics at different sites within the RR. The few studies that have done so examined flow at two sites only (dorsal and ventral sacs [Ellis et al., 1979; Dixon et al., 1983; Ellis et al., 1994; Poppi et al., 2001] or dorsal sac and reticulum [Balch, 1950]) or used such infrequent sampling (every 6 h at most) that identifying differences across sites is difficult (Walz et al., 2004). Understanding flow kinetics at different sites within the RR and how they integrate together may explain the overall pattern of particle flow dynamics and passage from the RR as a whole.

The objective of this study was to determine Yb marker profiles at multiple sites within the RR (dorsal sac, ventral sac, ventral blind sac, reticulum) when three forage (bromegrass, low-fiber alfalfa, high-fiber alfalfa) were fed.

MATERIALS AND METHODS

Animals and Diets

Three hays, a bromegrass (**BG**; *Bromus inermis*), a low-fiber alfalfa (**LFA**; *Medicago sativa*), and a high-fiber alfalfa (**HFA**), were fed to one multiparous and three primiparous lactating Holstein cows (mean BW of 499 ± 50 kg; mean±SD) fitted with a permanent rumen cannula. Hays were chopped through a TMR mixer (New Direction Equipment, Sioux Falls, SD) before feeding. All procedures involving the animals were approved by the Animal Care and Use Committee, University of Missouri-Columbia. The experimental design was an incomplete 3x3 Latin square, with four cows in the first period (with two cow replicates for HFA) and three in the second period (one

primiparous cow was removed midway during collection phase of the second period due to illness).

Marker Preparation

Eight kilograms of chopped BG, HFA, and LFA were soaked overnight in approximately 125 L of distilled H_2O to remove soluble material and subsequently dried to 105°C on 1-mm i.d. wire screens. Dried forage was then soaked overnight in a distilled H_2O solution containing 12.5 mg $YbCl_3 \cdot 6H_2O \cdot g\ DM^{-1}$ with pH adjusted to 3.00 with H_2SO_4 (to remove Yb from acid-labile binding sites) To remove loosely-bound Yb, labeled forage was washed on 1-mm i.d. wire screens once per hour for six hours, until wash water ran clear. Absence of Yb in washwater was confirmed using a phosphate buffer with pH = 10 (Teeter, 1984).

Passage trial

During an initial adjustment phase, animals were housed in free-stall barns of the University of Missouri-Columbia Foremost Dairy Center. Adjustment was 9 d during the first period and 6 d during the second. Length of adjustment was longer during the first period because animals were fed a total mixed ration (467 $g \cdot kg\ DM^{-1}$ concentrate) prior to first period and displayed poor intakes during the initial days of adjustment; prior to the second period, animals were fed the experimental all-forage diets and showed little initial intake depression. Animals were fed approximately 110% ad libitum intake of BG, HFA, or LFA diets through electronic feeding gates (American Calan, Inc., Northwood, NH). Fresh diet was provided at 06:00, 14:00, and 22:00 and orts removed at 06:00 the following day.

During the following 3-d collection phase, animals were fed 110% of DM intake established during last 3 d of adjustment. Fresh diet was fed and orts removed at same times as during adjustment. To facilitate intense sampling on collection day 1, on that day animals were housed in tie-stall barns of University of Missouri-Columbia Foremost Dairy Center. Thereafter animals were transferred to free-stall barns for the remaining collection days. Approximately 100 g of feed and orts were sampled once daily for all collection days; samples were placed in sealed plastic bags then stored at <0°C to await chemical analysis.

At 08:00 of collection day one, animals were dosed approximately 350 g Yb-marked forage (BG, HFA, or LFA, corresponding with diet fed) by placing the marked forage in the mid-dorsal rumen sac (DS) (Figure 4.1). The marked forage was firmly embedded in the center of the rumen mat in the DS but not mixed within. Between 100 and 200 mL of digesta contents were sampled from the DS, mid-ventral sac (VS), caudo-ventral blind sac (VBS), and ventral reticulum (RT) (Figure 4.1) at 0 (predosing), 1, 2, 3, 4, 6, 8, 10, 12, 16, 20, 24, 28, 32, 36, 40, 44, 48, 54, 60, 66, and 72 h relative to dosing (Figure 4.1). Samples were collected using a 250 mL plastic container. To sample from sites below the DS (VS, VBS, RT), the container was cupped with one hand (avoiding inadvertent sampling of the DS) and led down the wall of the rumen (avoiding mixing of DS with other sample sites). Immediately after sampling, sampled contents were removed from containers, strained through two layers of cheesecloth, returned to containers, and stored at <0°C to await further processing.

Chemical Analyses

After thawing, orts and feed samples were ground with a Wiley mill (Arthur H. Thomas Company, Philadelphia, PA) to pass through a 1-mm screen and analyzed for DM by drying at 105°C for 24 h; neutral detergent fibre (NDF) including residual ash (using heat-stable α-amylase and sodium sulphite) and acid detergent fibre (ADF) according to Van Soest et al. (1991) in an ANKOM^{200} Fiber Analyzer (ANKOM Technology); and total N by combustion analysis (LECO FP-428; LECO Corporation, St. Joseph, MI).

After thawing, rumen contents samples were dried to a 55°C oven to a constant mass. Subsamples were analyzed for DM by drying at 105°C for 24 h. Yb was extracted from contents using ethylenediaminetetraacetic acid solution and its concentration analyzed using atomic absorption spectrophotometry (S Series AA Spectrometer; Thermo Electron Corporation, Beverly, MA), as described by Hart and Polan (1984).

Regression with Yb Profile Data

Examination of the raw marker profiles revealed considerable stochastic variation ("noise") that tended to mask the overall shapes of the profiles. To reduce this variation and better visualize the underlying shape of the profiles, we applied both parametric and non-parametric regressions to the original profile observations (hereto referred to as the raw observations). A non-parametric regression has the advantage of flexibility, as it does not rely on or assume any structured (i.e., parametric) equation form and can thus fit a range of curve shapes. While less flexible, a parametric regression (i.e., a regression that uses a structured equation form) has the advantage of delivering parameter estimates,

which can be used for quantitatively summarizing and comparing the results of fitted curve shapes.

The non-parametric regression was a local regression model (a robust local averaging procedure) fitted using LOCFIT package of R (Loader, 1999). The model chosen was a local quadratic model with Gaussian kernel and nearest neighbor bandwidth of 0.4, parameters which visually provided the smoothest fit while minimizing underestimation at profile peaks and overestimation at early sampling times. Using the local regression model, values of marker concentration were predicted at each of the original sampling times (0 thorugh 72 h) to construct a dataset of smoothed values. The smoothed dataset was subjected to the following data editing procedures. First, all 0 h smoothed observations were adjusted to 0 ppm, as the 0 h observation was defined as 0 ppm during spectrometric analysis. Also, all values <0 ppm were raised to 0 ppm, which was defined as the minimum concentration of marker during spectrometric analysis.

The parametric models included the two-compartmental models of Pond et al. (1988) and Ellis et al. (1994). These models assume gamma-distributed residences times in the first compartment and exponentially-distributed times in the second, sequential compartment. The equation form of these models is the following:

$$Y(t) = C \cdot [\delta^n e^{-k \cdot t} - e^{-\lambda \cdot t} \cdot \sum_{i=1}^{n} \frac{\delta^i (\lambda \cdot t)}{(n-i)!}]$$

where *Y(t)* is the concentration of marker at time *t*, *C* is the initial concentration of marker entering the first compartment, *n* is the order of the gamma-distribution associated with the first compartment, λ is the passage rate in the first compartment, *k* is the passage rate in the second compartment, and $\delta = \lambda/(\lambda - k)$. The order *n* can assume integer values

≥1, and the optimal value of n is determined during model fitting procedures. We found a model with $n = 2$ yielded lowest the value of Akaike's information criterion (data not shown) and thus was optimal (see Chapter 2 for use of Akaike's information criterion for model selection). Following the convention of Pond et al. (1988) and Ellis et al. (1994), we refer to this optimal model as G2→G1→O. Fitted concentrations from this model are constrained to 0 and ≥0 ppm at $t = 0$ and > 0 h, respectively, and thus it was not necessary to edit the fitted data in the manner done for the local regression.

Calculation of Mean Residence Time

We calculated mean residence time (MRT) from the raw observations, local regression, and G2→G1→O model numerically using the equation of Thielemans (1978):

$$MRT = \frac{\sum C_t \cdot t \cdot dt}{\sum C_t \cdot dt} \qquad [1]$$

where t is the sampling time (h), the time between marker administration and the midpoint of the successive sampling times; C_t is the concentration of Yb in sample taken at t; and dt is the interval (h) between the successive sampling times. For the G2→G1→O model, which is a continuous equation (not discrete as required by Eq. 1), marker concentration values at each of original sampling points (0 to 72 h) were predicted using the model, and values of C_t thusly calculated from these predicted values.

For the G2→G1→O model, MRT was additionally calculated analytically using model parameters and the equation

$$MRT = n/\lambda + 1/k \qquad [2]$$

(Pond et al., 1988; Ellis et al, 1994).

Eq. 2 is more robust and accurate than Eq. 1 because it is the exact analytical expression for MRT for the G2→G1→O model, whereas Eq. 1 is only its numerical, discrete approximation. The main limitation of the numerical method (Eq. 1) is that it accounts for residence time accumulated only to the last sampling point; it consequently underestimates MRT if additional residence time accumulates thereafter (usually indicated by >0 ppm at the last sampling point). The analytical method (Eq. 2) effectively extrapolates beyond the final sampling time and is not liable to such underestimation.

For raw observations and local regression, we calculated MRT only numerically (Eq. 2) because appropriate analytical expressions cannot be derived, as this requires continuous, parametric models. For the G2→G1→O model, we calculated MRT both analytically (for better potential accuracy) and numerically (for better comparison with MRT values calculated numerically using raw observations and local regression).

Peak Marker Concentration

We determined the time of peak marker concentration for each marker profile according to (1) local regression and (2) G2→G1→O models. We did not assess the time of peak concentration using raw observations because the presence stochastic variation in these observations entailed that the observation with highest concentration may not represent a meaningful physiological peak, but rather an observation which was highest only by chance.

ANOVA and Other Statistical Procedures

Intake of DM, NDF, ADF, and N ($kg \cdot [100\ kg\ BW \cdot d]^{-1}$) was calculated using mass and chemical composition of feed and orts as well as BW.

Intake (DM, NDF, ADF, N), time of peak marker concentration (determined from local regression or G2→G1→O models), and MRT (calculated using raw observations, local regression, or G2→G1→O models in conjunction with Eq. 1 or 2, where appropriate) were analyzed using PROC GLM of SAS (SAS Institute, Inc., Cary, NC) with cow, diet, period, and site as fixed effects. Main effects of cow, period, diet, and site were determined using an *F*-test. When the *F*-test was significant ($P < 0.05$), a Tukey's test was used to identify significant differences between the means.

For comparison of approaches to calculate MRT, we linearly regressed (PROC REG of SAS) MRT values calculated using raw observations (in conjunction with Eq. 1) against values calculated using local regression (in conjunction with Eq. 1) and G2→G1→O models (in conjunction with Eq.. 1 or 2), giving 3 regressions in total.

RESULTS

Forage Composition and Intake

Table 4.1 reports chemical composition of LFA, HFA, and BG forage diets. Concentrations of NDF and ADF increase and N decrease in the order of LFA, HFA, and BG. There is a large difference in NDF (approximately 150 g·kg DM^{-1}) and N (approximately 15 g·kg DM^{-1}) between LFA and BG, with HFA intermediate.

Table 4.2 reports voluntary intake of DM, NDF, ADF, and N of LFA, HFA, and BG diets. Diet significantly influenced intake of DM ($P = 0.022$), with intake of HFA tending to be higher than BG ($P = 0.058$). Diet did not influence NDF, ADF, or N intakes ($P = 0.259$, 0.788, 0.125; Table 4.2). For all chemical fractions, effect of cow was highly significant ($P = 0.012$ or lower; Table 4.2). Intakes were not affected by period for any chemical fraction ($P = 0.050$ or higher; Table 4.2).

General Shape of Yb Marker Profiles

Figure 4.2 shows Yb marker profiles for period 1 (DS, VS, VBS, and RT sites for cows 270, 957, 963, and 968) to illustrate general profile shapes. Considerable stochastic variation is present in the raw observations (shown as symbols in Figure 4.2). The non-parameteric, local regression (producing a set of smooth observations connected by solid, linear splines in Figure 4.2) reduces this variation. It reveals that for most, but not all, profiles, marker concentration follows a biphasic curve, ascending steadily to a peak between 1 and 16 h then declining exponentially thereafter.

Like the local regression, the parameteric regression (the G2→G1→O model; shown as smooth, dotted lines in Figure 4.2) fits the data as a biphasic curve. In some cases, the fit is close to the raw observations and similar to the non-parametric, local regression (e.g., RT of cow 270 in Figure 4.2). In other cases, relative to raw observations and the local regression, the G2→G1→O model appears to peak too early (e.g., VBS of cow 968 in Figure 4.1) or too low (DS of cow 270 in Figure 4.2) or decline too slowly after peak (VS of cow 963 in Figure 4.2).

Visual comparison among profiles revealed that marker concentration peaked in the DS earliest and more sharply relative to other sites, and latest and least sharply in the VBS. Few other consistent differences in shape were found attributable to cow, diet, period, or site.

Comparison of Methods Used to Calculate MRT

Figure 4.3 shows the relationship between MRT values computed with raw observations vs. local regression. The best-fit line for the relationship (Y =

[0.96±0.02]·X + [1.12±0.38]) has a high R^2 (0.993) and low root mean squared error (RMSE; 0.386).

Figure 4.4A shows the relationship between MRT values computed with raw observations vs. G2→G1→O model, using the analytical method (Eq. 2). The best-fit line for the relationship (Y = [1.01±0.26]·X+[5.29±6.45]) has a low R^2 (0.367) and very high RMSE (6.492). Though neither slope nor intercept are significantly different from 1 or 0 (slope: $P = 0.974$; intercept: $P = 0.420$), visually, MRT values calculated using raw observations are systematically smaller than those calculated from the G2→G1→O model, with only 3 of 28 total observations falling below the line $x = y$.

Figure 4.4B shows the relationship between MRT values computed with raw observations (using the numerical method; Eq. 1) vs. G2→G1→O model (using the analytical method; Eq. 2). The best-fit line for the relationship (Y = [0.28±0.018]·X+[18.8±4.4]) has a very low R^2 (0.086) and moderately high RMSE (4.41). Values of MRT calculated using raw observations are not systematically smaller than those calculated with the G2→G1→O model and the numerical method (Figure 4.4B).

Differences in MRT by Cow, Diet, Period, and Site

For raw observations, MRT averaged (mean± SEM) 24.4 ± 4.0 h. This value did not differ by diet ($P = 0.434$), and there existed only weak to moderate trends for period ($P = 0.187$) and site ($P = 0.113$). Statistics were similar for MRT calculated using local regression (owing to agreement between MRT values using each of the source data; Figure 4.3) and are not presented for brevity.

For raw observations, there was a significant main effect for cow ($P = 0.036$). Mean MRT for cow 963 (27.8 ± 1.9 h; mean ± SEM) tended to be higher than that of cow 968 (20.3 ± 1.9 h) ($P = 0.070$), but no other pair-wise comparisons between cows approached significance ($P = 0.228$ or higher). Statistics were again similar for MRT calculated using local regression and not presented.

Differences in Marker Concentration Peak by Cow, Diet, Period, and Site

Assessed using local regression, as described in Materials and Methods, peak concentration time averaged (mean±SEM.) 7.6 ± 2.9 h. This value tended to differ by site ($P = 0.0824$). There were no statistical differences between periods ($P = 0.354$) and diet ($P = 0.5630$). The only significant main effect was for cow ($P = 0.004$), with marker concentration peaking later for cow 963 (10.8 h) than for cow 270 (5.7 h; $P = 0.011$) and 968 (4.7 h; $P = 0.034$).

DISCUSSION

Forage Composition and Intake

The decrease in NDF and ADF and decrease in N in the order of LFA, HFA, and BG was expected; LFA and HFA so named because of these observed differences in chemical composition, and legumes typically have lower NDF and ADF but higher N than grasses (NRC, 2001). The large difference in NDF and N between LFA and BG (with HFA intermediate) ensures a range of forge qualities were used in this experiment.

Intake of legumes is typically higher than that of grasses on a DM basis (Mertens, 1973). This explains why intake of HFA tended to be higher than BG. It was unexpected that intake of LFA was not significantly higher than BG, also. Mertens (1985, 1987) suggested that, when physically restricted, intake should remain constant across diets (1.1

to 1.2 kg NDF·[100 kg BW·d]$^{-1}$). This is within the general range observed in this experiment (Table 4.2) and explains why diet did not influence NDF intake. Similar ADF intake across diets is a consequence of similar NDF intakes combined with similar dietary ratios of ADF to NDF across diets (0.756, 0.690, and 0.648 for LFA, HFA, and BG). Given large differences in N content across diets, we expected N intake to differ by diet, though statistically they did not. Despite the absence of a strong statistical difference, numerical differences were great, with mean N intake of LFA 183% greater than BG (Table 4.2).

Stochastic Variation in Yb Marker Profiles

The substantial stochastic variation in raw observations (Figure 4.2) is probably due to violation of two common assumptions in marker analysis (1) uniform, instantaneous mixing of marked material and (2) steady-state conditions (i.e., constant influx, efflux, and pool size of unmarked material) (Shipley and Clark, 1972). The thick digesta consistency encountered with these forage diets (especially in the compact DS) very likely prevented uniform marker mixing within sampling sites, creating local sampling regions with highly variable Yb concentrations and stochasticity in sampling concentration. Intermittent meal consumption (animals fed most heavily near delivery of fresh feed at 06:00, 14:00, and 22:00) and non-constant digesta passage (Aitchison et al., 1986) very likely caused fluctuation in digesta pool size (violating steady-state conditions) and marker concentration in turn. Very frequent feed delivery (e.g., every hour) would have reduced such fluctuation (c.f., Ulyatt et al., 1984), but we chose not employ very frequent feeding because it strays far from typical management practice and might produce unrepresentative physiological responses. The stochastic variation of

marker concentration is made more conspicuous by the intense frequency of sample collection (every 1 h for the first 4 h, then at least every 4 h for first 48 h). In studies with similar sampling intensity, the level of stochastic variation in dorsal rumen (Balch, 1950; Ellis et al., 1994) and RT (Balch, 1950) sampling sites was similar.

Regression Models to Visualize Marker Profiles

To reduce stochastic variation and better visualize the underlying shape of the profiles, we applied both non-parametric (local quadratic) and parametric (G2→G1→O) regressions to the raw observations. Because it often peaked too early, too low, or declined too slowly after peak, the parametric regression (G2→G1→O) model visually appeared to fit the data inconsistently and at times poorly. From this somewhat subjective assessment, the G2→G1→O model does not appear appropriate to visualize the data, even though it reduced stochastic variation. By contrast, the non-parameteric, local regression reduced this variation while visually fitting the peak and other regions of the marker profiles well. It tentatively appears to be an appropriate tool by which to smooth the raw data and help detect the underlying shapes they imply.

Mean residence time is the time expected for an average particle to escape from a sampling site. It is a function of marker concentration over time (Eq. 1) and thus closely reflects marker profile shape. Consequently, comparing MRT values calculated using different source data (raw data, local regression model, G2→G1→O model) permits us to determine whether these source data imply similar or different profile shapes. From this comparison, we can test our visual finding that the local regression fit accurately reflects the shape of the raw data, but the G2→G1→O model fit does not.

We found close agreement between MRT values computed using raw observations vs. local regression, as indicated by the high R^2 and low RMSE of their regression (Figure 4.3). This close agreement suggests that the underlying shapes implied by these source data are indeed similar. Thus, the local regression successfully reduced stochastic variation in the raw observations without changing the underlying shapes they formed, further supporting the use of the local regression to visualize marker profiles.

We found poor agreement between MRT values computed with raw observations vs. G2→G1→O model. However, the nature of this poor agreement appeared to differ whether we used analytical (Eq. 2) or numerical methods (Eq. 1) to calculate MRT of G2→G1→O model. When we used the analytical method, R^2 was moderate and RMSE was high, indicating marginal precision but high total error. When we used the numerical method, R^2 and RMSE were lower, indicating worse precision but less error overall. Total error is lower because MRT values calculated using raw observations are not systematically smaller than those calculated with the G2→G1→O model and the numerical method (Figure 4.4B), unlike in the prior regression where the analytical method was used throughout. The absence of systematic differences when the numerical method was used for the G2→G1→O model—but their presence when the analytical method was used instead—demonstrates that the numerical method can underestimate MRT relative to the analytical method.

In any event, the poor agreement between MRT values computed with raw observations vs. G2→G1→O model, regardless of MRT calculation methods used, suggests that the underlying shapes implied by these source data differ. This suggests the

fit of the G2→G1→O model can poorly reflect the raw observations, dovetailing with earlier visual findings. The G2→G1→O is thus not appropriate to visualize the marker profile data. This finding also suggests that the kinetic parameters estimated from the G2→G1→O (which reflect the shape of model fit) might poorly describe marker profiles in some cases. For these reasons, we will not present or further discuss MRT, parameter estimates, peak concentration times, or other values associated with the G2→G1→O model.

In contrast to our findings, Ellis et al. (1979), Dixon et al. (1983) (for large particles), Poppi et al. (2001), and Walz et al. (2004) reported that two pool-compartmental models (such as the G2→G1→O model used here) fit RR marker profile data well. However, for all studies except Dixon et al. (1983), sampling intensity was relatively low (at most every 3.5 [Ellis et al., 1979], 4 [Poppi et al., 2001], or 6 [Walz et al., 2004] h), which tends to artificially improve model fit. Ellis et al. (1994), who used a similar sampling frequency as we did, noted large deviations between observed marker concentration and that predicted by the G2→G1→τ→O model (the G2→G1→O model with a time delay) for the dorsal rumen. With fecal excretion data and intense sampling frequency, Matis et al. (1989) noted that the G*n*→G1→O family of models (to which G2→G1→O belongs) qualitatively displayed poor fit to peak concentration observations, the principal problem we found with the G2→G1→O model applied to our RR data. None of these prior reports (whether finding the two-compartmental model adequate or not) critically appraised two-compartmental models by comparing (1) their fit to a non-parametric regression or (2) MRT values calculated from them with those calculated from raw observations. Our more critical appraisal, which used both of these comparisons,

strongly suggests that two-compartmental models require improvement in order to accommodate RR marker profiles.

Differences in Yb Marker Profiles by Cow, Diet, Period, and Site

The local regression reveals the marker profiles have an underlying biphasic shape. This general finding is consistent with Balch (1950) for the dorsal rumen and RT when long hay was fed; Ellis et al. (1979) for large particles in the "upper" and "lower" rumen; Ellis et al. (1994) for the ventral rumen; and Poppi et al. (2001) for the raft and ventral rumen. However, an initial ascending phase was not present in Balch (1950) for the dorsal rumen and RT when ground hay was fed; Ellis et al. (1979) for small particles in the "upper" and "lower" rumen; and Walz et al. (2004) for most (9 out of 144) profiles for five sites in the reticulorumen, though this may be due the limited number of sampling points (only 2 within first 16 h) in this dataset. The biphasic shape present in most, but not all, of our profiles and prior studies demonstrates that particle flow from the RR usually does not follow simple first-order kinetics (which would produce one monotonically descending phase), despite the common assumption that is does (e.g., Waldo, 1972; Ørskov and McDonald, 1979).

The lack of consistent differences in marker profile shape across cow, diet, period, and site (except in the peak region between DS and VBS) was striking. In some cases profile shapes from different cows, sites, diets, or all three appeared very similar, such as DS and VBS profiles of cow 957 as well as DS profiles of cow 270 and 968 in Figure 4.2. In Walz et al. (2004), few differences may be found visually among the many sites sampled, but it was not clear whether similarity was due to true physiological

differences or due to infrequent (every 6 h at most) sampling scheme (causing low resolution of profiles).

As explained above, MRT is a quantitative measure that closely reflects underlying marker profile shape. We compared MRT values by cow, diet, period, and site to quantitatively test our visual finding that profile shapes were similar across these factors. Peak marker concentration time is another aspect of marker profile shape that could be assessed quantitatively, and we compared these values across factors with the same aim.

Our finding that neither MRT nor peak marker concentration differed by diet or period suggests these factors did not consistently affect marker profile shape. Site affects marker profile marginally at most; while peak marker concentration tended to differ by site, there were no such differences in MRT. Cow, however, significantly affected both MRT and peak marker concentration. This finding, along with our other statistical and visual and results, suggests that cow and cow alone exerted a strong and consistent effect on profile shape.

Difference between Dosing and Sampling Sites within the DS

For two DS profiles (cows 968 and 270 of period 1; Figure 4.2), marker concentration peaks at the first non-zero hour sampling time (hour 1), whereas it more gradually ascends (reaching a peak between 4 to 16 h) in the five other DS profiles (as shown in Figure 4.2 for cows 957 and 963). If sampling and dosing site within the DS were the same, marker concentration should peak immediately by sampling hour 1 (the first sampling point after dosing), when the marker dose is undispersed and creates a region of high Yb concentration (as observed for cows 968 and 270 of period 1). If

dosing site differs from sampling site, marker will be absent from sampling site at first but disperse there over time, creating a protracted ascending phase (as observed for the other 5 profiles). Consequently, one can infer sampling and dosing site within the DS were the same for cows 968 and 270 of period 1 but differed for all other profiles.

Difference between DS sampling and dosing sites was also observed by Ellis et al. (1979), Poppi et al. (2001) and Walz et al. (2004) and emphasizes that mixing in the DS is neither instantaneous nor uniform. It is unclear why dosing and sampling sites in the DS differ in the majority, but not all, profiles in this study.

Particle Flow Kinetics in the RR

Several studies have attempted to elucidate RR particle flow kinetics either radiologically or by monitoring distribution of particle size and density. These studies taken together suggest the following. Newly ingested particles enter the upper cranial sac (**CS**), where RR wall contractions propel them into DS (Ehrlein, 1980; Wyburn, 1980; Deswysen and Ehrlein, 1981). Particles are trapped in the tightly-woven DS digesta, owing to their high buoyancy (from entrapped gas) and large initial particle size (Evans et al., 1973; Sutherland, 1988). Over time, buoyancy decreases (as gas escapes) as does particle size, permitting particles to escape from the DS and enter the ventral rumen (Evans et al., 1973; Sutherland, 1988) as liquid flow washes them downwards (Erhlein, 1980). In the more liquid ventral rumen, particles flow in a circular motion through the VS and VBS while they sediment (Waghorn and Reid, 1977; Wyburn, 1980). Once they completely sediment onto the ventral rumen wall, contractions carry them to the CS and then the RT (Wyburn, 1980; Erlein, 1980). In the RT, larger, more buoyant particles are either (1) ejected back to the CS or (2) aspirated upwards during rumination and re-

deposited into the DS after traveling through the cranial rumen (Ehrlein, 1980; Wyburn, 1980; Sutherland, 1988). Small and dense particles in the RT are trapped by honeycomb cells of the RT and conveyed to the reticulo-omasal orifice, where they escape into the omasum (Reid, 1984).

This view suggests particle flow occurs primarily in the sequence CS→DS→VS →VBS↔VS↔RT↔omasum or CS→DS, which generally follows with the order of RR wall contractions (RT→CS→DS→VS→VBS) (Erlein, 1980). By endoscopic observation of dyed particles, Lirette and Milligan (1990) propose circular movement of digesta following in the opposite direction (DS→RT→CS→VS→VBS→caudo-dorsal blind sac→DS), but this isolated suggestion is difficult to accept over multi-faceted evidence to the contrary. According to the probable flow sequence CS→DS→VS→VBS↔VS↔RT↔omasum or CS→DS, MRT values should be in the order $MRT_{DS} < MRT_{VS} \approx MRT_{VBS} < MRT_{RT}$ (where MRT_i refers to MRT of the i^{th} site) because of the order in which particles enter and exit these sites.

However, in our dataset, there was no significant difference in MRT by site—i.e., differences in MRT by site, if any, are so small that they are masked by variability in MRT across replicates. Similarity in MRT between the dorsal and ventral rumen was also found in data of Dixon et al. (1983) (compared within particle size class) and Ellis et al. (1994). Within diet, Walz et al. (2004) also found similarity in MRT across five sites in the RR (craniodorsal rumen, DS, caudodorsal rumen, VS, RT), though from examining their data in isolation it is not clear whether this similarity arose simply from difficulty to discriminate differences with the infrequent sampling interval (every 6 h at most). It is unclear if MRT differences exist between dorsal and ventral rumen in Poppi et al. (2001)

because the authors claim, without presenting statistical test results, that kinetic parameters (from which MRT is calculated) are similar but MRT differ across sites. Values in our dataset did not follow the expected MRT order ($MRT_{DS} < MRT_{VS} \approx MRT_{VBS} < MRT_{RT}$) even on a numerical basis, with the numerical order MRT_{VS} (21.5 h) < MRT_{RT} (23.1 h) < MRT_{VBS} (25.0 h) < MRT_{DS} (26.7 h) (SEM = 1.8 h).

Similar MRT values across sites suggests that once a particle escapes from the DS for the final time (see below), it resides in the ventral regions (VS, VBS, RT) only shortly before escaping; only under this condition can MRT_{VS}, MRT_{VBS}, and MRT_{RT} not be appreciably greater than MRT_{DS}, as found in this study. In support of this idea, Poppi et al. (2001), who modeled flow of Yb-marked stem and leaf through the DS and VF, found that particle escape from the VS must occur rapidly relative to the DS. Also, Welch (1982) found plastic particles arrived in the RT quickly (within ~35 min) after original placement in the VS.

This conclusion does not rule out the possibility that particles to spend appreciable time in the ventral regions at some point during their residence in the RR. Indeed, we could envision the following scenario consistent with the MRT results of this study: after a sojourn in the DS, particles (1) exit the DS and enter the VS, (2) spend appreciable time in the ventral regions (VS, VBS, RT), (3) are recycled into the DS (via rumination then re-deposition into the CS), (4) exit the DS and enter the VS once more, then (5) continue steps 2-4 or quickly escape from the VS, VBS, and finally RT (via reticulo-omasal orifice). Particles can follow steps 2-4 and still ultimately result in $MRT_{DS} \approx MRT_{VS} \approx MRT_{VBS} \approx MRT_{RT}$ because the way in which residence time is accrued by particles. If particles re-enter the DS (via recycling) after residing in the

ventral regions (VS, VBS, RT), the residence time they accumulate in the DS will include that accrued in the VBS, VS, and RT prior to being recycled. This process results in similar residence times across sites, and consequently MRT (calculated from the residence time distribution) will also then be similar. However, whether or not recycling occurs, the order of MRT values found in this experiment again demonstrate that once a particle escapes from the DS the final time, it must escape from the ventral regions (VS, VBS, RT) soon after entry. Figure 4.5 illustrates the findings of the above discussion, assuming the direction of flow between sites follows that delineated beforehand.

The above discussion and Figure 4.5 imply that if appreciable recycling of particles from the RT to the DS does not occur, escape from the DS is the limiting process to passage from the RR, consistent with suggestions by Evans et al. (1973), Fainchey (1986), and Sutherland (1988). If appreciable recycling does occur, escape from the DS need not be rate-limiting, consistent with the contention by Mathison et al. (1994) that escape through the reticulo-omasal orifice, not the DS, limits passage. Determining the extent of such recycling, in conjunction with these results, could hence demonstrate how strongly the DS acts as a barrier to passage from the RR.

Because the conclusions above (i.e., those illustrated in Figure 4.5) are founded on a negative finding (i.e., lack of MRT differences across sites), their strength relies on our experiment's power to detect MRT differences across sites. According to a power analysis (Kutner et al. 2004), an *F*-test could detect a difference of 7.99 h—specifically, the difference between sites with highest and lowest MRT values—in our data with a statistical power ($1-\beta$) of at least 0.8 and level of significance (α) of 0.05. In other words, if the true range of MRT values across sites was greater than 8 h, our experiment would

have had a reasonable chance (≥80%) to find a significant ($P < 0.05$) difference in MRT values across sites. Thus, our experiment is relatively sensitive in detecting differences in MRT values across sites, our negative finding is meaningful, and the conclusions made from this finding have merit.

Limitations of our Analysis

The chief limitation of our analysis is our inability to find a suitable model to deliver kinetic parameter estimates. Because they describe marker profile shape quantitatively and concisely, kinetic parameter estimates would allow us to compare particle flow kinetics more thoroughly and rigorously than our analysis above.

We reported some results (MRT values) gathered with the G2→G1→O model because we could achieve model fit to the data. Our original goal in this study was to build a more compelx compartmental model that represents bidirectional flow through each of the sampling sites (DS, VS, VBS, RT). In so doing, we could quantify the net direction of flow through the sites, determine the flow paths of particles within the RR, and consequently test view of particle flow kinetics delineated by radiological and particle analysis studies (Evans et al., 1973; Waghorn and Reid, 1977; Erlein, 1980; Wyburn, 1980; Deswysen and Ehrlein, 1981; Sutherland, 1988). However, fitting data to this model (and, later, highly simplified versions thereof) led to failed convergance, very poor fit (negative R^2), parameter values that approached either 0 or infinity, or a combination of these problems.

We attribute the poor model fit to the stochastic variation in the data (which violates the ideal compartmental behavior assumed by these models) and difficulty in estimating sizes of sampling sites (which were not measured in this experiment). We

caution future researchers who attempt to build a similarly complex model. Poppi et al. (2001) were able to build a compartmental model that simulated flow through the DS and VS alone, though inferring particle flow dynamics through the entire RR from examining only 2 sites is questionable. Our approach of comparing MRT values, along with radiological and particle studies, offer the most cohesive picture of particle flow kinetics in the RR achievable at this time.

CONCLUSION

In our experiment, variability in marker profile shape (indicated by visual assessment and values of MRT and peak marker concentration time) remains largely unexplained by diet, site, and period; only cow has a consistent effect on profile shape. Because profile shape relates to particle flow kinetics and parameters linked to it (e.g., digestibility and voluntary intake), the source of this variation is important for future efforts to uncover.

Development of a parametric model suitable to quantitatively represent particle flow in the RR is imperative. Only once such a model is developed can marker data be quantitatively examined and compared to the fullest extent possible.

Our inference that a particle quickly leaves the RR after escaping the DS the final time has an important practical implication: designing feed products to immediately enter the ventral rumen (bypassing the DS) and resist regurgitation guarantees their quick passage from the RR.

Table 4.1. Chemical composition of high-quality alfalfa (LFA), low-quality alfalfa (HFA), and bromegrass (BG) forage diets fed to cows during passage trial

	Diet					
	LFA		HFA		BG	
Chemical composition (g·kg DM^{-1})	mean	SEM	mean	SEM	mean	SEM
DM, $g \cdot kg^{-1}$	888	6	887	2	884	4
NDF	451	22	520	24	603	39
ADF	341	20	359	20	392	61
N	35.2	1.9	23.5	1.0	20.6	2.3

Table 4.2. Voluntary intake of bromegrass (BG), high-quality alfalfa (LFA), and low-quality alfalfa diets (HFA) fed to cows during passage trial

	Diet				*P*-values		
Intake (kg·[100 kg BW·d]$^{-1}$)	BG	LFA	HFA	SEM	diet	period	cow
DM	1.82	2.11	2.32	0.24	0.022	0.050	<0.001
NDF	1.23	0.94	1.16	0.27	0.259	0.385	0.016
ADF	0.89	0.74	0.79	0.22	0.789	0.207	0.012
N	0.038	0.070	0.059	0.10	0.125	0.659	<0.001

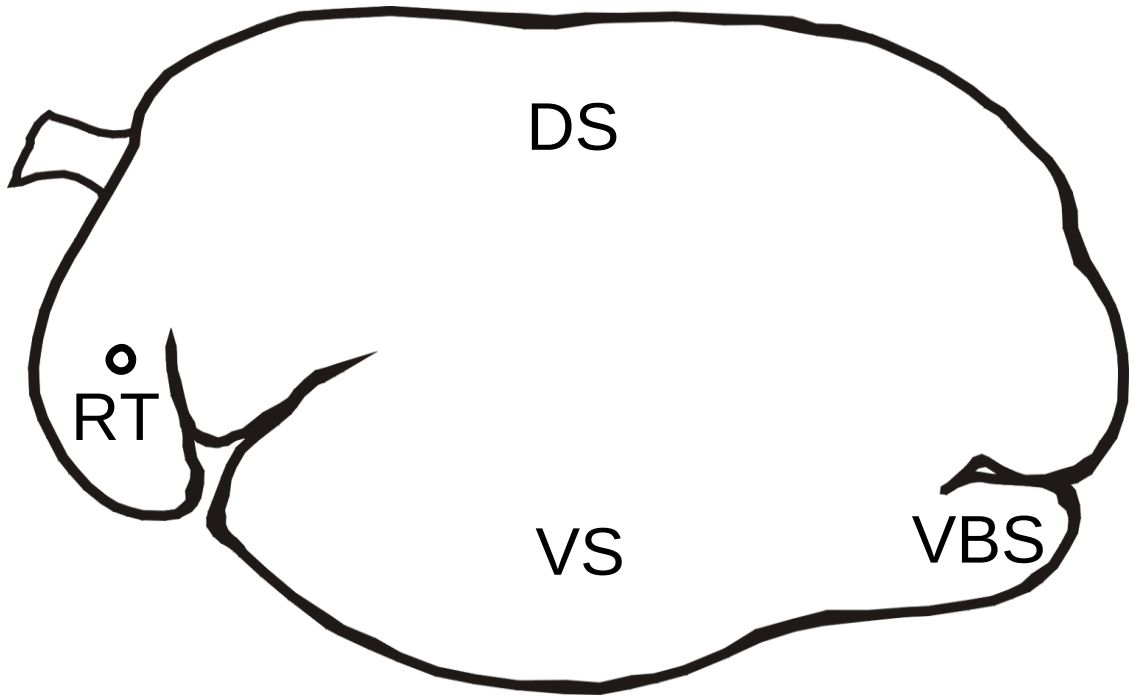

Figure 4.1. Location of dosing (mid-dorsal sac [DS]) and sampling sites (DS, mid-ventral sac [VS], caudo-ventral blind sac [VBS], ventral reticulum [RT]) within the reticulorumen.

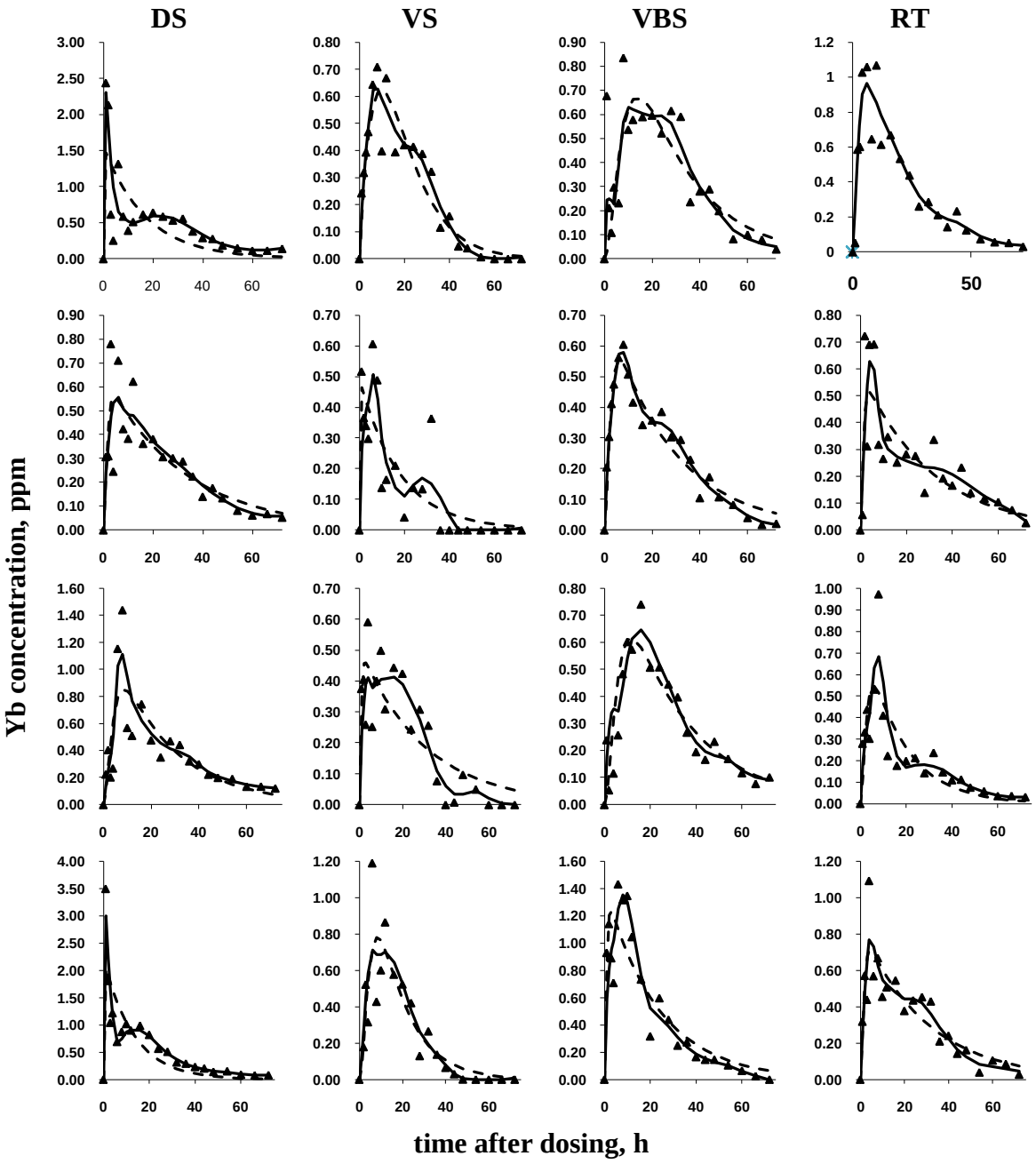

Figure 4.2. Yb marker profile in (from left to right) dorsal sac (DS), mid-ventral sac (VS), caudo-ventral blind sac (VBS), and ventral reticulum (RT) for cows (from top to bottom) 270, 957, 963, and 968 during period 1. Raw observations are shown with filled triangle symbols (▲). Observations given by local regression model (with Gaussian kernel and nearest neighbor bandwidth of 0.4) are connected by linear splines (solid lines); symbols are omitted for clarity. Fit of G2→G1→O model is shown by dotted lines.

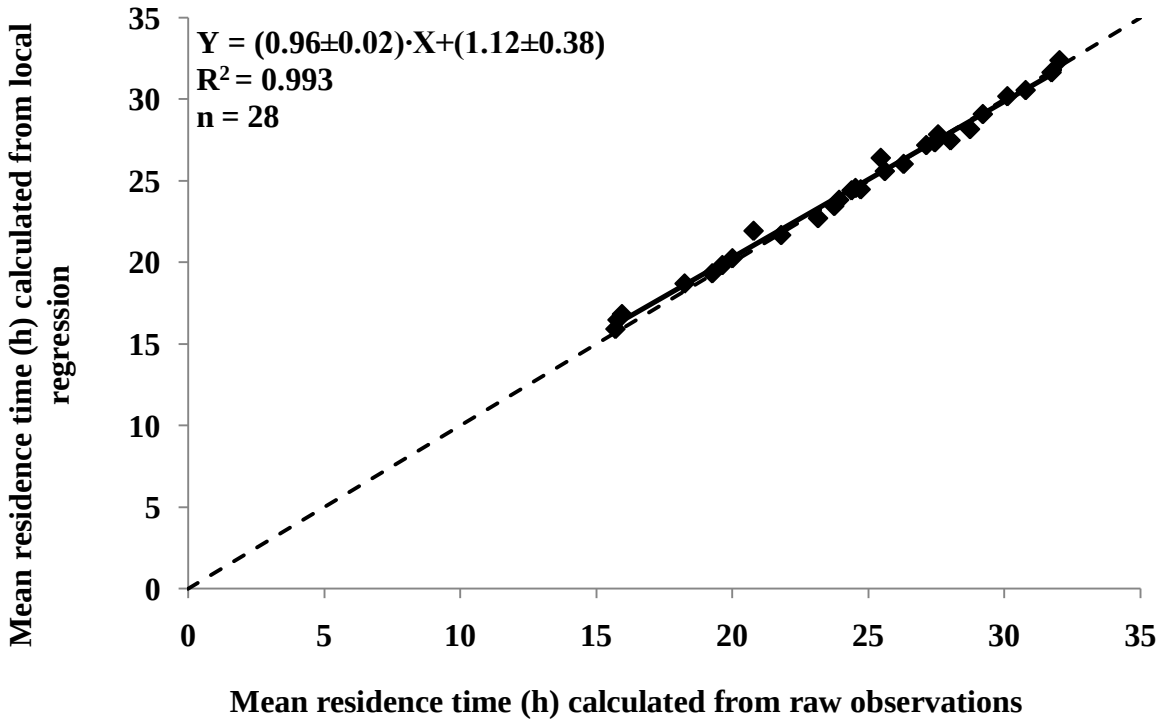

Figure 4.3. Comparison of mean retention time values calculated using raw observations and local regression model. In each case, the numerical method (Eq. 1) was used for calculation. Dotted and solid lines represent $x = y$ and best-fit regression, respectively.

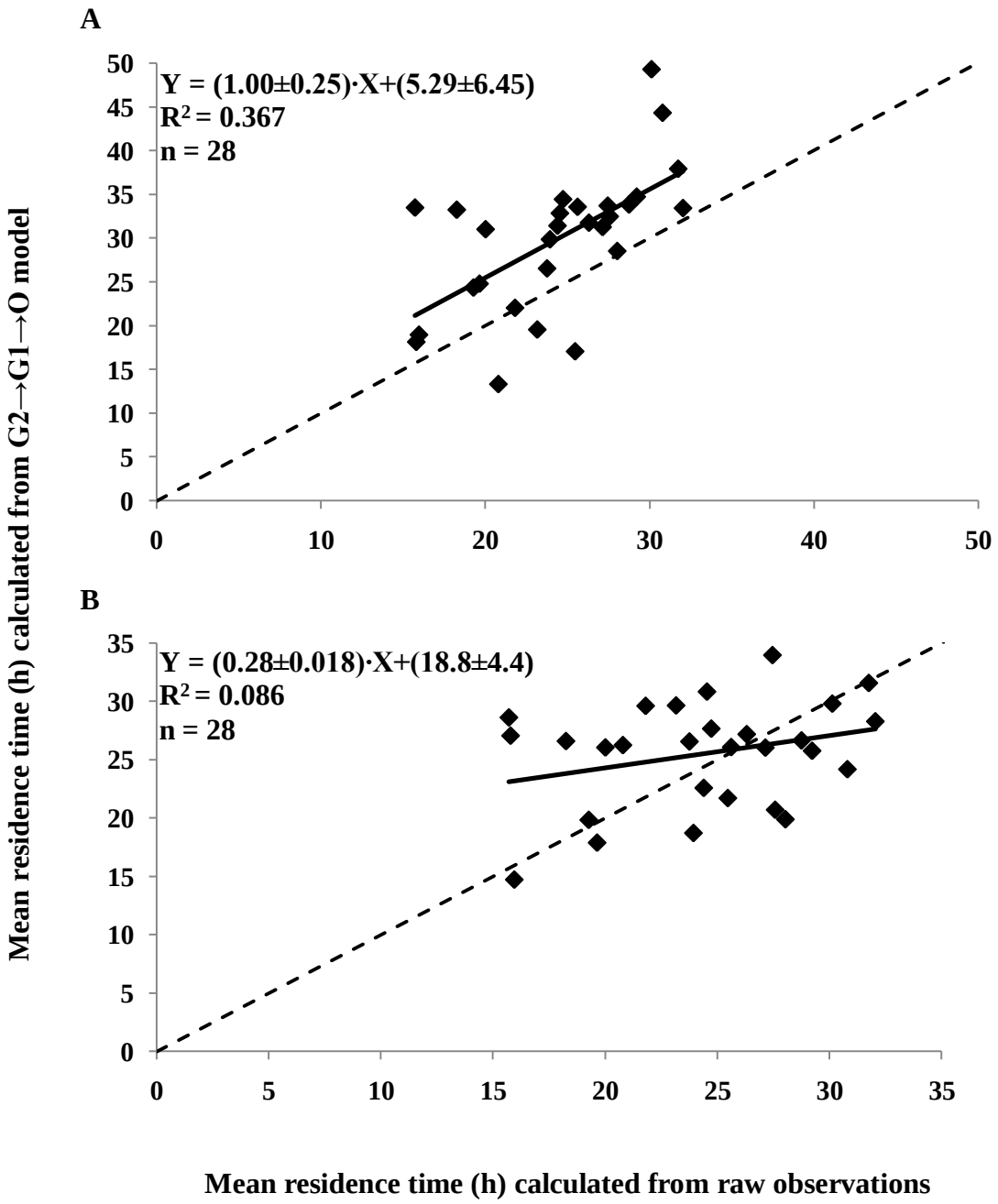

Figure 4.4. Comparison of mean retention time values calculated using raw observations and the numerical method (Eq. 1) with those of the G2→G1→O model and (A) the analytical method (Eq. 2) or (B) numerical method (Eq. 1). Dotted and solid lines represent $x = y$ and best-fit regression, respectively.

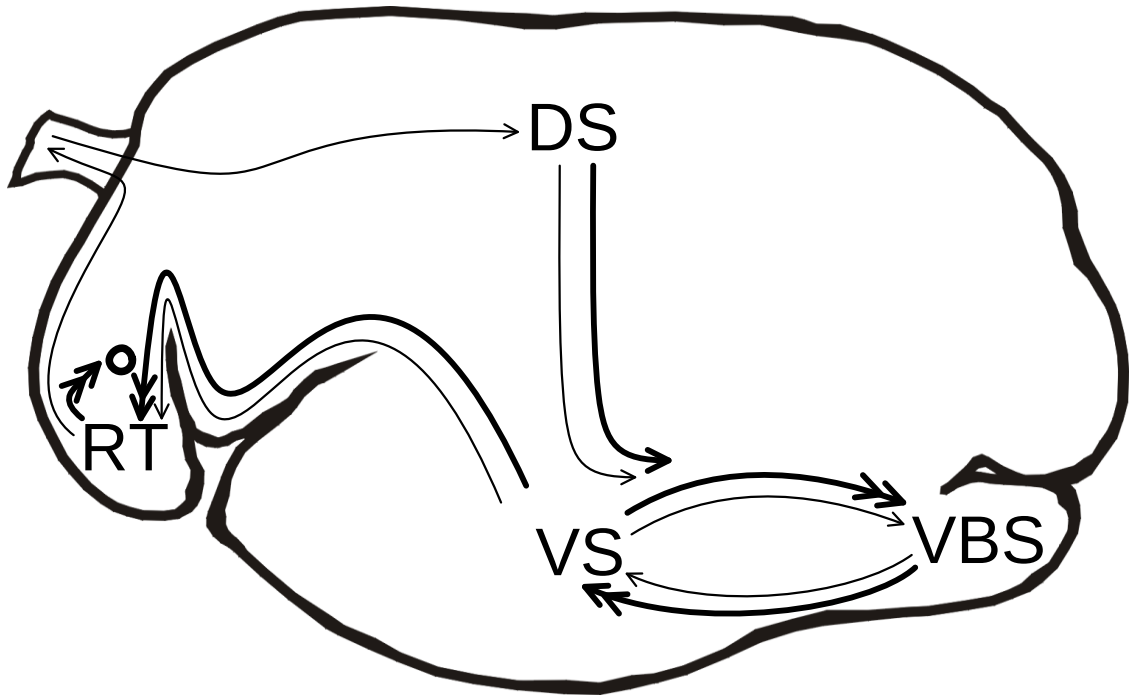

Figure 4.5. Proposed kinetics of particle flow across sampling sites (mid-dorsal sac [DS], mid-ventral sac [VS], caudo-ventral blind sac [VBS], ventral reticulum [RT]) in the reticulorumen. Thin and thick arrows represent particle flow paths when particles will and will not be subsequently recycled to the DS (via regurgitation during rumination). Double-headed arrows indicate particle escape occurs very quickly from the site where the arrow originates; single-headed arrows indicates escape can occur either quickly or slowly. See text for justification of this representation.

CHAPTER 5

A MECHANISTIC MODEL FOR PREDICTING INTAKE OF FORAGE DIETS BY RUMINANTS

ABSTRACT

Accurate voluntary feed intake (VFI) prediction is critical to the productivity and profitability of ruminant livestock production systems. Simple empirical models have been used to predict VFI for decades but are inflexible, restrictive, and poorly accommodate many feeding conditions, such as those of developing countries. We have developed a mechanistic model to predict VFI over a range over a range forage diets (low- and high-quality grasses and legumes) by wild and domestic ruminants of varying physiological states (growth, lactation, gestation, non-productive). Based on chemical reactor theory, the model represents the reticulorumen, large intestine, and blood plasma as continuous stirred reactors and the small intestine as a plug flow reactor. Predicted VFI is that which (1) fulfills an empirical relationship between chemostatic and distention feedbacks observed in the literature, and (2) leads to steady-state conditions. In all model validations, agreement with observed feed intake was high ($R^2 > 0.9$, root mean square prediction error < 1.4 $kg \cdot d^{-1}$). Root mean square prediction error for our model was only 67% of that of the Beef NRC model, the leading empirical prediction system for cattle. These results together demonstrate that our model can predict ruminant VFI more broadly and accurately than prior methods and, by consequence, serve as a crucial tool to ruminant livestock production systems.

INTRODUCTION

Predicting voluntary feed intake (**VFI**) is critical to the profitability and productivity of ruminant livestock production systems (Yearsley et al., 2001). Since their introduction in the 1960s (Conrad et al., 1964), multiple regression and other simple empirical equations (Forbes, 2007) have been embraced for VFI prediction. Typically, these equations are parameterized with data encompassing a narrow range of biological conditions (e.g., focusing on only one animal species, physiological state, environment, and dietary type; Forbes, 2007) because correlations between predictor variables and VFI vary across conditions. Whereas these equations can have good predictive power within the specific conditions used for parameterization, extrapolation is not appropriate due to the equations' purely empirical basis (Yearsley et al., 2001). Because they have generally been developed for conventional feeding situations in developed countries (cattle and sheep fed high-quality temperate forages and grain), these equations can be restrictive, particularly for novel feeding situations (such as for new or unconventional livestock species; NRC, 1991, 2007) or in developing countries (where goats, in addition to sheep and cattle, and poor-quality tropical forages are mainstays; Timon and Hanrahan, 1986; Chenost and Kayouli, 1997).

In contrast to empirical models, mechanistic models estimate VFI by modeling underlying intake regulation mechanisms (Illius and Allen, 1994; Illius et al., 2000; Yearsley et al., 2001). Their broader biological aims and reliance on more than one dataset for parameterization grants them wider applicability than empirical models. However, their historically low precision, in addition to more theoretically-focused aims, has led to little adoption in practice.

The objective of this study was to develop and evaluate a mechanistic model that reliably predicts VFI over a range of forage diets by wild and domestic ruminants of varying physiological states.

MATERIALS AND METHODS

Our model of VFI represents digestive events within the ruminant gastrointestinal tract (**GIT**). It is based on chemical reactor theory (Penry and Jumars, 1987) and compartmental modeling (Jacquez, 1985) and is mechanistic, dynamic, and deterministic (Thornley and France, 2007).

General Structure

The model's representation of digestion begins with feed being consumed and entering the reticulorumen (**RR**), modeled as a continuously-stirred reactor (after Penry and Jumars, 1987; Mertens and Ely, 1979) Nutrients in the food include soluble carbohydrate (**SCHO**; low molecular weight carbohydrates, pectins, and fructans), insoluble, non-fibrous carbohydrate (**InNFC**; starch and other insoluble non-structural polysaccharides), digestible hemicellulose (**DHEM**), indigestible hemicellulose (**IHEM**), digestible ADF (**DADF**), indigestible ADF (**IADF**), soluble protein (**SP**; amino acids, short-chain peptides, hydrophilic proteins), insoluble digestible protein (**InDP**), indigestible CP (protein bound to ADF and lignin nitrogen), lipid (FAT), and ash. Metabolites generated from fermentation of feed include VFA and ammonia (NH3).

Once in the RR, these entities enter into their respective RR compartments (with the exception of ash and indigestible CP, which are assumed to be inert and not explicitly represented). Entities exit their RR compartments via (1) microbe (MICRO) mediated hydrolysis (InNFC, DHEM, DADF, InDP), (2) uptake by MICRO (SCHO, SP, NH3), (3)

absorption through the RR wall (VFA, NH3), and (4) passage through the RR-omasal orifice (all entities). SCHO and SP taken up by MICRO are used for MICRO growth or fermentation. Growth produces MICRO biomass, comprised of InDP, InNFC, FAT, and nucleic acids (**NcAc**). Fermentation of excess SCHO and SP produces VFA and NH3.

Entities that pass through the RR-omasal orifice flow through the omasum are exposed abomasal acid hydrolysis, which converts a fraction of InDP to SP. They then enter the small intestine (**SI**), represented as a plug flow reactor (after Penry and Jumars, 1987). Once entities enter their respective compartments, they can exit via (1) hydrolysis by SI enzymes (InNFC, InDP), (2) absorption through the SI wall (SCHO, SP, FAT, NH3, NcAc), and (3) passage through the ileocecal junction (all entities). Entities that pass through the ileocecal junction enter large intestine (**LI**) compartments.

The LI is modeled as a continuously-stirred reactor and constructed almost identically to the RR (after Danfaer, 1990). Entities exit their compartments via routes similar to those in the RR. For simplicity, the model does not directly simulate MICRO uptake of NcAc, though it is observed experimentally (Wallace et al., 1997); for this reason, the model immediately converts NcAc entering the LI to equivalent amounts of SCHO and NH3 (which MICRO take up) to effectively permit MICRO to take up NcAc. Passed, undigested material is excreted in the feces.

Absorbed amino nitrogen and NH3 is transferred to a blood plasma urea space (modeled as a continuously-stirred reactor; after Baldwin, 1995), where they are converted to urea and excreted into the urine or into the GIT as an endogenous secretion. Endogenous protein (assumed for simplicity to be entirely SP) is also secreted into the

GIT through the saliva or other sources (e.g., sloughing of GIT epithelium, mucin secretions by goblet cells, enzymatic secretions).

Viscera and other organs outside the GIT are not included explicitly, though some of their functions that determine intake and digestibility are implicit; for example, conversion of NH3 to urea is a function of the liver and kidneys, though neither is represented in the model.

Model Equations

We used a system of differential equations to quantify the fluxes of nutrients, metabolites, and MICRO across compartments and spaces, as described above. These equations follow the general format

$$\frac{d < \text{size of compartment } j >}{dt} = < \text{inflow to compartment } j > - < \text{outflow from compartment } j >$$

where t = time and <inflow to compartment j> and <outflow from compartment j> are the sums of all processes causing entity j to flow into and out of compartment j, respectively.

Equations describing digestive events in the RR, LI, SI, and plasma are provided in Table 5.1, and supporting auxiliary equations are presented in Table 5.5. Equations for a MICRO submodel are presented in Table 5.6. Miscellaneous equations are given in Table 5.7. All other equations are provided below in the text. Units, abbreviations, and symbols used in these equations are provided in Appendix 1.

Feedback Signals and Prediction of VFI

In simulating digestion for a given level of VFI (kg DM·d^{-1}), the model computes two key parameters: (1) RR fill with space-occupying NDF (kg·100 kg BW^{-1}), (2) the

quantity of nutrients and metabolites the gastrointestinal tract absorbs per unit time, with NE (expressed in units of NE_m [Mcal·100 kg BW^{-1}·h^{-1}]) and protein (kg·100 kg BW^{-1}·h^{-1}) of particular importance. Both of parameters have been proposed to regulate intake in the ruminant (Forbes, 2007). We compared the computed value of these two parameters to optimal or reference values by taking the ratio between reference and actual parameter values. We define the ratio of optimal (C_r) to actual (NEI) NE intake as the chemostatic feedback signal (C_s)—i.e.,

$$C_s = \frac{C_r}{NEI}$$

The value of C_r is equal to the energy required to reach genetic production potential (defined here as the production level expected from an individual of a given species, BW, physiological state, production stage, and sex under optimal nutritional, environmental, and managerial conditions) and computed as described below. We additionally define the ratio of reference (D_r) to actual ($<^{RR}NDF>$) RR fill with NDF as the distention feedback signal (D_s)—i.e.,

$$D_s = \frac{D_r}{<^{RR}NDF>}$$

We define D_r as $<^{RR}NDF>$ when $C_s = 1$ and set its value to 1.7 kg·100 kg BW^{-1}, a value found by applying the model to a calibration dataset (Mertens, 1973). We used NDF as a measure of RR fill following its historic use in the literature (Mertens, 1987) and because its use led to higher system stability (faster and higher convergence rates during model solution procedures) relative to other potential measures.

To find an empirical relationship between C_s and D_s, we calculated values of C_s and D_s from two studies in the literature (Bernal-Santos, 1989; Bosch et al., 1992a,b).

We estimated C_s from milk output and BW reported by the two studies in conjunction with energy requirement equations of the NRC (2000, 2001). Following our definition of genetic potential, we assume that milk output realized on these high-quality diets approached the animals' genetic potential. We estimated D_r from the value of indigestible NDF (Bernal-Santos, 1989) or lignin (Bosch et al., 1992a,b) when $C_s = 1$, the definition of the reference value for RR fill. We used indigestible NDF and lignin instead of NDF (as in the model) because these measures of RR fill were most consistently related to C_s across these datasets (though NDF gave greater system stability in the model). We found that C_s and D_s followed the relationship

$$D_s = C_s^{\alpha} \quad [1]$$

where α is a shape parameter found by regression (using log-transformed values with PROC REG of SAS; SAS Institute, Inc., Cary, NC) and equal to (mean±SEM) -0.78±0.16 ($P < 0.001$; Figure 5.1).

Eq. 1 was derived under circumstances where the dietary energy:protein ratio was low, though high ratios strongly reduce intake (Moore and Kunkle, 1995). To accommodate diets with high ratios, we added a feedback signal for energy:protein, using an equation form proposed by Fisher (1996)

$$P_s = 1 - \gamma \cdot e^{-e^{(\delta - \varepsilon \cdot NE:P)}}$$

where P_s = energy:protein feedback signal; *NE:P* = ratio of NE to protein absorption from the GIT (Mcal·kg^{-1}); and γ, δ, and ε = shape parameters (unitless). The value of γ (0.7) is from Fisher (1996) and δ and ε (6, 0.17) were found by applying the model to a calibration dataset (Mertens, 1973). This signal describes the fraction of VFI realized

when energy:protein feedback occurs relative to the case where no feedback occurs. After incorporating this signal, the relationship between C_t and D_t can be shown to become

$$D_s = \frac{C_s^{\alpha}}{P_s} \qquad [2]$$

We solved the model's system of differential equations to find a level of VFI (predicted VFI) that (1) yields values of C_s, D_s, and P_s that fulfill Eq. 2 and (2) lead to steady-state conditions. After Fisher (1996), we solved the equations by encoding them into Microsoft Excel 2007 (Microsoft Corporation, Seattle, WA) and applying Euler's method with time step Δt between 0.001 and 0.01 d. We considered convergence reached when fractional change in VFI between iterations was less than $1 \cdot 10^{-6}$, and the final solution was insensitive to the time step used.

Other Notes on Model Structure

We have modeled many digestive processes as following simple first-order and Michaelis-Menten saturation kinetics, as in previous, related models (Penry and Jumars, 1987; Illius and Allen, 1994). However, in accordance with experimental observations (Hungate, 1966; Chapter 2), we represented passage in the RR with two sequential passage rates (Blaxter et al., 1956) and hydrolysis in the RR and LI with age-dependent kinetics (following a second-order Erlang distribution; Matis, 1972). We have devised "subcompartments" (c.f., Table 5.4) as mathematical artifices to represent these complex kinetic schemes with only simple first-order equations.

We use the term "compartment" loosely when referring to SI entities; compartments are strictly defined as well-mixed spaces (Jacquez, 1985), but by definition

there is no longitudinal mixing in plug flow reactors. We assume that secretion of endogenous protein into the SI occurs evenly along the SI length.

Given the importance of the microbial ecosystem in the ruminant animal (Hungate, 1966), we included within the model a submodel of MICRO (Table 5.6). MICRO, which are represented as one homogenous entity, take up SCHO, SP, and NH3 according to Michaelis-Menten kinetics. After discounting total SCHO uptake for a MICRO maintenance energy requirement, the first-limiting nutrient (SCHO or N) determines growth. A portion of SCHO is used as a carbon source for MICRO biomass synthesis and a portion fermented for energy to drive growth. Any SCHO or SP remaining (as a result of being non-limiting to growth) is fermented, mirroring the observation that copious amounts of SCHO (van Kessell and Russell, 1996) and SP (Russell et al., 1983) are fermented in such cases.

In addition to D_s, C_s, and P_s, which directly modulate VFI, our model includes a protein feedback (P_d) that indirectly affects intake by modifying degradation rates of insoluble nutrients according to ratio of N:SCHO taken up by microbes (Eq. 3a,b, Table 5.7). This feedback follows a Michaelis-Menten relationship. We predict the slow-passage rate of particles from the RR ($^{RR}k_{p2}^{j}$) from indigestible NDF fill of the RR, employing Michaelis-Menten kinetics and assuming all particles pass at the same rate as INDF (Eq. 19, Table 5.5). The equation for *NEI* (Eq. 4, Table 5.7) follows standard conventions, except for the use of the heat increment of eating (H_e; see Appendix 2).

Model Parameters

Model inputs include forage chemical composition (NDF, ADF, CP, ash) as well as forage type (early or late-cut alfalfa, C_3 grass, C_4 grass, grass/legume mixture), which

determine dietary degradation characteristics. C_r is calculated by estimating genetic production potential (by locating a study that reports productive output under optimal conditions), then NE (expressed in NE_m equivalents) required to reach that production level (referencing Blaxter, 1989; NRC, 2000, 2001, 2007). All other parameters are constants estimated from 65 publications (Appendix 2, Tables 5.8 – 5.14) and our own unpublished data. The model currently accommodates one-ingredient diets containing only forage because of the complexity and number of model equations.

Model Validation

We compared model-predicted VFI with actual values from 15 studies reporting ad libitum consumption of all-forage diets by 14 bovid, 4 cervid, and 1 giraffid species during gestation, lactation, growth, or non-productive physiological states. Studies and species included are given in Table 5.1, and descriptive statistics of these studies are given in Table 5.2. We focused on all-forage diets because these are the most pervasive one-ingredient diets (as required by the model), though we included a wide range of dietary qualities (Table 5.2).

We conducted validations with the full dataset (n = 158) and a subset of domestic species (cattle, sheep, goats) only (n = 118). We also compared performance of our model with that of the NRC (2000) using the 43 cattle observations (including growing, lactating, gestating, and non-productive animals) within our validation dataset to which we could apply the NRC (2000) equations. We assessed mean and linear biases of model predictions using residual analysis (St-Pierre, 2003).

RESULTS AND DISCUSSION

Validation Results

We found good agreement between model-predicted and actual values of VFI for the full dataset ($\text{actual VFI} = [0.99 \pm 0.02] \cdot \text{predicted VFI} + [0.35 \pm 0.16]$; R^2 = 0.910, root mean square prediction error [RMSPE], 1.35 kg·d^{-1}, n = 158), indicated by high R^2 and low RMSPE (Figure 5.2A). Residual analysis (St-Pierre, 2003) revealed statistically significant but numerically minor biases in both intercept (-0.28 kg·d^{-1}; P = 0.008) and slope (-0.076; P = 0.001).

The model over-predicted the two giraffe observations in the validation dataset (from Foose, 1982; circled in Figure 5.2A). Foose (1982) and those who have studied his work (Owen-Smith, 1988) noted qualitatively that giraffes were reluctant, for unspecified reasons, to consume hay; our model's over-prediction of giraffe VFI underscores for these qualitative behavioral observations. Omitting the giraffe observations increases R^2 (0.942) and lowers RMSPE (1.05 kg·d^{-1}) and reduces biases in both intercept (-0.19 kg·d^{-1}; P = 0.025) and slope (-0.039; P = 0.045).

For livestock species (cattle, sheep, goat) alone, we found marginally higher agreement ($\text{actual VFI} = [0.97 \pm 0.02] \cdot \text{predicted VFI} + [0.17 \pm 0.13]$; R^2 = 0.955, RMSPE = 0.96 kg/d, n = 118; Figure 5.2B) than for the full dataset with giraffe observations removed. We attribute this higher agreement to the likely higher precision with which we could compute C_r for domestic species; energy requirement equations are reasonably well-established for domestic species (NRC, 2000, 2001, 2007), but equations for cervids are based on limited data (NRC, 2007), and equations for most other wild species have not been published (forcing us to use an imprecise interspecific equation; Blaxter, 1989).

There were no significant biases in either intercept (P = 0.697) or slope (P = 0.385). These results demonstrate our model, with few exceptions, predicts VFI reliably across a wide range of diet qualities, ruminant species, and physiological states.

We compared predictive performance of our model and that of the NRC (2000), one of the most widely-accepted and general empirical prediction systems for cattle (particularly in North America). Agreement between model-predicted and actual values of VFI for our model ($\text{actual VFI} = [0.81 \pm 0.06] \cdot \text{predicted VFI} + [1.89 \pm 0.63]$; R^2 = 0.812, RMSPE = 1.55 kg/d) was appreciably better than for the NRC (2000) ($\text{actual VFI} = [0.48 \pm 0.05] \cdot \text{predicted VFI} + [4.23 \pm 0.50]$; R^2 = 0.700, RMSPE = 2.31 kg/d) in terms of R^2 and RMSPE (Figure 5.3A,B). Further, there were no biases in intercept or slope for our model (intercept: P = 0.674; slope: P = 0.971) but large and significant biases in intercept (0.783 $kg \cdot d^{-1}$; P = 0.014) and slope (0.462; P = 0.004) for the NRC (2000). Gestation observations from Stanley et al. (1993) (circled in Figure 5.3A) were moderately over-predicted by our model for indeterminate reasons. These observations were present in the validations above, but their outlying behavior is more conspicuous here because comparatively few observations were included in this validation (n = 43). When these observations were removed, predictive performance of our model (R^2 = 0.958, RMSPE = 1.09 kg/d) was elevated even more highly above that of the NRC (2000) (R^2 = 0.724, RMSPE = 2.45 kg/d) and more consistent with level of precision in previous validations.

We note that to predict cattle VFI, the NRC (2000) employs four distinct empirical equations (one each for growing calves, growing yearlings, gestating and non-lactating, and gestating and lactating cattle). Our model uses the same equation set for all

physiological states and animal types. Though not specifically designed for cattle or certain physiological states, our system predicts cattle VFI of forage diets with superiority to that of the empirical NRC (2000). This point demonstrates how the mechanistic model proposed here can exceed both the breadth and precision of an empirical system.

Comparison with Prior Mechanistic Models.

Our mechanistic model is one of several previously developed (Illius and Allen, 1994; Illius et al., 2000; Yearsley et al., 2001). Table 5.3 summarizes the predictive performance of models that have been validated, showing that most have low precision, large slope and intercept biases, or both. For this reason, mechanistic models have been regarded primarily as research and not predictive tools (Illius et al., 2000; Yearsley et al., 2001). Only two models, Chilibroste et al. (1997) and our own, display good predictive power within their validation datasets (Table 5.3). Whereas the model of Chilibroste et al. (1997) displays a high R^2 value (0.949), its practicability as a universal VFI prediction model is uncertain because its performance was (1) evaluated only with cattle, (2) not directly compared to other models, (3) likely exaggerated by its small validation dataset size (n = 18). From this perspective, our model stands uniquely as a reliable, practical, and universal VFI prediction system.

Though the complexity of mechanistic models makes it difficult to definitively determine reasons for their predictive performance, we believe that our mechanistic model performs well because it integrates several intake-regulating mechanisms according to an empirical relationship (Figure 5.1), capturing a broad number of mechanisms known the regulate intake (Forbes, 2007) and representing them realistically.

Other models may perform poorly because they either focus exclusively on one intake-regulating mechanism (Illius and Allen, 1994; Illius et al., 2000) or integrate multiple regulation mechanisms according to a theoretical relationship only (Fisher, 1996).

Model Limitations

Despite good agreement between actual and model-predicted VFI, the model's structure is necessarily limited in certain aspects. We model the effects and integration of feedback signals only at a gross level (Eq. 2) and not the specific means by which such effects are mediated (e.g., hormonal and neuronal pathways; Forbes, 2007). The effect of this simplification on VFI-prediction is uncertain, but does prohibit investigation and further understanding of how VFI is regulated at a fine degree of resolution.

Our model cannot account for VFI-depression occurring under special conditions, such as deficiency or excess of micronutrients, extreme temperatures, presence of plant secondary metabolites or other toxins, or endocrinal involvement during estrus and late pregnancy (Forbes, 2007). The model's omission of endocrine-mediated VFI depression may partially explain its systematic over-prediction of gestation observations from Stanley et al. (1993) (Figure 5.3A), though we note gestation observations from two other studies (Table 5.1) were well-predicted.

Another limitation of the model is its accommodation of only one dietary ingredient. Expanding the model to accommodate more complex diets is a goal of future work.

Potential Model Applications

An important feature of the model is its ability to predict reliably over a wide range of animal species and forage qualities. The model should serve as an appropriate

predictive tool for application to small ruminants and poor-quality forages, which are mainstays of livestock production in developing countries (Timon and Hanrahan, 1986; Chenost and Kayouli, 1997) but for which few empirical intake prediction systems (excepting sheep) have been developed. By the same reasoning, the model may be suitable to accommodate new or unconventional ruminant livestock species and breeds (NRC, 1991, 2007); these animals have similarly been ignored by empirical systems although they have considerable economic promise in developed and developing countries alike and, in the latter, may help solve the problem of low meat and milk availability (NRC, 1991). Our model can serve as a valuable tool to livestock production systems, such as those in developing countries, that animal production research has largely neglected.

Rook et al. (1991) previously concluded that a universal model of ruminant VFI prediction is unattainable, and that a battery of empirical equations (each equation specific to a biological condition) be developed and applied instead. Though animal scientists have tacitly accepted the conclusions of Rook et al. (1991) (even as developing such as monumental battery of equations has doubtful practicability), our model's ability to predict intake over a wide range of physiological states and dietary qualities illustrates that a universal model of VFI can indeed be developed. As the model is refined (such as expansion to accommodate several dietary ingredients) and the world's population and demand for animal products climbs (Delgado, 2003), the model's VFI prediction will become of crucial value to improving profitability and productivity of ruminant livestock systems. The model has other useful applications. Because it can consistently deliver accurate food intake predictions when external constraints (e.g., limited food availability,

competition) are absent, our model can provide baseline predictions for VFI capacity that could be highly valuable to ecological investigations.

APPENDIX 1

Units

Entity (nutrient, metabolite, or microbes; MICRO) compartment size and flow (by absorption, hydrolysis, intake, passage, or uptake) have units of kg·100 kg BW^{-1} and kg·100 kg $BW^{-1}·h^{-1}$. Fractional rate constants have units of h^{-1}. Affinity, inhibition, and maximum velocity constants (except for MICRO) are in kg·100 kg BW^{-1}, kg·100 kg BW^{-1}, and kg·100 kg $BW^{-1}·h^{-1}$. MICRO maximum velocity constants are kg·kg $MICRO^{-1}·h^{-1}$. MICRO growth has units of kg MICRO·100 kg $BW^{-1}·h^{-1}$. Heat of combustion and heat increments are in $Mcal·kg^{-1}$ and $Mcal^{-1}·Mcal^{-1}$.

Miscellaneous units not included above are defined in the text where they are introduced. Exceptions to the conventions above are also indicated in the text where appropriate.

Abbreviations

<u>Space abbreviations</u>

AB = abomasum

RR = reticulorumen

OMA = omasum

LI = large intestine

plasma = blood plasma space

SI = small intestine

urine = urinary space

Nutrient, MICRO, and metabolite compartment abbreviations

CP = crude protein

DADF = potentially digestible acid detergent fiber

DHEM = potentially digestible hemicellulose

DM = dry matter

IADF = indigestible acid detergent fiber

ICP = indigestible crude protein

IHEM = indigestible hemicellulose

InDP = insoluble potentially digestible protein

InNFC = insoluble non-fibrous carbohydrate

FAT = lipid

MICRO = microbes

NDF = neutral detergent fiber

NH3 = ammonia

DP = potentially digestible protein

PU = plasma urea

SCHO = soluble carbohydrate

SP = soluble protein

Process, *k*, abbreviations

a = absorption

e = excretion

h = hydrolysis

L = soluble entity passage rate

p1 = insoluble entity fast passage rate

p2 = insoluble entity slow passage rate

p = passage rate (no designation as fast or slow nor soluble or insoluble)

u = uptake

Other abbreviations

C_3 = C_3 grass

C_4 = C_4 grass

ECA = early-cut alfalfa

GL = grass-legume mixture

LCA = late-cut alfalfa

MRT = mean residence time

Symbols and Notation

Compartment and subcompartment symbols

$<^{i}j>$ = size of compartment of entity *j* in space *i*

e.g., $<^{RR}DHEM>$ = size of compartment of DHEM in RR

$<^{i}j_{m}>$ = size of the subcompartment *m* of entity *j* in space *i*

e.g., $<^{RR}DHEM_{1A}>$ = size of 1A subcompartment of DHEM in RR

$<^{i}j_{m1+m2}>$ =size of the sum of *m1* and *m2* subcompartments, where *m1* and *m2* are any subcompartments within a parent compartment *j*

e.g., $<^{RR}DHEM_{1A+2A}>$ = size of the sum 1A and 2A subcompartments of DHEM in RR

Rate constant symbols

${}^{i}k_{k}^{j}$ = age-independent rate for process *k* pertaining to nutrient *j* in space *i*

e.g., ${}^{RR}k_{p1}^{DHEM}$ = slow passage rate of DHEM from the RR

${}^{i}\lambda_{k}^{j}$ = age-dependent rate for process *k* pertaining to nutrient *j* in space *i*

${}^{i}\lambda_{k}^{j}$ *=age-dependent rate without the effect of ${}^{i}P_{d}$

MICRO SYMBOLS

${}^{i}microG$ = actual MICRO growth in space *i*

${}^{i}microG \mid SP$ = actual MICRO growth supported by SP in space *i*

${}^{i}microG \mid NH3$ = actual MICRO growth supported by NH3 in space *i*

${}^{i}pmicroG \mid N$ = potential MICRO growth supported by N (from SP and NH3) in space *i*

${}^{i}pmicroG \mid SCHO$ = potential MICRO growth supported by SCHO in space *i*

$R_{microG|l}^{j|biomass}$ = requirement for nutrient *j* for incorpotation into biomass in MICRO growth supported by nitrogen source *l* (NH3,SP) (kg *j*·kg MICRO^{-1})

$R_{microG|l}^{j|ferment}$ = requirement for nutrient *j* for fermentation into biomass in MICRO growth supported by nitrogen source *l* (NH3, SP) (kg *j*·kg MICRO^{-1})

R_{microM}^{SCHO} = minimal requirement for SCHO for maintenance (kg SCHO·kg MICRO^{-1}·h^{-1})

ϕ = shape parameter for SP uptake (unitless)

Other symbols and notation

$A_{InDP,SP}$ =fraction of InDP flowing from RR hydrolyzed to SP in abomasum (kg InDP·kg SP^{-1})

${}^{RR}E^{PU}_{saliva}$ =endogenous input of PU into the RR from inflow of saliva

${}^{i}E^{SP}_{s}$ = endogenous input of SP into space *i*

${}^{RR}E^{SP}_{saliva}$ = endogenous input of SP into the RR from inflow of saliva

${}^{RR}E^{SP}_{wall}$ =endogenous input of SP into the RR from epithelial sloughing of RR wall

f^{j} = fraction of nutrient *j* in diet (kg·kg DM^{-1})

${}^{i}ferment^{j}$ = quantity of nutrient *j* fermented by MICRO in space *i*

H^{j}_{c} = heat of combustion of nutrient *j* (Mcal·Mcal^{-1})

H^{j}_{m} = heat increment of metabolism of nutrient *j*

H_{e} = heat increment of eating

INTAKE = voluntary feed intake

${}^{i}J^{j}_{k|l}$ =inhibition constant for nutrient *j* in the process *k* involving nutrient *l* in space *i*

e.g., ${}^{RR}J^{NH3}_{e|PU}$ = inhibition constant for NH3 in the excretion of PU into the RR

${}^{urine}k^{PU}_{e}$ = excretion of PU through urine (L·100 kg BW^{-1}·h^{-1})

${}^{i}K^{j}_{k|l}$ =affinity constant for nutrient *j* in the process *k* involving nutrient *l* in space *i*

${}^{i}K^{SCHO:SP}_{P_d}$ = affinity constant for P_d

NEI = actual NE intake

NE:P =absorption of NE:absorption of CP (Mcal·kg^{-1})

${}^{i}O^{j}$ = outflow of nutrient *j* from space *i* by passage

${}^{i}P_d$ = protein feedback signal that affects degradation rates in space *i* (unitless)

t = time

tt = SI mean residence time

${}^{i}v_{u}^{j}$ = uptake of entity j by MICRO in space i

${}^{i}V_{k}^{j}$ = maximum rate of process k for nutrient j into space i

${}^{i}V_{\max}^{Pd}$ = maximum value of the fraction by which ${}^{i}P_{d}$ can increase degradation rates of insoluble nutrients (unitless)

VFA^{SP} =VFA from SP fermentation (kg·100 kg BW^{-1})

VFA^{SCHO} =VFA from SCHO fermentation (kg·100 kg BW^{-1})

$Y_{j,l}$ = yield of entity l from entity j (kg l·kg j^{-1})

APPENDIX 2

Refer to Appendix 1 for units, abbreviations, and symbols.

Conversion Factors

In order to convert values from literature sources to be consistent with units used in the model, molecular masses of nutrients were assumed to be 17, 60, 110, 134, 162, and 675 g·mol^{-1} for NH3, PU, protein, CHO, and FAT (Dijkstra et al., 1992); 60, 74, 88, and 102 g/mol for acetate, butyrate, propionate, and valerate; and 67.3 and 79.3 g·mol^{-1} for VFA^{SCHO} and VFA^{SP} (calculated using average molar proportions for CHO and protein fermentation reported by Murphy [1984]). The volume of the RR, SI, LI, and plasma spaces were assumed to be 11, 1.3, 2.4, and 79.5 L·100 kg BW^{-1}, typical of sheep and cattle (Grovum and Hecker, 1973; Grovum and Williams, 1973; McAllan, 1981; Dixon and Nolan, 1982; Dixon and Milligan, 1984; Barry et al., 1985; Baldwin, 1995; Pitt et al., 1996). We also assumed 1.26 mol N·mol SP^{-1} (Dijkstra et al., 1992).

Protein Feedback Signal that Affects Degradation Rates

To estimate parameter values for ${}^{i}P_d$, we used the data of Houser (1970), which report the effect of adding urea to the in vitro degradation rate of Pangola grass OM, with the following assumptions: (1) all nutrient disappearance was due to MICRO uptake, (2) all non-CP OM that disappeared was CHO, (3) 75% of grass CP disappeared, (4) all urea disappeared, and (5) ${}^{i}V_{\max}^{P_d}=1$ (so that $\lim_{SP:SCHO\to\infty}[{}^{i}P_d \cdot {}^{i}\lambda_h^j *]={}^{i}\lambda_h^j$). By regression (PROC NLIN of SAS; SAS Institute, Inc., Cary, NC) we found ${}^{i}K_{P_d}^{N:SCHO}=31.7$ (and ${}^{i}V_{\max}^{P_d}=1$ by definition).

Absorption, Hydrolysis, and Passage Rates

Values for ${}^{SI}V_a^{SCHO}$ and ${}^{SI}K_{a|SCHO}^{SCHO}$ were set to $8.30\cdot10^{-2}$ and $1.64\cdot10^{-4}$ (Cant et al., 1996). The value of ${}^{RR}k^{NH3}$ is from Baldwin (1995) and ${}^{SI}k^{NH3}$ and ${}^{LI}k^{NH3}$ are typical values calculated from the literature for sheep (Hecker, 1971; Grovum and Williams, 1973; Nolan et al., 1976; McAllan, 1981; Dixon and Nolan, 1983, 1984, 1986; Siddons et al., 1985; Sklan et al., 1985b; Table 5.8). An estimate of $<{}^{i}NH3>$ is required to calculate ${}^{i}k^{NH3}$, and when unavailable in a report, was taken from Hecker (1971) (assuming 1 kg·L SI digesta^{-1} and all non-protein nitrogen is NH_3) for the SI and from Dixon and Nolan (1982) for the LI.

To estimate ${}^{SI}k_a^{NcAc}$, ${}^{SI}k_a^{FAT}$, ${}^{SI}k_a^{SP}$, and we first constructed curves that relate nutrient absorption to time spent in the SI. We constructed these curves using data from McAllan (1981) and Sklan (1985a,b; for nutrient absorption, assuming all nutrient disappearance is due to absorption) and Grovum and Williams (1973; for segmental

MRT). We then applied regression (PROC NLIN of SAS) to estimate ${}^{SI}k_a^{SP}$, ${}^{SI}k_a^{FAT}$, and ${}^{SI}k_a^{NcAc}$. For FAT and SP disappearance curves, we resolved two distinct first-order rates. We used the slow rates as estimates for ${}^{SI}k_a^{i}$, assuming the fast rate was that associated with rapid resorption of endogenous secretions (Sklan [1985a,b] show that resorption of many endogenous enzymes is rapid).

We estimated ${}^{SI}k_h^{InDP}$ as 0.73 with the same technique for estimating ${}^{SI}k_a^{SP}$, ${}^{SI}k_a^{FAT}$, and ${}^{SI}k_a^{NcAc}$, using data from Sklan (1985b; for InDP hydrolysis, assuming all disappearance is due to hydrolysis) and Grovum and Williams (1973; for segmental MRT). In absence of sufficient data for direct estimation, ${}^{SI}k_h^{InNFC}$ was set to 0.50 to yield starch a digestibility value within the range summarized by Owens et al. (1986) for an SI MRT of 2h.

Values for ${}^{i}\lambda_h^{i}$ are from NRC (2000) for InNFC (using the approximate conversion factor $0.59635 \cdot {}^{i}\lambda_h^{i} = {}^{i}k_h^{j}$; Pond et al., 1988) and Chapter 2 for all other parameters (Table 5.9). These parameter values generally vary by diet type (ECA, LCA, C_3, C_4, GL).

The value of ${}^{RR}k_L^{j}$ is estimated using the following equation (Illius and Gordon, 1991):

$${}^{RR}k_L^{j} = 0.176 \cdot (f^{SCHO} + f^{InNFC} + f^{SP} + f^{InDP}) + 0.145 \cdot (f^{DHEM} + f^{DADF}) + 2.31 \cdot 10^{-5} \cdot BW$$

.

The value of ${}^{RR}k_{p1}^{j}$ was set to 0.10 (Ellis et al., 2000). The value of ${}^{RR}K_{p2|j}^{IHEM+IADF}$ was set to 1 (after Figure 5.16.7(a) from Ellis et al. [2000]), and ${}^{RR}V_{p2}^{j}$ was set to 0.083,

double the maximum INDF outflow rate from Figure 5.16.7(a) in Ellis et al. (2000). We doubled the outflow rate because calculating passage rate directly from total INDF (or any other nutrient) outflow yields a passage rate that is the composite of ${}^{RR}k_{p1}^{j}$ and ${}^{RR}k_{p2}^{j}$ (rather than ${}^{RR}k_{p2}^{j}$ alone). We found that doubling INDF outflow rate empirically yielded values of ${}^{RR}k_{p2}^{j}$ that closely matched values calculated from the graph using the direct numerical method (by partitioning MRT between that associated with ${}^{RR}k_{p2}^{j}$ and ${}^{RR}k_{p1}^{j}$, assuming ${}^{RR}k_{p1}^{j}$ = 0.10), and resulted in a much simpler expression for ${}^{RR}k_{p2}^{j}$ compared with direct MRT partitioning.

Values of *tt* and ${}^{LI}k_{p}^{j}$ were set to 2.00 and 0.065 according to typical values for sheep, cattle, and goats (*tt*: Coombe and Kay, 1965; Grovum and Williams, 1973, 1977; Warner, 1981; Barry et al., 1985; Gregory et al., 1985; Gregory and Miller, 1989; Ellis et al., 2002; Walz et al., 2004; ${}^{LI}k_{p}^{j}$: Coombe and Kay, 1965; Grovum and Hecker, 1973; Hecker and Grovum, 1975; Grovum and Williams, 1977; Warner, 1981; Dixon and Nolan, 1982; Faichney and Boston, 1983; Barry et al., 1985; de Vega et al., 1998; Ellis et al., 2002; Walz et al., 2004).

Endogenous Protein and PU

Values of ${}^{RR}E_{saliva}^{SP}$ and ${}^{RR}E_{saliva}^{PU}$ are calculated as salivation rate multiplied by salivary concentration of PU and SP, respectively. Salivation rate is calculated from the equations of Baldwin (1995), with time spent ruminating estimated from NDF concentration (Murphy et al., 1983) and the default feed intake (9 kg·d^{-1}) in Baldwin (1995). Salivary concentration of SP and urea were taken to be $1.10 \cdot 10^{-4}$ kg·L (Dijkstra

et al., 1992) and 0.65 of that in the plasma space (Bailey and Balch, 1961; Somers, 1961; Doyle et al., 1982; Cirio et al., 2000; Piccione et al., 2006), and thus

$$^{RR}E^{SP}_{saliva} = 4.58\cdot 10^{-4}\{[0.850 + 0.796\cdot(f^{DHEM} + f^{IHEM}\, f^{DADF} + f^{IADF})]\cdot BW^{0.75} + 0.0163\cdot BW\}/BW$$

$$^{RR}E^{PU}_{saliva} = 8.06\cdot 10^{-4}\cdot <^{plasma}PU>\cdot\{[0.850 + 0.796\cdot(f^{DHEM} + f^{IHEM}\, f^{DADF} + f^{IADF})]\cdot BW^{0.75} + 0.0163\cdot BW\}/BW$$

.

Values of $^{RR}V^{PU}_{e}$, $^{RR}K^{PU}_{e|PU}$, and $^{RR}J^{NH3}_{e|PU}$ were set to $1.32\cdot10^{-2}\cdot$BW$^{-0.25}$, $1.47\cdot10^{-3}$, and $8.45\cdot10^{-2}$ (Baldwin, 1995). The value of $^{RR}E^{SP}_{wall}$ was set to $9.05\cdot10^{-6}$, typical for cattle and sheep (MacRae and Reeds, 1980; Ørskov, 1982; Ørskov and MacLeod, 1982, 1983; Ørskov et al., 1986). Values for $^{i}E^{SP}$ and $^{i}k^{PU}_{e}$ for all other spaces were those typical for cattle, sheep, and goats ($^{i}E^{SP}$: Harrop, 1974; Ørskov and MacLeod, 1982; Dixon and Milligan, 1984; Dixon and Nolan, 1985; Siddons et al., 1985; Ørskov et al., 1986; Van Bruchem et al., 1997; Ouellet et al., 2002; $^{i}k^{PU}_{e}$:

Nolan et al., 1976; von Engelhardt and Hinderer, 1976; Dixon and Nolan, 1983, 1986; Dixon and Milligan, 1984; Siddons et al., 1985; Kohn et al., 2005; Table 5.10).

MICRO Submodel

The value for $^{i}V^{SCHO}_{u}$ was set to 1.11 (Dijkstra et al., 1992). In absence of sufficient data for direct estimation, $^{RR}K^{SCHO}_{u|SCHO}$ and $^{LI}K^{SCHO}_{u|SCHO}$ were set heuristically to 0.20 and $7.58\cdot10^{-3}$ to result in first-order uptake rates within the general range (typically 0.75 to 4·h^{-1}) of "A" CHO fraction digestion rates suggested by Sniffen et al. (1992).

Parameter values for MICRO uptake of NH3 and SP were estimated by applying regression (PROC NLIN of SAS) to data of Atasoglu et al. (1999; Table 5.11). We made

the following assumptions: (1) $Y_{MICRO,InDP}$ = 0.42 (Dijkstra et al., 1992), (2) ${}^{i}\nu_{u}^{SCHO}$=1.1 (${}^{RR}\nu_{u}^{SCHO}$ when $<{}^{i}SCHO>$ is large; required to calculate average SCHO concentration), and (3) values of ${}^{i}K_{u|SP}^{SCHO}$ and ${}^{i}K_{u|NH3}^{SCHO}$ from Dijkstra et al. (1992).

The value of $Y_{MICRO,InNFC}$ was set to 0.20 (Reichl and Baldwin, 1975) and $Y_{MICRO,InDP}$, $Y_{MICRO,FAT}$, and $Y_{MICRO,NcAc}$ were set to 0.42, 0.11, and 0.13 (Dijkstra et al., 1992). Values for $R_{microG|NH3}^{SCHO|biomass}$, $R_{microG|NH3}^{SCHO|ferment}$, $R_{microG|SP}^{SCHO|biomass}$, $R_{microG|SP}^{SCHO|ferment}$, $R_{microG|NH3}^{NH3}$, and $R_{microG|SP}^{SP}$ were set to were set to 1.13, 1.12, 0.52, 0.88, 0.12, and 0.59 (Dijkstra et al., 1992) and R_{microM}^{SCHO} was set to 0.042 (Isaacson et al., 1975).

Heat of Combustion and Heat Increment

Values of H_{c}^{j} for SCHO, InNFC, HEM, cellulose, lignin, InDP, SP, FAT, and PU are those reported by Blaxter (1989) for α-D-glucose, xylan, starch, cellulose, lignin, myosin, grain lipids, and urea (Table 5.12). Values for $H_{c}^{VFA^{SCHO}}$ and $H_{c}^{VFA^{SP}}$ were calculated using H_{c}^{j} of individual VFA (Blaxter, 1989) and average VFA molar proportions for CHO and protein fermentation reported by Murphy (1984).

Values of H_{m}^{j} for all entities but FAT are those reported by Blaxter (1989) for ruminants "below maintenance" (Table 5.12). Values of $H_{m}^{VFA^{SCHO}}$ and $H_{m}^{VFA^{SP}}$ are calculated using H_{m}^{j} for individual VFA (Blaxter, 1989) and the average VFA molar proportions from Murphy (1984). We could not find a literature value of H_{m}^{FAT} for ruminants near maintenance, and so we adopted a typical value of H_{m}^{FAT} for monogastic species (Blaxter 1989; Table 5.12). Because H_{m}^{j} are set to values for near or below

maintenance, they are most appropriate for calculation of NE_m, explaining our convention to express NE in units of NE_m throughout the model (e.g., in calculation of C_r).

Typical literature values of H_{eat} (as reported by Blaxter, 1989) are 0.05. However, H_{eat} is classically defined as a constant fraction of ME, whereas the model implicitly defines it as a fraction of total ME less heat losses due to fermentation and metabolism (c.f. Eq. 4, Table 5.7). Because ME less fermentation and metabolism heat losses is about 20% smaller than total ME, we set H_{eat} to 0.04, 20% less than the typical value of 0.05.

Yield Parameters for Diet Composition

Values of $Y_{j,l}$ are from Stefanon et al. (1996) for $Y_{NFC,SCHO}$; Chapter 2 for $Y_{HEM,DHEM}$, $Y_{ADF,DADF}$, and $Y_{CP,DP}$; and T.J. Hackmann, J.D. Sampson, and J.N. Spain (unpublished results) for $Y_{DP,SP}$ (Table 5.13). Parameter values generally differ by diet type.

Miscellaneous Yield and Other Parameters.

Values for $Y_{NcAc,NH3}$ and $Y_{NcAc,SCHO}$ were back-calculated from the amount of SCHO and NH3 for NcAc synthesis reported by (Dijkstra et al., 1992; Table 5.14). Values for $Y_{SCHO,VFA}$ and $Y_{SP,VFA}$ are averages for CHO and protein from Murphy (1984). All other miscellaneous $Y_{i,j}$ values were calculated using conversion factors explained above.

The value of $A_{InDP,SP}$ was set to 0.50, based on data from Crooker et al. (1982) reporting the fraction of feed N remaining after in vitro incubation in the AB fluid (after

prior incubation in situ in the RR). Values for f^{NFC} and f^{FAT} are those reported by NRC (2001).

Table 5.1. Studies and species used in model validation

Name			
Latin	Common	Physiological state	Reference[1]
Bison bison	American bison	non-productive	4
Bison bonasus	European bison	non-productive	4
Bos gaurus	Gaur	non-productive	4
Bos taurus	Domestic cattle	non-productive	4,10,14,15
		gestating	5,12
		growing	1,5,15
		lactating	5,8,12
Boselaphus tragocamelus	Nilgai	non-productive	4
Bubalus bubalis	Asian water buffalo	non-productive	4
Capra aegagrus hircus	domestic goat	non-productive	10,11
Capreolus capreolus	Roe deer	non-productive	14
Capra ibex nubiana	Nubian ibex	non-productive	13
		lactating	13
Cervus canadensis	North American elk	non-productive	4,6
Cervus duvaucelii	Barasingha	non-productive	4
Cervus elaphus	Red deer	non-productive	11,14
Giraffa camelopardalis	Giraffe	non-productive	4
Kobus ellipsiprymnus	Waterbuck	non-productive	4
Odocoileus hemionus	Mule deer	non-productive	6
Oryx gazelle	Gemsbok	non-productive	4
Ovis aries	Domestic sheep	non-productive	3,4,7,9,10
		gestating	2
		growing	3,9
		lactating	2,7
Ovis canadensis	Bighorn sheep	non-productive	6
Syncerus caffer	African buffalo	non-productive	4
Taurotragus oryx	Common eland	non-productive	4

[1]Key to references: *1* Colburn (1968), *2* Foot and Russel (1979), *3* Egan and Doyle (1982), *4* Foose (1982), *5* Hunter and Siebert (1986), *6* Baker and Hobbs (1987), *7* Weston (1988), *8* Hatfield et al. (1989), *9* Weston et al. (1989), *10* Reid et al. (1990), *11* Domingue et al. (1991), *12* Stanley et al. (1993), *13* Gross et al. (1996), *14* van Wieren (1996), *15* Varel and Kreikemeier (1999).

Table 5.2. Descriptive statistics of studies used in model validation[1,2]

	Dietary composition				Digestibility							
Item	NDF	ADF	CP	NE_m[3]	DM	OM	NDF	ADF	CP	BW	VFI	VFI
	-----g·kg DM^{-1}-----			Mcal·kg DM^{-1}	g·g^{-1}	g·g^{-1}	g·g^{-1}	g·g^{-1}	g·g^{-1}	kg	g DM·100 g BW^{-1}	kg DM·d^{-1}
Mean	562	366	147	1.23	0.619	0.606	0.578	0.555	0.806	223	2.44	4.72
Min	351	261	36	0.71	0.460	0.442	0.370	0.392	0.541	16	0.47	0.29
Max	787	551	231	1.77	0.747	0.781	0.834	0.745	0.975	907	4.89	17.2
SD	105	56	52	0.20	0.067	0.092	0.105	0.087	0.124	210	0.81	4.26
N	158	158	158	158	39	53	89	55	51	158	158	158

[1]Studies include Colburn (1968), Foot and Russel (1979), Egan and Doyle (1982), Foose (1982), Hunter and Siebert (1986), Baker and Hobbs (1987), Weston (1988), Hatfield et al. (1989), Weston et al. (1989), Reid et al. (1990), Domingue et al. (1991), Stanley et al. (1993), Gross et al. (1996), van Wieren (1996), Varel and Kreikemeier (1999).

[2]VFI = voluntary feed intake

[3]Values NE_m are estimated using equations of NRC (2001).

Table 5.3. Performance of mechanistic models used to predict feed intake of ruminants

model	species	physiological state[2]	feed	expression for VFI[3]	best-fit line[1]			
					slope	intercept	R^2	n
Mertens and Ely (1979, 1982)	Sheep	growth (?), non-productive	C_3 and C_4 grass, legume, grass/legume mixture	kg·100 kg $BW^{-1}·d^{-1}$	0.39	1.33	0.262	166
Hyer et al. (1991a,b)	Cattle	growth, non-productive (?)	C_3 and C_4 grass, legume	$kg·d^{-1}$	0.79[4]	3.92[4]	NA	42
Illius and Gordon (1991)	Sheep, cattle	growth, non-productive	C_3 and C_4 grass	g·kg $BW^{-0.73}·d^{-1}$	0.98±0.03	NA	0.606	25
Illius and Gordon (1992)	Domestic and wild ungulates	non-productive	C_3 grass	g·kg $BW^{-0.73}·d^{-1}$	0.77±0.03	NA	0.641	27
Fisher (1996)	Cattle	growth (?)	C_3 and C_4 grass, legume	kg·100 kg $BW^{-1}·d^{-1}$	NA	NA	0.504	38
Chilibroste et al. (1997)	Cattle	lactating, gestating, growth, non-productive (?)	C_3 grass, C_4 grass, and legume-concentrate diets	$kg·d^{-1}$	1.03±0.06[5]	0.03±0.81[5]	0.949[5]	18
our model	Domestic and wild ruminants	gestating, growth, lactating, non-productive	C_3 and C_4 grass, legume, grass/legume mixture	$kg·d^{-1}$	0.99±0.02	0.35±0.16	0.910	158

[1]Values line (mean±SE) refer to line *actual VFI = slope·predicted VFI + intercept*.
[2]Model reports and references therein did not always report physiological state; uncertainty in physiological state, where present, is indicated with "?".
[3]VFI = voluntary feed intake
[4]Found by digitizing Figure 5.1 of Hyer et al. (1991b).
[5]Calculated using data in original report of Chilibroste et al. (1997).

Table 5.4. Main system of differential equations used in the mechanistic model to represent digestive events in the RR, SI, LI, and plasma[1]

Space	Compartment	Subcompartment	Equation	
RR	SCHO		$\frac{d<^{RR}SCHO>}{dt} = (INTAKE \cdot f^{SCHO} + <^{RR}INFC_{2A+2B}> \cdot {}^{RR}\lambda_h^{INFC} + <^{RR}DHEM_{2A+2B}> \cdot {}^{RR}\lambda_h^{DHEM} + <^{RR}DADF_{2A+2B}> \cdot {}^{RR}\lambda_h^{DADF}) - ({}^{RR}v_u^{SCHO} + <^{RR}SCHO> \cdot {}^{RR}k_L^{SCHO})$	[1]
	InNFC	1A	$\frac{d<^{RR}InNFC_{1A}>}{dt} = INTAKE \cdot f^{InNFC} - <^{RR}INFC_{1A}> \cdot ({}^{RR}\lambda_h^{InNFC} + {}^{RR}k_{p1}^{InNFC})$	[2]
		2A	$\frac{d<^{RR}InNFC_{2A}>}{dt} = <^{RR}InNFC_{1A}> \cdot {}^{RR}\lambda_h^{InNFC} - <^{RR}InNFC_{2A}> \cdot ({}^{RR}\lambda_h^{InNFC} + {}^{RR}k_{p1}^{InNFC})$	[3]
		1B	$\frac{d<^{RR}InNFC_{1B}>}{dt} = <^{RR}InNFC_{1A}> \cdot {}^{RR}k_{p1}^{InNFC} - <^{RR}InNFC_{1B}> \cdot ({}^{RR}\lambda_h^{InNFC} + {}^{RR}k_{p2}^{InNFC})$	[4]
		2B	$\frac{d<^{RR}InNFC_{2B}>}{dt} = (<^{RR}InNFC_{2A}> \cdot {}^{RR}k_{p1}^{InNFC} + <^{RR}InNFC_{1B}> \cdot {}^{RR}\lambda_h^{InNFC}) - <^{RR}InNFC_{2B}> \cdot ({}^{RR}\lambda_h^{InNFC} + {}^{RR}k_{p2}^{InNFC})$	[5]
	DHEM	1A	Replace “InNFC” in Eq. 2 with “DHEM” throughout	[6]
		2A	Replace “InNFC” in Eq. 3 with “DHEM” throughout	[7]
		1B	Replace “InNFC” in Eq. 4 with “DHEM” throughout	[8]
		2B	Replace “InNFC” in Eq. 5 with “DHEM” throughout	[9]
	IHEM	A	$\frac{d<^{RR}IHEM_A>}{dt} = INTAKE \cdot f^{IHEM} - <^{RR}IHEM_A> \cdot {}^{RR}k_{p1}^{IHEM}$	[10]
		B	$\frac{d<^{RR}IHEM_B>}{dt} = <^{RR}IHEM_A> \cdot {}^{RR}k_{p1}^{IHEM} - <^{RR}IHEM_B> \cdot {}^{RR}k_{p2}^{IHEM}$	[11]
	DADF	1A	Replace “InNFC” in Eq. 2 with “DADF” throughout	[12]
		2A	Replace “InNFC” in Eq. 3 with “DADF” throughout	[13]
		1B	Replace “InNFC” in Eq. 4 with “DADF” throughout	[14]

		2B	Replace “InNFC” in Eq. 5 with “DADF” throughout	[15]
	IADF	A	Replace “IHEM” in Eq. 10 with “IADF” throughout	[16]
		B	Replace “IHEM” in Eq. 11 with “IADF” throughout	[17]
	SP		$\frac{d<^{RR}SP>}{dt} = (INTAKE \cdot f^{SP} + {}^{RR}E^{SP} + <^{RR}InDP_{2A+2B}> \cdot {}^{RR}\lambda_h^{InDP}) - ({}^{RR}v_u^{SP} + <^{RR}SP> \cdot {}^{RR}k_L^{SP})$	[18]
	InDP	1A	Replace “INFC” in Eq. 2 with “InDP” throughout	[19]
		2A	Replace “INFC” in Eq. 3 with “InDP” throughout	[20]
		1B	Replace “INFC” in Eq. 4 with “InDP” throughout	[21]
		2B	Replace “INFC” in Eq. 5 with “InDP” throughout	[22]
	FAT	A	Replace “IHEM” in Eq. 10 with “FAT” throughout	[23]
		B	Replace “IHEM” in Eq. 11 with “FAT” throughout	[24]
	NH3		$\frac{d<^{RR}NH3>}{dt} = [{}^{RR}ferment^{SP} \cdot Y_{SP,NH3} + (<^{plasma}PU> \cdot {}^{RR}k_e^{PU} + {}^{RR}E_{saliva}^{PU}) \cdot Y_{PU,NH3}] -$ $[<^{RR}NH3> \cdot ({}^{RR}k_L^{NH3} + {}^{RR}k_a^{NH3}) + {}^{RR}v_u^{NH3}]$	[25]
	MICRO		$\frac{d<^{RR}MICRO>}{dt} = {}^{RR}microG - <^{RR}MICRO> \cdot {}^{RR}k_{p2}^{MICRO}$	[26]
SI	SCHO	SCHO	$\frac{d<^{SI}SCHO>}{dt} = (<^{RR}SCHO> \cdot {}^{RR}k_L^{SCHO} + <^{SI}INFC> \cdot {}^{SI}k_h^{INFC}) -$ $(<^{SI}SCHO> \cdot {}^{SI}k_a^{SCHO} + {}^{SI}O^{SCHO})$	[27]
	InNFC	InNFC	$\frac{d<^{SI}InNFC>}{dt} = (<^{RR}InNFC_{1B+2B}> \cdot {}^{RR}k_{p2}^{INFC} + <^{RR}MICRO> \cdot {}^{RR}k_{p2}^{MICRO} \cdot Y_{MICRO,InNFC}) -$ $(<^{SI}InNFC> \cdot {}^{SI}k_h^{InNFC} + {}^{SI}O^{InNFC})$	[28]
	SP	SP	$\frac{d<^{SI}SP>}{dt} = [<^{RR}SP> \cdot {}^{RR}k_L^{SP} + (<^{RR}InDP_{1B+2B}> \cdot {}^{RR}k_{p2}^{InDP} +$ $<^{RR}MICRO> \cdot {}^{RR}k_{p2}^{MICRO} \cdot Y_{MICRO,InDP}) \cdot A_{InDP,SP} + {}^{OMA+AB}E^{SP} + {}^{SI}E^{SP} + <^{SI}InDP> \cdot {}^{SI}k_h^{InDP}) -$ $(<^{SI}SP> \cdot {}^{SI}k_a^{SP} + {}^{SI}O^{SP})$	[29]

	InDP	InDP	$\frac{d<^{SI}InDP>}{dt} = [(<^{RR}InDP_{1B+2B}>\cdot^{RR}k_{p2}^{InDP} + <^{RR}MICRO>\cdot^{RR}k_{p2}^{MICRO} \cdot Y_{MICRO,InDP}) \cdot (1 - A_{InDP,SP})] -$ $(<^{SI}InDP>\cdot^{SI}k_h^{InDP} + {}^{SI}O^{InDP})$	[30]
	FAT	FAT	$\frac{d<^{SI}FAT>}{dt} = (<^{RR}FAT_B>\cdot^{RR}k_{p2}^{FAT} + <^{RR}MICRO>\cdot^{RR}k_{p2}^{MICRO} \cdot Y_{MICRO,FAT}) - (<^{SI}FAT>\cdot^{SI}k_a^{FAT}$ $+ {}^{SI}O^{FAT})$	[31]
	NcAc	NcAc	$\frac{d<^{SI}NcAc>}{dt} = <^{RR}MICRO>\cdot^{RR}k_{p2}^{MICRO} \cdot Y_{MICRO,NcAc} - (<^{SI}NcAc>\cdot^{SI}k_a^{NcAc} + {}^{SI}O^{NcAc})$	[32]
	NH3	NH3	$\frac{d<^{SI}NH3>}{dt} = (<^{RR}NH3>\cdot^{RR}k_L^{NH3} + <^{plasma}PU>\cdot^{SI}k_e^{PU}Y_{PU,NH3}) - (<^{SI}NH3>\cdot^{SI}k_a^{NH3} + {}^{SI}O^{NH3})$	[33]
LI	SCHO		$\frac{d<^{LI}SCHO>}{dt} = ({}^{SI}O^{SCHO} + {}^{SI}O^{NcAc} \cdot Y_{NcAc,SCHO} + <^{LI}InNFC_2>\cdot^{LI}\lambda_h^{InNFC} +$ $<^{LI}DHEM_2>\cdot^{LI}\lambda_h^{DHEM} + <^{LI}DADF_2>\cdot^{LI}\lambda_h^{DADF}) - ({}^{LI}v_u^{SCHO} + <^{LI}SCHO>\cdot^{LI}k_p^{SCHO})$	[34]
	InNFC	1	$\frac{d<^{LI}InNFC>}{dt} = {}^{SI}O^{InNFC} - <^{LI}InNFC_1>\cdot({}^{LI}\lambda_h^{InNFC} + {}^{LI}k_p^{InNFC})$	[35]
		2	$\frac{d<^{LI}InNFC>}{dt} = <^{LI}InNFC_1>\cdot^{LI}\lambda_h^{InNFC} - <^{LI}InNFC_2>\cdot({}^{LI}\lambda_h^{InNFC} + {}^{LI}k_p^{InNFC})$	[36]
	DHEM	1	$\frac{d<^{LI}DHEM>}{dt} = <^{RR}DHEM_{1B+2B}>\cdot^{RR}k_{p2}^{DHEM} - <^{LI}DHEM_1>\cdot({}^{LI}\lambda_h^{DHEM} + {}^{LI}k_p^{DHEM})$	[37]
		2	$\frac{d<^{LI}DHEM>}{dt} = <^{LI}DHEM_1>\cdot^{LI}k_p^{DHEM} - <^{LI}DHEM_2>\cdot({}^{LI}\lambda_h^{DHEM} + {}^{LI}k_p^{DHEM})$	[38]
	DADF	1	Replace “DHEM” in Eq. 3 with “DADF” throughout	[39]
		2	Replace “DHEM” in Eq. 4 with “DADF” throughout	[40]

	SP		$\frac{d<^{LI}SP>}{dt}=(^{SI}O^{SP}+^{SI}O^{NcAc}\cdot Y_{NcAc,SP}+<^{LI}InDP_2>\cdot^{LI}\lambda_h^{InDP}+^{LI}E^{SP})-(^{LI}v_u^{SP}+<^{LI}SP>\cdot^{LI}k_p^{SP})$	[41]
	InDP	1	Replace "InNFC" in Eq. 2 with "InDP" throughout	[42]
		2	Replace "InNFC" in Eq. 3 with "InDP" throughout	[43]
	NH3		$\frac{d<^{LI}NH3>}{dt}=[^{SI}O^{NH3}+^{SI}O^{NcAc}\cdot Y_{NcAc,NH3}+^{LI}ferment^{SP}\cdot Y_{SP,NH3}+$ $(<^{plasma}PU>\cdot^{LI}k_e^{PU}+^{LI}E^{PU})\cdot Y_{PU,NH3}]-[<^{LI}NH3>\cdot(^{LI}k_p^{NH3}+^{LI}k_a^{NH3})+^{LI}v_u^{NH3}]$	[44]
	MICRO		$\frac{d<^{LI}MICRO>}{dt}=^{LI}microG\mid actual-<^{LI}MICRO>\cdot^{LI}k_p^{MICRO}$	[45]
plasma	PU		$\frac{d<^{plasma}PU>}{dt}=<^{SI}SP>\cdot^{SI}k_a^{SP}\cdot Y_{SP,PU}-[^{RR}E_{saliva}^{PU}+<^{plasma}PU>\cdot(^{RR}k_e^{PU}+^{SI}k_e^{PU}$ $+^{LI}k_e^{PU}+^{urine}k_e^{PU})]$	[46]

[1]See Appendix 1 for explanation of symbols, abbreviations, and unit conventions.

Table 5.5. Auxiliary equations for the main system of differential equations of the mechanistic model[1,2]

Category	Equation	
f^{j}	$f^{SCHO} = Y_{NFC,SCHO} \cdot f^{NFC}$	[1]
	$f^{InNFC} = (1 - Y_{NFC,SCHO}) \cdot f^{NFC}$	[2]
	$f^{DHEM} = Y_{HEM,DHEM} \cdot (f^{NDF} - f^{ADF})$	[3]
	$f^{IHEM} = (1 - Y_{HEM,DHEM}) \cdot (f^{NDF} - f^{ADF})$	[4]
	$f^{DADF} = Y_{ADF,DADF} \cdot f^{ADF}$	[5]
	$f^{IADF} = (1 - Y_{ADF,IADF}) \cdot f^{ADF}$	[6]
	$f^{SP} = Y_{CP,DP} \cdot Y_{DP,SP} \cdot f^{CP}$	[7]
	$f^{InDP} = Y_{CP,DP} \cdot (1 - Y_{DP,SP}) \cdot f^{CP}$	[8]
${}^{SI}O^{j}$	${}^{SI}O^{SCHO} = <^{RR}SCHO> \cdot {}^{RR}k_L^{SCHO} \cdot \exp(-{}^{SI}k_a^{SCHO} \cdot tt) + \frac{<^{RR}SCHO> \cdot {}^{RR}k_L^{SCHO} \cdot [{}^{SI}k_h^{InNFC} - {}^{SI}k_a^{SCHO} + \exp({}^{SI}k_h^{InNFC} \cdot tt) \cdot {}^{SI}k_a^{SCHO} - \exp({}^{SI}k_a^{SCHO} \cdot tt) \cdot {}^{SI}k_a^{SCHO}]}{{}^{SI}k_a^{SCHO} \cdot ({}^{SI}k_h^{InNFC} - {}^{SI}k_a^{SCHO})}$	[9]
	${}^{SI}O^{InNFC} = <^{RR}InNFC_{1B+2B}> \cdot {}^{RR}k_{p2}^{InNFC} \cdot \exp(-{}^{SI}k_a^{InNFC} \cdot tt)$	[10]
	${}^{SI}O^{SP} = {}^{SI}E^{SP} \cdot \frac{1 - \exp(-{}^{SI}k_a^{SP} \cdot tt)}{{}^{SI}k_a^{SP} \cdot tt} + {}^{SI}I^{SP} \cdot \exp(-{}^{SI}k_a^{SP} \cdot tt) + \frac{{}^{SI}I^{InDP} \cdot [{}^{SI}k_h^{InDP} - {}^{SI}k_a^{SP} + \exp({}^{SI}k_h^{InDP} \cdot tt) \cdot {}^{SI}k_a^{SP} - \exp({}^{SI}k_a^{SP} \cdot {}^{SI}k_a^{SP})]}{{}^{SI}k_a^{SP} \cdot ({}^{SI}k_h^{InDP} - {}^{SI}k_a^{SP})} +$	[11a]
	where	
	${}^{SI}I^{SP} = <^{RR}SP> \cdot {}^{RR}k_L^{SP} + (<^{RR}InDP_{1B+2B}> \cdot {}^{RR}k_{p2}^{InDP} + <^{RR}MICRO> \cdot {}^{RR}k_{p2}^{MICRO} \cdot Y_{MICRO,InDP}) \cdot A_{InDP,SP} + {}^{OMA+AB}E^{SP}$	[11b]
	and	

	${}^{SI}I^{InDP} = (<{}^{RR}InDP_{1B+2B}> \cdot {}^{RR}k_{p2}^{InDP} + <{}^{RR}MICRO> \cdot {}^{RR}k_{p2}^{MICRO} \cdot Y_{MICRO,InDP}) \cdot (1 - A_{InDP,SP})$	[11c]
	${}^{SI}O^{InDP} = {}^{SI}I^{InDP} \cdot \exp(-{}^{SI}k_a^{InDP} \cdot tt)$	[12]
	${}^{SI}O^{FAT} = (<{}^{RR}FAT_2> \cdot {}^{RR}k_{p2}^{FAT} + <{}^{RR}MICRO> \cdot {}^{RR}k_{p2}^{MICRO} \cdot Y_{MICRO,FAT}) \cdot \exp(-{}^{SI}k_a^{FAT} \cdot tt)$	[13]
	${}^{SI}O^{NcAc} = <{}^{RR}MICRO> \cdot {}^{RR}k_{p2}^{MICRO} \cdot Y_{MICRO,FAT} \cdot \exp(-{}^{SI}k_a^{FAT} \cdot tt)$	[14]
	${}^{SI}O^{NH3} = <{}^{plasma}PU> \cdot {}^{SI}k_e^{PU} \cdot Y_{PU,NH3} \cdot \frac{1 - \exp(-{}^{SI}k_a^{NH3} \cdot tt)}{{}^{SI}k_a^{NH3} \cdot tt} + <{}^{RR}NH3> \cdot {}^{RR}k_L^{NH3} \cdot \exp(-{}^{SI}k_a^{NH3} \cdot tt)$	[15]
miscellaneous	${}^{i}\lambda_h^j = {}^{i}\lambda_h^j * {}^{i}P_d$	[16]
	${}^{RR}k_e^{PU} = \frac{{}^{RR}V_e^{PU} \cdot <{}^{plasma}PU>}{1 + {}^{RR}K_{e\|PU}^{PU} / <{}^{plasma}PU> + <{}^{RR}NH3> / {}^{RR}J_{e\|PU}^{NH3}}$	[17]
	${}^{SI}k_a^{SCHO} = \frac{{}^{SI}V_a^{SCHO} \cdot <{}^{SI}SCHO>}{1 + {}^{SI}K_{a\|SCHO}^{SCHO} / <{}^{SI}SCHO>}$	[18]
	${}^{RR}k_{p2}^{j} = \frac{{}^{RR}V_{p2}^{j} / (<{}^{RR}IHEM> + <{}^{RR}IADF>)}{1 + {}^{RR}K_{p2\|j}^{IHEM+IADF} / (<{}^{RR}IHEM> + <{}^{RR}IADF>)}$	[19]
	${}^{RR}E^{SP} = {}^{RR}E_{wall}^{SP} + {}^{RR}E_{saliva}^{SP}$	[20]

[1]See Appendix 1 for explanation of symbols, abbreviations, and unit conventions

.

Table 5.6. Equations for MICRO submodel of the mechanistic model[1]

Equation	
$${}^{i}v_u^{SCHO} = \frac{<{}^{i}MICRO>\cdot {}^{i}V_u^{SCHO}}{1+{}^{i}K_{u\|SCHO}^{SCHO}/<{}^{i}SCHO>}$$	[1]
$${}^{i}v_u^{SP} = \frac{<{}^{i}MICRO>\cdot {}^{i}V_u^{SP}}{1+({}^{i}K_{u\|SP}^{SP}/<{}^{i}SP>)^{\phi}+{}^{i}K_{u\|SP}^{SCHO}/<{}^{i}SCHO>}$$	[2]
$${}^{i}v_u^{NH3} = \frac{<{}^{i}MICRO>\cdot {}^{i}V_u^{NH3}}{1+{}^{i}K_{u\|NH3}^{NH3}/<{}^{i}NH3>+{}^{i}K_{u\|NH3}^{SCHO}/<{}^{i}NH3>+<{}^{i}SP>/{}^{i}J_{u\|NH3}^{SP}}$$	[3]
$${}^{i}microM = <{}^{i}MICRO>\cdot R_{microM}^{SCHO}$$	[4]
$${}^{i}pmicroG\|SCHO = \frac{{}^{i}microG\|NH3\cdot({}^{i}v_u^{SCHO}-{}^{i}microM)}{{}^{i}microG\cdot(R_{microG\|NH3}^{SCHO\|biomass}+R_{microG\|NH3}^{SCHO\|ferment})} + \frac{{}^{i}microG\|SP\cdot({}^{i}v_u^{SCHO}-{}^{i}microM)}{{}^{i}microG\cdot(R_{microG\|SP}^{SCHO\|biomass}+R_{microF\|SP}^{SCHO\|ferment})}$$	[5]
$${}^{i}pmicroG\|N = \frac{{}^{i}v_u^{NH3}}{R_{microG\|NH3}^{NH3\|biomass}} + \frac{{}^{i}v_u^{SP}}{R_{microG\|SP}^{SP\|biomass}}$$	[6]
$${}^{i}microG = \min({}^{i}pmicroG\|SCHO, {}^{i}pmicroG\|N)$$	[7]
$${}^{i}microG\|NH3 = \frac{{}^{i}v_u^{NH3}}{R_{microG\|NH3}^{NH3\|biomass}}$$	[8]
$${}^{i}microG\|SP = microG - microG\|NH3$$	[9]
$${}^{i}ferment^{SCHO} = {}^{i}v_u^{SCHO} - ({}^{i}microG\|NH3\cdot R_{microG\|NH3}^{SCHO\|biomass} + {}^{i}microG\|SP\cdot R_{microG\|SP}^{SCHO\|biomass})$$	[10]
$${}^{i}ferment^{SP} = {}^{i}v_u^{SP} - {}^{i}microG\|SP\cdot R_{microG\|SP}^{SP\|biomass}$$	[11]
$${}^{i}VFA^{SCHO} = {}^{i}ferment^{SCHO}\cdot Y_{SCHO,VFA}$$	[12]
$${}^{i}VFA^{SP} = {}^{i}ferment^{SP}\cdot Y_{SP,VFA}$$	[13]

[1]Refer to Table 5.4 for the main system of differential equations.

[2]See Appendix 1 for explanation of symbols, abbreviations, and unit conventions.

Table 5.7. Miscellaneous equations in the mechanistic model[1]

Equation		Note
$<^{RR}NDF>=<^{RR}DHEM>+<^{RR}IHEM>+<^{RR}DADF>+<^{RR}IADF>$	[1]	c.f. main text
$NE:P=\frac{NEI}{<^{SI}SP>\cdot^{SI}k_a^{SP}}$	[2]	c.f. main text
$^{i}P_d=\frac{^{i}V_{\max}^{P_d}}{1+N:SCHO/^{i}K_{P_d}^{SP:SCHO}}$ where $N:SCHO=\frac{(^{i}v_u^{SP}+^{i}v_u^{NH3}\cdot Y_{NH3,SP})}{^{i}v_u^{SCHO}}$	[3a] [3b]	
$NEI=[<^{SI}FAT>\cdot^{SI}k_a^{FAT}\cdot H_c^{FAT}\cdot(1-H_m^{FAT})+(<^{SI}SP>\cdot^{SI}k_a^{SP}-^{RR}E^{SP}-^{OM+AB}E^{SP}-^{SI}E^{SP}-^{LI}E^{SP})\cdot H_c^{SP}\cdot(1-H_m^{SP})+$ $<^{SI}SCHO>\cdot^{SI}k_a^{SCHO}\cdot H_c^{SCHO}\cdot(1-H_m^{SCHO})+(^{RR}VFA^{SCHO}+^{LI}VFA^{SCHO})\cdot H_c^{VFA^{SCHO}}\cdot(1-H_m^{VFA^{SCHO}})+$ $(^{RR}VFA^{SP}+^{LI}VFA^{SP})\cdot H_c^{VFA^{SP}}\cdot(1-H_m^{VFA^{SP}})+<^{SI}NcAc>\cdot^{SI}k_a^{NcAc}\cdot H_c^{NcAc}\cdot(1-H_m^{NcAc})-$ $<^{plasma}PU>\cdot^{urine}k_e^{PU}\cdot H_c^{PU}]\cdot(1-H_e)$	[4]	

[1]See Appendix 1 for explanation of symbols, abbreviations, and unit conventions.

Table 5.8. Estimated parameter values for absorption rates[1,2]

	space *i*		
nutrient *j*	RR	SI	LI
SCHO	-----	c.f. Eq. 18, Table 5.5	-----
InNFC	-----	-----	-----
SP	-----	3.75	-----
InDP	-----	-----	-----
NH3	0.52	1.50	0.35
FAT	-----	0.91	-----
NcAc	-----	2.80	-----

[1]See Appendix 1 for explanation of symbols, abbreviations, and unit conventions.
[2]See Appendix 2 for literature sources and methods used for parameter estimation.

Table 5.9. Estimated parameter values for age-dependent hydrolysis rates[1,2]

	diet				
nutrient *j*	ECA	LCA	C_3	C_4	GL
InNFC	0.50	0.50	0.50	0.50	0.50
DHEM	0.21	0.23	0.10	0.06	0.13
DADF	0.15	0.15	0.10	0.07	0.08
InDP	0.23	0.26	0.13	0.09	0.23

[1]See Appendix 1 for explanation of symbols, abbreviations, and unit conventions.
[2]See Appendix 2 for literature sources and methods used for parameter estimation.

Table 5.10. Estimated parameter values for endogenous protein and PU secretion[1,2]

	space				
parameter	RR	OM + AB	SI	LI	urine
${}^{i}E^{SP}$	-----	$3.15 \cdot 10^{-6}$	$2.10 \cdot 10^{-5}$	$2.05 \cdot 10^{-6}$	-----
${}^{i}k_e^{PU}$	c.f. Eq. 17, Table S4	-----	$2.75 \cdot 10^{-2}$	$1.10 \cdot 10^{-2}$	$6.30 \cdot 10^{-2}$

[1]See Appendix 1 for explanation of symbols, abbreviations, and unit conventions.
[2]See Appendix 2 for literature sources and methods used for parameter estimation.

Table 5.11. Estimated parameter values for MICRO uptake of NH3 and SP[1,2]

space	parameter							
	${}^{i}V_{u}^{NH3}$	${}^{i}K_{u\|NH3}^{NH3}$	${}^{i}K_{u\|NH3}^{SCHO}$	${}^{i}J_{u\|SP}^{NH3}$	${}^{i}V_{u}^{SP}$	${}^{i}K_{u\|SP}^{SP}$	${}^{i}V_{u\|SP}^{SCHO}$	ϕ
RR	$1.96 \cdot 10^{-2}$	$1.24 \cdot 10^{-2}$	$2.84 \cdot 10^{-2}$	$1.24 \cdot 10^{-2}$	1.06	$1.93 \cdot 10^{-1}$	$3.00 \cdot 10^{-2}$	1.22
SI	$1.96 \cdot 10^{-2}$	$2.70 \cdot 10^{-3}$	$6.18 \cdot 10^{-3}$	$2.70 \cdot 10^{-3}$	1.06	$4.20 \cdot 10^{-2}$	$6.55 \cdot 10^{-3}$	1.22

[1]See Appendix 1 for explanation of symbols, abbreviations, and unit conventions.
[2]See Appendix 2 for literature sources and methods used for parameter estimation.

Table 5.12. Estimated parameter values for heat of combustion and heat increment parameter values[1,2]

nutrient or metabolite j	H_c^j	H_m^j
SCHO	4.15	0.00
SP	5.96	0.19
FAT	9.36	0.05
VFA^{SCHO}	2.53	0.14
VFA^{SP}	4.27	0.12

[1]See Appendix 1 for explanation of symbols, abbreviations, and unit conventions.
[2]See Appendix 2 for literature sources and methods used for parameter estimation.

Table 5.13. Estimated yield parameter values for diet composition[1,2]

Diet	Parameter				
	$Y_{NFC,SCHO}$	$Y_{HEM,DHEM}$	$Y_{ADF,DADF}$	$Y_{CP,DP}$	$Y_{DP,SP}$
ECA	0.51	0.63	0.54	0.89	0.34
LCA	0.51	0.58	0.51	0.92	0.28
C_3	0.70	0.59	0.58	0.85	0.35
C_4	0.70	0.54	0.52	0.78	0.31
GL	0.61	0.44	0.56	0.89	0.34

[1]See Appendix 1 for explanation of symbols, abbreviations, and unit conventions.
[2]See Appendix 2 for literature sources and methods used for parameter estimation.

Table 5.14. Estimated miscellaneous parameter values[1,2]

j and l in $Y_{j,l}$		
j	l	value
SP	NH3	0.20
NH3	SP	5.13
PU	NH3	0.58
SP	PU	0.34
NcAc	NH3	0.22
NcAc	SCHO	0.63
SCHO	VFA^{SCHO}	0.76
SP	VFA^{SP}	0.50

[1]See Appendix 1 for explanation of symbols, abbreviations, and unit conventions.
[2]See Appendix 2 for literature sources and methods used for parameter estimation.

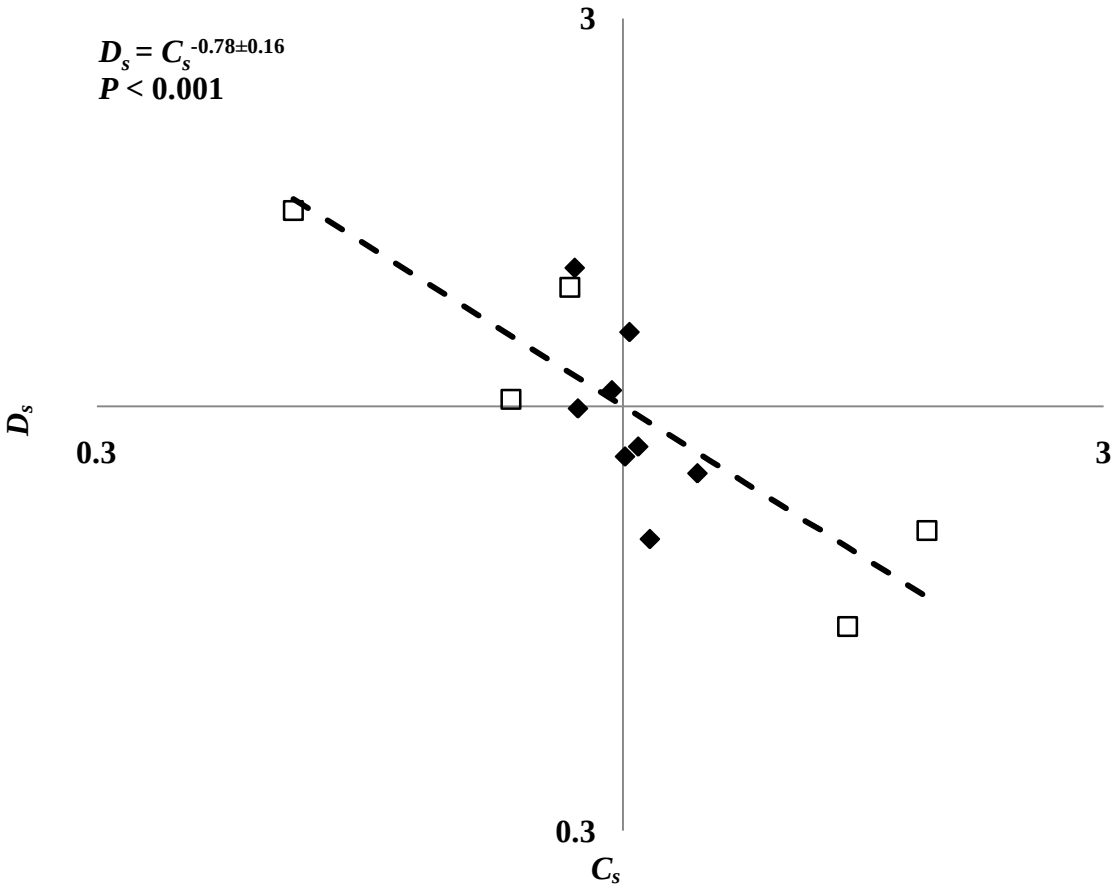

Figure 5.1. Empirical relationship between chemostatic (C_s) and distention (D_s) feedbacks derived from Bernal-Santos (1989) (□) and Bosch et al. (1992a,b) (♦). We estimated C_s and D_s according to methods described in the text. The dotted line is the regression line. The plot is semi-logarithmic.

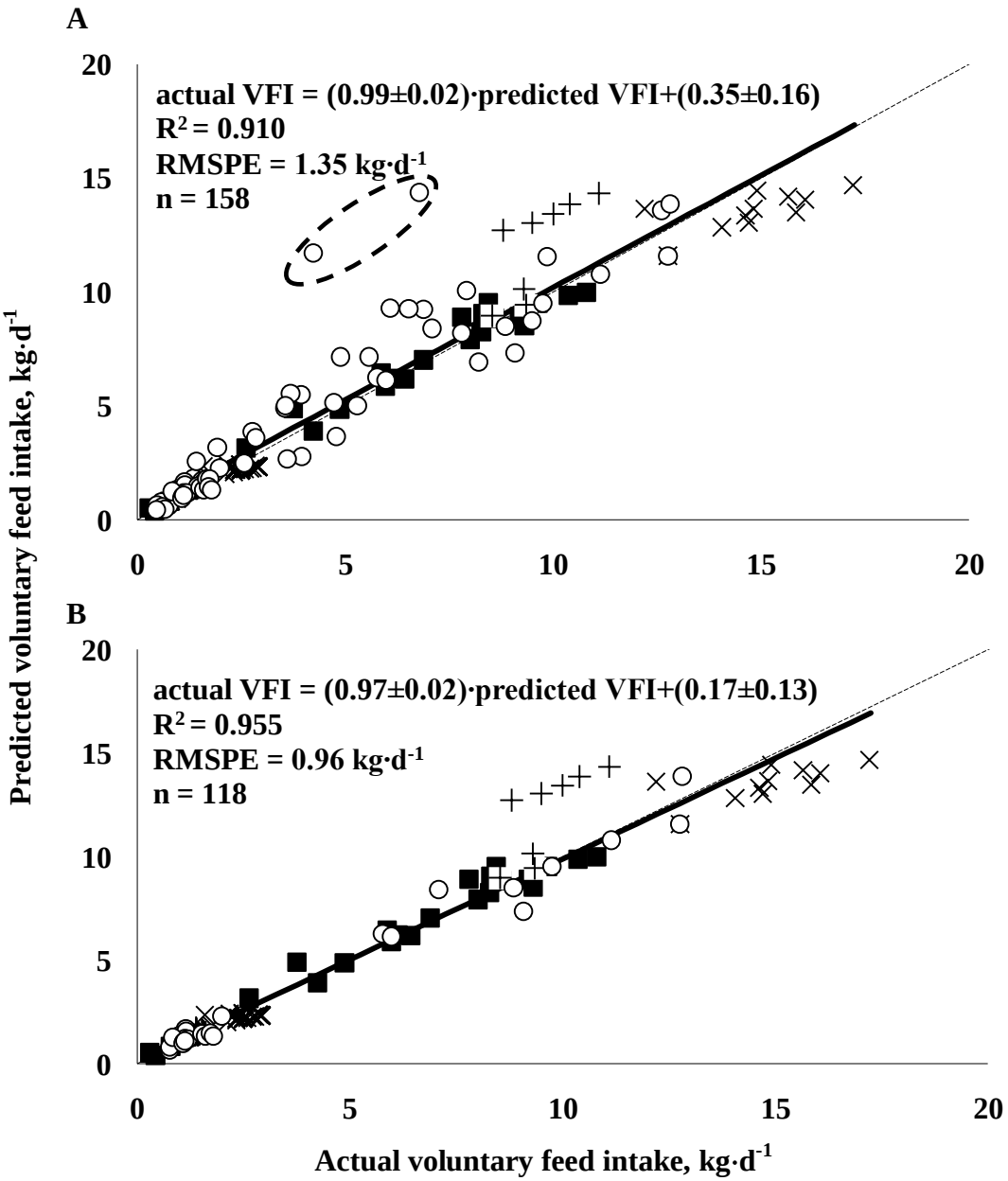

Figure 5.2. Comparison between actual and model-predicted voluntary feed intake (VFI; $kg \cdot d^{-1}$) of forage diets by ruminant species of various physiological states (growth [■], gestation [+], lactation [x], non-productive [○]). (A) All species (14 bovids, 4 cervids, and 1 giraffid). (B) Livestock species only. Circled in (A) are giraffe observations from Foose (1982) that our model systematically over-predicted. Dotted and solid lines represent x = y and the best-fit linear regression, respectively.

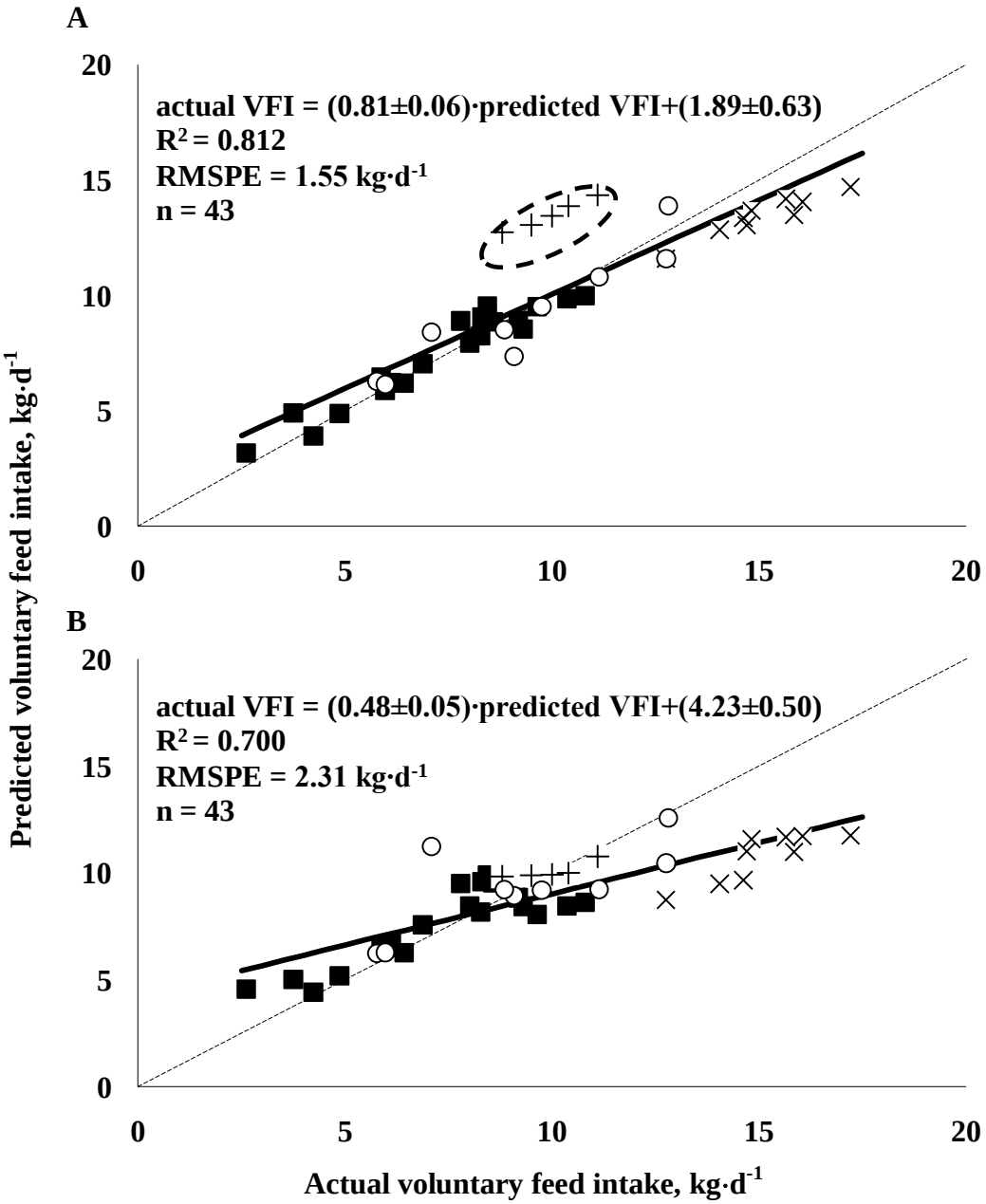

Figure 5.3. Comparison between actual voluntary feed intake (VFI; $kg \cdot d^{-1}$) and that predicted by (A) our mechanistic model and (B) the empirical equations of the NRC (2000) for cattle of various physiological states (growth [■], gestation [+], lactation [x], non-productive [○]). Circled in (A) are gestation observations from Stanley et al. (1993) that our model moderately over-predicted. Dotted and solid lines represent x = y and the best-fit linear regression, respectively.

CHAPTER 6

PRESSURE FOR LARGE BODY MASS IN THE RUMINANTIA: THE ROLE OF NUTRITIONAL RESOURCE LIMITATIONS

ABSTRACT

Explaining determinants of BW is a critical because BW accounts for 75% of variation in mammalian life history traits. Our objective was to determine whether nutritional resource limitations could exert pressure for large BW. We focus on the Ruminantia because there has been a clear pressure for large BW within this clade (median body BW is approximately 45 kg) and because we developed a ruminant food intake model key to this analysis. We found that increasing BW increases physiologically potential nutrient intake relative to metabolic requirements. The adaptive costs of increasing relative nutrient intake with increased BW (e.g., 20% increase in metabolic rate) underscore the impact of nutritional resource limitations on ruminant fitness. Tendency towards large BW, as evidenced by extant and fossil ruminants, is an evolutionary strategy adopted by the Ruminantia to overcome these nutritional resource limitations. Similar principles may partially explain BW evolution in other mammals.

INTRODUCTION

Body mass is highly correlated to a range of physiological variables (Peters, 1983) and overall accounts for 75% of variation in mammalian and avian life history traits (Calder, 1984). As such, BW is a crucial biological parameter and elucidating evolutionary pressures determining BW is important. The Ruminantia, an herbivorous mammalian

clade, is a suitable group with which to study pressures for large BW. Whereas the median BW of all extant mammals is approximately 90 g (Smith et al., 2003), the median BW of extant ruminant species is approximately 45 kg (van Wieren, 1996; Smith et al., 2003), with no species less than approximately 2 kg (van Wieren, 1996; Smith et al., 2003) and several extant and extinct species that have exceeded 1000 kg (Clauss et al., 2003).

There are a number of general advantages of large BW that may have selected for large BW within the Ruminantia. As discussed in part by Clauss et al. (2003) and Capellini and Gosling (2007), increasing BW increases daily travelling distance (Garland, 1983) and locomotory velocity (Peters 1983), increasing home range (Harested and Bunnell, 1979; Peters, 1983; Owen-Smith, 1988), foraging range, and ability to flee from predators (Altman, 1987). Large BW enhances the ability to stand defensively against predators (megaherbivores act indifferently or aggressively towards encroaching predators whereas small herbivores flee; Owen-Smith, 1988). It can provide better access to resources difficult spatially to reach, as for the giraffe in the African browsing ungulate guild (Woolnough and du Toit, 2001). Success in contests for mates also increases with increasing BW (Andersson, 1994). The difference between lower critical temperature and normal body temperature increases with increasing BW (Peters, 1983), permitting greater tolerance to cold. Further, with increasing BW, energy storage (in the form of adipose deposits) increases relative to metabolic requirements (Calder, 1984).

Whereas these advantages are well-documented and perhaps contributed to the pattern of large BW within Ruminantia, the advantage of large BW emphasized most frequently is embodied by the Bell-Jarman principle (Geist, 1974). This principle asserts

that increased BW grants an advantage in resource acquisition because metabolic requirements scale with $BW^{0.75}$ whereas physiologically potential intake of digestible nutrients (i.e., intake that is determined only by the internal physiological restrictions, not food availability, competition, or other factors) should scale with BW^{1} (though this proposed intake scaling pattern was not tested). Because intake rate increases over metabolic rate with increasing BW, poorer-quality foods could be selected by larger ruminants (Bell, 1970; Jarman, 1974), implying a fitness benefit associated with and pressure for large BW when poor-quality foods predominate.

Demment and Van Soest (1985) proposed a variant of this hypothesis by suggesting that because gut contents scale with BW^{1} and metabolic rate scales with $BW^{0.75}$, residence time should increase, permit more extensive digestion of the diet, and result in higher digestible nutrient intake relative to metabolic requirements with increasing BW. They used this reasoning to explain the lower BW limit of herbivores. Illius and Gordon (1991, 1992) and Gordon and Illius (1996) found through mechanistic modeling that intake scaled approximately with $BW^{0.8\text{-}0.9}$, again suggesting an advantage with increasing BW. Neither Demment and Van Soest (1985) or Illius and Gordon (1991, 1992) presented empirical data that directly support their contentions that digestible nutrient intake increases with increasing BW.

A major limitation of these hypotheses is their tacit assumption that nutritional resource limitations have appreciably impacted fitness. The possibility that resource-acquisition adaptations have exerted pressure for large BW exists, but the probability of this scenario remains unknown. Further, these hypotheses do not consider the importance of other resource-acquisition adaptations associated with increasing BW (larger foraging

range, better access to resources difficult to reach), making it difficult to assess the true importance of enhanced physiologically potential digestible nutrient intake. Another limitation of these hypotheses, as indicated in the discussion above, is their ultimate conclusions concerning the nutritional advantages with increasing BW often lack critical comparison with empirical data.

In this study we re-examine the core hypothesis that large BW within Ruminantia are explained by greater physiologically potential digestible nutrient intake with increasing BW. We also explore the corollary hypothesis that resource limitations have impacted the fitness of ruminants and ultimately generated selective pressure for large BW. We examine these hypotheses by considering how reticulorumen digesta contents scale with BW and inferring fitness implications of different scaling patterns. Finally, we apply, to non-ruminants, our finding that ruminants evolved large BW as a likely strategy to overcome nutritional resource limitations.

METHODS

Scaling of PPDMI and DDM with BW

To empirically test the Bell-Jarman principle and its variants, we compiled literature data to derive the allometric relationship relating BW to digestible DM (**DDM**) and physiologically potential DMI (**PPDMI**). We define PPDMI as intake determined by only internal, physiological constraints (gastrointestinal tract [**GIT**] capacity, chemostatis, lipostasis, other physiological regulation) and not external constraints like food availability, competition, or other factors. In order to provide a controlled analysis and accommodate other factors, we employed the following selection criteria in choosing literature sources:

(1) Diets offered must consist of entirely forage, excepting vitamin and mineral supplements. Compared to mixed forage-concentrate diets, all-forage diets permit limited dietary selection by animals. They also allow better comparison between empirical results and that of our mechanistic model (see below), which accommodates forage diets only.

(2) Very similar or identical diets must be offered to all species within a study, permitting the effect of diet on PPDMI to be removed (see below).

(3) Animals must be of mature size and a non-productive physiological state (i.e., non-lactating, non-gestating), ensuring a uniform animal type across studies.

(4) To fulfill the definition of PPDMI, forage must be made freely available at all times and other measures taken such that food availability does not limit intake.

(5) Studies must include three or more animal species. This criterion allows regression outliers within a study to be better detected; because an allometric equation requires two df (intercept and scaling parameter), at least three species are required to detect outliers within a study.

Five studies met these criteria and were thus selected. They included 19 species with a BW range of 17.2 to 907 kg. Table 6.1 lists these studies and species, and Table 6.2 reports descriptive statistics of these studies.

We examined the relationship between PPDMI ($kg \cdot d^{-1}$) and DDM ($g \cdot g\ DM^{-1}$) with the following analysis of covariance (**ANCOVA**) model:

$$Y = a + diet + b \cdot BW + diet \times BW$$

where Y = independent variable (DMD or log-transformed PPDMI), *diet* = diet type within study, BW = log-transformed BW (the covariate), *diet* x BW = diet x BW

interaction term, a = intercept term, and b = scaling parameter. We did not logarithmically-transform DMD because doing so did not improve linearity. Because *diet* x *BW* terms were not significant for PPDMI ($P = 0.960$) or DMD ($P = 0.706$) regressions, we dropped the interaction term and re-ran the regressions. We re-expressed and reported the PPDMI regression equation in the exponential form

$$Y = a \cdot BW^{b}$$

With exception of the DDM regression (inappropriate to express in the exponential form because we used untransformed values of DDM), all allometric equations subsequently discussed are reported in this exponential form.

For Foose (1982) and van Weiren (1996), DMD was not reported, and OM digestibility (**OMD**) was used a proxy. Its use as a proxy is supported by several reasons beyond statistical necessity. First, ash comprises a relatively small fraction of DM relative to other macronutrients (mean concentration ± SD was 0.073±0.031 $g \cdot g^{-1}$), digestibility of ash was found highly variable (-0.090±0.369) but appeared to have no apparent relationship with BW (Domingue et al., 1991), and the *diet* covariate in the ANCOVA removes any systematic differences between studies that reported DDM and those that reported OMD. Consequently, differences between DDM and OMD should be minor and unrelated to BW, and differences across studies that report DDM and OMD should be removed, justifying the use of OMD as a proxy for DDM.

We identified two giraffe observations in the dataset, those for grass and alfalfa from Foose (1982), as outliers and subsequently removed them. Each fell far below the PPDMI regression line, as indicated visually and by the large negative value of their studentized residuals, -2.467 (alfafa) and -3.389 (grass). Owen-Smith (1988) also

identified these giraffe observations as outliers in his own regression analysis of Foose's (1982) data.

Allometric Equations for Scaling of RR Parameters with BW

We took allometric equations relating BW with reticulorumen (RR) volume (L), RR DM contents (kg), basal metabolic rate (BMR; $kcal \cdot d^{-1}$), and field metabolic rate (FMR; $kcal \cdot d^{-1}$) from van Wieren (1996), Illius and Gordon (1992), Blaxter (1989), and Nagy et al. (1999), respectively (Table 6.3). The allometric equation for BMR from Blaxter (1989) is that reported for Artiodactyla, and that for FMR from Nagy et al. (1999) is for all eutharian mammals. Illius and Gordon (1992) reported that the scaling parameter for the RR DM contents equation did not differ from 1, and, as done by those authors, we report a regression with a scaling parameter set to 1.

We derived allometric equations relating BW with RR wet matter (WM) contents (kg) and RR tissue WM (kg). For the former, we used data from nine studies on 22 species (Table 6.1), with BW ranging from 3.69 to 807.5 kg. For the latter, we used data from 10 studies on 18 species (Table 6.1), with BW ranging from 20.7 to 807.5 kg. In order to estimate *a* and *b*, we used a simple linear regression model with log-transformed RR tissue mass and log-transformed BW as dependent and independent variables. We could not use an ANCOVA because too few studies listed multiple species.

Though the scaling parameters of RR-related parameters differ from 1 numerically, all approach 1 and parameters for two equations (RR DM contents, RR tissue mass) do not differ statistically. For brevity they will be referenced as scaling to 1 precisely.

For comparison, we determined values of RR-related parameters for the hypothetical case where they scale with $BW^{0.75}$. To compute these values, values of *b* in the RR-parameter prediction equations (Table 6.3) were changed to 0.75, while the original values of *a* were retained. Where we refer to parameter values when RR size scales with $BW^{0.75}$, we refer to parameter values calculated with $b = 0.75$ (and *a* equal to original values). By the same token, where we refers to RR size scaling with BW^{1}, we refer to parameter values calculated with original values of *b* (which approach 1) and *a*—i.e., with prediction equations in Table 6.3.

Calculation of FMR and Other Parameters when RR Size Scales with $BW^{0.75}$ vs. BW^{1}

Using the following methods, we calculated FMR and other parameters when the RR size scales with BW^{1} vs. a hypothetical case where it scales with $BW^{0.75}$.

Total BW can be partitioned into (1) RR tissue WM and contents and (2) remaining tissue as follows:

$$BW = \text{RR tissue WM and WM contents} + \text{RR-free BW} \quad [1]$$

Here and throughout this analysis, we impose the condition that individuals with RR size$\propto BW^{0.75}$ and RR size$\propto BW^{1}$ are identical in all ways except those immediately impacted by RR size. We recognize that parameters even distantly related to RR size could change over evolutionary time if RR size scaling changed, but we assume general similarity between scaling cases in order to study the impact of changing RR size scaling in isolation. Following this assumption, parameter values when RR size$\propto BW^{0.75}$ vs. BW^{1} are identical when expressed on a RR-free basis—e.g., RR-free BW is identical when RR size$\propto BW^{0.75}$ vs. BW^{1}. Here and throughout we assign subscripts to the RR-dependent parameters to designate their value when RR$\propto BW^{0.75}$ vs. BW^{1}; let "1"

designate the case when scaling is with BW^1 and "2" when scaling is with $BW^{0.75}$—e.g., BW_2 is BW when RR size$\propto BW^{0.75}$. Additionally, we append the subscript "0" to BW and other parameters to indicate their value when the RR is absent—e.g., BW_0 is RR-free BW. For BW, we thus have

$$BW_i = BW_0 + [RR\ tissue\ and\ WM\ contents]_i \quad [2]$$

where i = 1 or 2 in order to designate whether parameters pertain to the case where RR parameters$\propto BW^1$ or $BW^{0.75}$, respectively.

Acceleration is given by the general formula

$$a = (P \cdot t)/(\text{mass} \cdot d) \quad [3]$$

where a = acceleration ($m \cdot s^{-2}$), P = power (W), t = time (s), *mass* = mass (kg), d = distance (m). Because RR size does not immediately affect muscle size or strength, we assume that power delivered by the muscles, P, is identical in each case (i.e., $P_1 = P_2$). With $mass_i = BW_i$ and for identical t and d, the ratio of a_1 to a_2 is

$$a_1/a_2 = BW_1/BW_2 \quad [4]$$

To give an index of the absorptive and secretive capacity of the RR, we define the term relative absorptive/secretive capacity (**RASC**):

$$RASC = \text{RR SA/RR volume} \quad [5]$$

where SA = surface area (m^2). The use of this ratio as an index reflects that (1) metabolite absorption (such as that of short-chain fatty acids and NH_3) and secretion (such as that of urea) rates from the RR are proportional to RR epithelial SA, and (2) the load of metabolites required to be absorbed and secreted should increase with RR volume (because size of fermentation contents directly increase with RR volume and so too will acid and NH_3 production and microbial urea-N requirement). Thus, with increasing

RASC, requirements for absorption and secretion are more fully met, making larger values of RASC potentially more advantageous. Under the case of geometric similarity, SA increases with $V^{2/3}$. Setting V to the volume of the RR, $RASC_i$ is

$$RASC_i = V_i^{2/3}/V_i^1 = V_i^{-1/3} \quad [6]$$

In his classic investigation of the stomach structure of 27 African ruminant species, Hoffman (1973) remarks that the RR "occupies almost three-quarters of the peritoneal cavity" (p. 23). Following this observation, it is assumed that fraction of space not occupied by the RR is 0.3 when RR$\propto$BW^1. To calculate the value of this fraction when RR size$\propto$BW$^{0.75}$, first, the total volume of peritoneal space (L) when RR$\propto$BW^1 is calculated as

$$[volume\ of\ peritoneal\ space]_1 = [RR\ volume]_1 / 0.7 \quad [7]$$

where 0.7 represents the fraction of peritoneal space occupied by the RR when RR size$\propto$BW^1. For this analysis, the volume of the peritoneal space when RR$\propto$BW$^{0.75}$ is the same as that when RR$\propto$BW^1 (i.e., there is geometric similarity for peritoneal cavity size and architecture). The fraction of peritoneal space not occupied by the RR when RR$\propto$BW$^{0.75}$ is then

$$[fraction\ of\ peritoneal\ space\ not\ occupied\ by\ the\ RR]_2 = [RR\ volume]_2 / [volume\ of\ peritoneal\ space]_1 \quad [8]$$

As mentioned above, FMR when RR size$\propto$BW^1 (FMR_1) is estimated from an equation from Nagy et al. (1999). After accounting for several changes that occur when RR size changes scaling from BW^1 to BW$^{0.75}$, we can calculated FMR_2 from FMR_1. This section discusses the scaling-related changes that impact FMR, including changes in RR

metabolic rate, activity costs, and heat increment (HI). Because of its detail, the precise calculation of FMR_2 is relegated to Appendix 1.

A large component of BMR (and thus FMR) is the metabolism of the GIT (McBride and Kelly, 1990), which includes the RR. To calculate the metabolic rate of RR tissue (kcal·d^{-1}) when RR size$\propto$BW$^{0.75}$ and BW^{1}, we multiple estimated RR tissue WM (Table 6.2) by the mass-specific metabolic rate of RR tissue, 929 kcal·kg RR tissue DM^{-1}·d^{-1} (average cattle values summarized by Cant et al. [1996]). Further assuming RR tissue WM is 0.825 g water·g tissue WM^{-1} (Smith and Baldwin 1974), we have

$$RR\ metabolic\ rate = 929 \cdot RR\ tissue\ WM \cdot (1\text{-}0.825). \quad [9]$$

We reason that changing RR size scaling affects FMR also by changing activity expenditures. This reasoning is fundamentally based on the work of Taylor et al. (1980), which demonstrated with rats, dogs, humans, and horses that carrying a load increases O_2 production during movement relative to the case where no load is carried. Specifically, they found that the relationship

$$O_2\ production\ of\ loaded\ animal\ during\ movement\ /\ O_2\ production\ of\ loaded\ animal\ during\ movement = 1.01\ mass\ of\ animal,\ loaded\ /\ mass\ of\ animal,\ unloaded \quad [10]$$

Because the relationship found by Taylor et al. (1980) was independent of locomotion speed and gait, we reason that O_2 production during standing (locomotion speed = 0) is increased by carrying a load in the same manner as when locomotion speed >0. We assume that O_2 production is directly proportional to heat production so that ratio of heat production for the loaded and unloaded animal follows the mass relationship given in Eq. 10. We also envision the RR tissue WM and WM contents as a "load" carried by the

ruminant similar in effect as external loads applied by Taylor et al. (1980). Finally, we define activity to consist of either standing or movement. (Some may consider eating as an activity, but we classify and account for it as a component of HI, as discussed later.) Applying the above logic and assumptions to Eq. 10 yields the following relationship

$$[\textit{heat release during activity}]_i / [\textit{heat release during activity}]_0 = BW_i / BW_0 \quad [11]$$

The HI component of FMR is the increase in heat production following consumption of a meal and primarily includes heat released from microbial fermentation, eating (mastication, rumination, and other digestive processes), and nutrient metabolism (arising from the inherent inefficiency of assimilating absorbed nutrients) (Blaxter, 1989). It is often expressed as a fraction of metabolizable energy intake (MEI)—i.e.,

$$HI = MEI \cdot (1-k) \quad [12]$$

where k = efficiency of use of ME (Mcal NE·Mcal ME^{-1}).

Under conditions of energy stasis, carrying a load (e.g., that of the RR contents and tissue) increases the HI. Carrying a load increases energetic expenditures, as indicated by the effect carrying a load on heat production (Eq. 11). To maintain energy stasis, carrying a load necessitates that MEI must be increased, which, by Eq. 12, increases heat increment. From Eq. 11 and 12, as well as calculated RR metabolic rate, FMR_2 we calculate FMR_1, as detailed in the appendix.

The allometric equation for PPDMI (see Results) was used to estimate $PPDMI_1$. As discussed below, we found PPDMI would scale with $BW^{0.75}$ if RR hypothetically scaled with $BW^{0.75}$. To estimate $PPDMI_2$, the value of b was changed to 0.75 while original value of the coefficient a was unchanged.

To help illustrate the change in FMR and other parameters when RR scales with $BW^{0.75}$ vs. BW^{1}, parameter values were calculated at discrete values of BW. Body weight values chosen were 2, 50, 100, 500, 1000, 1500, and 3000 kg. These values range from the smallest (*Madoqua saltiana swaynei, Neotragus pygmaeus, Tragulus javanicus*) to largest (the extinct Sivatheriinae) ruminants and included the largest extant bovid (*Bison bison, Bos gaurus, Bubalus bubalis*) and giraffid (*Giraffa camelopardalis*) along with several intermediate points for comparison. Body weights for smallest and largest extant ruminants were from those summarized by van Weiren (1996) and Clauss et al. (2003), respectively, and that for the largest extinct ruminant in the upper end of the range estimated by Clauss et al. (2003). To help illustrate change in parameter values when RR size scales with $BW^{0.75}$ vs. BW^{1}, we calculated the ratio of parameters values when RR size$\propto BW^{0.75}$ vs. BW^{1}.

Investigating PPDMI Scaling with a Mechanistic Model of Ruminant Digestion

We hypothesized that PPDMI scales with $BW^{0.875}$ because RR DM contents scale with BW^{1} and metabolic rate scales with $BW^{0.75}$. We further hypothesized that PPDMI would scale with $BW^{0.75}$ if RR DM contents were to hypothetically scale with $BW^{0.75}$. To test these hypotheses, we used a mechanistic model of ruminant digestion developed in Chapter 6. A brief description of the model is provided in Appendix 2.

In the model, we set RR DM contents and metabolic rate (more precisely, optimal RR fill and energetic demands, respectively; see appendix) to scale with BW^{1} and $BW^{0.75}$, respectively (their empirical patterns). With these scaling patterns, the model was used to predict PPDMI of a high-quality C_3 grass (500 g NDF, 300 g ADF, 150 g CP, 90 g ash·kg DM^{-1}) by an ox (maintenance energetic demands of 65 kcal·kg $BW^{0.75}$; NRC

2000, assuming empty BW = 0.85 full BW). We varied mature BW of the ox in increments from 1 to 2000 kg and predicted-PPDMI at each increment recorded. Scaling of model-predicted PPDMI with BW was determined using a one-way ANOVA, with BW as the factor. Different forage types and qualities, as well as ruminant species (with corresponding metabolic rates), were later used. It was found that the scaling of predicted-PPDMI with BW was insensitive to forage and animal species, and thus results for the alfalfa and ox alone are subsequently presented.

Next, we set RR DM contents and metabolic rate both set to scale with (1) $BW^{0.75}$ or (2) BW^{1}. For these two scaling patterns, we used the model to determine PPDMI over a wide range of BW, and determined scaling of model-predicted PPDMI with BW with an ANOVA. Again, final scaling results were insensitive to forage and animal types selected.

Body Mass Distributions of Fossil and Extant Ruminants

We estimated and compared BW of fossil ruminants to those of extant ruminants to determine the change in BW of ruminants over evolutionary time. Our approach in summarizing and estimating BW of fossil species largely follows that of Janis (2000). We took data for fossil ruminants from chapters of Janis et al. (1998), a comprehensive and standardized source for the North American (NA) Tertiary fossil record. We included all genera of NA Tertiary ruminant families (Hypertragulidae, Leptomerycidae, Antilocapridae, Dromomerycidae, Moschidae) except those of the Bovidae and Cervidae. We excluded these groups because they represent rare and recent migrants (late Miocene) in the NA Tertiary (Webb, 1998a). We estimated BW using reported dental measurements (average m2 or, when unavailable, average M2 lengths) with prediction

equations of Janis (1990). Appearance dates were those reported in chapters of Janis et al. (1998). We took BW for extant ruminants from van Wieren (1996).

We examined relationship between estimated BW (kg) of fossil ruminants and date of appearance (millions of years relative to present) with the ANCOVA model:

$$\log BW = a + family + b \cdot time + family \times time$$

where *log BW* = log-transformed BW, *family* = taxonomic family (Hypertragulidae, Leptomerycidae, Antilocapridae, Dromomerycidae, Moschidae), *time* = date of appearance, *family x time* = family x time interaction, *a* = intercept term, and *b* = slope term.

RESULTS

Scaling of PPDMI with BW

The allometric equation relating BW with PPDMI for 18 species (BW range 17.2 – 817 kg)

$$PPDMI = 10^{(-1.36 \pm 0.0756 + diet)} \cdot BW^{(0.875 \pm 0.0324)}$$

where values presented are parameter means±SE (n = 51, root mean square prediction error [RMSPE] = 1.20 kg·d^{-1}, R^2 = 0.967). Lower and upper ninety-five percent confidence limits for *b* are 0.810 and 0.941. The *BW* term and overall regression and were highly significant ($P < 0.001$ for each), as was the *diet* term ($P < 0.001$), which, for brevity, is not given numerical values in the equation above but ranged from -0.205 to 0.094 across diets.

Scaling of DDM with BW

The allometric equation relating BW with DDM for 19 species (BW range 17.2 – 907 kg) of ruminants is

$$DDM = (0.524 \pm 0.049) + (0.0152 \pm 0.0206 + diet) \cdot \log(BW)$$

where parameter means±SE are given parenthetically (n = 53, RMSPE = 0.0102 g· g^{-1}, R^2 = 0.944). The overall regression was highly significant ($P < 0.001$), as was the *diet* term ($P < 0.001$), which, for brevity, is not given numerical values in the equation above but ranged from -3.806 to 19.000 across diets. In contrast, the BW term did not approach significance ($P = 0.465$).

Scaling Results of the Mechanistic Model

We used a mechanistic model to predict PPDMI under three scenarios: (1) metabolic rate and RR DM contents scale with $BW^{0.75}$ and BW^{1}, respectively, (2) metabolic rate and RR DM contents each scale with BW^{1}, and (3) metabolic rate and RR DM contents each scale with $BW^{0.75}$. Figure 6.1 shows model-predicted PPDMI under these three scenarios for a hypothetical ox (ranging in BW from 1 to 2000 kg) consuming a C_3 grass; results are similar for different forage and animal types, and only those of the ox and grass are presented for brevity.

Under scenario #1, in which metabolic rate and RR DM contents scale according to their observed patterns, PPDMI scales with $BW^{0.901 \pm 0.0005}$ (mean±SE). Under scenario #2, when we set RR DM contents to artificially scale with $BW^{0.75}$, PPDMI only scales with $BW^{0.76 \pm 0.002}$. Under scenario #3, where metabolic rate was artificially set to scale with BW^{1}, PPDMI scales with $BW^{1 \pm 0.00001}$.

Value of Physiological Parameters when RR Size Scales With $BW^{0.75}$ vs. BW^{1}

Table 6.4 and 6.5 reports the value of RR volume RR WM contents, RR tissue WM, FMR, RASC, and fraction of peritoneal space not occupied by the RR when RR size$\propto BW^{0.75}$ vs. BW^{1}, respectively. In Table 6.5, BW when RR size$\propto BW^{1}$ is reported

alongside BW when RR size$\propto BW^{0.75}$ to facilitate comparison between Tables 4 and 5. The values of RR volume RR WM contents, RR tissue WM, and FMR increase with increasing BW when RR size$\propto BW^{0.75}$ and BW^{1}, but increase more rapidly when RR size$\propto BW^{1}$. The value of RASC decreases with increasing BW because SA increases more slowly than does volume with increasing RR size. It decreases more rapidly when RR size$\propto BW^{1}$. The fraction of peritoneal space not occupied by the RR remains constant for RR size$\propto BW^{1}$, as defined in Methods, but it increases with RR size$\propto BW^{0.75}$.

To further facilitate comparison between the cases where RR size$\propto BW^{0.75}$ vs. BW^{1}, Table 6.6 reports the fraction of parameter values expected when RR size$\propto BW^{0.75}$ vs. BW^{1}. Values of the most important parameters (FMR, fraction of peritoneal space not occupied by the RR, RASC, maximum locomotory acceleration, and PPDMI) only are included for brevity (the importance of other parameters is solely for calculation of FMR_2). Maximum locomotory acceleration and PPDMI are not included in previous tables, where absolute values of parameters are reported, because calculation of absolute values for locomotory acceleration require parameter values not estimated in this study and calculation of absolute values of PPDMI depends on dietary quality, which varies considerably. In Table 6.6, values for FMR and PPDMI are less than unity for all BW and decrease with increasing BW. The fraction of peritoneal space, RASC, and maximum locomotory acceleration are greater than unity at all BW and increase with increasing BW.

BW of Fossil Ruminants over the NA Tertiary

Figure 1.6 shows estimated BW of fossil ruminants over the NA Tertiary. Visually, there is a consistent and approximately log-linear increase in BW manifested

across all families, except Gelocidae (which is relatively small for its appearance date). Formally, the ANCOVA indicates that BW increased, on average, 9.11% per million years; this rate of increase is both highly significant ($P < 0.001$ for *time*) and invariant across families ($P = 0.142$ for *time* x *family* interaction).

DISCUSSION

Scaling of PDDMI and DDM with BW

The mean and 95% confidence limits of *b* for the allometric equation relating BW with PPDM suggest that scaling of potential PPDMI is less than isometric but higher than metabolic rate. By contrast, most reviews in animal ecology find that PPDMI scales with $BW^{0.75}$ for ruminants and other herbivores (review by Clauss et al. [2007]). For ruminants, at least, this $BW^{0.75}$ scaling is likely artificially low. Across feeding trials, low BW species are typically provided higher-quality diets than those of high BW (c.f., supplement to Clauss et al. [2007]). Because consumption of higher-quality diets should be greater than that of low-quality diets, PPDMI by low-BW animals is artificially inflated and PPDMI of high-BW animals artificially lowered when compared concurrently. This leads the value of b to be underestimated when data across experiments are compiled and diet-related variation not removed, as in most reviews.

The value of *b* in this investigation would not be susceptible to such underestimation because diet effects are removed by employing an ANCOVA, supporting the validity of our value of *b*. Additional support for our finding of *b* comes from Reid et al. (1990), who summarized ruminant livestock feeding trials (involving domestic cattle, sheep, and goats) in which diet attributes were kept constant across BW,

and thus diet-related variation was controlled. They found PPDMI scaled approximately with $BW^{0.9}$, similar to the scaling found in this study.

In its allometric equation for DDM, DDM did not scale significantly with BW ($P = 0.465$). This finding, along with a highly-significant term for diet ($P < 0.001$), suggests that DDM is affected primarily by dietary factors and not BW. Demment and Van Soest (1985), Illius and Gordon (1991, 1992), and Gordon and Illius (1994), among others, have argued that digesta retention time should increase with increasing BW, permit more extensive digestion of DM, and lead to higher DDM. Our results suggest that either (1) retention time does not appreciably increase with increasing BW, as supported by an extensive review by Clauss et al. (2007), or (2) retention time does not appreciably limit DDM.

The allometric equations relating PPDMI and DDM demonstrate that digestible nutrient intake scales with $BW^{0.875}$; digestible nutrient intake is the product of PPDMI, which scales with $BW^{0.875}$, and DDM, which scales with BW^{0}. The scaling for digestible nutrient intake is thus higher than that for metabolic requirements, revealing a mechanism for the Bell-Jarman principle. The Bell-Jarman principle suggests increasing BW grants greater tolerance to poor-quality food, and was developed to explain patterns of dietary selection across BW in ruminants and other ungulates (Geist, 1974) and has since been applied to a wide range of mammals, including primates (Gaulin, 1979) and sciurids (Tyser and Moermond, 1983). Despite extensive observational data and conceptual arguments (Demment and Van Soest, 1985; Illius and Gordon, 1991, 1992; Gordon and Illius, 1996) consistent with the hypothesis, to our knowledge no study has directly verified a possible underlying mechanism of the principle. Importantly, the

results of this study show that for ruminants, the large-BW advantages described by the Bell-Jarman principle arise from an advantage in PPDMI (not DDM), in contrast to the oft-cited argument of Demment and Van Soest (1985) but in general agreement with Illius and Gordon (1991, 1992) and Gordon and Illius (1996).

Expanding upon the Bell-Jarman principle, these results suggest that because of their PPDMI-advantage, large ruminants can select a poorer-quality diet than small ruminants and still meet basal requirements. Further, they suggest large ruminants can more greatly exceed their basal requirements than small ruminants when selecting the same diet, permitting a higher production level (e.g., of milk, conceptus, and other body tissue). This might be one route by which selective pressure for larger BW is exerted. The likelihood of this scenario is determined by the probability that intake of digestible nutrients is a limiting factor to fitness and is determined appreciably by the PPDMI-advantaged mechanism described here (i.e., in comparison to other mechanisms by which large BW may increase nutrient consumption, as discussed in the introduction).

Scaling Results of the Mechanistic Model

When we set both RR DM contents and metabolic rate to their empirically-observed scaling patterns, the mechanistic model predicted a PPDMI scaling pattern ($BW^{0.901}$) very close to the empirical pattern found in this dataset ($BW^{0.875}$) and that found by Reid et al. (1990) ($BW^{0.9}$). By contrast, when we changed either RR DM and metabolic rate scaling from its empirically observed pattern to an artificial one ($BW^{0.75}$ for RR DM, BW^{1} for metabolic rate), PPDMI scaling shifted dramatically from $BW^{0.9}$ to either $BW^{0.76}$ (when RR DM$\propto BW^{0.75}$) or BW^{1} (when metabolic rate $\propto BW^{1}$). These results together suggest PPDMI scales with $BW^{0.875}$ as the result of metabolic rate scaling

with $BW^{0.75}$ and RR DM contents scaling with BW^{1}. Similarly, they show that the BW-related advantage in PPDMI arises from RR DM size scaling with $BW^{>0.75}$ (BW^{1} specifically).

In their models, Illius and Gordon (1991, 1992) and Gordon and Illius (1996) found that PPDMI scaled approximately with $BW^{0.8\text{-}0.9}$, as well. However, they explained the scaling pattern as resulting from an interaction between scaling of retention time (which they contend scales with $BW^{0.27}$) and digestion rate (which scales with BW^{0}; see Illius and Gordon [1991]). Their explanation also predicts that intake scaling should change with diet quality, but comparison with empirical data show this not be the case (diet x BW term in the allometric analysis was not significant; P = 0.960), suggesting that their scaling explanation is incorrect.

These model findings suggest the consequences of RR scaling with BW^{1} vs. $BW^{0.75}$ be further examined: why should RR size scale with BW^{1} if scaling with $BW^{0.75}$ causes no disadvantage in PPDMI with increasing BW?

Adaptive Costs and Benefits of RR Size Scaling with $BW^{0.75}$ vs. BW^{1}

Results in Tables 4, 5, and 6 imply a ruminant with RR size$\propto BW^{0.75}$ has several major advantages over a similarly-sized individual with RR size$\propto BW^{1}$. The individual with RR size$\propto BW^{0.75}$ is expected to have lower heat production and energetic requirements, indicated by values of FMR. Such an individual would also have greater space for fat storage and organ differentiation, indicated by values of fraction of peritoneal space unoccupied by RR; ability to absorb and secrete necessary nutrients and metabolites from the RR, indicated by RASC; and ability to flee from predators, indicated by values of maximum locomotory acceleration. Furthermore, these relative

advantages increase with increasing BW, becoming considerable at high BW. By changing RR size scaling from BW^1 to $BW^{0.75}$ for the largest extant ruminant (1500 kg), we expect FMR to decrease by nearly 20% while the fraction of peritoneal space, RASC, and locomotory acceleration to increase more than 250, 150, and 120%. The composite impact of these advantages on fitness are difficult to quantitate precisely but must be great.

In the midst of these advantages, scaling RR size with $BW^{0.75}$ vs. BW^1 brings one key disadvantage. From Table 6.6, there exists a clear disadvantage in PPDMI, with PPDMI of the largest extant ruminant only about 0.4 when RR size$\propto BW^{0.75}$ vs. BW^1. According to the Bell-Jarman principle and the discussion above, this would cause an animal with RR size$\propto BW^{0.75}$ to be less tolerant of poor-quality food or maintain a lower production level than an individual with RR size$\propto BW^1$.

There are a few related disadvantages associated with RR size$\propto BW^{0.75}$ vs. RR size$\propto BW^1$. Decreased RR size would lower RR storage capacity, both long- and short-term. Decreased long-term storage of food and water would decrease long-term capacity for intake (effectively PPDMI), and thus render no different disadvantages than discussed above. Decreased short-term storage would lower short-term intake capacity as the RR would be filled more quickly during feeding. Among other effects, this could increase predation risk. Lower short-term intake capacity would decrease the amount of nutrients that could be acquired in one foraging bout, increase the number of foraging bouts required to meet daily nutrient requirements, increase the required foraging frequency, and hence could force animals to forage during times of day when predation risk is higher. Note that this disadvantage is still fundamentally related to physiological intake

limitations, which PPDMI reflects (albeit more so on the long- than short-term timescale).

In sum, there exist a number of potential adaptive benefits to scaling RR size with $BW^{0.75}$ vs. BW^{1} whereas there exists only one core disadvantage, decreased PPDMI. However, despite the severity of the relative costs of RR size$\propto BW^{1}$, RR size is observed to scale with BW^{1}. This suggests that advantage gained from increasing PPDMI with increasing BW must be great. For the fitness benefit of PPDMI to be considerable, nutritional resources must have been limiting. This, in turn, demonstrates that nutritional resource limitations, at root, have generated selective force for large BW. In sum, this analysis suggests that fitness of ruminants is limited by acquisition of nutritional resources, and development of large BW is a key strategy of coping with these limitations.

Note that the approach above does not directly assess the importance of other resource-acquisition adaptations associated with increasing BW (larger foraging range, better access to resources difficult to reach). These other adaptations may well exert selective pressure, but we emphasize that PPDMI still has appreciable, if predominant, importance relative to these adaptations. Again, if PPDMI were not appreciable, RR size would scale with $BW^{0.75}$ instead of BW^{1} due to the myriad adaptive costs of RR size$\propto BW^{1}$.

Nutritional Resource Limitations and Evolution of Body Size in the Ruminantia

The principles demonstrated above strongly suggest that nutritional resource limitations are largely, if not predominantly, responsible for the pattern of large body sizes in the Ruminantia. It is tempting to speculate that nutritional resource limitations

are not just presently responsible for large BW but, mediated by foregut fermentation, have contributed to the evolution of large BW in the Ruminantia.

At their emergence in the NA fossil record during the middle Eocene, the primitive Hypertragulidae were small (<4 kg; Figure 1.6), as was their likely ancestor, the rabbit-sized Diacodexis (Rose, 1982). As observed in Figure 1.6, ruminant BW progressively increased with the rise Leptomerycidae during the middle Eocene and Antilocapridae, Dromomerycidae, and Moschidae in the Early to Late Miocene, though the Gelocidae of the Late Miocene is curiously small (approximately 1.3 kg). The results of the ANCOVA, indicating a steady BW increase of 9.11% per million years, statistically verify the visually apparent trend in Figure 1.6.

Increase in body size over evolutionary time has been noted for many mammals (Alroy, 1998), and several explanations for increase in body size exist (e.g., sexual selection [Andersson, 1994]). We posit that, at least for the ruminants, this increase in BW may have been actuated by nutritional resource limitations. We suggest that the evolution of foregut fermentation and rumination (occurring approximately 40 million years before present; Janis, 1976; Jermann et al., 1995) provided a means for PPDMI to increase with increasing BW (via scaling of RR with $BW^{>0.75}$), and that resource limitations pressured for increasing BW because of this advantage gained in PPDMI. Further support for this argument depends on testing the evolution of many specific features (e.g., forestomach scaling with $BW^{>0.75}$) that currently have not been tested.

Implications for Non-Ruminant Species

Because the mechanistic model used in this analysis accommodates only ruminant species, the analysis cannot be extended quantitatively beyond ruminants. Qualitatively, however, some links can be made to non-ruminant species.

The analysis suggests the fitness of any mammal with a large GIT is impacted by nutritional resource limitations. Ruminants are renowned for large RR size, but other herbivores have similar mass of fermentation contents in their total GIT as ruminants (Parra, 1978; Clauss et al., 2007). Even some non-herbivores have large GIT sizes, with *Mustela erminea* having a GIT tissue WM of 27 g·100 g BW^{-1} (Chivers and Hladik, 1980). Computational results in Tables 4, 5, and 6 demonstrate that a reduction in GIT size causes dramatic decreases in FMR while increases in RASC, acceleration, and peritoneal space unoccupied by the GIT. This shows several potential adaptive benefits of small GIT size. If we assume enlarged GIT size enhances nutrient extraction and storage with few other benefits, as demonstrated for ruminants and might be expected intuitively, we conclude that nutrient extraction and storage must be highly important to any mammal with a large GIT, such that these benefits exceed the benefits of a small GIT. For nutrient extraction and storage to be of such importance, it follows that nutritional resource limitations impact the fitness of these species. This in some ways may seem like an intuitive point, but the calculations here underscore the depth of this impact on fitness.

Concluding whether increased BW is a strategy adopted by non-ruminants to overcome these limitations (as in the ruminant) is more speculative. To firmly advance nutritional resource limitations as an ecological and evolutionary force increasing BW in

non-ruminants, digestible nutrient intake scaling with BW needs to be precisely quantified (avoiding the biased approach of a simple compilation technique) and explained mechanistically, as we have done for ruminants. At the present time, our preliminary analysis with ruminants suggests that increased nutrient extraction with increased BW may be an important force driving evolution of large BW.

APPENDIX 1

We partition FMR into the following components

$$FMR_i = [\text{heat released during activity, excluding HI}]_i + [\text{heat released during rest, excluding HI}]_i + HI_i \quad [1]$$

To calculate FMR_2, we calculate the value of these components for FMR_1, convert these values to ones independent of RR-scaling patterns (i.e., where $i = 0$), and use these RR-independent values to calculate components of FMR_2.

We define

$$[\text{heat released during rest, excluding HI}]_1 = BMR_1 \cdot (1\text{-}activity) \quad [2]$$

where *activity* = fraction of day spent lying (not standing or moving) ($d \cdot d^{-1}$). The value of *activity* is set equal to 0.533, the average value for 18 ruminant species compiled by Mysterud (1998). Eq. 2 assumes that when heat increment is excluded, metabolic rate during rest is equal to BMR—i.e., there is no activity during rest.

We additionally define

$$HI_1 = FMR_1 \cdot (1\text{-}k). \quad [3]$$

This equation assumes that animals eat to maintain energy stasis, which requires MEI equal FMR (which has units of ME). It also assumes that the same *k* value can be applied all maintenance and activity functions associated FMR, which is supported by the

observation of Clapperton (1964) that sheep at rest (with predominantly maintenance expenditures) exhibited the same value of *k* as walked on a treadmill (which had significant activity expenditures). The value of *k* was taken to be 0.7, a reasonable value for ruminant and other herbivores with significant food fermentation (Blaxter 1989).

Next we calculate

$$[\textit{heat released during rest}]_1 = [\textit{heat released during rest, excluding HI}]_1 + HI_1 \cdot (1\text{-}\textit{activity}) \quad [4]$$

This calculation assumes the heat generated through the HI is dispersed evenly during periods of rest and activity, which is reasonable because the events associated with heat increment (eating, fermentation, digestion) occur during rest and activity both. Next we find

$$[\textit{heat released during periods of activity}]_1 = FMR_1 - [\textit{heat release during rest}]_1 \quad [5]$$

where FMR_1 is estimated from Nagy (1999). This quantity is corrected for the HI as follows

$$[\textit{heat released during periods of activity, excluding HI}]_1 = [\textit{heat released during movement and standing}] - \textit{activity} \cdot [\textit{heat increment }]_1 \quad [6]$$

We calculate the following using a rearrangement of Eq. 11

$$[\textit{heat released during activity}]_0 = [\textit{heat released during activity}]_1 \cdot BW_0/BW_1 \quad [7]$$

and then corrected for HI as follows

$$[\textit{heat released during activity, excluding HI}]_0 = [\textit{heat released during activity}]_0 - HI_1 \cdot \textit{activity}. \quad [8]$$

Because we assume individuals with RR size$\propto BW^{0.75}$ and RR size$\propto BW^{1}$ are identical in all ways except those immediately impacted by RR size (Methods), we can use the result of Eq. 8 (wherein the RR is hypothetically absent and thus not affected by RR size) as a basis to calculate FMR_2.

We now calculate components of FMR_2. We anticipate carrying a load has minimal effect on heat release at rest (when excluding HI) because the additional weight of the load is predominantly supported by the ground, not muscular work. As such, we assume

$$[\textit{heat released during rest, excluding HI}]_2 = [\textit{heat released during rest, excluding HI}]_1.$$

Using a rearrangement of Eq. 11 of the main text, we find

$$[\textit{heat released during activity}]_2 = ([\textit{heat released during activity}]_0)\cdot BW_2/BW_0. \quad [9]$$

where, additionally,

$$[\textit{heat released during activity}]_0 = [\textit{heat released during activity, excluding HI}]_0 + HI_2 \cdot \textit{activity}. \quad [10]$$

Note that HI_2 is not yet solved (see below). Values of $[\textit{heat released during rest, excluding HI}]_2$, HI_2 and, critically, FMR_2, are solved simultaneously using Eq. 2 and three following:

$$[\textit{heat released during activity, excluding HI}]_2 = [\textit{heat released during activity}]_2 - [HI]_2 \cdot \textit{activity} \quad [11]$$

$$FMR_2 = [\text{heat released during rest, excluding heat increment}]_2 + [\text{heat released during activity, excluding HI}]_2 + HI_2 \quad [12]$$

$$HI_2 = FMR_2 \cdot (1-k). \quad [13]$$

The forms of these equations, and the assumptions used in formulating them, are analogous to those used when RR size$\propto BW^1$.

APPENDIX 2

The mechanistic model of ruminant digestion employed in this study was formulated in Chapter 5. The model is based on chemical reactor theory (Penry and Jumars 1986, 1987) and represents the RR, large intestine, and blood as continuously-stirred reactors and the small intestine as a plug flow reactor. To simulate digestion, it uses a system of differential equations to represent flows of nutrients (indigestible NDF; digestible NDF; indigestible ADF; digestible ADF; soluble non-structural carbohydrate; and insoluble non-structural carbohydrates; soluble protein; insoluble, indigestible protein; insoluble, digestible protein; lipid), metabolites (NH_3, urea, SCFA), and microbes within and across these reactors.

In simulating digestion for a given level of PPDMI, the model computes two key parameters: (1) RR fill with space-occupying NDF (kg·100 kg BW^{-1}), (2) the quantity of nutrients and metabolites the gastrointestinal tract absorbs per unit time, with NE (expressed in units of NE_m [Mcal·100 kg $BW^{-1}\cdot h^{-1}$]) and protein (kg·100 kg $BW^{-1}\cdot h^{-1}$) of particular importance. Both of parameters have been proposed to regulate intake in the ruminant (Forbes, 2007). We compared the computed value of these two parameters to optimal or reference values by taking the ratio between reference and actual parameter

values. We define the ratio of optimal (C_r) to actual (NEI) NE intake as the chemostatic feedback signal (C_s)—i.e.,

$$C_s = \frac{C_r}{NEI}$$

The value of C_r is equal to the energy required to reach genetic production potential (defined here as the production level expected from an individual of a given species, BW, physiological state, production stage, and sex under optimal nutritional, environmental, and managerial conditions) and computed as described below. We additionally define the ratio of reference (D_r) to actual ($<^{RR}NDF>$) RR fill with NDF as the distention feedback signal (D_s)—i.e.,

$$D_s = \frac{D_r}{<^{RR}NDF>}$$

We define D_r as $<^{RR}NDF>$ when $C_s = 1$ and set its value to 1.7 kg·100 kg BW^{-1}, a value found by applying the model to a calibration dataset (Mertens, 1973). We used NDF as a measure of RR fill following its historic use in the literature (Mertens, 1987) and because its use led to higher system stability (faster and higher convergence rates during model solution procedures) relative to other potential measures.

We found an empirical relationship between chemostatic and distention feedbacks from two studies in the literature (Bernal Santos, 1989; Bosch et al., 1992a,b), summarized by the equation

$$D_s = C_s^{\alpha} \qquad [3]$$

where α is a shape parameters found by regression (using log-transformed values of variables) and equal to (mean±SE) -0.78±0.16 (MSE = 0.16, $P < 0.001$).

Eq. 1 was derived under circumstances where the dietary energy:protein ratio was low, though high ratios strongly reduce intake (Moore and Kunkle, 1995). To accommodate diets with high ratios, we added a feedback signal for energy:protein, using an equation form proposed by Fisher (1996)

$$P_s = 1 - \gamma \cdot e^{-e^{(\delta - \varepsilon \cdot NE:P)}}$$

where P_s = energy:protein feedback signal; *NE:P* = ratio of NE to protein absorption from the GIT (Mcal·kg^{-1}); and γ, δ, and ε = shape parameters (unitless). The value of γ (0.7) is from Fisher (1996) and δ and ε (6, 0.17) were found by applying the model to a calibration dataset (Mertens, 1973). This signal describes the fraction of PPDMI realized when energy:protein feedback occurs relative to the case where no feedback occurs. After incorporating this signal, the relationship between C_t and D_t can be shown to become

$$D_s = \frac{{C_s}^{\alpha}}{P_s} \qquad [2]$$

We solved the model's system of differential equations to find a level of PPDMI (predicted PPDMI) that (1) yields values of C_s, D_s, and P_s that fulfill Eq. 2 and (2) lead to steady-state conditions.

We assumed that the energetic demands of an animal at the maintenance, non-productive state (as in the validation studies) are equal to maintenance metabolic rate; that is, the animal "seeks" to maintain energy stasis. We predicted maintenance metabolic rate and thus C_r with Blaxter (1989) and NRC (2000, 2001, 2007) in conjunction with species and BW data given in the published report. Other inputs for the model include chemical composition of the forage (NDF, ADF, CP, ash) as well as

forage type (alfalfa [including cutting, if available], C_3 grass, C_4 grass, grass/legume mixture), which determine the degradation characteristics of the diet. All other parameters were constants estimated from 65 published reports and our own unpublished data (Hackmann, T.J., Sampson, J.D., and Spain, J.N., unpublished). Because of the complexity and number of equations used in the model, the model currently accommodates diets with only one ingredient (including more than one dietary ingredient would require multiplicity of equations).

In discussing the model in Methods and elsewhere, we use the terms metabolic rate and RR DM contents and as synonyms for energetic demands and RR NDF fill, respectively. Given the definition of energetic demands as maintenance metabolic rate above, the use of metabolic rate as a synonym for energetic demands is ensuant. The high correlation between RR DM and NDF contents (r = 0.975; Hackmann, T.J., unpublished summary of 20 cattle studies) suggests that the two can be used synonymously, also.

As discussed in Chapter 5, good agreement between model-predicted and actual values of PPDMI was found in a validation with 15 studies (including the 5 studies used in determining the empirical relationship between PPDMI and BW) reporting ad libitum consumption of all-forage diets by 14 bovid, 4 cervid, and 1 giraffid species during gestation, lactation, growth, or non-productive physiological states (R^2 = 0.910, root mean square prediction = 1.35 $kg \cdot d^{-1}$). The good agreement circumstantially suggests that the underlying mechanisms in the model are represented correctly and in accordance with real biological phenomena, making the model appropriate for mechanistic analysis of PPDMI scaling with BW.

Table 6.1 Species used to derive allometric equations relating several physiological parameters (PPDMI, DDM, RR WM contents, RR tissue WM) to BW

Species name		Equations[2]		
binomial	common	PPDMI	RR WM contents	RR tissue WM
Aepyceros melampus	Impala		X	X
Alces alces	North American moose		X	X
Antidorcas marsupialis	Springbok		X	X
Bison bison	American bison	X		
Bison bonasus	European bison	X		
Bos gaurus	Gaur	X		
Bos taurus	Domestic cattle	X		X
Boselaphus tragocamelus	Nilgai	X		
Bubalus bubalis	Asian water buffalo	X		
Capra aegagrus hircus	Domestic goat	X		
Capreolus capreolus	Roe deer	X	X	X
Cervus canadensis	North American elk	X		X
Cervus duvaucelii	Barasingha	X		
Cervus elaphus	Red deer	X	X	X
Cervus nippon	Sika deer		X	X
Connochaetes taurinus	Blue wildebeest		X	X
Dama dama	Fallow deer		X	X
Gazella granti	Grant's gazelle		X	
Gazella thomsoni	Thomson's gazelle		X	
Giraffa camelopardalis	Giraffe	X	X	
Hemitragus jemlahicus	Himalayan Tahr		X	X
Kobus ellipsiprymnus	Waterbuck	X	X	
Litocranius walleri	Gerenuk		X	
Neotragus moschatus	Suni		X	
Odocoileus hemionus	Mule deer	X		
Odocoileus virginianus	White-tailed deer		X	X
Oryx gazelle	Gemsbok	X	X	X
Ovibos moschatus	Muskoxen		X	X
Ovis aries	Domestic sheep	X		X
Ovis canadensis	Bighorn sheep	X		
Rangifer tarandus	Reindeer		X	X
Syncerus caffer	African buffalo	X	X	X
Taurotragus oryx	Common eland	X	X	
Tragelaphus strepsiceros	Greater kudu		X	X

PPDMI = physiologically potential DMI, RR = reticulorumen, WM = wet mass

[2]An "X" below indicates that the species in the corresponding row was used in the derivation of the allometric equation in the corresponding column.

Table 6.2. Descriptive statistics of studies used to determine empirical relationship between BW and PPDMI and DDM[1,2]

Item[3]	n	mean	min	max	SD
Diet					
NDF, $g \cdot kg^{-1}$ DM	52	575	351	787	147
ADF, $g \cdot kg^{-1}$ DM	52	388	261	501	60
CP, $g \cdot kg^{-1}$ DM	52	13.3	36	231	69
NEm, Mcal· kg DM^{-1} [4]	52	1.23	0.71	1.77	0.304
Animal					
BW, kg	52	275.3	17.2	907	232
DDM, $g \cdot g^{-1}$ DM	18	0.566	0.460	0.687	0.568
DOM, $g \cdot g^{-1}$ OM	41	0.613	0.445	0.781	0.117
PPDMI, kg·(100 kg $BW \cdot d)^{-1}$	52	1.90	0.467	3.86	0.67
PPDMI, $kg \cdot d^{-1}$	52	4.37	0.458	12.81	3.41

[1]Studies include Foose (1982), Baker and Hobbs (1987), Reid et al. (1990), Domingue et al. (1991), and van Weiren (1996).
[2]PPDMI = physiologically potential DMI, DDM = digestible DM
[3]OMD = digestible OM
[4]NE_m estimated using equations of NRC (2001)

Table 6.3. Allometric equations[1] which relate RR and energetic parameters with BW[2,3]

Parameter[4]	coefficient *a*	Scaling parameter *b*	r^2	P	BW range	Species *n*	Source
					kg		
RR volume, L	0.241	0.925	0.94	<0.001	4.1 – 750.8	25	van Wieren (1996)
RR WM contents, kg	0.0703	1.11	0.976	<0.001	3.69 – 807.5	22	literature compilation
RR DM contents, kg	0.0091	1.15	0.972	NA	4.2 - 702	11	Illius and Gordon (1992)
RR DM contents, scaling parameter = 1	0.023	1	NA	NA	4.2 - 702	11	Illius and Gordon (1992)
RR tissue WM, kg	0.0206	0.983	0.977	<0.001	20.7 – 807.5	18	literature compilation
RR tissue WM, scaling parameter = 1	0.0190	1	NA	NA	20.7 – 807.5	18	literature compilation
BMR, $kcal \cdot d^{-1}$	68.4	0.75	NA	NA	NA	NA	Blaxter (1989)
FMR, $kcal \cdot d^{-1}$	208.3	0.772	0.959	<0.001	NA	58	Nagy et al. (1999)

[1]Equations are of the form $Y = a \cdot BW^b$

[2]RR = reticulorumen

[3]Unit and logarithmic conversions have been applied to equations in original sources, in order to standardize their units and form

[4]WM = wet matter, BMR = basal metabolic rate, FMR = field metabolic rate

Table 6.4. Expected values of some digestive, energetic, and other parameters when RR size scales with BW[1] [1,2]

BW	Remark	RR volume	RR WM contents[3]	RR tissue WM[3]	FMR[4]	RASC[5]	Fraction of peritoneal space not occupied by RR
kg		L	kg	kg	$kcal \cdot d^{-1}$	m^{-1}	$L \cdot L^{-1}$
2	Smallest ruminant	0.459	0.151	0.0407	356	1.30	0.3
50		9.00	5.32	0.963	4270	0.491	0.3
100		17.1	11.4	1.90	7290	0.388	0.3
500		75.8	67.9	9.26	25200	0.236	0.3
1000	Largest bovid	144	146	18.3	43100	0.191	0.3
1500	Largest giraffid	209	229	27.3	59000	0.168	0.3
3000	Largest extinct ruminant	397	492	53.9	101000	0.136	0.3

[1]RR = reticulorumen, BW = body weight

[2]Values calculated using regression equations in Methods (shown partially in Table 6.2)

[3]WM = wet mass

[4]FMR = field metabolic rate

[5]RASC = relative absorptive/secretive capacity

Table 6.5. Expected values of some digestive, energetic, and other parameters when RR size scales with $BW^{0.75}$ [1,2]

BW when RR∝BW[1]	BW when RR∝$BW^{0.75}$	Remark	RR volume	RR WM contents[3]	RR tissue WM[3]	FMR[4]	RASC[5]	Fraction of peritoneal space not occupied by RR
kg	kg		L	kg	kg	kcal·d-1	m^{-1}	$L \cdot L^{-1}$
2	1.96	Smallest ruminant	0.406	0.118	0.0346	349	1.35	1.35
50	45.4		4.54	1.32	0.387	3860	0.604	0.604
100	89.5		7.64	2.22	0.651	6500	0.508	0.508
500	432		25.5	7.43	2.18	21700	0.340	0.340
1000	851	Largest bovid	42.9	12.5	3.66	36400	0.286	0.286
1500	1270	Largest giraffid	58.2	16.9	4.96	49300	0.258	0.258
3000	2490	Largest extinct ruminant	97.9	28.5	8.34	82800	0.217	0.217

[1]RR = reticulorumen, BW = body weight
[2]Values calculated using regression equations in Methods (shown partially in Table 6.2)
[3]WM = wet mass
[4]FMR = field metabolic rate
[5]RASC = relative absorptive/secretive capacity

Table 6.6. Change in some digestive, energetic, and other parameters when RR size scaling is changed from BW^{1} to $BW^{0.75}$ [1]

BW when $RR \propto BW^{1}$ (kg)	Remark	Fraction of parameter value when $RR \propto BW^{0.75}$ relative its value when $RR \propto BW^{1}$ [2]				
		FMR[3]	Fraction of peritoneal space not occupied by RR	RASC[4]	Maximum locomotory acceleration	PPDMI[5]
2	Smallest ruminant	0.980	1.27	1.04	1.02	0.917
50		0.905	2.16	1.26	1.10	0.613
100		0.891	2.29	1.31	1.12	0.562
500		0.859	2.55	1.44	1.16	0.460
1000	Largest bovid	0.845	2.64	1.50	1.17	0.422
1500	Largest giraffid	0.837	2.68	1.53	1.18	0.401
3000	Largest extinct ruminant	0.822	2.76	1.60	1.20	0.368

[1] RR = reticulorumen, BW = body weight

[2] Values calculated as ratio between values expected for $BW^{0.75}$ and BW^{1}, using equations in the text

[3] FMR = field metabolic rate

[4] RASC = relative absorptive/secretive capacity

[5] PPDMI = physiological potential dry DMI.

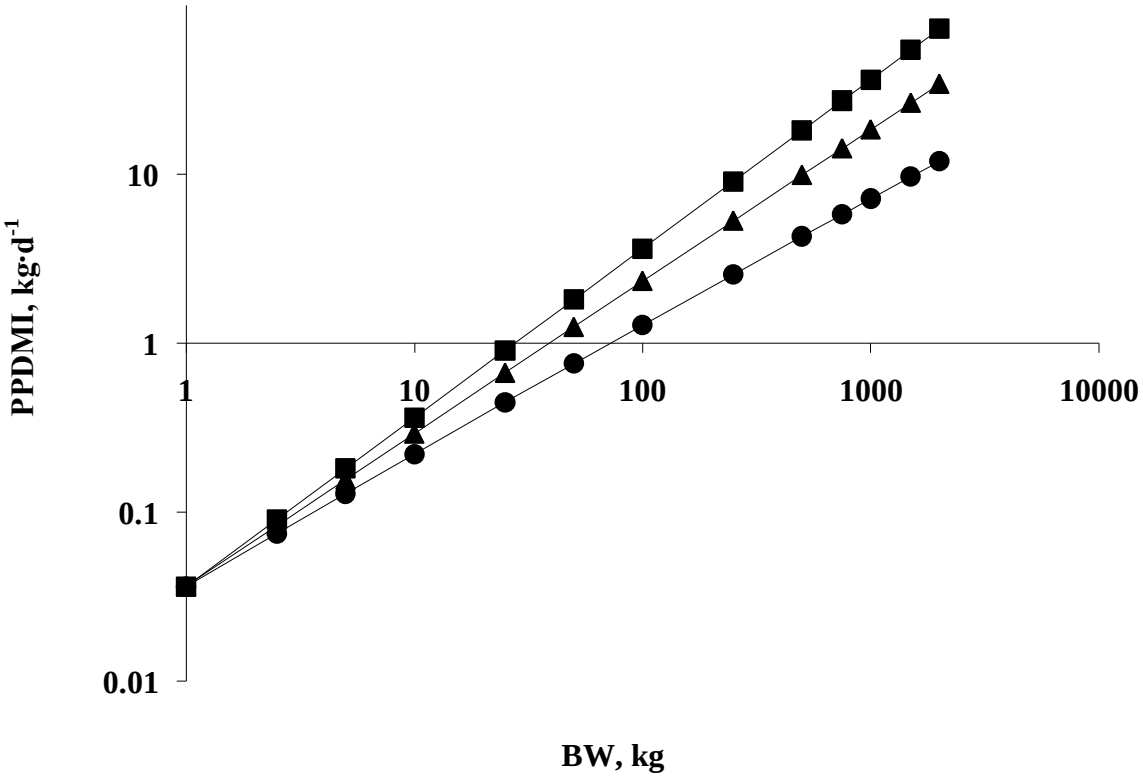

Figure 6.1 Relationship between model-predicted physiologically potential DMI (PPDMI) and BW under three scenarios (1) metabolic rate and RR DM contents scale with $BW^{0.75}$ and BW^{1}, respectively (▲) (2) metabolic rate and RR DM contents each scale with BW^{1} (■), and (3) metabolic rate and RR DM contents each scale with $BW^{0.75}$ (●). Results shown are those for hypothetical ox (ranging in BW from 1 to 2000 kg) consuming a high-quality C_3 grass; scaling results are similar for different forage and animal types.

CHAPTER 7

PERSPECTIVES FROM RUMINANT ECOLOGY AND EVOLUTION USEFUL TO RUMINANT LIVESTOCK RESEARCH AND PRODUCTION

ABSTRACT

This chapter presents insights ruminant ecology and evolution that can be utilized in livestock research. The first ruminants evolved about 50 million years ago and were small (<5 kg) forest-dwelling omnivores. Today there are almost 200 living ruminant species in 6 families. Wild ruminants number about 75 million, range from about 2 to more than 800 kg, and generally prefer at least some browse in their diet. Eight species have been domesticated within the last 12,000 years. Their combined population currently numbers 3.6 billion. In contrast to wild ruminants, domestic species naturally prefer at least some grass in their diets, are of larger BW (roughly from 35 to 800 kg), and, excepting reindeer, belong to one family (Bovidae). Wild ruminants thus have a comparatively rich ecological diversity and long evolutionary history. Studying them gives a broad perspective that can augment ruminant research and production. Allometric equations, often used in ecology, relate BW to physiological measurements from several species (typically both wild and domestic). Their utility is to predict or explain values of physiological parameters from BW alone. Voluntary feed intake is proportional to $BW^{0.9}$ across wild and domestic ruminant species. This proportionality suggests that physical and metabolic factors regulate intake simultaneously, not mutually exclusively as often presumed. Studying the omasum in wild species suggests it

functions primarily in particle separation and retention and only secondarily in absorption and other roles. Studies on the African Serengeti show that multiple species, when grazed together, feed such that they use grasslands more completely. They support use of mixed-species grazing systems in production agriculture. When under metabolic stress, wild species will not rebreed but rather extend lactation (to nourish their current offspring). This bolsters the suggestion that lactation length be extended in dairy operations. Cooperation between animal scientists and ecologists could generate valuable insight.

INTRODUCTION

As an applied field, animal science borrows variously from classical physiology, endocrinology, biochemistry, genetics, and nutrition, among other disciplines. Seldom though does it draw from ecological and evolutionary research. For ruminant research, at least, this is not because of a dearth of excellent material on the subject, with classic works such as Hoffman (1973), Clutton-Brock et al. (1982), Foose (1982), and Owen-Smith (1988) and more recent material compilations as Vbra and Schaller (2000) and Prothero and Foss (2008).

In his general ruminant nutrition text, Van Soest (1994) presents a fairly comprehensive account of ruminant ecology and evolution—perhaps the most comprehensive in an animal science work. However, as may be expected from a general text, Van Soest's (1994) account lacks detail and syntheses few explicit connections between ruminant ecology and evolution and applied livestock research. Some individual manuscripts (e.g., Walker 1994, Knight 2001) have drawn more detailed and direct

connections. While valuable in their own right, these manuscripts have a limited scope and lack a thorough introduction to ruminant ecology and evolution.

Chapter 1 has reviewed key points of ruminant ecology and evolution. This chapter briefly recapitulates these points then shows where they offer insight into livestock research and production. We draw on both our original ideas and some presented previously. The focus on nutrition and physiology in this review reflects our own expertise, not a lack of importance of other fields (e.g., reproduction, behavior, genetics).

ECOLOGY, EVOLUTION, AND DOMESTICATION OF RUMINANTS

Details of the discussion below are found in Chapter 1. A ruminant is any artiodactyl that possesses a rumen, reticulum, omasum or isthmus homologous to the omasum, and abomasum. Ruminants also possess certain skeletal features—e.g., fusion of cubiod and navicular bones in the tarsus—that are useful in fossil identification.

Ruminant Families

Except where noted, details of the discussion below are from Nowak (1999) and Feldhamer et al. (2007). The six extant (i.e., non-extinct) ruminant families include the Tragulidae, Moschidae, Bovidae, Giraffidae, Antilocapridae, and Cervidae. The Tragulidae (chevrotains) and Moschidae (musk deer) are small forest-dwelling, deer-like ruminants. Members of both families are hornless, and males have large upper canines instead. The Tragulidae are phylogenetically and morphologically primitive—they have even been called "living fossils" (Janis, 1984))—and lack a true omasum (Langer, 1988). The remaining families, the Bovidae (e.g., cattle, sheep, goats, antelope), Giraffidae

(giraffe and okapi), Cervidae (true deer; e.g., white-tailed deer, caribou, moose), and Antilocapridae (pronghorn), include species familiar to most readers.

There are 5 additional extinct families, the Hypertragulidae, Leptomerycidae, Gelocidae, Palaeomerycidae, and Dromomerycidae (Carroll, 1988). The Hypertragulidae, Leptomerycidae, and Gelocidae were small, hornless ruminants that probably most closely resembled moschids or tragulids (Webb and Taylor, 1980; Webb, 1998b). The Palaeomerycidae and Dromomerycidae are medium-to-large-sized with giraffe-like horns but deer-like limb proportions (Janis and Scott, 1987). Their ecological niche probably resembled that of a subtropical deer (Jannis and Manning, 1998b).

Evolution

The Hypertragulidae first appeared about 50 million years ago in SE Asia (Métais and Vislobokov, 2007) and were soon followed by the Tragulidae and Leptomerycidae (Colbert, 1941; Métais et al., 2001). The Gelocidae appeared at approximately 40 million years ago (**Ma**) (Genry, 2000). All but the Tragulidae eventually migrated to North America (Webb, 1998b). These groups were rabbit-sized at first, though their size increased progressively over time (Chapter 6). They probably were reclusive, forest-dwelling omnivores (Webb, 1998b). They did not have extensive foregut fermentation or rumination until about 40 Ma (Jermann et al., 1995).

The remaining families evolved around 18 to 23 Ma in Eurasia (Antilocapridae, Cervidae, Moschidae, Dromomerycidae, Bovidae, Palaeomerycidae) and Africa (Giraffidae) (Gentry, 2000). Many (Bovidae, Cervidae, Moschidae, Dromomerycidae, Antilocapridae) migated to North America (Janis and Manning, 1998a,b; Webb, 1998b), though the Bovidae and Cervidae did not migrate until relatively late (5 Ma) (Webb,

1998a, 2000). By 2 Ma, Cervidae migrated to South America (Webb, 2000). Body mass of these groups was larger (20 to 40 kg; Janis, 1982) and increased over time. The first of these groups lived in open woodlands and ate primarily grass and leaves (Janis, 1982; DeMiguel et al., 2008). When grasslands expanded about 5 to 11 Ma, some species began including more grass in their diets (Semprebon et al., 2004; Semprebon and Rivals, 2007).

Ecological Characteristics

Except where noted, details of the discussion below are from van Wieren (1996). Today there exist nearly 200 ruminant wild species (Nowak, 1999), most of which are Bovidae and Cervidae. A conservative estimate places the world population of wild ruminants at 75.3 million, with 0.28 million tragulids, 0.28 million moschids, 44.6 million cervids, 29.1 million bovids, 0.15 million giraffids, and 0.88 million antilocaprids (Chapter 1). Living ruminants are natively found on all continents except Antarctica and Australia, with most species are found in Africa and Eurasia. As a whole, ruminant species are evenly spread across open, ecotone, and forested habitats, but they prefer warm to other types of climates. Median BW of modern ruminants is 45 kg, near that expected from the historical trend. Species BW ranges greatly, from approximately 2 kg to 800 kg or more. For most of their evolutionary history, ruminant species were predominately or exclusively browsers (consume fruits, shoots, and leaves) (see above). Today, a plurality of ruminant species is still classified as browsers, and only about a quarter are grazers (consume grass and roughage).

Details of Domestication

Except where noted, details of the discussion below are from Clutton-Brock (1999). The goat was domesticated at approximately 10,000 B.C. in the Fertile Crescent of the Near East (Zeder and Hesse, 2000). Most of the other 8 domesticated ruminant species (sheep, European and Zebu cattle, water buffalo, mithan, reindeer, yak, Bali cattle) were brought under human control by 2,500 B.C. in either the Near East or southern Asia. The goat and other species were initially domesticated for meat, but reasons for domesticating other species included milk, draft, transportation, sacrifice, and barter. Each domestic species is probably derived from several wild species; at least 12 species can claim ancestry to the 9 domesticated species (Bruford et al., 2003). These 12 and possibly others were chosen for domestication because they were gregarious, submissive to human captors, unexcitable, and easy to breed.

Characteristics of Domestic Species

The total population size of domestic species is 3.57 billion (Chapter 1), nearly 50-fold larger than that of wild ruminants. All but reindeer belong to the family Bovidae. Most species are grazers, though goats, reindeer, and possibly sheep are intermediate feeders (consume either browse and grass) (Chapter 1). Body mass of domestic ruminants is larger than most wild ruminants. The smallest species (sheep, goat) are near the median BW of wild ruminants (45 kg) and many species (cattle, mithan, Bali cattle) approach the maximum observed in the wild (800 kg) (Chapter 1).

PERSPECTIVES REVELANT TO MODERN PRODUCTION SYSTEMS

Wild ruminants, past and present, prove much more diverse (in terms of phylogeny, behavior, diet, and otherwise) than domestic ruminants. Further, the 50 million year

evolutionary history of the ruminant extends far before domestication. Studying ruminant ecology and evolution gives a broad perspective of what ruminants are and how they came to be—much broader than achieved through studying domestic species alone. This broad perspective can augment or even challenge the status quo of livestock research and management, which has been established using a much narrower perspective. The following presents some examples how principles in ruminant ecology and evolution can offer insight into livestock research and production.

Predicting Values of Physiological Parameters from BW

Body mass has a clear influence on the value of many physiological parameters. For example, the greater feed intake of a cow relative to a goat, intuitively, is largely attributable to greater BW of the cow. The exact, quantitative relationship between a physiological parameter and BW is often less obvious, however.

Allometric equations (Peters, 1983; Schmidt-Nielson, 1984; Calder, 1984) quantitatively express these relationships with the formula

$$y = a \cdot BW^{b}$$

where y is the value of a physiological parameter and a and b are intercept and scaling parameters, respectively. Values of a and b are found empirically by regressing BW against y for several species (Figure 7.1). By using observations from multiple ruminant species (including wild ones), one is provided a robust yet widely-applicable equation that gives a benchmark prediction for a physiological parameter from BW alone. Some uses of these predictions for livestock research include (1) serving as a first approximation for a physiological value for a species when one has not been measured

directly and (2) explaining to what extent observed differences between livestock species are attributable to BW (i.e., act as a control for BW in comparisons).

The allometric equation for metabolic rate (e.g., Blaxter, 1989) is widely-known and applied, but there are many others much less so. Examples of allometric equations are given in Table 7.1, including those for predicting anatomical, ingestive and digestive, energetic, reproductive, and other physiological parameters. For illustration, expected values of these parameters for two different BW (50 and 500 kg) are shown. Note that many equations have a very high R^2 (>0.95) and thus can be expected to be precise; others have much lower R^2 values (as low as 0.18) and should be applied more cautiously.

Equations listed in Table 7.1 represent a broad survey of the many available in the literature. For more allometric equations, the reader should refer to the sources referenced in the table, and Scott (1990) for equations predicting post-cranial skeletal dimensions; Clauss et al. (2008) for masseter muscle mass; Hofmann et al. (2008) for salivary gland mass; Robbins et al. (1995) for parotid salivary gland mass and digestive parameters; Illius and Gordon (1991) and Gordon and Illius (1994) for mean retention time, particle breakdown rate, and other digestive parameters; Illius and Gordon (1999) for ingestive parameters related to foraging; Clauss et al. (2002) for fecal particle size; and Mystrud (1998) for activity time.

The equations given in Table 7.1 have been derived using both wild and domestic ruminant species. Note that one can parameterize allometric equations using other approaches. Domestic species alone can be used, as only 2 species observations are technically required to estimate the 2 parameters (3 if error is to be estimated). However,

with so few species observations, an outlier from any one species can unduly affect parameter estimates. Wild species should thus be included to increase the number of observations and the robustness of parameter estimates. At the opposite end, non-ruminant species (wild or domestic) can be included in addition to ruminants. In this case, phylogenetic differences across the wide range of species, if not controlled for statistically, may make the resultant equation very general but also very imprecise and potentially biased. For example, adding marsupials to the allometric equation for metabolic rate would make the equation more widely applicable (viz., for marsupials) but would skew the regression because marsupials have characteristically low metabolic rates (Dawson and Hulbert, 1970). A good balance between precision, generality, and robustness is thus found by including domestic and wild ruminant species and these alone.

Role of Physical and Metabolic Factors in Regulating Feed Intake

Besides the two general uses of allometric equations explained above, some allometric equations can be applied to draw deeper, more complex inferences. For example, the allometric equation for feed intake demonstrates that forage intake is regulated by physical and metabolic factors simultaneously.

Physiological regulation of feed intake is important to livestock production systems because feed intake impacts animal performance and operation costs. Of the many proposed regulation mechanisms (Forbes, 2007), physical (Allen, 1996) and metabolic regulation (Illius and Jessop, 1996) are often suggested to predominate. Generally these two regulation mechanisms (physical, metabolic) are typically considered operate on a mutually exclusive basis, with intake of low-energy, bulky diets (usually

forages) regulated only physically and high-energy, highly-degradable diets regulated only metabolically (Conrad et al., 1964; Baumgardt, 1970).

Theoretical arguments have suggested that these two and more regulation mechanisms operate simultaneously (Fisher et al., 1987; Fisher, 1996), as do experiments in which VFA is infused and physical ballast is placed in the rumen simultaneously (Forbes, 1996). A recent examination of feed intake behavior of wild and domestic ruminants (Chapter 6) considerably strengthens the case for simultaneous regulation. Because reticulorumen digesta contents and volume are nearly proportional to BW^{1} (i.e., proportionally do not change with BW; Table 7.1), one would expect feed intake be proportional to BW^{1}, also, if physical regulation only were operating. On other hand, because metabolic rate is proportional to $BW^{0.75}$ (Table 7.1), one would expect feed intake be proportional to $BW^{0.75}$, also, if metabolic regulation acted alone. However, in a summary 19 species from 5 studies, we (Chapter 6) found that intake of forage is proportional to $BW^{0.875\pm0.032}$ (Table 7.1), with lower and upper 95% percent confidence limits of $BW^{0.810}$ and $BW^{0.941}$. This agrees with the finding that for livestock species (cattle, sheep, goats) intake scales with $BW^{0.9}$ (Minson 1990, Reid et al., 1990).

The mean value of the scaling parameter (~0.9) and its 95% confidence limits fall in between values expected if intake were regulated only physically (1) and metabolically (0.75). Intuitively, this suggests that physical and metabolic regulation operate simultaneously for forage diets, contrary to the classical suggestion physical regulation alone should occur; mechanistic modeling described in Chapter 6 confirmed this suggestion. Though lack of controlled data disallowed a similar examination with non-all forage diets, the wide range in quality of the forage diets (predicted NE_m ranged from

0.71 to 1.77 Mcal·kg DM^{-1}) suggests the results are not simply constrained to a narrow range of forages. Because this simultaneous regulation is apparent across wild and domestic species alike, it can be inferred that it is highly conserved evolutionarily and deeply-seated.

Conrad et al. (1964), who originally proposed that metabolic and physical regulation are mutually exclusive, also used allometry to support their arguments. They concluded that for high-producing dairy cows, intake scaled with $BW^{0.73}$ for low-digestibility (>66.7% DDM) and BW^{1} for high-digestibility (<66.7% DDM) diets, consistent with mutually exclusive regulation. This conclusion is, at the very least, oversimplified. For high-digestibility diets, scaling parameter values were ~0.73 for only 2 of their 5 regressions; all others were lower (≤0.62). The upper 95% confidence limits of these 2 favorable regressions (0.962 and 1.03) do not rule out intake scaling with $BW^{0.9}$ or even possibly BW^{1}. This, and considering that intake was only poorly related to BW (R^2 = 0.074 or lower), indicates that this dataset is poor for discriminating intake scaling patterns. Detailed results are not presented for low digestibility diets, but the above suggests one should remain skeptical of their conclusion that intake scales with BW^{1} for these diets. While intriguing for their time, the allometric analysis of Conrad et al. (1964) and conclusions based thereon must be rejected over our more discriminating analysis.

Primary Function of the Omasum

Whereas functions of the rumen, reticulum, and abomasum are well-delineated, the chief function of the omasum remains somewhat a mystery. It may help retain and separate particles, as (1) large particles tend to become trapped between the omasal

laminae while small particles and liquid pass through quickly (Bost, 1970; Langer, 1988), and (2) large particles can be ejected from the omasum back into the reticulum (via the reticuloomasal orifice) (Ehrlein, 1980). It may more generally serve as a suction-pump that regulates flow of digesta (both liquid and particles) from the reticulum to the abomasum (Stevens et al., 1960), though some question this purported ability (Bost, 1970; Langer, 1988). It may also be an absorptive organ; the omasum absorbs approximately 12.5, 50, 35, 25, 10, and 50% of water, VFA, ammonia, sodium, potassium, and CO_2 that enter (Engelhardt and Hauffe, 1975). Some fiber digestion (7 to 9% of total tract; Ahvenjärvi et al., 2000, 2001) also occurs in the omasum. Finally, some claim the omasum reduces particle size (via purported grinding of digesta between laminae), though evidence for this function is at best circumstantial (Bost, 1970).

To establish the primary function of the omasum, we will review the omasal form and function of several wild species and suggest how and why the omasum evolved. In tragulids, a true omasum is not present at all; where it should be found there exists only an isthmus instead (Langer, 1988). As shown in Figure 7.2, this isthmus (also called a transisiton zone by some) is short, narrow, and with only small, subtle longitudinal folds (Agungpriyono et al., 1992). Though it does not form a distinct compartment like a true omasum, it is still histologically distinct from the reticulum and abomasum (Agungpriyono et al., 1995). Considering this evidence and that the Tragulidae are otherwise primitive (Figure 1.5), this isthmus probably resembles a very early form of omasum, as concluded by other authors (see Langer [1988]). Because the isthmus lacks structures to retain digesta within it, its contribution to absorption, fiber fermentation, absorption, and particle size reduction must be minimal. Its poor structural development

also precludes it from acting as a suction-pump to regulate digesta flow. However, the isthmus likely helps retain particles as its small aperture should allow only fine particles to pass into the abomasum and subsequently through the rest of the tract (Langer, 1988).

In small browsing Pecoran species, which are more advanced than the tragulids, the omasum forms a distinct compartment, but it still tends to be small and has few laminae (Hoffman, 1973; Langer, 1988, Hoffman, 1989; van Wieren, 1996). Hoffman (1989) concluded that its simple structure permits it to serve little more than a "sieving screen" that prevents large particles from entering the abomasum. In large, grazing ruminants (such as cattle), the omasum is large and with many laminae (Hoffman, 1973; Langer, 1988; Hoffman, 1989; van Wieren, 1996). Whereas the omasum in these species still helps retain particles (Langer, 1988), its large surface area may additionally contribute to absorption (Hoffman, 1973; Hoffman, 1989) and presumably other more advanced functions (e.g., fiber fermentation).

We thus find a progression in omasal form and function from the tragulids to browsing then grazing Pecoran ruminants. This progression suggests the omasum originally evolved as a simple isthmus that acted as a "flood-gate" (Bost, 1970) to retain particles. Compartmentalization, well-developed laminae, and complex motor activity subsequently evolved to support absorption, fiber fermentation, and suction-based digesta flow control. These more derived functions indeed have some adaptive benefit, particularly for grazers, where they may help process large amounts of refractory fiber (Hoffman 1973, 1989; Van Soest 1994). Still, considering that the particle retention function is pervasive across all species and the impetus for the omasum's evolution, this function is almost certainly of primary importance.

Dietary Niche Separation and Mixed-Species Grazing

Certain elements of this argument have also been presented by Walker (1994). Studies on the African Serengeti support the use of mixed-species grazing systems—i.e., systems in which pastures are stocked with more than one livestock species simultaneously. In their seminal studies, Bell and Gwynne (Gwynne and Bell, 1968; Bell 1970, 1971) showed that when an occupied area of the Serengeti plains becomes overgrazed, African buffalo and zebra are the first to migrate into long, ungrazed regions of long, poor-quality grass. As they remove the top herbage layer (stems and leaves of mature grasses), they expose lower, high-quality layers (stems, leaves, and fruits of immature grass and browse), which wildebeest, topi, and Thompson's gazelle then graze as they move in succession. By occupying different dietary niches, these ruminants and zebras together not only successfully occupy the same habitat but use grasslands more efficiently and completely.

Two primary reasons explain why these species occupy different dietary niches and thus can exist sympatrically (i.e., in the same geographic area). First, these species exhibit innately different dietary selectivities (i.e., feeding classes) that would immediately suggest the observed dietary niches; the buffalo and zebra are strict grazers, the wildebeest and topi are more selective grazers, and the Thompson's gazelle is an intermediate feeder (Gwynne and Bell, 1968; Bell 1970, 1971; Hofmann 1973, 1989). Second, these species range greatly in BW; the Thompson's gazelle and buffalo, the largest and smallest of the species, weigh 16 and 447 kg (Gwynne and Bell, 1968; Bell, 1970, 1971). Because voluntary feed intake scales with $BW^{0.9}$ while metabolic requirements scale only with $BW^{0.75}$ (Table 7.1), nutrient intake increases relative to

metabolic requirements with increasing BW. Consequently, large species can adapt to poor-quality material because they can consume relatively large amounts to meet their metabolic requirements, while smaller species are constrained to higher-quality material because they can eat relatively little (Bell, 1970, 1971, Jarman, 1974; Chapter 6). This principle (the Bell-Jarman principle; Geist, 1974) further reinforces innate selectivity differences to establish different dietary niches.

Significantly, major livestock species (goat, sheep, cattle) differ greatly in feeding class or BW or both (Table 1.5). Probably as a combination of these factors, species choose diets that overlap incompletely: goats choose more browse, cattle choose more grass, and sheep are intermediate (Figure 7.3). Diets should be even less similar than Figure 7.3 might suggest because (1) Figure 7.3 shows ranges that apply to single-species grazing, and cattle shift to poorer-quality diets in their range when grazing with sheep (Walker, 1994), (2) sheep eat plant biomass soiled by cattle feces, which cattle themselves avoid (Nolan and Connolly, 1989), and (3) the rough expression of botanical composition shown in Figure 7.3 ignores other ways diets can differ (e.g., by plant species or part). Livestock species thus have ample opportunity to separate their dietary niches when grazed concurrently.

Given this probable dietary niche separation, one might expect mixed-grazing systems to lead more complete utilization of pasture and higher combined level of animal productivity (as more pasture is transformed into animal tissue). In support, Vallentine (1990) observed that extent of pasture use can be increased by 25% by using multi- vs. single-species grazing, and Walker (1994) found that multi-species grazing increased

animal gain by 9 and 24% per unit area compared to sheep- and cattle-only systems, respectively.

There exist some legitimate, practical limitations to mixed-species grazing, such as elevated facility costs and predation risk of sheep and goats (Vallentine, 1990). However, most barriers are social, based on tradition and prejudice towards species (Walker, 1994). The enhanced production and efficiency of the systems vs. conventional ones—as expected from the archetypal mixed-grazing system on the Serengeti—challenges these barriers.

Extended Lactation

Elements of this discussion are derived from Knight (2001). The aim of many dairy cow operations is a 305-d lactation with a 12 to 14 month calving interval. This requires cattle be rebred by 100 d following parturition, soon after peak lactation, when they experience a negative energy balance (Bauman and Currie, 1980) and other metabolic stress that severely reduces fertility (Chagas et al., 2007). With pregnancy rates of U.S. breeds averaging about 25% (Animal Improvement Programs Laboratory, 2008), this management strategy is largely untenable.

An alternative management approach, forwarded by Knight (1984) and others, is to purposely extend lactation as long as possible and thus avoid early rebreeding. This approach, compared to current practice, indeed appears better supported by ecological observations. When in severe metabolic stress (poor body condition or nutritional plane) during lactation, many wild species (muskoxen [Adamczewski et al., 1998], red deer [Loudon et al., 1983; Albon et al. 1986], caribou [Gerhardt et al., 1997]) will not rebreed or do so only at low rates. Instead of rebreeding, they may extend lactation and thus

invest in their current young (caribou: White and Luick, 1984; muskoxen: Knight, 2001). In muskoxen, this extended lactation can exceed 1 year (Adamczewski et al. 1997). As explained by Knight (2001), extending lactation is presumably a maternal strategy to maximize fitness (the most important biological drive of organisms); investing in current offspring by extending lactation is safer and, in the long-term, more profitable than producing new offspring when necessary nutritional resources are inadequate.

These observations of wild species suggest that when under metabolic stress, the ruminant animal is evolutionary entrained to continue lactation rather than rebreed. Attempting to rebreed the high-producing dairy cow soon after parturition is a direct fight against this entrained response. If producing replacement heifers is not a major production goal, it might make more sense to rebreed less frequently and exploit the physiological capacity and drive for extended lactation shown in wild ruminants.

Though this argument for extended lactation is largely conceptual, growing experimental evidence suggests practicing extended lactation is viable and profitable. Lactation has been maintained naturally in goats for 4 years (Linzell, 1973) and in cattle nearly 2 years (Auldist et al., 2007); with bovine somatropin supplementation, it has been maintained for more 2 years in cattle (van Amburgh et al., 1997). Milk production far into an extended lactation is less than around peak, but it is more than production of a rebred animal during late pregnancy and its dry period (Figure 7.4). Pre-designed experiments have demonstrated that, over the long term, extending lactation up to 16 months (and sometimes longer) does not decrease daily production (van Amburgh et al., 1997; Rehn et al., 2000; Arbel et al., 2001; Österman and Bertilsson, 2003; Salama et al., 2005; Auldist et al., 2007). In some cases, extending lactation has increased either total

milk (second lactation of primiparous cows; Arbel et al., 2001) or component (protein and fat of goats; Salama et al., 2005) yields. The economic advantage of extended lactation ranged from \$0.12 to 0.21·(d calving interval)-1 among treatment groups in Arbel et al. (2001) and \$0.75·(d productive life)-1 in van Amburgh et al. (1997). (Note that earlier studies claiming no positive economic response [e.g., Holmann et al., 1984] were observational or theoretical, not experimental.) Though more research is clearly needed, these preliminary results suggest that the biological principles of extended lactation, as illuminated by wild ruminants, may be of great service to livestock production systems.

CONCLUSIONS

By offering a comparative vantage point, ruminant ecological and evolutionary research can offer great insight into livestock research. This research can reinforce and augment some conventional livestock practices, and if we allow, challenge and help revise others. With further dialogue and cooperation between animal scientists and ecologists, the insights that ruminant ecology and evolution have to offer should grow in number and usefulness.

Table 7.1. Some allometric equations useful for predicting physiological parameter values from BW[1,2]

Category	Physiological parameter	Equation parameters		r^2	Predicted value for BW of		Source[3]
		a	*b*		50 kg	500 kg	
Anatomical	Reticulorumen volume, L	0.241	0.925	0.940	8.99	75.61	van Wieren (1996)
	Skull length, cm	6.18	0.337	0.960	23.1	50.2	Janis (1990)
Ingestive and digestive	Voluntary feed intake at maintenance, kg DM·d^{-1}	0.0437[4]	0.875	0.967	1.34	10.05	Chapter 6
	Maximum intake rate, g WM·min^{-1} [5]	0.738	0.621	0.754	8.37	34.96	data from Shipley et al. (1994)
	Chewing rate during rumination, s^{-1}	2.53	-0.141	0.660	1.46	1.05	data from Langer (1988)
	Reticulorumen DM contents, kg	0.0091	1.15	0.972	0.82	11.56	Illius and Gordon (1992)
Energetic	Basal metabolic rate, kcal·d^{-1}	68.4	0.75	NA	1,286	7,232	Blaxter (1989)
Reproductive	Age at sexual maturity, months	8.86	0.156	0.250	16.3	23.4	van Wieren (1996)
	Reproductive output, young·yr^{-1}	2.54	-0.167	0.180	1.32	0.90	van Wieren (1996)
	Gestation length, d	129	0.125	0.556	210	280	data from Peréz-Barbería and Gordon (2005)
Other	Respiratory frequency, s^{-1}	1.27	-0.221	0.215	0.54	0.32	data from Mortola and Lanthier (2005)

[1]Equations are of the form $Y = a \cdot BW^b$

[2]Unit, logarithmic, and other conversions have been applied to equations in original sources, in order to standardize their units and form

[3]The phrase "data from" preceding a source, where present, indicates that we performed the allometric regression using ruminant data (averaged by species) originally reported by that source.

[4]*b* and predicted values reported in this table are for the 58% NDF, 19% CP mature alfalfa hay of van Wieren (1996); in the original equation, *b* is adjusted by a fixed-effect term for diet, which allows intake to be predicted for other diet types, but this term was omitted here for simplicity.

[5]WM = wet matter.

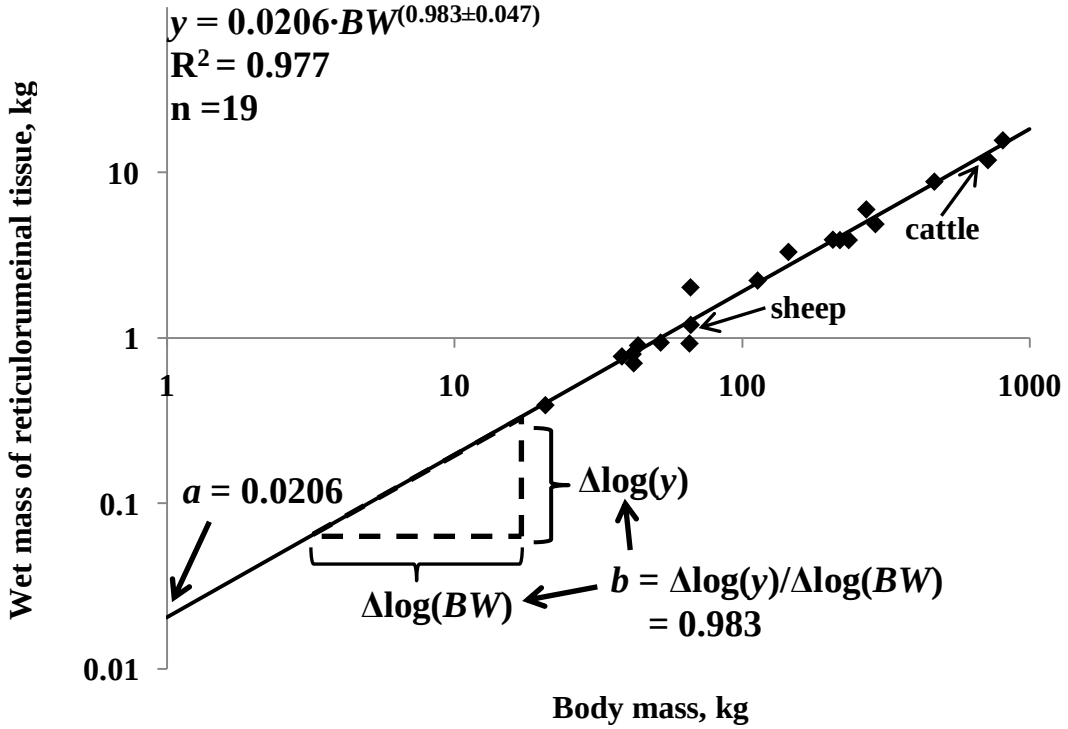

Figure 7.1. Graph of the allometric relationship between BW (kg) and wet mass of reticulorumen tissue (kg), illustrating the general principles of allometric equations. Tissue mass observations of individual ruminant species are shown with symbols (♦), with observations of sheep and cattle labeled. Solid line indicates best-fit allometric equation, with intercept parameter *a* and scaling parameter *b* defined graphically. Note plot is semi-logarithmic. Data from sources listed in Table 6.1.

Images removed for electronic publication because copyright permission could not be obtained. Reader is referred to Figures 5A and 2 of source (Agungpriyono et al., 1992) for original images.

Figure 7.2. The isthmus in the stomach of the lesser mouse deer (*Tragulus javanicus*), a member of the family Tragulidae. (A) The isthmus (arrow) in relation to the reticulum ("R") and abomasum ("1"). Note its narrow aperture and subtle longitudinal folds. (B) The isthmus in relation to the entire stomach, showing its small size. 1 = reticulum, 2 = rumen, 3 = abomasum, 4 = reticular groove, 5 = isthmus. Scale bar in (A) and (B) is 5 mm. Reproduced from Agungpriyono et al. (1992).

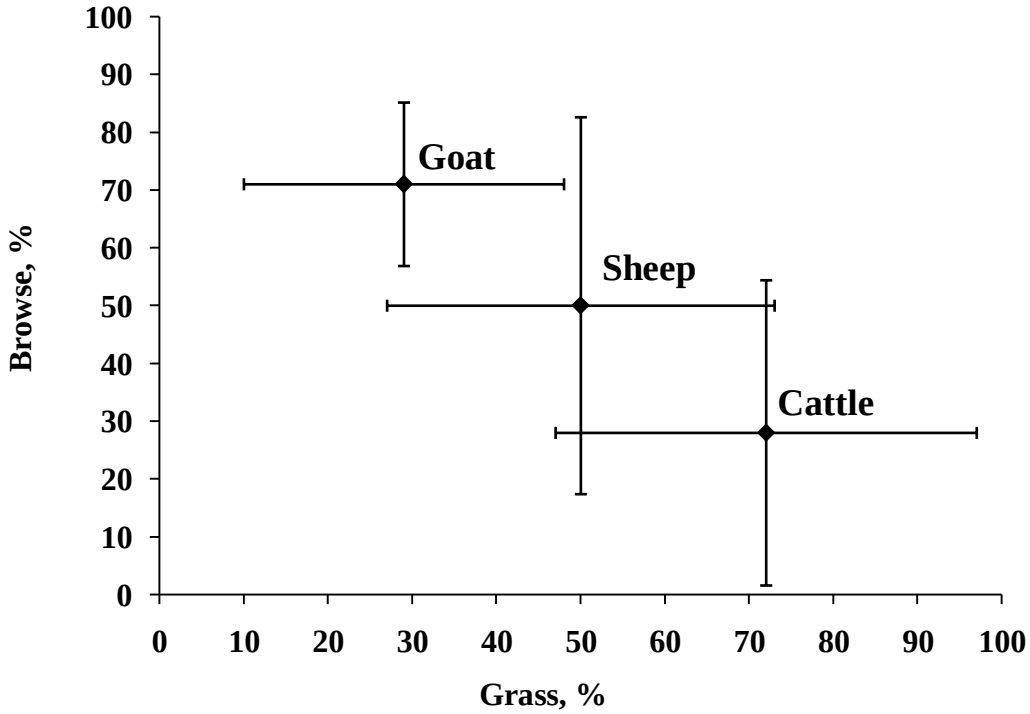

Figure 7.3. Botanical composition (% grass and browse) of diets chosen by goat (n = 13), sheep (n = 105), and cattle (n = 121) on pasture. Bars delineate mean ± SD. Data from Van Dyne et al. (1980).

Image removed for electronic publication because copyright permission could not be obtained. Reader is referred to Figure 1 of source (Salama et al., 2005) for original image.

Figure 7.4. Milk production of extended vs. conventional lactations of multiparous Muriciano-Granadina goats milked once daily. Open (○) and closed (●) symbols represent production of goats managed for kidding intervals of 12-months (K12) and 24-months (K24), respectively. Arrows labeled (a) and (b) highlight where milk production of extended lactation is greater (during pregnancy and dry period of K12 goats) and less (during peak lactation of K12 goats) than conventional lactation. First and second asterisks near *x*-axis indicate times that K12 and all goats were rebred, respectively. Figure modified from Salama et al. (2005).

REFERENCES

Adamczewski, J. Z., P. F. Flood, and A. Gunn. 1997. Seasonal patterns in body composition and reproduction of female muskoxen (Ovibos moschatus). J. Zool. 241: 245-269.

Adamczewski, J. Z., P. J. Fargey, B. Laarveld, A. Gunn, and P.F. Flood. 1998. The influence of fatness on the likelihood of early-winter pregnancy in muskoxen (Ovibos moschatus). Theriogenology 50:605–614.

Agungpriyono, S, Y. Yamamoto, N. Kitamura, J. Yamada, K. Sigit, and T. Yamashita. 1992. Morphological study on the stomach of the lesser mouse deer (Tragulus javanicus) with special reference to the internal surface. J. Vet. Med. Sci. 54:1063-1069.

Agungpriyono, S., J. Yamada, N. Kitamura, K. Sigit, Y. Yamamoto, A. Winarto, and T. Yamashita. 1995. Light microscopic studies of the stomach of the lesser mouse deer (Tragulus javanicus). Eur. J. Morphol. 33:59-70.

Ahvenjärvi, S., A. Vanhatalo, P. Huhtanen, and T. Varvikko. 2000. Determination of reticulo-rumen and whole-stomach digestion in lactating cows by omasal canal or duodenal sampling. Br. J. Nutr. 83:67–77.

Ahvenjärvi, S., B. Skiba, and P. Huhtanen. 2001. Effect of heterogeneous digesta chemical composition on the accuracy of measurements of fiber flow in dairy cows. J Anim Sci. 79:1611-1620.

Aitchison, E. M., M. Gill, M. S. Dhanoa, and D. F. Osbourn. 1986. The effect of digestibility and forage species on the removal of digesta from the rumen and the voluntary intake of hay by sheep. Br. J. Nutr. 56:463-476.

Albon, S.D., B. Mitchell, B.J. Huby, and D. Brown. 1986. Fertility in female red deer (Cervus elaphus) : the effects of body composition, age and reproductive status. J. Zool. 209:447–460.

Allen, M. S., and D. R. Mertens. 1988. Evaluating constraints on fiber digestion by rumen microbes. J. Nutr. 118:261-270.

Allen, M.S. 1996. Physical constraints on voluntary intake of forages by ruminants. J. Anim. Sci. 74:3063-3075.

Alory, J. 1998. Cope's rule and the dynamics of body mass evolution in North American fossil mammals. Science 280:731-734.

Altman, S. A. 1987. The impact of locomotor energetic on mammalian foraging. J. Zool. Lond. 211: 215-225.

Andersson, M. 1994. Sexual Selection. Princeton University Press, Princeton, NJ.

Animal Improvement Programs Laboratory. 2008. Cow genetic trends. United States Department of Agriculture, Beltsville, MD. http://aipl.arsusda.gov/eval/summary/trend.cfm Accessed Oct. 13, 2008.

Arbel, R., Y. Bigun, E. Ezra, H. Sturman, D. Hojman. 2001. The effect of extended calving intervals in high lactating cows on milk production and profitability. J. Dairy Sci. 84:600-608.

Atasoglu, C., and C. Valdés, C. J. Newbold, and R. J. Wallace. 1999. Influence of peptides and amino acids on fermentation rate and de novo synthesis of amino acids by mixed micro-organisms from the sheep rumen. Br. J. Nutr. 81:307-314.

Auldist, M. J., G. O'Brien, D. Cole, K. L. Macmillan, and C. Grainger. 2007. Effects of varying lactation length on milk production capacity of cows in pasture-based dairying systems. J. Dairy Sci. 90:3234-3241.

Bailey, C. B., and C. C. Balch. 1961. Saliva secretion and its relation to feeding in cattle. 2. The composition and rate of secretion of mixed saliva in the cow during rest. Br. J. Nutr. 15:383-402.

Baker, D. L., and N. T. Hobbs. 1987. Strategies of digestion: digestion efficiency and retention time of forage diets in montane ungulates. Can. J. Zool. 65:1978-1984.

Balch, C. C. 1950. Factors affecting the utilization of food by dairy cows; the rate of passage of food through the digestive tract. Br. J. Nutr. 4:361-388.

Baldwin, R. L. 1995. Modeling ruminant digestion and metabolism. Chapman and Hall, London, UK.

Barry, T. N., G. J. Faichney, and C. Redekopp. 1985. Gastro-intestinal tract function in sheep infused with somatostatin. Aust. J. Biol. Sci. 38:393-403.

Bauman, D. E., and W. B. Currie. 1980. Partitioning of nutrients during pregnancy and lactation: a review of mechanisms involving homeostasis and homeorhesis. J. Dairy Sci. 63:1514-1529.

Baumgardt, B. R. 1970. Regulation of feed intake and energy balance. Pages 235-253 in Physiology of Digestion and Metabolism in the Ruminant. A. T Phillipson, ed. Oriel Press, Newcastle upon Tyne, UK.

Bell, R. H. V. 1970. The use of the herb layer by grazing ungulates in the Serengeti. Pages 111-123 in Animal Population in Relation to Their Food Resources. A. Watson, ed. Blackwell Scientific, New York.

Bell, R. H. V. 1971. A grazing ecosystem in the Serengeti. Sci. Am. 224:86-93.

Bernal-Santos, M. G. 1989. Dynamics of rumen turnover in cows at various stages of lactation. PhD Diss. Cornell Univ., Ithica, NY.

Blaxter, K. L. 1989. Energy Metabolism in Animals and Man. Cambridge Univ. Press, Cambridge, UK.

Blaxter, K. L., N. M. McGraham, and F. W. Wainman. 1956. Some observations on the digestibility of food by sheep and on related problems. Br. J. Nutr. 10:69-91.

Boda, J. M., P. Riley, and T. Wegner. 1962. Tissue glycogen levels in relation to age and some parameters of rumen development in lambs. J. Anim. Sci. 21:252-257.

Bosch, M. W., S. Tamminga, G. Pos, C. P. Leffering, and J. M. Muylaert. 1992a. Influence of stage of maturity of grass silages on digestion processes in dairy cows. 1. Composition, nylon bag degradation rates, fermentation characteristics, digestibility and intake. Livestock Prod. Sci. 32:245-264.

Bosch, M. W., S. Tamminga, G. Post, C. P. Leffering, and J. M. Muylaert. 1992b. Influence of stage of maturity of grass silages on digestion processes in dairy cows. 2. Rumen contents, passage rates, distribution of rumen and faecal particles and mastication activity. Livestock Prod. Sci. 32:265-281.

Bost, J. 1970. Omasal physiology. Pages 52-65 in Physiology of Digestion and Metabolism in Ruminants. A. T. Phillipson, ed. Oriel Press, Newcastle upon Tyne, UK.

Brown, W. F., and Pitman, W.D. 1991. Concentration and degradability of nitrogen and fibre fractions in selected tropical grasses and legumes. Trop. Grass. 25:305-312.

Bruford, M. W., D. G. Bradley, and G. Luikart. 2003. DNA markers reveal the complexity of livestock domestication. Nat Rev. Genet. 2003 4:900-910.

Calder, W. A., III. 1984. Size, Function, and Life History. Harvard Univ. Press, Cambridge, MA.

Canbolat, O., Kamalak, A., Ozkan, C. O., Erol, A., Sahin, M., Karakas, E., and E. Ozkose. 2006. Prediction of relative feed value of alfalfa hays harvested at different maturity stages using in vitro gas production. Livestock Res. Rural Dev. http://www.cipav.org.co/lrrd/lrrd18/2/canb18027.htm Accessed March 23, 2007.

Cant, J. P., B. W. McBride, and W. J. Croom, Jr. 1996. The regulation of intestinal metabolism and its impact on whole animal energetics. J. Anim. Sci. 74:2541-2553.

Capellini, I., and L. M. Gosling. 2007. Habitat primary production and the evolution of body size within the hartebeest clade. Biol. J. Linn. Soc. 92:431-440.

Carroll, R. L. 1988. Vertebrate Paleontology and Evolution. W.H. Freeman & Co., New York, NY.

Chagas, L. M., J. J. Bass, D. Blache, C. R. Burke, J. K. Kay, D. R. Lindsay, M. C. Lucy, G. B. Martin, S. Meier, F. M. Rhodes, J. R. Roche, W. W. Thatcher, and R. Webb. 2007. New perspectives on the roles of nutrition and metabolic priorities in the subfertility of high-producing dairy cows. J. Dairy Sci. 90:4022-4032.

Chenost, M., and C. Kayouli. 1997. Roughage Utilization in Warm Climates. FAO Animal Production and Health Paper no. 135. Food and Agriculture Organization of the United Nations, Rome, IT.

Cherney, D. J. R., Patterson, J. A., and R. P. Lemenager. 1990b. Influence of in situ bag rinsing technique on determination of dry matter disappearance. J. Dairy Sci. 73:391-397.

Cherney, D. J., Mertens, D. R., and J. E. Moore. 1990a. Intake and digestibility by wethers as influenced by forage morphology at three levels of forage offering. J. Anim. Sci. 68:4387-4399.

Chilibroste, P., C. Aguilar, and F. García. 1997. Nutritional evaluation of diets. Simulation model of digestion and passage of nutrients through the rumen-reticulum. Anim. Feed Sci. Tech. 68:259-275.

Chivers, D.J., and C. M. Hladik. 1980. Morphology of the gastrointestinal tract in primates: comparisons with other mammals in relation to diet. J. Morphol. 166:337–386.

Church, D. C., and W. H. Hines. 1978. Ruminoreticular characteristics of elk. J. Wildl. Manage. 42:654-659.

Cirio, A., F. Méot, M. L. Delignette-Muller, and R. Biovin. 2000. Determination of parotid urea secretion in sheep by means of ultrasonic flow probes and a multifactorial regression analysis. J. Anim. Sci. 78:471-476.

Clapperton, J. L. 1964. The effect of walking upon the utilization of food by sheep. Br. J. Nutr. 18: 39-46.

Clauss, M., A. Schwarm, S. Ortmann, W. J. Streich, and J. Hummel. 2007 A case of non-scaling in mammalian physiology? Body size, digestive capacity, food intake, and ingesta passage in mammalian herbivores. Comp. Biochem. Physiol. A. 148:249–265.

Clauss, M., J. Hummel, F. Vercammen, and W. J. Streich. 2005. Observations on the macroscopic digestive anatomy of the Himalayan tahr (Hemitragus jemlahicus). Anat. Histol Embryol. 34:276-8.

Clauss, M., M. Lechner-Doll, and W. J. Striech. 2002. Faecal particle size distribution in captive wild ruminants: an approach to the browser/grazer dichotomy from the other end. Oecologia. 131:343-349.

Clauss, M., R. Frey, B. Kiefer, M. Lechner-Doll, W. Loehlein, C. Polster, G. E. Rössner, and W. J. Streich. 2003. The maximum attainable body size of herbivorous mammals: morphophysiological constraints on foregut, and adaptations of hindgut fermenters. Oecologia 136: 14–27.

Clauss, M., R. R. Hofmann, J. Hummel, J. Adamczewski, K. Nygren, C. Pitra, W. J. Streich, and S. Reese. 2006. Macroscopic anatomy of the omasum of free-ranging moose (Alces alces) and muskoxen (Ovibos moschatus) and a comparison of the omasal laminal surface area in 34 ruminant species. J. Zool. 270:346-358.

Clauss, M., R. R. Hofmann, W. J. Streich, J. Fickel, and J. Hummel. 2008. Higher masseter muscle mass in grazing than in browsing ruminants. Oecologia. 157:377-385.

Clutton-Brock, J. 1999. A Natural History of Domesticated Mammals. 2nd ed. Cambridge Univ. Press, Cambridge, UK.

Clutton-Brock, T. H., F. E. Guinness, and S. D. Albon. 1982. Red Deer: The Behaviour and Ecology of Two Sexes. University of Chicago Press, Chicago.

Coblentz, W. K., Fritz, J. O., Cochran, R. C., Rooney, W. L., and K. K. Bolsen. 1997. Protein degradation in response to spontaneous heating in alfalfa hay by in situ and ficin methods. J. Dairy Sci. 80:700-713.

Colbert, E. H. 1941. The osteology and relationships of Archaeomeryx, an ancestral ruminant. Am. Mus. Novit. 1135:1–24.

Colburn, M. W. 1968. Ingestion control, protein and energy requirements for maintenance, and metabolic size of growing ruminant animals. PhD Diss. Rutgers University, New Brunswick, NJ.

Conrad, H. D., J. W. Hibbs, and A. D. Pratt. 1964. Regulation of feed intake in dairy cows. I. Change in importance of physical and physiological factors with increasing digestibility. J. Dairy Sci. 47:54-62.

Conrad, H. R., A. D. Pratt, and J. W. Hibbs. 1964. Regulation of feed intake in dairy cows. I. Change in importance of physical and physiological factors with increasing digestibility. J. Dairy Sci. 47:54-62.

Coombe, J. B., and R. N. Kay. 1965. Passage of digesta through the intestines of the sheep: retention times in the small and large intestines. Br. J. Nutr. 19:325-338.

Crooker, B. A., J. H. Clark, and R. D. Shanks. 1982. Rare earth elements as markers for rate of passage measurements of individual feedstuffs through the digestive tract of ruminants. J. Nutr. 112:1353-1361.

Danfaer, A. 1990. A dynamic model of nutrient digestion and metabolism in lactating dairy cows. PhD Diss. National Institute of Animal Science, Foulam, DK.

Dawson, T.J., and A.J. Hulbert. 1970. Standard metabolism, body temperature, and surface area of Australian marsupials. Am. J. Physiol. 218:1233-1238.

de Vega, A., J. Gasa, C. Castrillo, and J. A. Guada. 1998. Passage through the rumen and the large intestine of sheep estimated from faecal marker excretion curves and slaughter trials. Br. J. Nutr. 80:381-389.

Delgado, C. L. 2003. Rising consumption of meat and milk in developing countries has created a new food revolution. J. Nutr. 133:3907S-3910S.

DeMiguel, D., M. Fortelius, B. Azanza, and J. Morales. 2008. Ancestral feeding state of ruminants reconsidered: earliest grazing adaptation claims a mixed condition for Cervidae. BMC Evol. Biol. 8:13

Demment, M.W., and P. J. Van Soest. 1985. A nutritional explanation for body-size patterns of ruminant and nonruminant herbivores. Am. Nat. 125: 641-672.

Deswysen, A.G., and H. J. Ehrlein. 1981. Silage intake, rumination and pseudo-rumination activity in sheep studied by radiography and jaw movement recordings. Br. J. Nutr. 46:327-335

Diamond J. 2002. Evolution, consequences and future of plant and animal domestication. Nature 418:700-707.

Dijkstra, J., H. D. Neal, D. E. Beever, and J. France. 1992. Simulation of nutrient digestion, absorption and outflow in the rumen: model description. J. Nutr. 122:2239-2256.

Dixon, R. M., and J. V. Nolan. 1982. Studies of the large intestine in sheep. 1. Fermentation and absorption in sections of the large intestine. Br. J. Nutr. 47:289-300.

Dixon, R. M., and J. V. Nolan. 1986. Nitrogen and carbon flows between the caecum, blood and rumen in sheep given chopped lucerne (Medicago sativa) hay. Br. J. Nutr. 55:313-332.

Dixon, R. M., and L. P. Milligan. 1984. Nitrogen kinetics in the large intestine of sheep given bromegrass pellets. Can. J. Anim. Sci. 64:103-111.

Dixon, R. M., J. J. Kennelly, and L. P. Milligan. 1983. Kinetics of [103Ru]phenanthroline and dysprosium particulate markers in the rumen of steers. Br. J. Nutr. 49:463-473.

Dixon, R.M., and J. V. Nolan. 1983. Studies of the large intestine in sheep. 3. Nitrogen kinetics in sheep given chopped lucerne (Medicago sativa) hay. Br. J. Nutr. 50:757-768.

Domingue, B. M. F., D. W. Dellow, P. R. Wilson, and T. N. Barry. 1991. Comparative digestion in deer, goats, and sheep. N.Z. J. Agric. Res. 34:45–53.

Doyle, P.T., J. K. Egan, and A. J. Thalen. 1982. Parotid saliva of sheep. I. Effects of level of intake and type of roughage. Aust. J. Agric. Res. 33:573-584.

East, R. 1999. African Antelope Database 1998. IUCN/SSC Antelope Specialist Group, Gland, CH

Egan, J. K., and P. T. Doyle. 1982. The effect of stage of maturity in sheep upon intake and digestion of roughage diets. Aust. J. Agric. Res. 33:1099-1105.

Ehrlein, H.J. 1980. Forestomach motility in ruminants. Film C 1328 des IWF, Goettingen, W. German. Publikationen zu Wissenschagtlichen Filmen, Sektion Medizin, Serie 5, No. 9/C 1328.

Ellis, W. C., J. H. Matis, and C. Lascano. 1979. Quantitating ruminal turnover. Fed Proc. 38:2702-6.

Ellis, W. C., J. H. Matis, T. M. Hill, and M. R. Murphy. 1994. Methodology for estimating digestion and passage kinetics of forages. Pages 682-753 in Forage Quality, Evaluation, and Utilization. G. C. Fahey, Jr, M. Collins, D. R. Mertens, and L. E. Moser, ed. American Society of Agronomy, Crop Science of America, Soil Science Society of America, Madison, WI.

Ellis, W. C., Mahlooji, M., and J. H. Matis. 2005. Models for estimating parameters of neutral detergent fiber digestion by ruminal microorganisms. J. Anim. Sci. 83:1591-1601.

Ellis, W.C., D. Poppi, and J. H. Matis. 2000. Feed intake in ruminants: kinetic aspects. Pages 335-363 in Farm Animal Metabolism and Nutrition. J. P. F. D'Mello, ed. CABI, Wallingford, UK.

Engelhardt, W. V., and R. Hauffe. 1975. Role of the omasum in absorption an secretion of water and electrolytes in sheep and goats. Pages 216–230 in Digestion and Metabolism in the Ruminant. I. W. McDonald and A. C. I. Warner, ed. University of New England Publishing Unit, Armidale, AU.

Evans, E. W., G. R. Pearce, J. Burnett, and S. L. Pillinger. 1973. Changes in some physical characteristics of the digesta in the reticulo-rumen of cows fed once daily. Br. J. Nutr. 29:357-376.

Faichney, G. J. 1986. The kinetics of particulate matter in the rumen. Pages 173-195 in Control of Digestion and Metabolism in Ruminants. L. P. Milligan, W. L. Grovum, and A. Dobson, ed. Prentice-Hall, Englewood Cliffs, NJ.

Faichney, G. J., and R. C. Boston. 1983. Interpretation of faecal excretion patterns of solute and particle markers introduced into the rumen of sheep. J. Agric. Sci (Camb). 101:575-581.

FAO. 2008a. Domestic Animal Diversity Information System. Food and Agriculture Organization of the United Nations, Rome, IT. http://lprdad.fao.org/ Accessed Sep. 9, 2008.

FAO. 2008b. FAO Statistical Databases. Food and Agriculture Organization of the United Nations, Rome, IT. http://faostat.fao.org/ Accessed Sep. 9, 2008.

Feldhamer, G. A., L. C. Drickamer, S. H. Vessey, J. F. Merrit, and C. Krajewski. 2007. Mammalogy: Adaptation, Diversity, Ecology. 3rd ed. The John Hopkins Univ. Press, Baltimore, MD.

Fernández, M. H, and E. S. Vrba. 2005. A complete estimate of the phylogenetic relationships in Ruminantia: a dated species-level supertree of the extant ruminants. Biol Rev. 80:269-302.

Fisher, D. S. 1996. Modeling ruminant feed intake with protein, chemostatic, and distention feedbacks. J. Anim. Sci. 74:3076-3081.

Fisher, D. S., J. C. Burns, and K. R. Pond. 1987. Modeling ad libitum dry matter intake by ruminants as regulated by distension and chemostatic feedbacks. J. Theor. Biol. 126:407-418.

Foose, T. J. 1982. Trophic strategies of ruminant versus nonruminant ungulates. PhD Diss. University of Chicago, Chicago, IL.

Foot, J. Z., and A. J. F. Russel. 1979. The relationship in ewes between voluntary food intake during pregnancy and forage intake during lactation and after weaning. Anim. Prod. 28:25-39.

Forbes, J. M. 1996. Integration of regulatory signals controlling forage intake in ruminants. J Anim Sci. 74:3029-3035.

Forbes, J. M. 2007. Voluntary Food Intake and Diet Selection in Farm Animals. 2nd ed. CABI, Wallingford, UK.

Garland, T., Jr. 1983. Scaling the ecological cost of transport to body mass in terrestrial mammals. Am. Nat. 121:571-87.

Gaulin, S. J.C. 1979. A Bell/Jarman model of primate feeding niches. Hum. Ecol. 7:1-20.

Geist, V. 1974. On the relationship of ecology and behavior in the evolution of ungulates: theoretical considerations. Pages 235-246 in The Behavior of Ungulates and Its Relation to Management. V. Geist and F. R. Walther, ed. IUCN Publications, New Series no. 24. IUCN, Morges, Switzerland.

Gentry, A. W. 2000. The ruminant radiation. Pages 11-25 in Antelopes, Deer, and Relatives: Fossil Record, Behavioral Ecology, Systematics, and Conservation. E. Vbra and G. B. Schaller. Yale Univ. Press, New Haven, CT.

Gerhart, K.L., D.E. Russell, D. van de Wetering, R.G. White, and R.D. Cameron. 1997. Pregnancy of adult caribou (Rangifer tarandus): evidence for lactational infertility. J. Zool. 242:17-30.

Giesecke, D., and N. O. Van Gylswyk. 1975 A study of feeding types and certain rumen functions in six species of South African wild ruminants. J. Agric. Sci. 85:75–83.

Gordon, I. J., and A. W. Illius. 1994. The functional significance of the browser-grazer dichotomy in African ruminants. Oecologia 98: 167-175.

Gordon, I. J., and A. W. Illius. 1996. The nutritional ecology of African ruminants: A reinterpretation. J. Anim. Ecol. 65:18-28.

Gregory, P. C., and S. J. Miller. 1989. Influence of duodenal digesta composition on abomasal outflow, motility and small intestinal transit time in sheep. J. Physiol. 413:415-431.

Gregory, P. C., S. J. Miller, and A. C. Brewer. 1985. The relation between food intake and abomasal emptying and small intestinal transit time in sheep. Br. J. Nutr. 53:373-380.

Gross, J. E., P. U. Alkon, and M. W. Demment. 1996. Nutritional ecology of dimorphic herbivores: digestion and passage rates in Nubian ibex. Oecologia. 107:170-178.

Grovum, W. L., and J. F. Hecker. 1973. Rate of passage of digesta in sheep. 2. The effect of level of food intake on digesta retention times and on water and electrolyte absorption in the large intestine. Br. J. Nutr. 30:221-230.

Grovum, W. L., and V. J. Williams. 1973. Rate of passage of digesta in sheep. 1. The effect of level of food intake on marker retention times along the small intestine and on apparent water absorption in the small and large intestines. Br. J. Nut. 29:13-21.

Grovum, W. L., and V. J. Williams. 1977. Rate of passage of digesta in sheep. 6. The effect of level of food intake on mathematical predictions of the kinetics of digesta in the reticulorumen and intestines. Br. J. Nutr. 38:425-36.

Gwynne, M. D., and R. H. V. Bell. 1968. Selection of vegetation components by grazing ungulates in the Serengeti National Park. Nature 220:390-393.

Harested, A. S. and F. L. Bunnell. 1979. Home range and body weight: a reevaluation. Ecology 60:389-402.

Harrop, C. J. F. 1974. Nitrogen metabolism in the ovine stomach. 4. Nitrogenous components of the abomasal secretions. J. Agric. Sci. 83:249-257.

Hatfield, P. G., D. C. Clanton, K. M. Eskridge, and D. W. Sanson. 1989. Forage intake by lactating beef cows differing in potential for milk production. J. Anim. Sci. 67:3018-3027.

Hecker, J. F. 1971. Ammonia in the large intestine of herbivores. Br. J. Nutr. 26:135-145.

Hecker, J. F., and W. L. Grovum. 1975. Rates of passage of digesta and water absorption along the larg intestines of sheep, cows and pigs. Aust. J. Biol. Sci. 28:161-167.

Heuvelink, G. B. M. 1998. Error Propagation in Environmental Modelling with GIS. Taylor & Francis, Bristo, PA.

Hoffman, R. R, and D. R. M. Stewart. 1972. Grazer or browser: a classification based on the stomach-structure and feeding habits of East African ruminants. Mammalia. 36:226-240.

Hoffman, R. R. 1989. Evolutionary steps of ecophysiological adaptation and diversification of ruminants: a comparative view of their digestive system. Oecologia 78:443–457.

Hofmann, R. R. 1973. The Ruminant Stomach: Stomach Structure and Feeding Habits of East African Game Ruminants. East African Literature Bureau, Nairobi, Kenya.

Hofmann, R. R., W. J. Streich, J. Fickel, J. Hummel, and M. Clauss. 2008. Convergent evolution in feeding types: salivary gland mass differences in wild ruminant species. J. Morphol. 269:240-257.

Holmann, F. J., C. R. Shumway, R. W. Blake, R. B. Schwart, and E. M. Sudweeks. 1984. Economic value of days open for Holstein cows of alternative milk yields with varying calving intervals. J. Dairy. Sci. 67:636-643.

Houser, R. H. 1970. Physiological effects of supplemental nitrogen and energy in sheep feed low-quality roughage. PhD Diss. U. Florida, Gainesville.

Hummel, J., M. Clauss, W. Zimmerman, K. Johanson, C. Nørgaard, Pfeffer E. 2005. Fluid and particle retention in captive okapi (Okapia johnstoni). Comp. Biochem. Phys. A. 140:426-446

Hungate, R. E. 1966. The rumen and its microbes. Academic Press, New York.

Hungate, R. E., G. D. Phillips, A. McGregor, D. P. Hungate, and H. K. Buechner. 1959. Microbial fermentation in certain mammals. Science 130:1192-1194.

Hunter, R. A, and B. D. Siebert. 1986. The effects of genotype, age, pregnancy, lactation and rumen characteristics on voluntary intake of roughage diets by cattle. Aust. J. Agric. Res. 37:549-560.

Hvelplund, T., and M. R. Weisbjerg. 2000. In situ techniques for the estimation of protein degradability and postrumen availability. Pages 233-258 in Forage Evaluation in Ruminant Nutrition. D. I. Givens, E. Owen, R. F. E. Axford, and H. M Omed, ed. CABI, Wallingford, UK.

Hyer, J. C., J. W. Oltjen, and M. L. Galyean. 1991a. Development of a model to predict forage intake by grazing cattle. J. Anim. Sci. 69:827-835.

Hyer, J. C., J. W. Oltjen, and M. L. Galyean. 1991b. Evaluation of a feed intake model for the grazing beef steer. J. Anim. Sci. 69:836-842.

Illius, A. W, and I. J. Gordon. 1991. Prediction of intake and digestion n ruminants and by a model of rumen kinetics integrating animal size and plant characteristics. J. Agric. Sci. (Camb). 116:145-157.

Illius, A. W, and N. S. Jessop. 1996. Metabolic constraints on voluntary intake in ruminants. J Anim Sci. 74:3052-3062.

Illius, A. W, N. S. Jessop, and M. Gill. 2000. Mathematical models of food intake and metabolism in ruminants. Pages 21-40 in Ruminant Physiology: Digestion, Metabolism, Growth and Reproduction. P. B. Cronjé, ed. CABI, Wallingford, UK.

Illius, A. W. and I. J. Gordon. 1991. Prediction of intake and digestion in ruminants by a model of rumen kinetics integrating animal size and plant characteristics. J. Agric. Sci. (Camb.) 116:145-157.

Illius, A. W., and I. J. Gordon. 1992. Modelling the nutritional ecology of ungulate herbivores: evolution of body size and competitive interactions. Oecologia. 89:428-434.

Illius, A. W., and M. S. Allen. 1994. Assessing forage quality using integrated models of intake and digestion by ruminants. Pages 969-890 In Forage Quality, Evaluation, and Utilization. G. C. Fahey, Jr., M. Collines, D. R. Mertens, and L. E. Moser, ed. ASA-CSSA-SSA, Madison, WI.

Illius, A.W., and I. J. Gordon, I.J. 1999. Physiological ecology of mammalian herbivory. Pages 71-96 in Vth International Symposium on the Nutrition of Herbivores. H.-J. G. Jung and G. C. Fahey, Jr., ed. American Society of Animal Science, Savoy, IL,

Isaacson, H. R., F. C. Hinds, M. P. Bryant, and F. N. Owens. 1975. Efficiency of energy utilization by mixed rumen bacteria in continuous culture. J. Dairy Sci. 58:1645-1659.

IUCN. 2008. European Mammal Assessment. http://ec.europa.eu/environment/nature/conservation/species/ema/species/all.htm Accessed Sep. 9, Cited 2008.

Jacobs, B. F., J. D. Kingston, and L. J. Jacobs. 1999. The origin of grass-dominated ecosystems. Ann. Mo. Bot. Gard. 86:590-643.

Jacquez, J. A. 1985. Compartmental Analysis in Biology and Medicine. University of Michigan Press, Ann Arbor, MI.

Janis, C. M. 2000. Patterns in the evolution of herbivory in large terrestrial mammals: the Paleogene in North America. Pages 168-222 in Evolution of Herbivory in Terrestrial Herbivores: Perspectives from the Fossil Record. H.-D. Sues, ed. Cambridge University Press, New York.

Janis, C. M. 1976. The evolutionary strategy of the Equidae and the origins of rumen and cecal digestion. Evolution 30: 757-774.

Janis, C. M. 1982. Evolution of horns in ungulates: ecology and paleoecology. Biol. Rev. 57:261-318.

Janis, C. M. 1984. Tragulids as living fossils. Pages 87-94 in Living Fossils. N. Eldredge and S. Stanley, ed. Springer-Verlag, New York.

Janis, C. M. 1990. Correlation of cranial and dental variables with body size in ungulates and macropodoids. Pages 255-300 in Body Size in Mammalian Paleobiology: Estimation and Biological Implications. J. Damuth and B.J . MacFadden, ed. Cambridge University Press, Cambridge.

Janis, C. M. 1993. Tertiary mammal evolution in the context of changing climates, vegetation, and tectonic events. Annu. Rev. Ecol. Syst. 24:467-500.

Janis, C. M., and E. Manning. 1998a. Antilocapridae. Pages 491- 507 in Evolution of Tertiary Mammals of North America: Volume 1, Terrestrial Carnivores, Ungulates, and Ungulatelike Mammals. C. M. Janis, K. M. Scott, L. L. Jacobs, ed. Cambridge Univ. Press: Cambridge, UK.

Janis, C. M., and E. Manning. 1998b. Dromomerycidae. Pages 477- 90 in Evolution of Tertiary Mammals of North America: Volume 1, Terrestrial Carnivores, Ungulates, and Ungulatelike Mammals. C. M. Janis, K. M. Scott, and L. L. Jacobs, ed. Cambridge Univ. Press: Cambridge, UK.

Janis, C. M., and K. M. Scott. 1987. The interrelationships of higher ruminant families with special emphasis on the members of the Cervoidea. Am. Mus. Novit. 2893:1-85.

Janis, C.M., K. M. Scott, and L. L. Jacobs, ed. 1998. Evolution of Tertiary Mammals of North America. Volume 1: Terrestrial Carnivores, Ungulates, and Ungulatelike Mammals. Cambridge University Press, Cambridge.

Jarman, P. J. 1974. The social organization of antelope in relation to their ecology. Behaviour 48: 215-266.

Jermann, T. M., J. G. Opitz, J. Stackhouse, and S. A. Benner. 1995. Reconstructing the evolutionary history of the artiodactyl ribonuclease superfamily. Nature 374:57-59.

Kaps, M., and W. Lamberson. 2004. Biostatistics for Animal Science. CABI Publishing, Cambridge, MA.

Knight, C. H. 1984. Mammary growth and development: strategies of animals and investigators. Symp. Zool. Soc. Lond. 51:147-170.

Knight, C. H., 2001. Lactation and gestation in dairy cows: flexibility avoids nutritional extremes. Proc. Nutr. Soc. 60:527–537.

Kohn, R. A., M. M. Dinneen, and E. Russek-Cohen. 2005. Using blood urea nitrogen to predict nitrogen excretion and efficiency of nitrogen utilization in cattle, sheep, goats, horses, pigs, and rats. J. Anim. Sci. 83:879-889.

Krishnamoorthy, U., C. J. Sniffen, M. D. Stern, and P. J. Van Soest. 1983. Evaluation of a mathematical model of rumen digestion and an in vitro simulation of rumen proteolysis to estimate the rumen-undegraded nitrogen content of feedstuffs. Br. J. Nutr. 50:555-568.

Kutner, M. H., C. J. Nachtsheim, J. Neter, and W. Li. 2004. Applied Linear Statistical Models. 5th ed.McGraw-Hill: New York.

Langer, P. 1988. The Mammalian Herbivore Stomach: Comparative Anatomy, Function and Evolution. Gustav Fischer Verlag, New York.

Linn, J. G., and N. P. Martin. 1989. Forage quality tests and interpretation. Univ. of Minnesota Ext. Ser. Publ. AG-FO-2637.

Linzell, J. L. 1973. Innate seasonal oscillations in the rate of milk secretion in goats. J. Physiol. 230:225–233.

Lirette, A., and L. P. Milligan. 1990. Endoscopic technique to follow the mixing and breakdown of colored forage particles in the rumino-reticulum of cattle. Can. J. Anim. Sci. 70:219-226.

Loader, C., 1999. Local Regression and Likelihood. Springer, New York.

Loudon, A.S.I., A. S. McNeilly, and J. A. Milne. 1983. Nutrition and. lactational control of fertility in red deer. Nature 302:145–147.

MacRae, J. C., and P. J. Reeds. 1980. Prediction of protein deposition in ruminants. Pages 225-249 in Protein Deposition in Animals. P. J. Buttery, and D. B. Lindsay, ed. Buttersworths, London.

Maloiy, G.M.O., E. T. Clemens, and J. M. Z. Kamau, 1982. Aspects of digestion and in vitro rumen fermentation rate in six species of East African wild ruminants J. Zoo. Lond. 197:345-353.

Mathison, G. W., E. K. Okine, A. S. Vaage, M. Kaske, and L. P. Milligan. 1995. Current understanding of the contribution of the propulsive activities in the forestomach to the flow of digesta. Pages 23-41 in Ruminant Physiology: Digestion, Metabolism, Growth, and Reproduction. Proceedings of the VIII International Symposium of Ruminant Physiology. W. von Engelhardt, S. Leonhard-Marek, G. Breves, and D. Giesecke, ed. Delmar Publ., Albany, NY, pp. 23-41.

Matis, J. H. 1972. Gamma time-dependency in Blaxter's compartmental model. Biometrics. 28:597–602.

Matis, J. H., T. E. Wehrly, and W. C. Ellis. 1989. Some generalized stochastic compartment models for digesta flow. Biometrics 45:703-720.

McAllan, A. B. 1981. Changes in the composition of digesta during passage through the small intestines of steers. Br. J. Nutr. 46:431-440.

McBride, B.W., and J. M. Kelly. 1990. Energy cost of absorption and metabolism in the ruminant gastrointestinal tract and liver: a review. J. Anim. Sci. 68:2997-3010.

McDonald, I. 1981. A revised model for the estimation of protein degradability in the rumen. J. Agric. Sci. 96:251–252.

McDowell, R. E. 1977. Ruminant Products: More than Meat and Milk. Winrock International Livestock Research and Training Center, Morrilton, AR

Mehrez, A. Z., and E. R. Ørskov. 1977. A study of the artificial fibre bag technique for determining the digestibility of feeds in the rumen. J. Agric. Sci. 88:645-650.

Mertens, D. R. 1973. Application of theoretical mathematical models to cell wall digestion and forage intake in ruminants. PhD Diss. Cornell Univ., Ithica, NY.

Mertens, D. R. 1985. Factors influencing feed intake in lactating cows: from theory to application using neutral detergent fiber. Pages 1-18 in Proceedings of the Georgia Nutrition Conference, Atlanta, GA. University of Georgia Press, Athens.

Mertens, D. R. 1987. Predicting intake and digestibility using mathematical models of ruminal function. J. Anim. Sci. 64:1548-1558.

Mertens, D. R. 1993. Kinetics of cell wall digestion and passage in ruminants. Pages 535-570 in Forage Cell Wall Structure and Digestibility. H. G. Jung, D. R. Buxton, R. D. Hatfield, and J. Ralph, eds. ASA-CSSA-SSSA, Madison, WI.

Mertens, D. R., and L. O. Ely. 1979. A dynamic model of fiber digestion and passage in the ruminant for evaluating forage quality. J. Anim. Sci. 49:1085–1095.

Mertens, D. R., and L. O. Ely. 1982. Relationship of rate and extent of digestion to forage utilization- dynamic model evaluation. J. Anim. Sci. 54:895-905.

Métais, G, and I. Vislobokova. 2007. Basal ruminants. Pages 189 – 212 in The Evolution of the Artiodactyls. D. R. Prothero and S. E. Foss, ed. The John Hopkins Univ. Press, Baltimore MD.

Métais, G., Y. Chaimanee, J. J. Jaeger, and S. Ducrocq. 2001. New remains of primitive ruminants from Thailand: evidence of the early evolution of the Ruminantia in Asia. Zool. Scr. 30:231-248.

Minson, D. J. 1990. Forage in Ruminant Nutrition. Academic Press, London, UK.

Moore, J. E, and W. E. Kunkle. 1995. Meeting energy requirements of beef cattle with forages and concentrates—a mathematical approach to supplementation and economic evaluation of forages of different qualities. Pages 190-197 in Proc. 50th Southern Pasture and Forage Crop Improvement Conf., Knoxville, TN.

Moore, J. E. 1994. Forage quality indices: Development and application. Pages 967-998 in Forage Cell Wall Structure and Digestibility. H. G. Jung, D. R. Buxton, R. D. Hatfield, and J. Ralph, eds. ASA-CSSA-SSSA, Madison, WI.

Moore, J. E., and D. J. Undersander. 2002. Relative forage quality: An alternative to relative feed value and quality index. Pages 16-32 in Proc. 13th Annual Florida Ruminant Nutr. Symp., Gainesville, FL.

Mortola, J. P., and C. Lathier. 2005. Breathing frequency in ruminants: a comparative analysis with non-ruminant mammals. Respir. Physiol. Neurobiol. 145:265-77.

Murphy, M. R. 1984. Modeling production of volatile fatty acids in ruminants. Pages 59-62 in Modeling Ruminant Digestion and Metabolism, Proc. of the 2nd Int. Workshop, Davis, CA.

Murphy, M. R., R. L. Baldwin, M. J. Ulyatt, and L. J. Koong. 1983. A quantitative analysis of rumination patterns. J. Anim. Sci. 56:1236-1240.

Mystrud, A. 1998. The relative roles of body size and feeding type on activity time of temperate ruminants. Oecologia 113:442-446.

Nagy, J. G., and W. L. Regelin. 1975. Comparison of digestive organ size of three deer species. J. Wildl. Manage. 39:621-624.

Nagy, K. A., I. A. Girard, and T. K. Brown. 1999. Energetics of free-ranging mammals, reptiles, and birds. Annu. Rev. Nutr. 19:247–277.

Nocek, J. E. 1988. In situ and other methods to estimate ruminal protein and energy digestibility: a review. J. Dairy Sci. 71:2051-2069.

Nolan, J. V., B. W. Norton, and R. A. Leng. 1976. Further studies of the dynamics of nitrogen metabolism in sheep. Br. J. Nutr. 35:127-147.

Nolan, T., and J. Connolly. 1989. Mixed versus mono grazing of steers and sheep. Anim. Prod. 48:519-533.

Nowak, R. M. 1999. Walker's Mammals of the World. Vol 2. 6th ed. John Hopkins Univ. Press: Baltimore, MD.

NRC. 1991. Microlivestock: Little-Known small Animals with a Promising Economic Future. Natl. Acad. Press, Washington, DC.

NRC. 2000. Nutrient Requirements of Beef Cattle. 7th updated ed. Natl. Acad. Press, Washington, DC.

NRC. 2001. Nutrient Requirements of Dairy Cattle, 7th rev. edn. Natl. Acad. Press, Washington, DC.

NRC. 2007. Nutrient Requirements of Small Ruminants: Sheep, Goats, Cervids, and New World Camelids. Natl. Acad. Press, Washington, DC.

Ohtaishi, N., and Y. Gao. 1990. A review of the distribution of all species of deer (Tragulidae, Moschidae and Cervidae) in China. Mamm. Rev. 20:125-144.

Oltjen, J. W., and J. L. Beckett. 1996. Role of ruminant livestock in sustainable agricultural systems. J. Anim. Sci. 74:1406-1409.

Ørskov, E. R. 1982. Protein Nutrition in Ruminants. Academic Press, New York.

Ørskov, E. R., and I. McDonald. 1979. The estimation of protein degradability in the rumen from incubation measurements weighted according to the rate of passage. J. Agric. Sci. 92:499-503.

Ørskov, E. R., and N. A. MacLeod. 1982. The flow of N from the rumen of cows and steers maintained by intraruminal infusion of volatile fatty acids. Proc. Nutr. Soc. 41:76A.

Ørskov, E. R., and N. A. MacLeod. 1983. Flow of endogenous N from the rumen and abomasum of cattle given protein-free nutrients. Proc. Nutr. Soc. 42:61A.

Ørskov, E. R., Hovell, F. D. DeB., and Mould, F. 1980. The use of the nylon bag technique for the evaluation of feedstuffs. Trop. Anim. Prod. 5:195–213.

Ørskov, E. R., N. A. MacLeod, and D. J. Kyle. 1986. Flow of nitrogen from the rumen and abomasum in cattle and sheep given protein-free nutrients by intragastric infusion. Br. J. Nutr. 56:241-248.

Österman, S., and J. Bertilsson. 2003. Extended calving interval in combination with milking two or three times per day: effects on milk production and milk composition. Livestock Prod. Sci. 82:139-149.

Ouellet, D. R., M. Demers, G. Zuur, G. E. Lobley, J. R. Seoane, J. V. Nolan, and H. Lapierre. 2002. Effect of dietary fiber on endogenous nitrogen flows in lactating dairy cows. J. Dairy Sci. 85:3013-3025.

Owens, F. N., R. A. Zinn, and Y. K. Kim. 1986. Limits to starch digestion in the ruminant small intestine. J. Anim. Sci. 63:1634-1648.

Owen-Smith, N. 1988. Megaherbivores: The Influence of Very Large Body Size on Ecology. Cambridge University Press, Cambridge.

Parra, R., 1978. Comparison of foregut and hindgut fermentation in herbivores. Pages 205-229 in The Ecology of Arboreal Folivores. G. G. Montgomery, ed. Smithsonian Institution Press, Washington, DC.

Penry, D. L, and P. A. Jumars. 1987. Modeling animal guts as chemical reactors. Am. Nat. 129:69-96.

Peréz-Barbería, J.F., and I. J. Gordon. 2005. Gregariousness increases brain size in ungulates. Oecologia 145:41-52.

Peters, R. H. 1983. The Ecological Implications of Body Size. Cambridge University Press, Cambridge.

Pfister, J. A., and J. C. Malechek.1986. Dietary selection by goats and sheep in a deciduous woodland of northeastern Brazil. J. Range Manage. 39:24–28.
Popenoe, H. 1981. The water buffalo: new prospects for an underutilized animal. Natl. Acad. Press, Washington, D.C.

Piccione, G., A. Foà, C. Bertolucci, and G. Coala. 2006. Daily rhythm of salivary and serum urea concentration in sheep. J. Circadian Rhythms. 4:16

Pitt, R. E., J. S. Van Kessel, D. G. Fox, A. N. Pell, M. C. Barry, and P. J. Van Soest. 1996. Prediction of ruminal volatile fatty acids and pH within the net carbohydrate and protein system. J. Anim. Sci. 74:226-244.

Pond, K. R., Ellis, W. C., Matis, J. H., Ferreiro, H. M., and J. D. Sutton. 1988. Compartment models for estimating attributes of digesta flow in cattle. Br. J. Nutr. 60:571-95.

Poppi, D. P., W. C. Ellis, J. H. Matis, and C. E. Lascano. 2001. Marker concentration patterns of labelled leaf and stem particles in the rumen of cattle grazing bermuda grass (Cynodon dactylon) analysed by reference to a raft model. Br. J. Nutr. 85:553-563.

Prothero, D. R, and S. E. Foss, ed. 2007. The Evolution of the Artiodactyls. The John Hopkins Univ. Press, Baltimore MD.

Rehn, H., B. Berglund, U. Emanuelson, G. Tengroth, and J. Philipsson. 2000. Milk production in Swedish dairy cows managed for calving intervals of 12 and 15 months. Acta Agric. Scand. Sect. A. Anim. Sci. 50:263-271.

Reichl, J. R., and R. L. Baldwin. 1975. Rumen modeling: rumen input-output balance models. J. Dairy Sci. 58:879-890.

Reid, C.S.W. 1984. The progress of solid feed residues through the ruminoreticulum: the ins and outs of particles. Pages 79-84 in Ruminant Physiology: Concepts and Consequences. S. K. Baker, J. M. Gawthorne, J. B. McIntosh, and D. B. Purser, ed. School of Agriculture, University of Western Australia, Perth..

Reid, R. L., G. A. Jung, J. M. Cox-Ganser, B. F. Rybeck, and E. C. Townsend. 1990. Comparative utilization of warm-and cool-season forages by cattle, sheep and goats. J. Anim. Sci. 68:2986-2994.

Robbins, C. T., D. E. Spalinger, and W. van Hoven. 1995. Adaptation of ruminants to browse and grass diets: are anatomical-based browser-grazer interpretations valid? Oecologia 103:208-213.

Rohweder, D. A., Barnes, R. F., and N. Jorgeson. 1978. Proposed hay grading standards based on laboratory analyses for evaluating quality. J. Anim. Sci. 47:747-759.

Rook, A. J., M. Gill, R. D. Willink, and S. J. Lister. 1991. Prediction of voluntary intake of grass silages by lactating cows offered concentrates at a flat rate. Anim. Prod. 52:407-420.

Rose, K. D. 1982. Skeleton of Diacodexis, oldest known artiodactyl. Science 216:621-623.

Russell, J. B., C. J. Sniffen, and P. J. Van Soest. 1983. Effect of carbohydrate limitation on degradation and utilization of casein by mixed rumen bacteria. J. Dairy Sci. 66:763-775.

Salama, A. A. K., G. Caja, X. Such, R. Casals, and E. Albanell. 2005. Effect of pregnancy and extended lactation on milk production in dairy goats milked once daily. J. Dairy Sci. 88:3894-3904

Sanson, D. W., and C. J. Kercher. 1996. Validation of equations used to estimate relative feed value of alfalfa hay. Prof. Anim. Sci. 12:162-166.

Schmidt-Neilson, K. 1984. Scaling, why is animal size so important? Cambridge University Press: Cambridge.

Scott, K. M. 1990. Postcranial dimensions of ungulates as predictos of body mass. Pages 301-36 in Body Size in Mammalian Paleobiology. J. Damuth and B. J. MacFadden, ed. Cambridge Univ. Press, Cambridge.

Scott, W. B. 1913. A History of Land Mammals of the Western Hemisphere. Macmillan, New York.

Semprebon, G., C. M. Janis, and N. Solounias. 2004. The diets of the Dromomerycidae (Mammalia: Artiodactyla) and their response to Miocene vegetational change. J. Vertebr. Paleontol. 24:427–444.

Semprebon, G.M., and F. Rivals. 2007. Was grass more prevalent in the pronghorn past? an assessment of the dietary adaptations of Miocene to recent Antilocapridae (Mammalia: Artiodactyla). Palaeogeogr. Palaeoclimatol. Palaeoecol. 253:332–347.

Seo, S., L. O. Tedeschi, C. G. Schwab, C. Lanzas, and D. G. Fox. 2006. Development and evaluation of empirical equations to predict feed passage rate in cattle. Anim. Feed Sci. Tech. 128:67-83.

Shipley, L. A., J. E. Gross, D. E. Spalinger, N. T. Hobbs, and B. A. Wunder. 1994. The scaling of intake rate in mammalian herbivores. Am. Nat. 143:1055-1082.

Shipley, R. A., and R. E. Clark. 1972. Tracer Methods for In Vivo Kinetics: Theory and Application. Academic Press, New York.

Short, H. L. 1964. Postnatal stomach development of white-tailed deer. J. Wildl. Manage. 28:445-458.

Siddons, R. C., J. V. Nolan, D. E. Beever, and J. C. MacRae. 1985. Nitrogen digestion and metabolism in sheep consuming diets containing contrasting forms and levels of N. Br. J. Nutr. 54:175-187.

Sklan, D., A. Arieli, W. Chalupa, and D. S. Kronfeld. 1985a. Digestion and absorption of lipids and bile acids in sheep fed stearic acid, oleic acid, or tristearin. J. Dairy Sci. 68:1667-1675.

Sklan, D., A. Arieli, W. Chalupa, and D. S. Kronfeld. 1985b. Digestion and absorption of protein along ovine gastrointestinal tract. J. Dairy Sci. 68:1676-1681.

Smith, F. A., S. K. Lyons, S. K. Morgan Ernest, K. E. Jones, D. M. Kaufman, T. Dayan, P. A. Marquet, J. H. Brown, and J. P. Haskell. 2003. Body mass of late quaternary mammals. Ecology 84:3403.

Smith, L. W., Goering, H. K., Waldo, D. R., and C. H. Gordon. 1971. In vitro digestion rate of forage cell wall components. J. Dairy Sci. 54:71-76.

Smith, L. W., H. K. Goering, and C. H. Gordon. 1972. Relationships of forage compositions with rates of cell wall digestion and indigestibility of cell walls. J. Dairy Sci. 55:1140-1147.

Smith, N. E., and R. L. Baldwin. 1974. Effects of breed, pregnancy, and lactation on weight of organs and tissues in dairy cattle. J. Dairy Sci. 57:1055-1060.

Sniffen, C. J., J. D. O'Connor, P. J. Van Soest, D. G. Fox, and J. B. Russell. 1992. A net carbohydrate and protein system for evaluating cattle diets: II. Carbohydrate and protein availability. J. Anim. Sci. 70:3562-3577.

Solounias, N. and S. M. C. Moelleken. 1992. Tooth microwear analysis of Eotragus sansaniensis (Mammalia: Ruminantia), one of the oldest known bovids. J. Vertebr. Paleontol. 12:113-121.

Solounias, N., W. S. McGraw, L-A. C. Hayek and L. Werdelin. 2000. The paleodiet of the Giraffidae. Pages 84-95 in Antelopes, Deer, and Relatives: Fossil Record, Behavioral Ecology, Systematics, and Conservation. E. Vbra and G. B. Schaller, ed. Yale Univ. Press, New Haven, CT.

Somers, M. 1961. Factors influencing the secretion of nitrogen in sheep saliva. 3. Factors affecting nitrogen fractions in the parotid saliva of sheep with special reference to the influence of ammonia production in the rumen and fluctuations in fluctuations in level of blood urea. Aust. J. Exp. Biol. 39:133-144.

Staaland, H., E. Jacobsen, and R. G. White. 1979. Comparison of the digestive tract in Svalbard and Norwegian reindeer. Arctic Alpine Res. 11:457-466.

Stanley, T. A., R. C. Cochran, E. S. Vanzant, D. L. Harmon, and L. R. Corah. 1993. Periparturient changes in intake, ruminal capacity, and digestive characteristics in beef cows consuming alfalfa hay. J. Anim. Sci. 71:788-795.

Stefanon, B, A. N. Pell, and P. Schofield. 1996. Effect of maturity on digestion kinetics of water-soluble and water-insoluble fractions of alfalfa and brome hay. J. Anim. Sci. 74:1104-1115.

Stensig, T., M. R. Weisbjerg, and T. Hvelplund. 1994. Estimation of ruminal digestibility of NDF from in sacco degradation and rumen outflow rate. Acta. Agric. Scand. Sect. A Anim. Sci. 44:96-109.

Stevens, C. E., A. F. Sellers, and F. A. Spurrell. 1960. Function of the bovine omasum in ingesta transfer. Am. J. Physiol. 198:449–455.

St-Pierre, N. R. 2003. Reassessment of biases in predicted nitrogen to the duodenum by NRC 2001. J Dairy Sci. 86:344-350.

Sutherland, T. M. 1988. Particle separation in the forestomach of sheep. Pages 43-73 in Aspects of Digestive Physiology in Ruminants. A. Dobson, and M. J. Dobson, ed. Comstock Publishing Associates, Ithaca, NY.

Takatsuki, S. 1988. The weight contributions of stomach compartments of sika deer. J. Wildl. Manage. 52:313-316.

Taylor, C. R., N. C. Heglund, T. A. McMahon, and T. R. Looney. 1980. Energetic cost of generating muscular force during running. J. Exp. Biol. 86:9-18.

Taylor, J. R. 1997. An Introduction to Error Analysis: The Study of Uncertainties in Physical Measurements. 2nd ed. University Science Books, Sausalito, CA.

Teeter, R. G, F. N. Owens, and T. L. Mader. 1984. Ytterbium chloride as a marker for particulate matter in the rumen. J. Anim. Sci. 58:465-473.

Thielemans, R. F., E. Francois, C. Bodart, and A. Thewis. 1978. Mesure du transit gastrointestinal chez le porc à l'aide des radiolanthanides. Comparaison avec le mouton. Ann. Biol. Anim. Biochim. Biophys. 18:237-247.

Thornley, J. H. M, and J. France. 2007. Mathematical Models in Agriculture. 2nd ed. CABI, Wallingford, UK.

Timon, V. M., and J. P. Hanrahan, ed. 1986. Small Ruminant Production in the Developing Countries. FAO Animal Production and Health Paper no. 54. Food and Agriculture Organization of the United Nations, Rome, IT.

Traxler, M. J., D. G. Fox, P. J. Van Soest, A. N. Pell, C. E. Lascano, D. P. Lanna, J. E. Moore, R. P. Lana, M. Vélez, and A. Flores. 1988. Predicting forage indigestible NDF from lignin concentration. J. Anim. Sci. 76:1469-1480.

Tyser, R.W. and T. C. Moermond. 1983. Foraging behavior in two species of different-sized sciurids. Am. Midland. Nat. 109:240-245.

Ulvevadet, B., and K. Klokov, eds. 2004. Family-Based Reindeer Herding and Hunting Economies and the Status and Management of Wild Reindeer/Caribou Populations. Centre for Saami Studies, Univ of Tromsø, Tromsø, Norway.

Ulyatt, M. J., G. C. Waghorn, A. John, C. S. W. Reid, and J. Monro. 1984. Effect of intake and feeding frequency on feeding behaviour and quantitative aspects of digestion in sheep fed chaffed lucerne hay. J. Agric. Sci. 102:645-657.

Vallentine, J. F. 1990. Grazing Management. Academic Press, San Diego, CA.

van Amburgh, M. E., D. M. Galton, D. E. Bauman, and R. W. Everett. 1997. Management and economics of extended calving intervals with use of bovine somatotropin. Livestock. Prod. Sci. 50:15-28.

Van Bruchem, J., J. Voigt, T. S. Lammers-Wienhoven, U. Schonhusen, J. J. Ketelaars, and S. Tamminga. 1997. Secretion and reabsorption of endogenous protein along the small intestine of sheep: estimates derived from 15N dilution of plasma non-protein-N. Br. J. Nutr. 77:273-286.

Van Dyne, G. M., N. R. Brockington, Z. Szocs, J. Duek, and C. A. Ribic. Large herbivore subsystem. Pages 269-537 in Grasslands, Systems Analysis and Man. A. I. Breymeyer and G. M. Van Dyne, ed. Cambridge Univ. Press, Cambridge, UK.

van Kessell, J. S., and J. B. Russell. 1996. The effect of amino nitrogen on the energetics of ruminal bacteria and its impact on energy spilling. J Dairy Sci. 79:1237-1243.

Van Milgen, J., M. R. Murphy, and L. L. Berger. 1991. A compartmental model to analyze ruminal degradation. J. Dairy Sci.74:2515–2529.

Van Soest, P. J. 1994. Nutritional Ecology of the Ruminant. 2nd ed. Cornell Univ. Press: Ithica, NY.

Van Soest, P. J. 1994. Nutritional Ecology of the Ruminant. 2nd ed. Cornell University Press, Ithaca, NY.

Van Soest, P. J., J. B. Robertson, and B. A. Lewis. 1991. Methods for dietary fiber, neutral detergent fiber and non-starch polysaccharides in relation to animal nutrition, J. Dairy Sci. 74:3568–3597.

Van Soest, P. J., M. E. Van Amburgh, and L. O. Tedeschi. 2000. Rumen balance and rates of fiber digestion. Pages 150-166 in Proceedings of the Cornell Nutrition Conference for Feed Manufacturers. Cornell University, Ithica, NY.

Van Soest, P. J., Mertens, D. R., and Deinum, B. 1978. Preharvest factors influencing quality of conserved forage. J. Anim. Sci. 47:712–720.

van Wieren, S. E. 1996. Digestive strategies in ruminants and nonruminants. PhD Dissertation, Wagenengen University.

Vanzant, E. S., R. C. Cochran, and E. C. Titgemeyer. 1998. Standardization of in situ techniques for ruminant feedstuff evaluation. J. Anim. Sci. 76:2717-2729.

Varel, V. H., and K. K. Kreikemeier. 1999. Low- and high-quality forage utilization by heifers and mature beef cows. J. Anim. Sci. 77:2774-2780.

Vbra, E., and G. B. Schaller, eds. 2000. Antelopes, Deer, and Relatives: Fossil Record, Behavioral Ecology, Systematics, and Conservation. Yale Univ. Press, New Haven, CT.Walker, J.W. 1994. Multispecies grazing: the ecological advantage. Sheep Res. J. (special issue) 52–64.

von Engelhardt, W., and S. Hinderer. 1976. Transfer of blood urea into the goat colon. Pages 57-58 in Tracer Studies on Non-Protein Nitrogen for Ruminants. Vol. 3. International Atomic Energy Agency, Vieanna, AU.

von Keyserlingk, M. A. G., M. L. Swift, R. Puchala, and J. A. Shelford. 1996. Degradability characteristics of dry matter and crude protein of forages in ruminants. Anim. Feed Sci. Tech. 57:291-311.

Waghorn, G. C., and C. S. W. Reid. 1977. Rumen motility in sheep and cattle as affected by feeds and feeding. Proc. N.Z. Soc. Anim. Prod. 37:176-181.

Waldo, D. R., L. W. Smith, and E. L. Cox. 1972. Model of cellulose disappearance from the rumen. J. Dairy Sci. 55:125-129.

Walker, J. W. 1994. Multispecies grazing: the ecological advantage. J. Sheep Res. Special Issue:52-64.

Wallace, R. J., R. Onodera, and R. A. Cotta. 1997. Metabolism of nitrogen-containing compounds. Pages 283-316 in The rumen microbial ecosystem. 2nd ed. P. N. Hobson, and C. S. Stewart, ed. Blackie Acedemic and Professional, London.

Walz, L. S., W. C. Ellis, T. W. White, J. H. Matis, H. G. Bateman, C. C. Williams, J. M. Fernandez, and L. R. Gentry. 2004. Flow paths of plant tissue residues and digesta

through gastrointestinal segments in Spanish goats and methodological considerations. J. Anim. Sci. 82:508-520.

Warner, A. C. I. 1981. Rate of passage of digesta through the gut of mammals and birds. Nutr. Abrst. Rev. B. 51:789-820.

Webb, S. D. 1998a. Cervidae and bovidae. Pages 508 - 10 in Evolution of Tertiary Mammals of North America: Volume 1, Terrestrial Carnivores, Ungulates, and Ungulate like Mammals. C. M. Janis, K. M. Scott, L. L. Jacobs, ed. Cambridge Univ. Press: Cambridge, UK.

Webb, S. D. 1998b. Hornless ruminants. Pages 463- 76 in Evolution of Tertiary Mammals of North America: Volume 1, Terrestrial Carnivores, Ungulates, and Ungulate like Mammals. C. M. Janis, K. M. Scott, L. L. Jacobs, ed. Cambridge Univ. Press: Cambridge, UK.

Webb, S. D. 2000. Evolutionary history of new world Cervidae. Pages 38 – 64 in Antelopes, Deer, and Relatives: Fossil Record, Behavioral Ecology, Systematics, and Conservation. E. Vbra and G. B. Schaller, ed. Yale Univ. Press, New Haven, CT.

Webb, S. D., and B.E. Taylor. 1980. The phylogeny of hornless ruminants and a description of the cranium of Archaeomeryx. Bull. Am. Mus. Nat. Hist. 167:120–157.

Weisbjerg, M. R., P. K. Bhargava, T. Hvelplund, and J. Madsen. 1990. Anvendelse af nedbrydningsprofiler i fodermiddelvurderingen. Beretning fra Statens Husdyrbrugsforsøg 679:33.

Weiss, W. P. 2002. Relative feed value of forage and dairy cows: A critical appraisal. Pages 127-140 in Proc. Tri-State Dairy Nutr. Conf., Ft. Wayne, IN.

Welch, J. G. 1982. Rumination, particle size and passage from the rumen. J. Anim. Sci. 54:885-894.

Wemmer, C. 1998. Deer: Status Survey and Conservation Action Plan. IUCN/SSC Antelope Specialist Group, Gland, CH.

Weston, R. H. 1988. Factors limiting the intake of feed by sheep. 12. Digesta load and chewing activities in relation to lactation and its attendant increase in voluntary roughage consumption. Aust. J. Agric. Res. 39:671-677.

Weston, R. H., J. R. Lindsay, D. W. Peter, and D. J. Buscall. 1989. Factors limiting the intake of feed by sheep. 14. Comparisons of voluntary feed consumption and

various transactions in the alimentary tract between lambs and sheep fed roughage diets. Aust. J. Agric. Res. 40:625-642.

White, R.G., and J.R. Luick. 1984. Plasticity and constraints in the lactational strategy of reindeer and caribou. Symp. Zool. Soc. Lond. 51:215-232.

Whitehead, G. K. 1972. Deer of the World. Constable, London.

Wiener, G., H. Jianlin, and L. Ruijun. 2003. The Yak. 2nd ed. Food and Agriculture Organization of the United Nations, Bangkok, TH.

Wiener, G., H. Jianlin, and L. Ruijun. 2003. The Yak. 2nd ed. Food and Agriculture Organization of the United Nations, Bangkok, TH.

Woolnough, A. P. and J. P. du Toit. 2001. Vertical zonation of browse quality in tree canopies exposed to a size-structured guild of African browsing ungulates. Oecologia 129: 585-590.

Wyburn, R. S. 1980. The mixing and propulsion of the stomach contents of ruminants. Pages 35-51 in Digestive Physiology and Metabolism in Ruminants. Y. Ruckebusch and P. Thivend, ed. AVI Publishing, Westport, CT.

Yearsley, J., B. J. Tolkamp BJ, and A. W. Illius. 2001. Theoretical development in the study and prediction of food intake. Proc. Nutr. Soc. 60:145-156.

Zachos, J., M. Pagani, L. Sloan, E. Thomas, and K. Billups. 2001. Trends, rhythms, and aberrations in global climate 65 Ma to present. Science. 292:686-693.

Zeder, M. A., and B. Hesse. The initial domestication of goats (Capra hircus) in the Zagros Mountains 10,000 years ago. Science. 287:2254-2257.

VITA

Timothy John Hackmann was born to Donald and Dianne Hackmann on 13 October, 1984 in St. Louis, MO. During his youth, he enjoyed the company of many pets—cats, dogs, fish, gerbils, toads, and turtles—but had no contact with livestock animals.

After graduating from Lindbergh High School, Timothy matriculated the University of Missouri-Columbia to study biology with the intention of entering veterinary school. He became aware of the existence of animal science after taking an introductory class there with Dr. James "Jimmy" Spain. He milked a cow for his first time (at age 20) in a subsequent class with Dr. Spain. During this time, Dr. Spain offered Timothy an opportunity in undergraduate research then convinced him to pursue a career as a researcher. After graduating summa cum laude with a B.S. (Hons.) in Biology, Timothy entered the M.S. program in Animal Sciences at the University of Missouri-Columbia under Dr. Spain's direction.

After 2 years of hard work, excitement, frustration, and sleep deprivation, Timothy earned a M.S. in December 2008. He will pursue a Ph.D. in Nutrition at The Ohio State University in 2009.